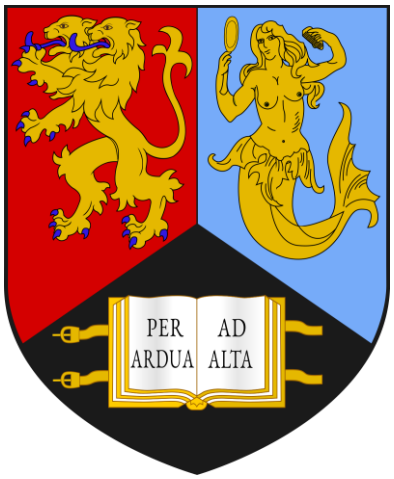
Establishing Human Pluripotent Stem Cell-Based Platforms with Autophagy Readouts to Investigate The Role of Autophagy in Cellular Homeostasis and Disease

by

Elena Seranova



A thesis submitted to

The University of Birmingham

for the degree of

DOCTOR OF PHILOSOPHY

Institute of Cancer and Genomic Sciences
College of Medical and Dental Sciences
The University of Birmingham
October 2020

UNIVERSITY OF
BIRMINGHAM

University of Birmingham Research Archive

e-theses repository

This unpublished thesis/dissertation is copyright of the author and/or third parties. The intellectual property rights of the author or third parties in respect of this work are as defined by The Copyright Designs and Patents Act 1988 or as modified by any successor legislation.

Any use made of information contained in this thesis/dissertation must be in accordance with that legislation and must be properly acknowledged. Further distribution or reproduction in any format is prohibited without the permission of the copyright holder.

Acknowledgments

This project would not be possible without the guidance and help of several people that supported me through my PhD journey.

First and foremost, I would like to thank my supervisor, Dr Sovan Sarkar, for his continuous support towards my PhD research, training and career development, and for giving me the chance to work on such exciting projects. I am also grateful to him for providing my PhD studentship through his UKIERI (UK-India Education and Research Initiative)–DST (Department of Science and Technology, Government of India) grant from the British Council.

I am grateful for the support of my secondary supervisor Dr Zania Stamataki, and our Indian collaborator Dr Dhiraj Kumar at International Centre for Genetic Engineering and Biotechnology in New Delhi, for their inputs on some parts of this project. I thank all the lab members who contributed to this research, and offered technical and moral support throughout the years in the lab. Special thanks to Dr Carl Ward, Ms Miruna Chipara, Mr Jorge Torresi, Dr Tatiana Rosenstock, Ms Adina Palhegyi, Dr Malgorzata Zatyka, Ms Surbhi Verma and Ms Congxin Sun.

I am indebted to all my friends and family for their emotional support and for always believing in me, for giving me courage when I needed it the most. In particular, I want to thank my mother Irina, Angelina and Olga for their unfailing support. Finally, I would like to thank Sami for his patience and his unwavering faith in me.

Abstract

Autophagy is a vital homeostatic pathway essential for cellular survival and human health. It primarily functions as an intracellular degradation process for the turnover of unwanted cytoplasmic materials such as aggregation-prone proteins, damaged organelles and invading pathogens. Defective autophagy contributes to the pathology of a myriad human diseases including neurodegeneration and infection, and thus therapeutic exploitation of autophagy presents an attractive opportunity. The work described in this thesis involves establishment of human embryonic stem cell (hESC) models of autophagy for studying its homeostatic role and developing screening platforms in physiologically-relevant human cell-types of interest. The autophagy-deficient (*ATG5*$^{-/-}$) hESC-based system was used to address how loss of autophagy leads to cytotoxicity; an important question relevant to neurodegeneration. The *ATG5*$^{-/-}$ hESCs and hESC-derived neurons exhibited basal cytotoxicity accompanied by a specific metabolic defect. Depletion of NADH was found to be mediating cytotoxicity during autophagy deficiency via mitochondrial depolarisation, since boosting cellular NADH levels improved cell viability and mitochondrial membrane potential in *ATG5*$^{-/-}$ neurons. This intervention was also cytoprotective in a human induced pluripotent stem cell (hiPSC)-based disease model of a neurodegenerative lysosomal storage disorder associated with autophagy dysfunction, and thus could be relevant for related neurodegenerative conditions. The autophagy reporter (mCherry-EGFP-LC3) hESC-based system was developed for identifying potent autophagy inducers enhancing pathogen clearance in macrophages; relevant for combating infection. The hESC-derived macrophages were characterised to confirm their cellular identity. These isogenic platforms can be of basic and biomedical relevance for mechanistic studies of autophagy regulation including human cell-type specific effects, and drug discovery of autophagy modulators for therapeutic applications in human diseases.

Declaration

The work presented in this thesis was carried out at the Institute of Cancer and Genomic Sciences in the University of Birmingham, Birmingham B15 2TT, UK, during the period of April 2017 to April 2020.

The work in this thesis is original, except where acknowledged by references.

No part of the work is being, or has been, submitted for a degree, diploma or any other qualification at any other University.

List of Figures

Figure 1.1. Mechanism of the autophagy process. 21

Figure 1.2. Regulation of autophagy by mTOR-dependent and mTOR-independent signaling pathways that are amenable to chemical perturbations. 25

Figure 1.3. Autophagy reporter and substrate based assay platforms and the impact of autophagy modulators at different stages of the autophagy process. 29

Figure 1.4. LC3 reporter-based in vitro screening platforms. 30

Figure 1.5. The impact of malfunctioning autophagy and the therapeutic benefits of autophagy modulators in diverse human diseases. 37

Figure 1.6. Impairment of autophagy in neurodegenerative disorders. 40

Figure 1.7. Cellular reprogramming for hiPSC generation and possible applications for hiPSC-based disease modelling and drug discovery. 45

Figure 2.1. Schematic representation of the impact and the genome editing strategy of *ATG5* gene disruption, and the list of hESC lines obtained. 58

Figure 2.2. Characterisation of *ATG5*$^{-/-}$ hESCs for pluripotency. 59

Figure 2.3. Characterisation of *ATG5*$^{-/-}$ hESCs for autophagy deficiency. 62

Figure 2.4. Rescue of functional autophagy in *ATG5*$^{-/-}$ hESCs via lipid nanoparticle-mediated *ATG5* mRNA delivery. 63

Figure 2.5. Autophagy-deficient hESCs exhibited increased cell death that could be rescued via lipid nanoparticle-mediated *ATG5* mRNA delivery. 65

Figure 2.6. Generation and characterisation of autophagy-deficient hESC-derived neural precursors and neurons. 68

Figure 2.7. Characterisation of autophagy-deficient hESC-derived neural precursors and neurons via immunoblotting for cell specific markers. 60

Figure 2.8. Phenotypic characterisation of *ATG5*$^{-/-}$ hESC-derived neural precursors and neurons for loss of autophagy. 72

Figure 2.9. Lipid nanoparticle-mediated *ATG5* mRNA delivery in autophagy-deficient neurons restored functional autophagic flux. 73

Figure 2.10. Increased cell death in autophagy-deficient hESC-derived neural precursors 75

Figure 2.11. Increased cell death in autophagy-deficient hESC-derived neurons. 76

Figure 2.12. Increased apoptotic nuclei in autophagy-deficient hESC-derived neurons. 77

Figure 3.1. Autophagy-deficient hESCs and neurons have perturbed metabolic profiles. 83

Figure 3.2. Perturbation of specific metabolites in autophagy-deficient hESCs and hESC-derived neurons. 84

Figure 3.3. Common negative and positive changes in metabolites in autophagy-deficient hESCs and hESC-derived neurons. 86

Figure 3.4. Alterations of the levels of energy carriers in autophagy-deficient hESCs and hESC-derived neurons. 87

Figure 3.5. Mitochondrial depolarisation and elevation in ROS in autophagy-deficient hESCs and hESC-derived neurons. 89

Figure 3.6. Increased mitochondrial fragmentation in autophagy-deficient hESCs and hESC-derived neurons. 91

Figure 3.7. Increased mitochondrial fragmentation in autophagy-deficient hESC-derived neural precursors. 92

Figure 3.8. Impaired mitophagy in autophagy-deficient hESC-derived neurons. 93

Figure 3.9. NAD/NADH boosting compounds rescued cell death in autophagy-deficient hESCs and hESC-derived neurons. 96

Figure 3.10. NAD/NADH boosting compounds improved axonal phenotype in autophagy-deficient hESC-derived neurons. 97

Figure 3.11. NAD/NADH boosting compounds increased cellular NADH levels and improved mitochondrial membrane potential in autophagy-deficient hESC-derived neurons without affected ATP/ADP levels. 98

Figure 3.12. NAD/NADH boosting compounds improved cell viability in Niemann-Pick type C1 (NPC1) disease patient hiPSC-derived neurons. 100

Figure 4.1. Schematic representation of the genome editing strategy in hESCs and the autophagy reporter readouts to monitor autophagosome turnover. 106

Figure 4.2. Phenotypic characterisation of mCherry-EGFP-hESCs. 107

Figure 4.3. Perturbations of autophagosome turnover readout in mCherry-EGFP-LC3 hESCs by modulation of autophagy. 109

Figure 4.4. Differentiation of hESCs into macrophages via monocytic cells. 112

Figure 4.5. Gating strategy implemented for FACS analysis of cell surface markers. 115

Figure 4.6. FACS analyses of surface markers in wild-type (parental WIBR3) hESC-derived monocytic cells. 117

Figure 4.7. FACS analyses of surface markers in autophagy reporter (mCherry-EGFP-LC3) hESC-derived monocytic cells. 118

Figure 4.8. Characterisation of wild-type hESC-derived macrophages. 122

Figure 4.9. FACS analyses of surface markers in autophagy reporter (mCherry-EGFP-LC3) hESC-derived monocytic cells. 123

Figure 4.10. Functional characterisation of autophagy reporter hESC-derived macrophages. 124

List of Tables

Table 4.1. Monocyte and macrophage surface markers 113

Table 6.1. List of primary and secondary antibodies for immunoblotting analysis 148

Table 6.2. List of primary and secondary antibodies for immunofluorescence 149

Table 6.3. List of primers for qPCR 150

Table 6.4. List of primary antibodies and isotype controls for FACS 156

List of Abbreviations

AAVS1	Adeno-associated virus integration site 1
AD	Alzheimer's disease
ADCC	Antibody-dependent cell-mediated cytotoxicity
ADP	Adenosine diphosphate
AIM	Atg8 family interacting motif
ALFY	Autophagy-linked FYVE protein
ALS	Amyotrophic lateral sclerosis
AMBRA1	Activating molecule in Beclin 1-regulated autophagy protein 1
AMP	Adenosine monophosphate
AMPK	AMP-activated protein kinase
APCs	Antigen-presenting cells
ASD	Autism spectrum disorder
ATG	Autophagy-related gene
ATP	Adenosine triphosphate
Baf A_1	Bafilomycin A_1
BMP4	Bone morphogenic protein 4
BRUCE	Baculovirus IAP repeat-containing ubiquitin-conjugating enzyme
Ca^{2+}	Calcium
Calpains	Ca^{2+}-dependent cysteine proteases
cAMP	3',5'-cyclic adenosine monophosphate
CRISPR	Clustered regularly interspaced short palindromic repeats
DAPI	4′,6-Diamidino-2-Phenylindole
DFCP1	Double FYVE domain containing protein 1
DMSO	Dimethyl sulfoxide
DNA	Deoxyribonucleic acid

EB	Embryoid body
ECM	Extracellular matrix
EGFP	Enhanced green fluorescent protein
ELISA	Enzyme-linked immunosorbent assay
ER	Endoplasmic reticulum
EPG5	Ectopic P-granules autophagy protein 5 homolog
ESX1	ESAT6-secretion system
ETC	Electron transport chain
FACS	Fluorescence activated cell sorting
FCCP	Carbonyl Cyanide-4-(Trifluoromethoxy)Phenylhydrazone
FDR	False discovery rate
FM	Full medium
FTD	Frontotemporal dementia
FIP200	Focal adhesion kinase family-interacting protein of 200 kDa
FYCO-1	FYVE and coiled-coil domain-containing protein 1
GABARAPs	γ-Aminobutyric acid receptor-associated proteins
GD	Gaucher disease
GM-CSF	Granulocyte-macrophage colony-stimulating factor
HBSS	Hanks balanced salt solution
HCS	High-content screening
HOPS	Homotypic fusion and protein sorting
HTS	High-throughput screening
IFNγ	Interferon gamma
IL10	Interleukin 10
IP_3	Inositol 1,4,5-trisphosphate
LBP	LPS together with LPS binding protein
LIR	LC3-interaction region

LNPs	Lipid nanoparticles
MAP1LC3	Microtubule-associated protein 1 light chain 3
mCherry	Monomeric Cherry
M-CSF	Macrophage colony stimulating factor
MEFs	Mouse embryonic fibroblasts
MR	Mannose receptor
MS	Mass spectrometry
MiNA	Mitochondrial network analysis
Mtb	Mycobacterium tuberculosis
NAD+	Nicotinamide adenine dinucleotide (oxidised form)
NADH	Nicotinamide adenine dinucleotide (reduced form)
NAM	Nicotinamide
NAMPT	Nicotinamide phosphoribosyltransferase
NBR	Nucleotide releasing buffer
NBR1	Neighbor of BRCA1 gene 1
NCL	Neuronal ceroid lipofuscinosis
NDP52	Nuclear dot protein of 52 kDa
NO	Nitric oxide
NMR	Nuclear magnetic resonance
NPC1	Niemann-Pick type C1
NPM	NP medium
NPs	Neural precursors
NR	Nicotinamide riboside
OCT4	Octamer-binding transcription factor 4
OD	Optical density
OPTN	Optineurin
OXPHOS	Oxidative phosphorylation

PARPs	Poly-ADP-ribose polymerases
PAS	Phagophore assembly site
PCA	Principal component analysis
PE	Phosphatidylethanolamine
PI	Propidium Iodide
PI3KC3-C1	Class III phosphatidylinositol-3-kinase complex 1
PI3P	Phosphatidylinositol 3-phosphate
PI4P	Phosphatidylinositol-4-Phosphate
PLEKHM1	Pleckstrin homology domain-containing family member 1
RILP	Rab-interacting lysosomal protein
ROS	Reactive oxygen species
RT	Room temperature
SCA3	Spinocerebellar ataxia type 3
SCF	Stem cell factor
SIRTs	Sirtuins
SNAREs	Soluble N-ethylmaleimide-sensitive factor-attachment protein receptors
SOX2	SRY (sex determining region Y)-box 2
SQSTM1	Sequestosome 1
SSEA4	Stage specific embryo antigen 4
STING	Stimulator of IFN genes
STX17	Syntaxin 17
TALENs	Transcription activator-like effector nucleases
TAX1BP1	Tax1 binding protein 1
TGFβ	Transforming growth factor beta
TECPR1	Tectonin beta-propeller repeat containing protein 1
TCA	Tricarboxylic acid

TFEB	Transcription factor EB
TMRE	Teramethylrhodamine
TOLLIP	Toll interacting protein
UBD	Ubiquitin-binding domain
ULK1	Unc-51-like kinase-1
UVRAG	UV radiation resistance associated gene
VEGF	Vascular endothelial growth factor
VPS34	Vacuolar protein sorting 34
WIPI2	WD repeat domain phosphoinositide-interacting protein 2
ZFNs	Zinc finger nucleases
hESCs	Human embryonic stem cells
hPSCs	Human pluripotent stem cells
hiPSCs	Human induced pluripotent stem cells
iMEFs	Inactivated mouse embryonic fibroblasts
mTOR	Mechanistic target of rapamycin
qPCR	Quantitative polymerase chain reaction
ΔΨm	Mitochondrial membrane potential

Table of contents

Chapter 1: Introduction 19

1.1. Overview 19

1.2. The autophagic machinery mediating the autophagy process 20

1.3. Signaling pathways regulating autophagy 24

1.4. Chemical modulators of autophagy 27

1.5. Methods for monitoring autophagy 28

1.5.1. Monitoring autophagy using LC3 based reporters 28

1.5.2. Monitoring autophagy by substrate clearance 32

1.6. Autophagy receptors for mediating selective autophagy 33

1.7. Role of autophagy in tissue and energy homeostasis 34

1.8. Role of autophagy in human diseases 35

1.8.1. Role of autophagy in neurodegenerative disorders 36

1.8.1.1. Role of autophagy in Niemann-Pick type C disease 39

1.8.2. Role of autophagy in infectious diseases 42

1.9. The importance of human pluripotent stem cells (hPSCs) in biological studies 43

1.9.1. Human pluripotent stem cells for studying basic biology and disease mechanisms 44

1.9.2. Human pluripotent stem cells in drug discovery and drug screening 46

1.10. Differentiation of hESCs into desired human cell-types 48

1.10.1. Neuronal differentiation 49

1.10.2. Macrophage differentiation 50

1.11. Aims and Hypotheses 53

Chapter 2: Establishment of autophagy-deficient human cellular platforms utilising hESCs 55

2.1. Overview 55

2.2. Introduction to the existing autophagy knockout models and the need for a hESC-based experimental platform 55

2.3. Results 57

2.3.1. Generation and characterisation of autophagy-deficient hESCs 57

2.3.2. Phenotypic characterisation of *ATG5*$^{-/-}$ hESCs for loss of autophagy 60

2.3.3. Nanoparticle-mediated *ATG5* mRNA delivery rescues autophagy deficiency 61

2.3.4. Increased cytotoxicity in autophagy-deficient hESCs 64

2.3.5. Optimisation of neuronal differentiation from hESCs 66

2.3.6. Establishment and characterisation of hESC-derived neural precursors and neurons 69

2.3.7. Characterisation of *ATG5*$^{-/-}$ hESC-derived NPs and neurons for loss of autophagy. 71

2.3.8. Increased cytotoxicity in *ATG5*$^{-/-}$ hESC-derived NPs and neurons 74

2.4. Chapter summary 78

Chapter 3: Metabolic and mitochondrial defects mediate cytotoxicity during autophagy deficiency 80

3.1. Overview 80

3.2. Introduction to the role of autophagy in metabolic homeostasis 81

3.3. Results 82

3.3.1. Metabolic defects in autophagy-deficient hESCs and neurons 82

3.3.2. Depletion of NADH is a common underlying perturbation in autophagy-deficient hESCs and neurons, and in other non-hESC model systems 85

3.3.3. Autophagy-deficient hESCs and neurons exhibit mitochondrial depolarisation and elevation in ROS 88

3.3.4. Autophagy-deficient hESCs and neurons are associated with mitochondrial fragmentation and impaired clearance of fragmented mitochondria 90

3.3.5. NAD/NADH boosting compounds improve neuronal and mitochondrial phenotypes, and rescue cell death in autophagy-deficient neurons 94

3.3.6. NAD/NADH boosting compounds improve cell viability in Niemann-Pick type C1 (NPC1) patient-derived disease-affected neurons 99

3.4. Chapter summary 101

Chapter 4: Establishment of autophagy reporter screening platform in human macrophages utilising hESCs 103

4.1. Overview 103

4.2. Introduction to the need for establishing autophagy reporter macrophage platform for identifying xenophagy inducers 104

4.3. Results 105

4.3.1. Characterisation of autophagy reporter hESCs stably expressing mCherry-EGFP-LC3 105

4.3.2. Challenges and mitigations of generation of autophagy reporter hESC-derived macrophages 110

4.3.3. Characterisation of cellular identity of hESC-derived monocytic cells 113

4.3.4. Characterisation of cellular identity and functionality of hESC-derived macrophages 119

4.4. Chapter summary 125

Chapter 5 126

Discussions 126

Chapter 5: Discussions 127
5.1. Summary and significance of principal findings 127
5.1.1. Establishment of human embryonic stem cell (hESC) models of autophagy deficiency and autophagy reporter 127
5.1.2. Elucidation of a mechanistic link between autophagy deficiency and cell death using autophagy-deficient hESC model 128
5.2. Biomedical implications 129
5.2.1. Implications of NADH boosting compounds in neurodegenerative diseases associated with dysfunctional autophagy (related to Chapters 2 and 3) 129
5.2.2. Implications of autophagy reporter macrophage platforms for drug discovery for infectious diseases (related to Chapter 4) 131
5.3. Study limitations 132
5.3.1. Study limitations related to hESC-derived autophagy-deficient cellular platforms (related to Chapter 2) 132
5.3.2. Study limitations related to the mechanistic link between autophagy deficiency and cell death (related to Chapter 3) 133
5.3.3. Study limitations related to hESC-derived autophagy reporter cellular platforms (related to Chapter 4) 134
5.4. Future work 135
5.4.1. Further work for studying the role of autophagy in cell death (related to Chapters 2 and 3) 135
5.4.2. Further work for developing and utilising the autophagy reporter cellular platforms (related to Chapter 4) 139
Chapter 6: Materials and Methods 143
6.1. Cell culture 143
6.1.1. Culture of human embryonic stem cells (hESCs) and human induced pluripotent stem cells 143
6.1.2. Human pluripotent stem cell culture: challenges and considerations 143
6.2. Differentiation of hESCs and hiPSCs into neural precursors and terminally differentiated neurons 144
6.3. Differentiation of hESCs into monocytic cells and macrophages 145
6.4. Lipid nanoparticle mediated mRNA delivery 146
6.5. Compounds and treatment 146
6.6. Analysis of autophagic vesicles by mCherry-EGFP-LC3 reporter 147
6.7. Immunoblotting analysis 147
6.8. Immunofluorescence analysis 149
6.9. Image acquisition of fixed cells 150
6.10. Gene expression analysis 150

6.11. Cell death analysis 151
6.11.1. TUNEL assay for apoptotic cells 151
6.11.2. Cytotoxicity assay 151
6.11.3. FACS analysis of live and apoptotic cells 152
6.11.4. DAPI staining for apoptotic nuclear morphology 152
6.12. NAD^+ and NADH measurements 153
6.13. ATP and ADP measurements 153
6.14. Mitochondrial ΔΨm and ROS measurements 153
6.15. MitoTracker staining and mitochondrial rod length analysis 154
6.16. Axonal length measurement in neurons 154
6.17. Metabolomics 155
6.17.1. LC-MS-based metabolomics 155
6.17.2. Metabolomics data analysis 155
6.18. Fluorescence Activated Cell Sorting (FACS) 156
6.19. Enzyme-linked immunosorbent assay (ELISA) 157
6.20. Phagocytosis assay 157
6.21. Statistical analyses 158
References 160
Appendix 226
Appendix 1: Publications of Elena Seranova 226
Appendix 2: Cover of Journal of Molecular Biology (April 2020) featuring hESC-derived neurons generated by Elena Seranova in Sovan Sarkar lab 227

Chapter 1

Introduction

Chapter 1: Introduction

Introduction sections 1.1, 1.2, 1.3, 1.4 and 1.6, and parts of 1.8, 1.9 and 1.10, have been published in my first-author review article: Seranova E., Palhegyi A.M., Verma S., Dimova S., Lasry R., Naama M., Sun C., Barrett T., Rosenstock T.R., Kumar D., Cohen M.A., Buganim Y., Sarkar S. Human induced pluripotent stem cell models of neurodegenerative disorders for studying the biomedical implications of autophagy. Journal of Molecular Biology 432(8): 2754-2798 (2020) [PMID: 32044344].

Introduction section 1.5 has been published in my first-author review article: Seranova E., Ward C., Chipara M., Rosenstock T.R., Sarkar S. In Vitro Screening Platforms for Identifying Autophagy Modulators in Mammalian Cells. Methods in Molecular Biology 1880: 389-428 (2019) [PMID: 30610712].

1.1. Overview

Macroautophagy (referred herein as autophagy) is a highly conserved catabolic pathway, which delivers undesirable cytoplasmic materials to the lysosomes for their degradation. It plays a constitutive role in the quality control of intracellular macromolecules and organelles, thus imperative for the maintenance of cellular and energy homeostasis that are vital for human health (Mizushima et al., 2008; Ravikumar et al., 2010). Autophagy is implicated in a myriad human physiology including development and immunity, whereas its malfunction contributes to the pathology of diverse human diseases including neurodegeneration, cancer and infectious diseases, amongst others (Jiang and Mizushima, 2013; Levine and Kroemer, 2008; Menzies et al., 2017). Of biomedical relevance, pharmacological modulation of autophagy imparts therapeutic benefits in experimental models of a range of human diseases, including neurodegenerative and infectious diseases (Galluzzi et al., 2017; Rubinsztein et al., 2012; Palhegyi et al., 2019; Seranova et al., 2017; Sharma et al., 2018). However, to fully exploit the therapeutic potential of autophagy, it is pertinent to understand how autophagy dysfunction mediates cytotoxicity, and to undertake drug discovery in disease-relevant human cell-types.

The aims of this thesis are to establish physiologically-relevant, human cellular platforms with autophagy readouts in order to understand the role of autophagy in cellular homeostasis, and to generate screening systems for identifying potent/tissue-specific autophagy inducers. Autophagy-deficient and autophagy reporter platforms

were established by utilising human embryonic stem cells (hESCs) for their ability to differentiate into the desired human cell-types, and genome editing for generating the autophagy phenotype. These isogenic hESC-based models were utilised to elucidate how loss of autophagy causes cell death in autophagy-deficient hESCs and hESC-derived neurons, and to establish chemical screening platforms in autophagy reporter hESCs and hESC-derived macrophages.

1.2. The autophagic machinery mediating the autophagy process

The initiation of the autophagy process in mammalian cells involves the genesis of the phagophore, which is an isolation membrane structure that is derived from the endoplasmic reticulum (ER)-emanating membrane domains termed as “omegasome” and/or from other sources like trans-Golgi, recycling endosomes, plasma membrane and mitochondria (Mercer et al., 2018; Tooze and Yoshimori, 2010). The phagophore expands to engulf intracellular autophagic cargo that comprises unwanted macromolecules like protein aggregates or damaged organelles like mitochondria, thereby sequestering the cargo in a double-membrane structure called the autophagosome. The cargo-loaded autophagosome then matures through fusion with the lysosome to form the autolysosome, thereby promoting the degradation of the autophagosomal content by the lysosomal digestive enzymes (Feng et al., 2013). Autophagosome maturation is generally a multistep process wherein the autophagosome initially fuses with the late endosome to form a hybrid organelle called amphisome, which acts as a sink for autophagic and endocytic cargo materials for delivery to the lysosomes; however, the autophagosome can also directly fuse with the lysosomes (Nakamura and Yoshimori, 2017; Zhao and Zhang, 2018) (Figure 1.1). The dynamic turnover of autophagosomes (autophagosome flux) and autophagic cargo (autophagic cargo flux) is collectively defined as autophagic flux.

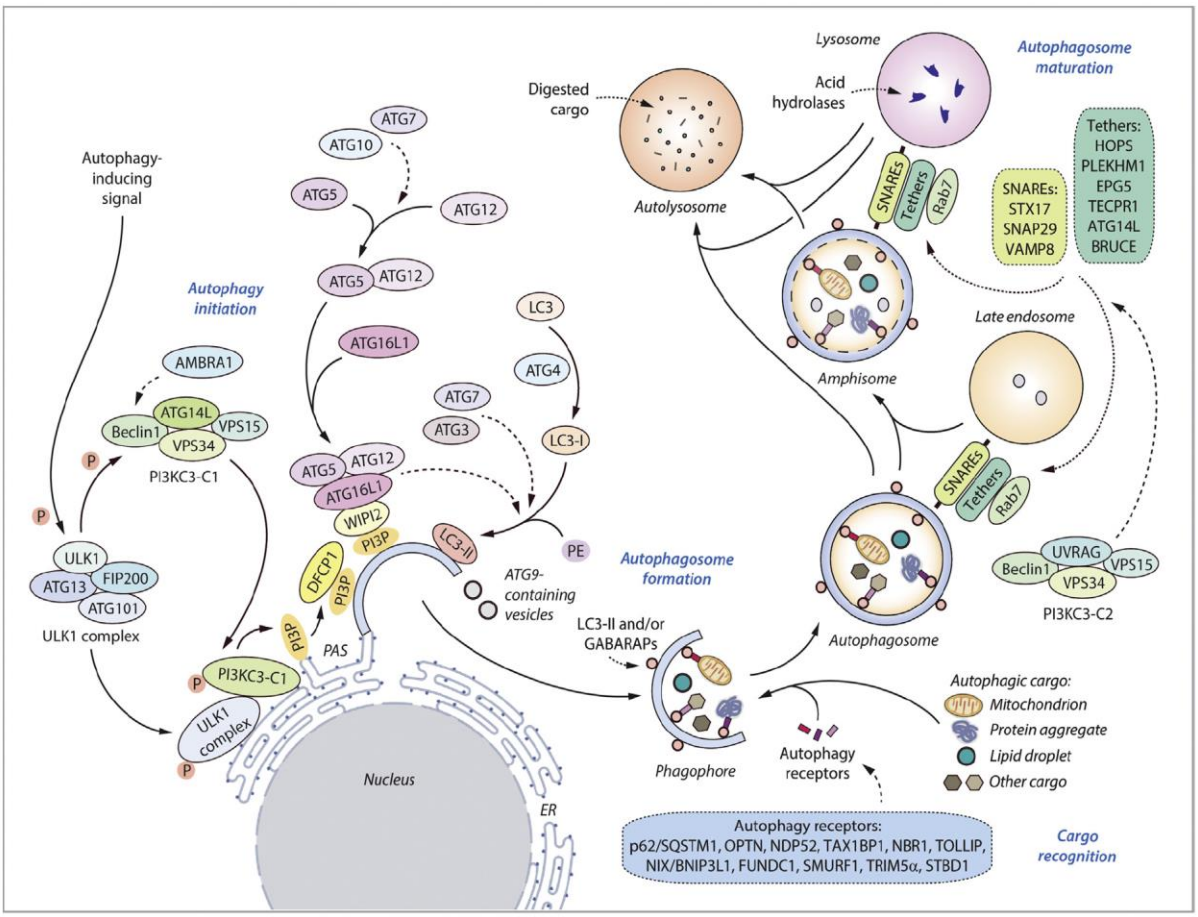


Figure 1.1. Mechanism of the autophagy process.

Autophagy encompasses multiple vesicular compartments and vesicle fusion events through which the autophagic cargo is degraded. This process initiates with the formation of phagophores at the phagophore assembly site (PAS). The autophagic machinery involving several autophagy-related (ATG) proteins enables the expansion of the phagophore to form autophagosomes. Autophagic cargo is engulfed in the autophagosomes during which specific autophagy receptors mediate selective cargo recognition. The autophagosomes either fuse with the late endosomes to form amphisomes and then with the lysosomes to form autolysosomes, or directly fuse with the lysosomes forming autolysosomes. These vesicle fusion events during autophagosome maturation are mediated by various SNAREs, tethering proteins and Rab7. The autophagic cargo is eventually degraded in the autolysosomes by the lysosomal acid hydrolases.

Figure reference: Seranova E. et al. Journal of Molecular Biology 432(8): 2754-2798 (2020).

The quantum leap in the explication of the molecular machinery controlling autophagy came from the genetic studies in yeasts by Ohsumi and colleagues during the 1990s, in which autophagy related (Atg) genes were identified (Mizushima, 2018). Since then, numerous studies have elucidated that this dedicated cohort of ATG proteins assembles into functional complexes that are activated and recruited to specific membrane structures to initiate the autophagy process (Mizushima, Yoshimori and Ohsumi, 2011; Klionsky et al., 2003) (Figure 1.1). The apical step in the initiation process involves the activation of the ULK1 (unc-51-like kinase-1) complex (Chan, Kir and Tooze, 2007), which consists of the serine/threonine-protein kinase ULK1 (mammalian orthologue of yeast Atg1) and three scaffold proteins that include FIP200 (focal adhesion kinase family-interacting protein of 200 kDa; also known as RB1CC1), ATG13, and ATG101 (Zachari and Ganley, 2017). Once activated, the ULK1 complex further phosphorylates a number of downstream targets, which culminate to promote autophagosome biogenesis from the phagophore assembly site (PAS) at the omegasome on the ER (Karanasios et al., 2013). An important phosphorylation target of the ULK1 complex to trigger phagophore nucleation is the class III phosphatidylinositol-3-kinase complex 1 (PI3KC3-C1) (Egan et al., 2015), consisting of VPS34 (vacuolar protein sorting 34; the catalytic subunit), Beclin 1, ATG14L and VPS15 (Kim et al., 2013). Specifically, the ULK1-mediated phosphorylation of PI3KC3-C1 results in phosphorylation of Beclin1 that activates the VPS34 lipid kinase, and subsequently the whole PI3KC3-C1 translocates to the PAS (Russell et al., 2013). This interaction between the components of PI3KC3-C1 leads to production of the phospholipid, phosphatidylinositol 3-phosphate (PI3P) at the PAS. PI3P then recruits the PI3P-binding proteins, such as WIPI2 (WD repeat domain phosphoinositide-interacting protein 2) and DFCP1 (double FYVE domain containing protein 1) to support the expansion of the phagophore membrane (Axe et al., 2008; Dooley et al., 2014). Phosphorylation of ATG9 by ULK1 also mediates the translocation of ATG9-positive vesicles to the PAS, where they supply lipid membrane to the expanding phagophore (Karanasios et al., 2016).

The elongation of the phagophore is regulated by two ubiquitin-like conjugation systems, which generate modified complexes of autophagy regulators (Mizushima et al., 1998; Ichimura et al., 2000) (Figure 1.1). The first ubiquitin-like reaction involves the conjugation of ATG12 to ATG5 that is catalyzed by the E1-like enzyme ATG7 and

the E2- like enzyme ATG10. The ATG5-ATG12 complex then non-covalently interacts with ATG16L1 to form the ATG5-ATG12-ATG16L1 ternary complex. The second of the ubiquitin-like reactions involves the conjugation of ubiquitin-like molecules of the ATG8 family with membrane-resident phosphatidylethanolamine (PE) (Mizushima, Yoshimori and Ohsumi, 2011; Geng and Klionsky, 2008). The human ATG8 family comprises of two subfamilies, microtubule-associated protein 1 light chain 3 (MAP1LC3 or LC3) and γ-aminobutyric acid receptor-associated proteins (GABARAPs), which are encoded by seven genes expressing LC3A, LC3B, LC3B2, LC3C, GABARAP, GABARAPL1 and GABARAPL2 (also called GATE-16) (Slobodkin and Elazar, 2013). Prior to lipidation, the ATG8 protein is processed at its C-terminal by a family of cysteine protease, ATG4 (Fernández and López-Otín, 2015). Further, ATG7 and ATG3 acting as the respective E1 and E2 enzymes, and ATG12-ATG5-ATG16L1 complex serving as an E3 ligase, conjugate ATG8 to PE, resulting in the incorporation of ATG8-PE in the growing phagophore that aids in phagophore expansion, autophagosome formation, and cargo recognition (Mizushima, Yoshimori and Ohsumi, 2011; Geng and Klionsky, 2008). One of the autophagosome markers generally used for studying autophagy is LC3B (referred herein as LC3), which via this conjugation reaction, gets converted from the cytosolic LC3-I form into the membrane-bound LC3-II form (Kabeya et al., 2000).

After biogenesis, the maturation of autophagosome occurs through fusion with the late endosome and lysosome that is primarily coordinated by three sets of proteins: Rab GTPases like Rab7, membrane tethering complexes, such as HOPS (homotypic fusion and protein sorting) complex, and SNARE (soluble N-ethylmaleimide-sensitive factor-attachment protein receptor) proteins like syntaxin-17 (STX17) and VAMP8 (Nakamura and Yoshimori, 2017, Zhao and Zhang, 2018) (Figure 1.1). Several effector proteins of active GTP-bound Rab7 drive autophagosome mobility and its fusion with the late endosomal and lysosomal compartments (Jager et al., 2004, Gutierrez et al., 2004). These include RILP (Rab-interacting lysosomal protein) (Jordens et al., 2001) and FYCO-1 (FYVE and coiled-coil domain-containing protein 1) (Pankiv et al., 2010), which respectively recruit dynein and kinesin motor proteins for the perinuclear transport of mature autophagosome. Other Rab7 effectors enabling vesicle fusion include PLEKHM1 (Pleckstrin homology domain-containing family member 1), which acts as an adaptor by binding to both the HOPS complex and

LC3/GABARAP (McEwan et al., 2015), and EPG5 (ectopic P-granules autophagy protein 5 homolog) that binds to LC3 and stabilises the autophagosomal SNARE complex (Wang et al., 2016). Interestingly, class III phosphatidylinositol-3-kinase complex 2 (PI3KC3-C2), comprising of VPS34, Beclin 1, VPS15, and UVRAG (UV radiation resistance associated gene protein), positively regulates autophagosome maturation via the association of UVRAG with the HOPS complex to activate Rab7 (Liang et al., 2008; Matsunaga et al., 2009). Besides HOPS, other tethering factors driving autophagosome fusion events are ATG14L (Diao et al., 2015) and TECPR1 (Tectonin beta-propeller repeat containing protein 1) (Chen et al., 2012). The SNAREs involved in autophagosome maturation form a complex between the autophagosomal Q-SNAREs STX17 and SNAP29, and the late endosomal/lysosomal R-SNARE VAMP8 (Itakura et al., 2012), which is mediated by ATG14L (Diao et al., 2015). Additional regulators of autophagosome maturation are GABARAPs (Nguyen et al., 2016), myosin VI (Tumbarello et al., 2012), BRUCE (Baculovirus IAP repeat-containing ubiquitin-conjugating enzyme) (Nguyen et al., 2016), and phosphoinositides like PI4P (phosphatidylinositol-4-phosphate) (Wang et al., 2015). In the final steps, the inner membrane of the autophagosome and the engulfed cytoplasm derived materials are degraded inside the autolysosome by the lysosomal acid hydrolases, which include proteases, such as cathepsins (Figure 1.1). The breakdown products are then recycled and serve as inputs for bioenergetics and anabolic pathways (Lahiri et al., 2019).

1.3. Signaling pathways regulating autophagy

Diverse signaling pathways regulate autophagy, but the most characterised one is nutrient signaling. Nutrient deprivation (starvation) induces autophagy by inhibiting the mechanistic target of rapamycin (mTOR), which is a serine/threonine-protein kinase that otherwise suppresses autophagy under nutrient sufficiency (Meijer et al., 2014) (Figure 1.2). mTOR forms two distinct protein complexes, which are mTOR complex 1 (mTORC1) and mTOR complex 2 (mTORC2) (Saxton and Sabatini, 2017), but only mTORC1 directly regulates autophagy by phosphorylating the ULK1 complex and suppressing the ULK1 kinase activity that is required to initiate autophagy (Zachari and Ganley, 2017). Besides ULK1 phosphorylation, mTORC1 can also indirectly inhibit autophagy by phosphorylating AMBRA1 (activating molecule in Beclin 1-

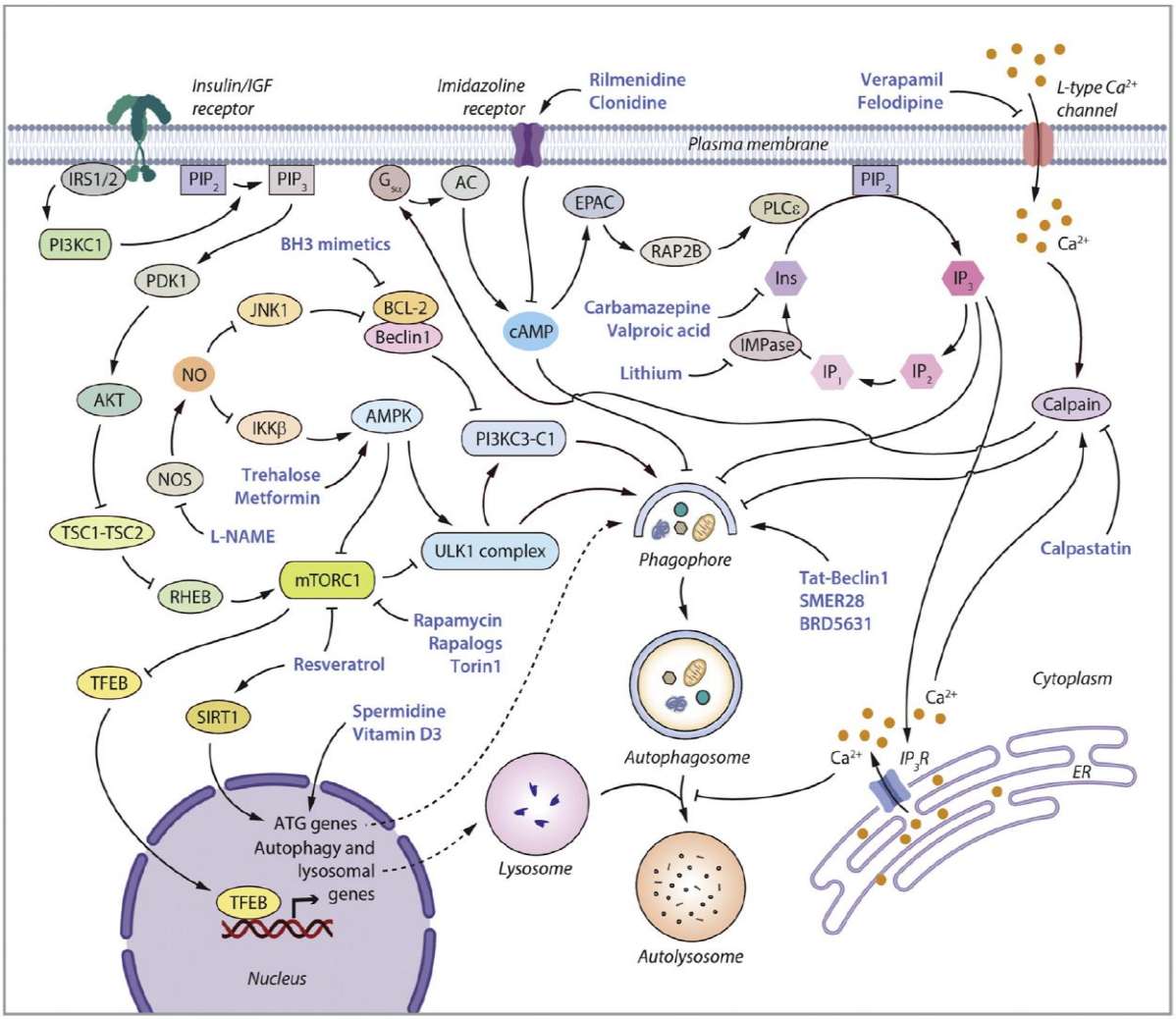


Figure 1.2. Regulation of autophagy by mTOR-dependent and mTOR-independent signaling pathways that are amenable to chemical perturbations.

Autophagy is classically regulated by the mechanistic target of rapamycin (mTOR) pathway, in which the downstream mediators are the ULK1 and PI3KC3-C1 complexes. AMPK can also directly influence ULK1 to govern autophagy. In addition, autophagy is regulated by mTOR-independent pathways involving IP_3, cAMP, Ca^{2+} and calpain. Various pharmacological inducers of autophagy acting on specific targets in these pathways are shown.

Figure reference: Seranova E. et al. Journal of Molecular Biology 432(8): 2754-2798 (2020).

regulated autophagy protein 1), which, in turn, could reduce ULK1 stability and its kinase activity (Nazio et al., 2013). Additionally, mTORC1 can prevent autophagy byphosphorylation-dependent cytoplasmic sequestration of TFEB (transcription factor EB), a master transcriptional regulator of genes involved in lysosomal biogenesis and autophagy (Settembre et al., 2011) (Figure 1.2). Particularly for the autophagy process, TFEB regulates the expression of genes required for autophagy initiation (BECN1, ATG9B, WIPI1), phagophore elongation (GABARAP, MAP1LC3B, ATG5), autophagosome maturation (UVRAG, RAB7) and cargo recognition (SQSTM1) (Di Malta, Cinque and Settembre, 2019). Likewise, another serine/threonine protein kinase, Akt, can phosphorylate TFEB independently of mTORC1 and prevent its nuclear translocation (Palmieri et al., 2017). Inhibition of mTORC1 or Akt activity promotes autophagy via nuclear localisation of TFEB to enable the transcription of the target genes (Palmieri et al., 2017; Settembre et al., 2012). Nuclear translocation of TFEB can also occur via its dephosphorylation by the phosphatase calcineurin, which is activated during the release of lysosomal Ca^{2+} through the Ca^{2+} channel mucolipin 1 (MCOLN1) (Medina et al., 2015). Another key regulator of autophagy is AMPK (AMP-activated protein kinase), which is activated during energy-deprived conditions (Meley et al., 2006). Activated AMPK can indirectly stimulate autophagy by suppressing mTORC1 activity via phosphorylation of RAPTOR (regulatory-associated protein of mTOR) and TSC2 (tuberous sclerosis complex 2) (Gwinn et al., 2008; Inoki et al., 2003). However, AMPK can directly induce autophagy independently of mTORC1 via binding to and phosphorylating ULK1 (Kim et al., 2011; Egan et al., 2010) (Figure 1.2). Furthermore, AMPK can phosphorylate Beclin 1 in PI3KC3eC1 that can be augmented by ATG14 to induce autophagy (Kim et al., 2013).

Apart from the regulation of autophagy by mTORC1 and AMPK, a number of mTORC1- independent autophagy pathways have also been described (Sarkar, 2013) (Figure 1.2). Most of these pathways involve second messenger molecules that negatively influence autophagy when their intracellular levels rise. These include IP_3 (inositol 1,4,5-trisphosphate) (Sarkar et al., 2005), Ca^{2+} (Williams et al., 2008; Ganleyet al., 2011), cAMP (3',5'-cyclic adenosine monophosphate) (Williams et al., 2008), and NO (nitric oxide) (Sarkar et al., 2011). While high levels of IP_3, cAMP, and NO suppress autophagosome biogenesis, Ca^{2+} has complex effects on autophagy that are not fully understood. For example, increased cytosolic Ca^{2+} via influx from

extracellular space through L-type Ca^{2+} channels inhibits autophagosome formation by activating the calpains (Ca^{2+}-dependent cysteine proteases), whereas efflux of stored ER Ca^{2+} via IP_3 receptors (IP_3R) blocks autophagosome maturation (Williams et al., 2008, Ganley et al., 2011). Some of these pathways are interconnected and form a cyclic loop, wherein high cAMP levels could increase IP_3 production via the cAMP sensor EPAC (exchange protein directly activated by cAMP), the small G-protein RAP2B and PLCε (phospholipase Cε), and subsequently IP_3 influences ER Ca^{2+} release through the IP_3R to elevate cytosolic Ca^{2+} (which also increases via L-type Ca^{2+} channels) that activates the calpains; which, in turn, could increase cAMP levels by cleaving and activating $G_{s\alpha}$ proteins (Williams et al., 2008). Both mTORC1 and mTORC1-independent pathways can be targeted by small molecules for modulating autophagy.

1.4. Chemical modulators of autophagy

Chemical modulation of autophagy can be achieved via directly inhibiting mTORC1 or by targeting the mTORC1-independent pathways (Sarkar, 2013; Rubinsztein at al., 2012) (Figure 1.2). Some of the mTOR inhibitors inducing autophagy include rapamycin (Blommaart et al., 1995) and its analogs (rapalogs) temsirolimus (CCI-779) (Ravikumar et al., 2004) and everolimus (RAD-001) (Kim et al., 2006), and Torin 1 (Thoreen et al., 2009). There are a number of mTOR-independent autophagy inducers acting via distinct mechanisms, which include lithium, carbamazepine, and valproic acid (Sarkar et al., 2005) (lowering intracellular inositol and IP_3 levels), trehalose (Sarkar et al., 2006; DeBosch et al., 2016) and metformin (Buzzai et al., 2007) (AMPK activation), verapamil (Williams et al., 2008), and felodipine (Siddiqi et al., 2019) (reduction in cytosolic Ca^{2+} levels), rilmenidine (Williams et al., 2008), (decrease in cAMP levels), L-NAME (Sarkar et al., 2011) (inhibition of NO production), and SMER28 (Sarkar et al., 2007) (mechanism not clear), amongst many others. Additional means of inducing autophagy include the natural compounds or nutritional supplements, such as resveratrol (Morselli et al., 2010; Park et al., 2016) (activation of sirtuin 1 and inhibition of mTOR), spermidine (Madeo et al., 2010) (increase in ATG gene expression), and vitamin D3 (Wang et al., 2008; Yuk et al., 2009) (increase in Beclin 1 and ATG gene expression), or via the autophagy-inducing peptide Tat-Beclin 1 (Shoji-Kawata et al., 2013), or via BH3 mimetics like ABT737 (Malik et al., 2011)

(disruption of Beclin 1–Bcl-2 interaction). The pharmacological modulation of autophagy has attracted significant biomedical interests for the treatment of myriad human diseases, including neurodegenerative disorders (Levine et al., 2015). For clinical applications, mTOR-independent autophagy inducers are considered to be safer with lesser side effects as compared to the mTOR inhibitors (Sarkar, 2013; Rubinsztein et al., 2012). This is because mTOR governs critical cellular processes like cell growth and protein synthesis (Saxton and Sabatini, 2017), and thus, inhibiting mTOR for inducing autophagy may not be ideal for long-term drug administration.

1.5. Methods for monitoring autophagy

To monitor autophagy, several methods have been developed that have evolved over time (Seranova et al., 2019; Panda et al., 2019). The commonly used methods for chemical and genetic screening approaches are based on the autophagy marker such as LC3, and the autophagy substrates like p62 (Figure 1.3). Some of these methods are described below.

1.5.1. Monitoring autophagy using LC3 based reporters

LC3 is the most commonly used autophagy marker (Klionsky et al., 2016; Yoshii and Mizushima, 2017). The phosphatidylethanolamine-conjugated LC3-II form associates specifically with the membrane of autophagosomes throughout their lifespan (Kabeya et al., 2000; Kabeya et al., 2004) (Figure 1.3). GFP-tagged LC3 (GFP-LC3) reporter is the most straightforward assay platform to determine perturbations in autophagic compartments by assessing GFP^+ puncta by fluorescence microscopy (Kabeya et al., 2000). Using this reporter, an autophagy inhibitor (which inhibits autophagosome formation) will decrease GFP^+ puncta, whereas both autophagy inducer (which induces autophagosome formation and subsequently autolysosome formation) and autophagy blocker (which prevents autophagosome maturation) will increase GFP^+ puncta (Figure 1.4a). However, this method will not allow distinguishing between an autophagy inducer and an autophagy blocker, because both the scenarios will increase autophagosome numbers and consequently the GFP^+ puncta. Nonetheless, GFP-LC3 reporter has been predominantly used in primary genetic or chemical screens because its readout is easy to measure, and the screen hits can be then subjected to secondary autophagy assays for further characterisation (Seranova et al., 2019).

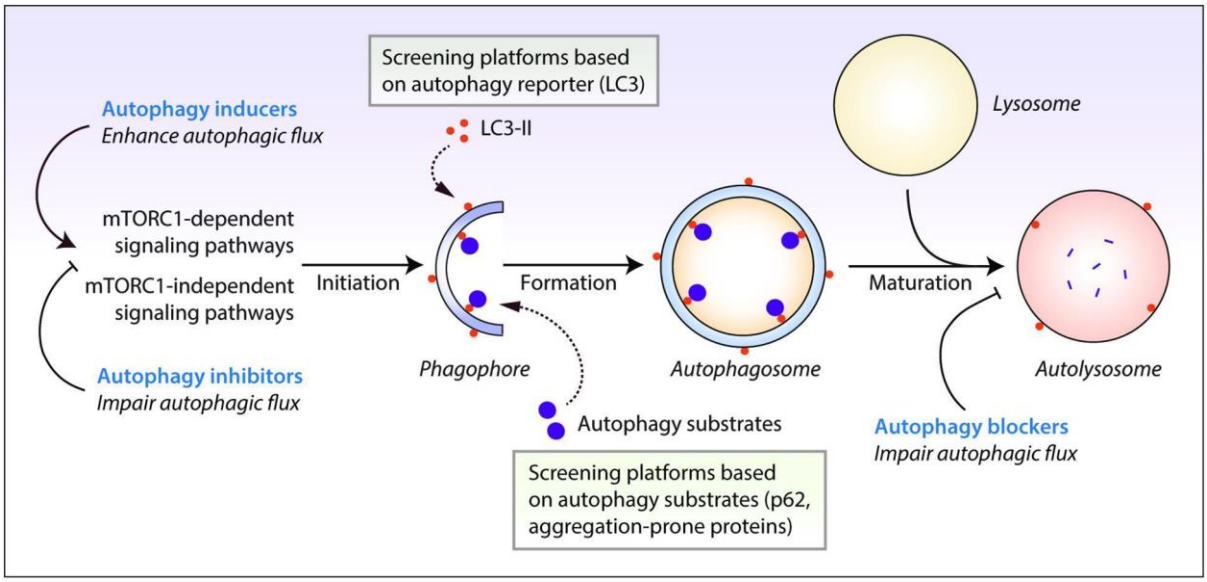


Figure 1.3. Autophagy reporter and substrate based assay platforms and the impact of autophagy modulators at different stages of the autophagy process.

Autophagy is regulated by the mechanistic target of rapamycin complex 1 (mTORC1) or mTORC1-independent pathways. This process initiates by the formation of phagophores that expand and engulf autophagy substrates to form autophagosomes, which then fuse with the lysosomes to form autolysosomes where the autophagic cargo is degraded. Autophagy inducers and inhibitors increase or decrease autophagosome formation, respectively, at the early stages of autophagy, whereas autophagy blockers prevent lysosomal degradation and/or autophagosome maturation at late stages of autophagy. Autophagic flux is thus enhanced by autophagy inducers but is retarded by autophagy inhibitors and blockers. Chemical screening methods for identifying autophagy modulators are commonly based on the readouts of perturbations in autophagy reporters such as LC3-II, or autophagy substrate clearance such as aggregation-prone proteins or p62/SQSTM1.

Figure reference: Panda P.K. et al. with Seranova E. Frontiers in Cell and Developmental Biology 7: 38 (2019).

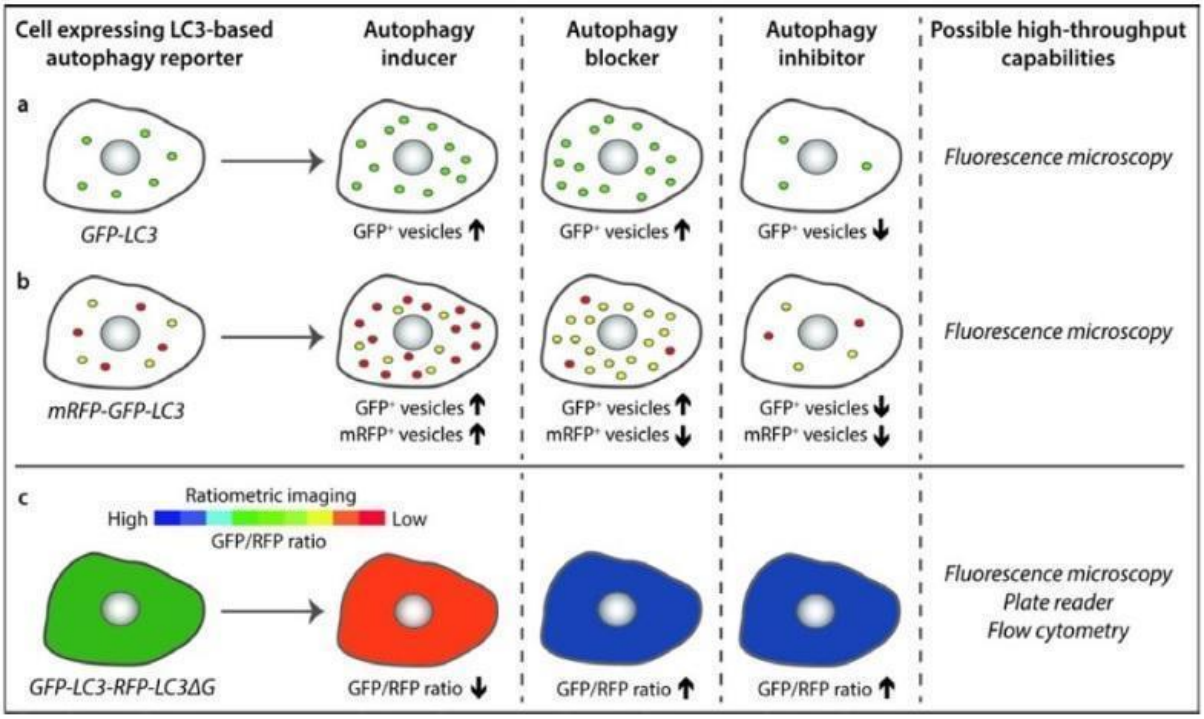


Figure 1.4. LC3 reporter-based in vitro screening platforms. Fluorescent-tagged LC3 reporters as indicated can be utilised as a screening platform to assess the effects of autophagy modulators on the perturbations in autophagosome number (using GFP-LC3 and mRFP-GFP-LC3) (**a**), autophagosome maturation (using mRFP-GFP-LC3) (**b**), or autophagosome/autophagic flux (using GFP-LC3-RFP-LC3ΔG) (**c**). Possible high throughput screening applications are indicated for each of the reporters. For GFP-LC3 reporter (**a**), an autophagy inducer will increase GFP^+ vesicles (by stimulating autophagosome formation), and an autophagy blocker will also increase GFP^+ vesicles (by preventing autophagosome maturation or lysosomal hydrolytic function), whereas an autophagy inhibitor will decrease GFP^+ vesicles (by inhibiting autophagosome formation). For mRFP-GFP-LC3 reporter (**b**) (where $mRFP^+/GFP^+$ vesicles are autophagosomes and $mRFP^+/GFP^-$ vesicles are autolysosomes), an autophagy inducer will increase $mRFP^+/GFP^+$ and $mRFP^+/GFP^-$ vesicles, and an autophagy blocker will increase $mRFP^+/GFP^+$ but decrease $mRFP^+/GFP^-$ vesicles, whereas an autophagy inhibitor will decrease $mRFP^+/GFP^+$ and $mRFP^+/GFP^-$ vesicles. For GFP-LC3-RFP-LC3ΔG reporter (**c**) (where GFP-LC3 undergoes degradation or recycling but RFP-LC3 remains in the cytosol as an internal control), an autophagy inducer will decrease GFP/RFP ratio (by enhancing autophagic flux), whereas an autophagy blocker or inhibitor will increase GFP/RFP ratio (by retarding autophagic flux).

Figure reference: Seranova E. et al. Methods in Molecular Biology 1880: 389-428 (2019).

A more specific readout for determining changes in autophagosome formation versus maturation is the tandem fluorescent tagged LC3 (mRFP-GFP-LC3) reporter. This reporter is pH-sensitive and can quantify the number of autophagosomes and autolysosomes by fluorescence microscopy: the autophagosomes emit both $mRFP^+$ and GFP^+ signals ($mRFP^+/GFP^+$), whereas the acidic autolysosomes emit only the acid-stable $mRFP^+$ signal ($mRFP^+/GFP^-$) because the GFP signal is acid-sensitive and gets quenched (Kimura, Noda and Yoshimori, 2007). Using this reporter, an autophagy inhibitor will decrease both autophagosomes and autolysosomes; an autophagy inducer will increase autolysosomes but may or may not increase autophagosomes depending on the speed of autophagosome flux at the time point assessed; whereas an autophagy blocker will increase autophagosomes but decrease autolysosomes (Kimura et al., 2007; Sarkar et al., 2009) (Figure 1.4b). Image-based chemical screens have also been undertaken in mammalian cells by employing the mRFP-GFP-LC3 reporter (Kuo et al., 2015; Chauhan et al., 2015; Pampaloni et al., 2017). Both the LC3-based reporters described above can be assessed manually by fluorescence microscopy and analysis software, as well as by automated high-throughput analysis. There are several variations of the tandem fluorescent-tagged LC3 reporter. For example, in the mRFP-GFP-LC3 construct, mRFP could be replaced by mCherry owing to its superior photostability over mRFP (Pankiv et al., 2007; N'Diaye et al., 2009; Shaner et al., 2005) Likewise, GFP can be substituted by mWasabi, which is a monomeric green fluorescent protein that is more acid sensitive than GFP, and, therefore, might provide more accurate measurement of autophagosome flux by precisely distinguishing autophagosome and autolysosome compartments (Zhou et al., 2012).

Although the GFP-LC3 and the mRFP-GFP-LC3 reporters can be used for low-, medium-, or high-throughput screens, the readouts can only be quantified by fluorescence image-based analysis. Recently, a new autophagic flux probe, GFP-LC3-RFP-LC3ΔG, has been designed that can have versatile high-throughput applications where the readouts can be quantified by various methodologies (Kaizuka et al., 2016). This construct has GFP-LC3 and RFP-LC3ΔG fused in tandem that can be cleaved by endogenous ATG4 family proteases into equimolar amounts. During autophagy, GFP-LC3 on the inner or outer autophagosomal membrane undergoes degradation or recycling, respectively, after fusion with the lysosomes. However, RFP-LC3ΔG has a

deletion in the C-terminal glycine and cannot be lipidated; therefore, it remains in the cytosol and serves as an internal control (Kaizuka et al., 2016). Thus, the readout of GFP/RFP ratio inversely correlates with the extent of autophagic flux. Using this reporter, an autophagy inhibitor or blocker will reduce autophagic flux and increase the GFP/RFP ratio, whereas an autophagy inducer will increase autophagic flux and reduce the GFP/RFP ratio (Figure 1.4c). These perturbations can be quantified by microplate reader, flow cytometry or ratiometric imaging with fluorescence microscopy.

1.5.2. Monitoring autophagy by substrate clearance

As an alternative to the LC3-based reporters, assay platforms pertaining to autophagic substrate degradation can also be used to monitor autophagy. In these methods, the clearance of specific autophagy substrate p62/SQSTM1 or neurodegeneration-associated aggregation-prone proteins, such as mutant huntingtin or α-synuclein, is measured as a readout (Sarkar et al., 2009; Ravikumar et al., 2008; Seranova et al., 2019; Panda et al., 2019). This assay depicts autophagic substrate flux and is informative of the overall autophagic flux. In p62-based assays, the levels of p62 inversely correlate with the extent of autophagic flux; for example, high flux reduces p62 whereas low flux accumulates p62. Chemical and genetic screens have been undertaken in mammalian cells using the p62/SQSTM1-based reporter platforms (Pietrocola et al., 2014; Hale et al., 2016; DeJesus et al., 2016; Strohecker et al., 2015; Tsuganezawa et al., 2013). However, it is possible that certain known autophagy modulators can influence the mRNA levels of p62 by affecting transcription (thereby complicating the readout at the protein level), and this effect can depend on the dose, time-point and the cell-type used (Klionsky et al., 2016). This could potentially complicate the autophagy analysis when p62 protein levels are measured as a readout. Therefore, it is important to assess the autophagy-specific degradation of p62 in the cell-type to be used, as well as characterising the positive and negative controls of the assay (with known autophagy inducers and inhibitors/blockers, respectively) that only affect p62 levels by regulating its autophagic degradation. The inducible p62 reporter constructs that have been established constitute attractive screening platforms for assessing autophagy modulators via flow cytometry, microplate reader or immunoblotting. These include the inducible GFP-p62 and p62-fLuc (Firefly luciferase) constructs (Larsen et al., 2010; Brown et al., 2016), and can overcome the issue related to readout complications at the protein level.

1.6. Autophagy receptors for mediating selective autophagy

The autophagic response to starvation is the bulk degradation of cytosolic materials that occurs in a nonselective manner. However, other types of cellular stresses, such as damaged organelles, aggregated proteins, or pathogens, require their selective sequestration into the autophagosomes for degradation. Based on the remarkable substrate specificity, selective autophagy is classified into aggrephagy (clearance of protein aggregates), mitophagy (clearance of mitochondria), pexophagy (clearance of peroxisomes), ribophagy (clearance of ribosomes), nucleophagy (clearance of nuclear envelope), reticulophagy (clearance of ER), lysophagy (clearance of lysosomes), xenophagy (clearance of pathogens), lipophagy (clearance of lipid droplets), and glycophagy (clearance of glycogen) (Gatica et al., 2018; Stolz et al., 2014). Selectivity in autophagy is conferred by the cargo receptor proteins, which tether the ubiquitinated cargo to the phagophore (Figure 1.1). All cargo receptors share common domains: the ubiquitin-binding domain (UBD) through which they bind the specific cargo (Kirkin et al., 2009), and the LC3-interaction region (LIR) motif via which the interaction with the expanding phagophore occurs (Johansen and Lamark, 2020). In mammalian cells, several cargo receptor proteins are recognised, which include p62 (sequestosome-1 or SQSTM1) (Pankiv et al., 2007), OPTN (optineurin) (Korac et al., 2012), NDP52 (nuclear dot protein of 52 kDa) (Thurston et al., 2009), TAX1BP1 (tax1 binding protein 1) (Tumbarello et al., 2015), NBR1 (neighbor of BRCA1 gene 1) (Kirkin et al., 2009), and TOLLIP (Toll Interacting protein) (Lu et al., 2014). These receptors could be recruited to different cargos in varying proportions and/or may also cooperate in substrate selection. For instance, p62/SQSTM1, NBR1, optineurin, and TOLLIP play a role in executing aggrephagy (Gatica et al., 2018).

Several studies have revealed an intrinsic connection between autophagy receptors and neurodegenerative diseases. Some of these findings reported that mutations in SQSTM1 could modify the genetic susceptibility to Alzheimer's disease (Cuyvers et al., 2015), frontotemporal dementia (van der Zee et al., 2014), and amyotrophic lateral sclerosis (Teyssou et al., 2013). Apart from ubiquitin-dependent selective autophagy, there is an arsenal of receptor proteins, which perform the process independent of ubiquitination (Khaminets et al., 2016). The most remarkable example is NIX, also known as BNIP3L1 (Bcl-2-interacting protein 3 like), which is a selective autophagy cargo receptor for mitophagy in reticulocytes during the final stage of erythroid

maturation (Sandoval et al., 2008). Others include FUNDC1 (FUN14 domain containing 1) (Liu et al., 2012), SMURF1 (SMAD-specific E3 ubiquitin-protein ligase 1) (Franco et al., 2017), TRIM5a (tripartite motif-containing protein 5a) (Mandell et al., 2014) and STBD1 (starch-binding domain-containing protein 1) (Jiang et al., 2011). Besides the cargo receptors, there are several key players like ALFY (autophagy-linked FYVE protein, also known as WDFY3), which does not harbor the UBD domain but acts as a scaffold by getting associated with the ubiquitinated protein aggregates and autophagosomal markers to facilitate aggrephagy (Filimonenko et al., 2010).

A role of selective autophagy is emerging in infectious diseases wherein the pathogens could affect both the house-keeping (homeostatic arm) and pathogen degradation (xenophagy arm) functions of the autophagy in the host cells (Sharma et al., 2018). For instance, when the DNA of *Mycobacterium tuberculosis (Mtb;* associated with tuberculosis) is released into the cytosol of the host cell, the foreign DNA is recognised by the STING (Stimulator of IFN genes)-dependent cytosolic sensing pathway that contributes to the ubiquitination of bacteria. This enables the subsequent delivery of the bacteria via the selective autophagic receptors p62 and NDP52 for autophagic degradation; a process termed xenophagy (Watson et al., 2015). However, the non-conventional ESAT6-secretion system (ESX1) of *Mtb* is known to play a role in mycobacterial virulence, in which the ESX1 machinery and its effectors like ESAT-6 selectively block xenophagy by disrupting pathogen-containing autophagosome maturation while keeping the overall autophagic flux intact in the host cell. This ensures not only the survival of the host cells but also the intracellular proliferation of *Mtb* (Chandra et al., 2015).

1.7. Role of autophagy in tissue and energy homeostasis

Multiple genetic studies in mouse models have demonstrated that autophagy plays a vital role in maintaining tissue and energy homeostasis (Mariño et al., 2011). A role of autophagy in energy homeostasis is elegantly shown in a study with autophagy-deficient mouse model, wherein the pups were unable to survive past the first day post-partum without food. This is because during this period, autophagy in tissues is upregulated and serves as a nutrient provider (Kuma et al., 2004). Likewise, a role of autophagy in tissue homeostasis is shown in mice with tissue specific autophagy knockout in the brain, which led to neurodegenerative phenotype with accumulation

of cytosolic inclusions, ubiquitinated protein aggregates, motor deficits, behavioral deficits and neuronal loss (Hara et al., 2006; Komatsu et al., 2006). Moreover, targeted abrogation of autophagy in the muscle and liver of normal mice also caused degeneration of the affected organs (Masiero et al., 2009; Komatsu et al., 2010). Furthermore, in multiple genetic models of autophagy deficiency including mice with knockout of *Atg5, Atg7, Ambra1* and *Atg6/Beclin-1*, increase in protein aggregates and apoptosis along with abnormal development and premature death have been documented (Mariño et al., 2007, Kuma et al., 2004, Hara et al., 2006, Nakai et al., 2007, Pua et al., 2006, Qu et al., 2007, Qu et al., 2003, Komatsu et al., 2005, Komatsu et al., 2006, Takahashi et al., 2007, Maria Fimia et al., 2007, Komatsu et al., 2005). Apart from the knockout of genes responsible for autophagy initiation contributing to this abnormal phenotype, the ablation of genes responsible for the lysosomal function also showed similar results. Mice deficient of *Lamp2, Cn3,* and *CtsB, CtsD* and *CtsL* also presented a neurodegenerative phenotype and increased cell death (Tanaka et al., 2000; Cao et al., 2006; Koike et al., 2005; Shacka et al., 2007; Felbor et al., 2002; Koike et al., 2005).

Overall, this robust genetic evidence points towards the fact that autophagy impairment potentially contributes to cytotoxicity; although the exact mechanism is poorly elucidated. One possible explanation might be the accumulation of autophagic substrates such as aggregate proteins or defective organelles. There has been evidence towards accumulation of reactive oxygen species (ROS) when damaged mitochondria are not recycled, which leads to cytotoxicity (Jin, 2006). Moreover, since autophagy is a catabolic process that contributes to the digestion and recycling of cytoplasmic components during starvation, its dysfunction might also result in impairments related to cellular metabolism (Lahiri et al., 2019). As such, autophagy is playing a crucial role in maintaining cellular bioenergetics (Lum et al., 2005), and thus, insufficient autophagy could affect cellular metabolism and energy homeostasis.

1.8. Role of autophagy in human diseases

Autophagy has been proven to be an indispensable mechanism involved in cellular survival and tissue homeostasis. This process contributes to the clearance of damaged organelles, aggregation-prone proteins and pathogens, amongst other autophagic cargo. However, malfunction of this process causes accumulation of

undesirable intracellular materials, and this perturbs cellular homeostasis and leads to cytotoxicity. Dysfunctional autophagy has been reported in a myriad of human diseases such as neurodegenerative disorders, cancer, myopathies, liver diseases, infectious and inflammatory diseases, and lysosomal and lipid storage disorders, to name a few (Figure 1.5) (Mizushima et al., 2008). Some of these diseases fall under the category of macromolecule storage disorders due to accumulation of proteins, carbohydrates and lipids, which could occur because of impairment in autophagy since this process is one of the primary clearance routes of these macromolecules (Palhegyi et al., 2019). Therefore, the therapeutic exploitation of autophagy and development of pharmacological inducers of autophagy are of great biomedical relevance. Particularly in the context of this thesis, the role of autophagy in neurodegenerative disorders and infectious diseases is described below.

1.8.1. Role of autophagy in neurodegenerative disorders

Multiple lines of evidence over the past decade have demonstrated that defective autophagy is a major contributing factor to the pathology of neurodegenerative disorders (Menzies et al., 2017; Nixon, 2013). Autophagy is crucial for ensuring cellular homeostasis in post-mitotic neurons (Stavoe and Holzbaur, 2019), and improper functioning of this process leads to neurodegeneration. This is evident from genetic studies in mice where brain-specific deletion of essential autophagy genes, such *Atg5* or *Atg7* to abrogate autophagy, resulted in a neurodegenerative phenotype (Hara et al., 2006; Komatsu et al., 2006). Indeed, autophagy dysfunction has been reported in almost all the neurodegenerative disorders investigated, such as, but not limited to, Alzheimer's disease (AD), Parkinson's disease (PD), Huntington's disease (HD) and amyotrophic lateral sclerosis (ALS) (Menzies et al., 2017, Sarkar, 2013, Seranova et al., 2020), as well as in certain neurodegenerative lysosomal storage disorders such as neuronal ceroid lipofuscinosis (NCL), Gaucher disease (GD) and Niemann-Pick type C1 (NPC1) disease (Seranova et al., 2017; Seranova et al., 2020). Since the selective autophagy process of aggrephagy is the main disposal route for a number of aggregation-prone proteins associated with neurodegeneration, impairment of autophagy in these contexts causes accumulation of these toxic species that affect neuronal viability (Rubinsztein, 2006; Nixon, 2013).

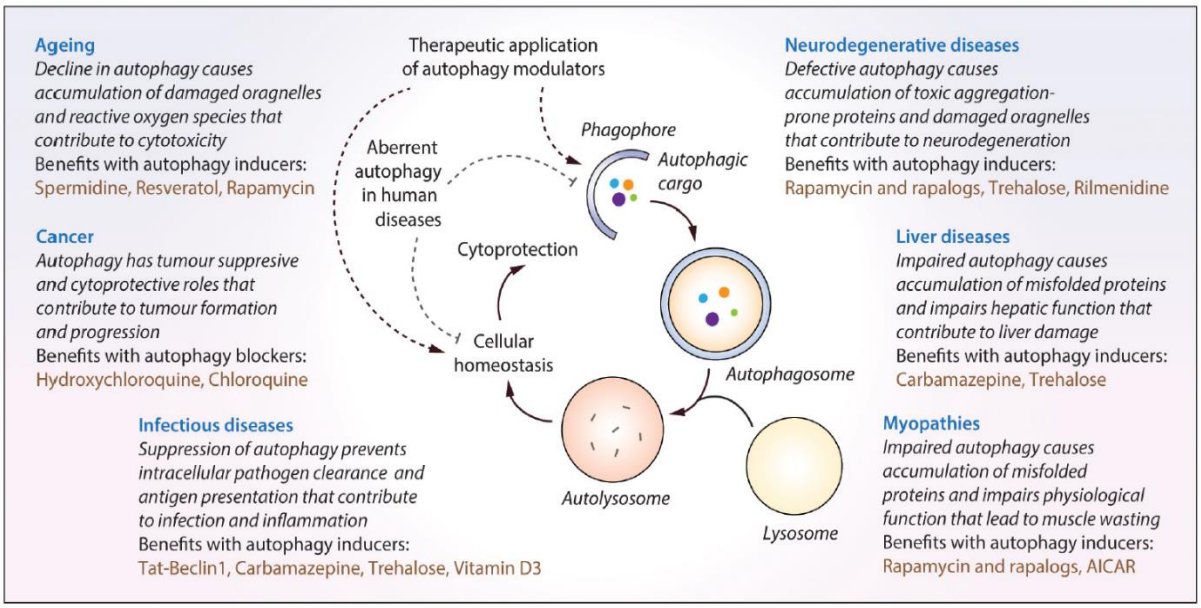


Figure 1.5. The impact of malfunctioning autophagy and the therapeutic benefits of autophagy modulators in diverse human diseases.

Autophagy is implicated in diverse human diseases due to its vital role in maintaining cellular homeostasis. Defective or aberrant autophagy contributes to the cytotoxicity underlying many pathological conditions whereas pharmacological upregulation of autophagy is beneficial in various transgenic models. Key autophagy modulators exerting therapeutic benefits in neurodegenerative disorders, cancer, infectious diseases, liver diseases, myopathies and lifespan extension, as well as the impact of malfunctioning autophagy in these contexts, are highlighted.

Figure reference: Panda P.K. et al including Seranova E. Frontiers in Cell and Developmental Biology 7: 38 (2019).

Autophagy has attracted significant attention for patient-derived hiPSC (human induced pluripotent stem cell)-based studies of neurodegenerative disorders. Since impairment of this vital homeostatic process contributes to neurodegeneration, defective autophagy is being utilised in recent years as a phenotypic readout in hiPSC-derived neurons (Jiménez-Moreno et al., 2017; Jungverdorben et al., 2017). This provides an appropriate disease-affected human cellular platform for investigating the mechanisms of autophagy dysfunction and the drug discovery of autophagy modulators for clinical translation to patients. Dysfunctional autophagy has been reported in several hiPSC models of neurodegenerative diseases; however, the nature of the autophagic defects is sometimes different between non-hiPSC (such as immortalised cell lines and mouse models) and hiPSC-based experimental systems (Figure 1.6) (reviewed extensively in Seranova et al., 2020). The use of patient-derived hiPSC models to generate disease-affected cell-types, such as neurons, may provide insights into the disease mechanisms in a manner relevant to human biology. These cellular platforms are also particularly important to evaluate the therapeutic potential of autophagy inducers that could be applicable to the patients.

Protein aggregates caused by aggregation-prone proteins such as mutant hungtingtin associated with Huntington's disease or tau in Alzheimer's disease are hallmarks of neurodegeneration, and levels of these proteins correlate with neurotoxicity (Krainc, 2010). Of biomedical relevance, chemical or genetic induction of autophagy could enhance the clearance of neurodegeneration-associated mutant proteins and ameliorate the disease phenotypes in transgenic animal models of various neurodegenerative disorders (Menzies et al., 2017; Sarkar, 2013; Rubinsztein et al., 2012; Levine et al., 2015; Sarkar et al., 2008). Several mTOR inhibitors have demonstrated their beneficial effects in neurodegenerative models *in vivo*. These include rapamycin and its analogs CCI-779 in fly and mouse models of AD, PD, HD, spinocerebellar ataxia type 3 (SCA3), prion disease and frontotemporal dementia (FTD) (Ravikumar et al., 2004; Berger et al., 2005; Sarkar et al., 2007; Menzies et al., 2009; Spilman et al., 2010; Cortes et al., 2012; Wang et al., 2012; Ozcelik et al., 2013; Jiang et al., 2014). Furthermore, mTOR-independent autophagy inducers including carbamazepine and lithium (inositol lowering agents), rilmenidine (cAMP reducing agent), trehalose (AMPK activator), SMER28 and BRD5631 (mechanisms not known) have demonstrated their neuroprotective properties in a plethora of *in vivo* models

such as mouse, zebrafish and *Drosophila*, but also in *in vitro* hiPSC models of AD, HD, FTD, ALS and NPC1 disease (Sarkar et al., 2005; Sarkar et al., 2006; Sarkar et al., 2007; Fornai et al., 2008; Williams et al., 2008; Rose et al., 2010; Zhang et al., 2011; Zhang et al., 2018; Shimada et al., 2012; Wang et al., 2012; Li et al., 2013; Maetzel, Sarkar et al., 2014; Kuo et al., 2015). These observations have led to the potential therapeutic possibilities for autophagy modulation in the contexts of several neurodegenerative and certain lysosomal storage disorders. However, it is worth noting that the therapeutic benefits of autophagy induction predominantly relies on the lysosomal degradative capability being functional. The role of autophagy in Niemann-Pick type C1 (NPC1) disease is described below in further details, because NPC1 hiPSC models were used in this study.

1.8.1.1. Role of autophagy in Niemann-Pick type C disease

Niemann-Pick type C (NPC) disease is a rare, autosomal recessive LSD characterised by neurodegeneration and hepatosplenomegaly (Vanier, 2013), and is associated with mutations predominantly in the *NPC1* gene (~95%) causing NPC1 disease (Loftus, 1997) or in the *NPC2* gene (~5%) causing NPC2 disease (Naureckiene, 2000, Patterson et al., 2012, Vanier, 2010). These genes encode NPC1 and NPC2 proteins, which respectively are lysosomal cholesterol transporter and lysosomal glycoprotein that play a role in the transport of cholesterol from late endosomes and lysosomes (Pallottini and Pfrieger, 2020). Mutations in these genes lead to abnormal accumulation of unesterified cholesterol and other lipids like sphingolipids in the brain, liver and spleen (Karten, Peake and Vance, 2009; Kwon et al., 2009). As in other LSDs (Seranova et al., 2017), autophagic flux is retarded due to defective autophagosome maturation as shown in mutant mouse and human cellular models of NPC1 and NPC2 disease (Figure 1.6), which are also associated with defective mitophagy and mitochondrial function (Sarkar et al., 2013; Lee et al., 2014; Guo et al., 2016; Ordonez et al., 2012). Multiple mechanisms shown for dysregulated autophagy in NPC1 disease include: disruption of SNARE complex formation between autophagosomes and late endosomal/lysosomal compartments involving Syntaxin-17 and VAMP8 to prevent autophagosome maturation (Sarkar et al., 2013); accumulation of sphingosine arising from diminished activity of sphingosine kinase and decreased levels of vascular endothelial growth factor (VEGF) to prevent autophagosome–lysosome fusion (Lee et al., 2014); and reduction in lysosomal Ca^{2+} stores (Lloyd-Evans et al., 2008). Despite

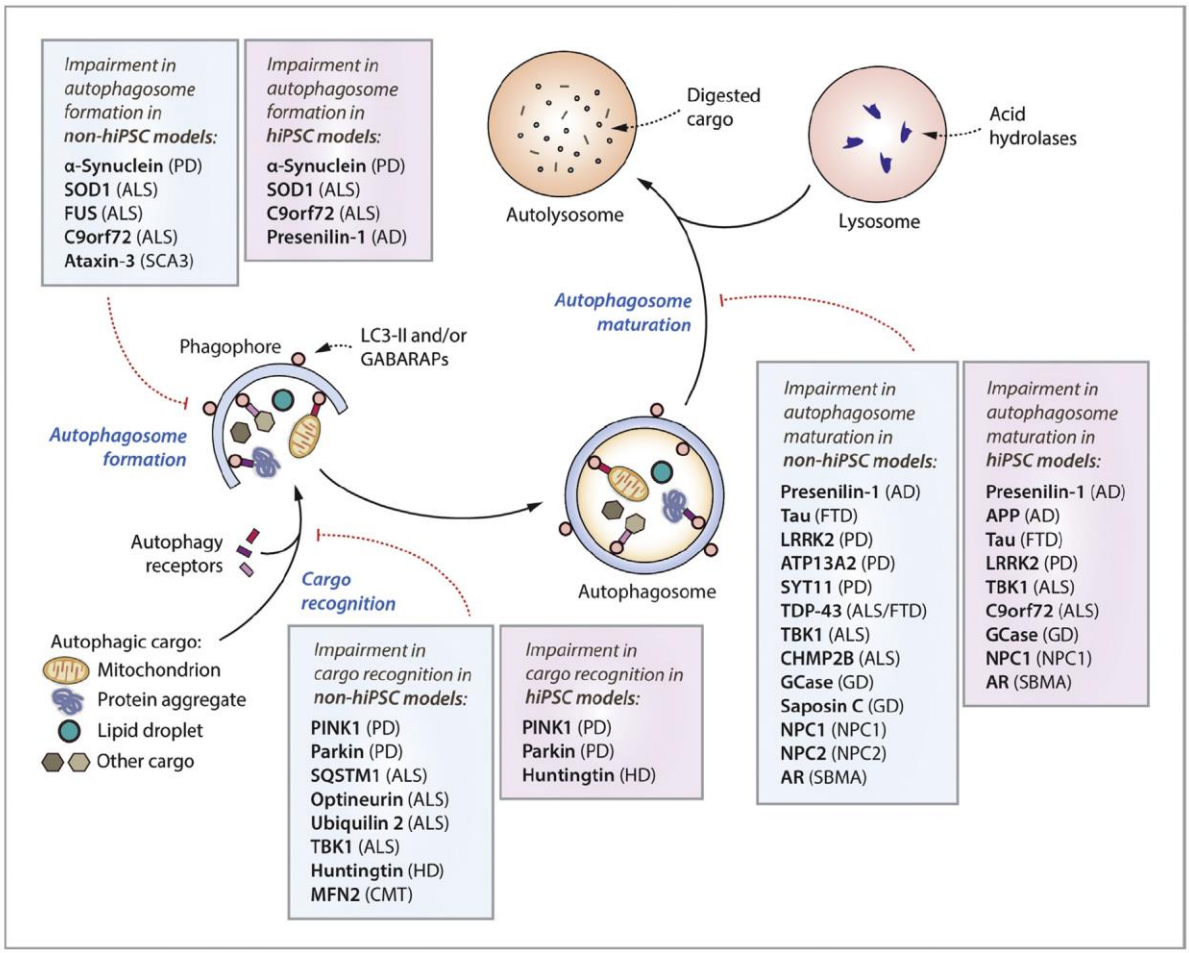


Figure 1.6. Impairment of autophagy in neurodegenerative disorders.

Impairment of autophagy at distinct stages of the process, such as at the level of autophagosome formation, cargo recognition, or autophagosome maturation, has been described in multiple neurodegenerative diseases. The impact on autophagy due to mutations or loss of disease associated proteins in non-hiPSC and hiPSC models is indicated (by red arrows). In addition, the point mutants of a synuclein and LRRK2 associated with PD also impair chaperone-mediated autophagy (not shown). Abbreviations: AD: Alzheimer's disease; ALS: Amyotrophic lateral sclerosis; APP: Amyloid-b precursor protein; AR: androgen receptor; ATP12A2: ATPase Cation Transporting 13A2; C9orf72: Chromosome 9 Open Reading Frame 72; CHMP2B: charged multivesicular body protein 2B; CMT: Charcot-Marie-Tooth disease; FTD: Frontotemporal dementia; FUS: Fused in sarcoma; GD: Gaucher disease; GCase: Glucocerebrosidase; HD: Huntington's disease; HTT: Huntingtin; LRRK2: Leucine-rich repeat kinase 2; MFN2: Mitofusin 2; NPC1: Niemann-Pick type C1; NPC2: Niemann-Pick type C2; PINK1: PTEN-induced kinase 1; PD: Parkinson's disease; SBMA: Spinal bulbar muscular atrophy; SCA3: Spinocerebellar ataxia 3; SQSTM1: Sequestosome 1; SOD1: superoxide dismutase 1; SYT11: Synaptotagmin 11; TBK1: TANK-binding kinase 1; TDP-43: TAR DNA-binding protein 43.

Figure reference: Seranova E. et al. Journal of Molecular Biology 432(8): 2754-2798 (2020).

a block in the multi-step route of autophagosome maturation, autophagy inducers improved autophagic flux in *Npc1* mutant mouse cells by facilitating direct autophagosome–lysosome fusion (bypass mechanism), which consequently also increased cell survival but did not reduce the cholesterol load (Sarkar et al., 2013).

As in non-hiPSC models, defective autophagic flux due to impaired autophagosome maturation, characterised by accumulation of autophagosomes and autophagy substrates like p62, was found in neurons and hepatic cells differentiated from multiple NPC1 hiPSC lines that also exhibited elevation in cholesterol (Lee et al., 2014; Maetzel, Sarkar et al., 2014; Dai et al., 2017). Genetic correction of a disease-causing *NPC1*$^{(I1061T)}$ mutation rescued the cellular phenotypes of defective autophagy and cholesterol accumulation in these NPC1 hiPSC-derived cells (Maetzel, Sarkar et al., 2014). Autophagic block associated with impaired mitophagy and mitochondrial fragmentation was also found in neurons derived from hESCs with shRNA-mediated NPC1 knockdown (Ordonez et al., 2012). Of therapeutic relevance, stimulating autophagy with rapamycin and various mTOR-independent autophagy inducers, such as carbamazepine, trehalose, verapamil and BRD5631, restored autophagic flux and improved cell viability in NPC1 hiPSC-derived neurons; however, only rapamycin and carbamazepine were effective in NPC1 hiPSC-derived hepatic cells (Maetzel, Sarkar et al., 2014; Kuo et al., 2015). The autophagy inducers were cytoprotective on their own without co-treatment of any cholesterol-lowering agents. In addition, recombinant VEGF treatment imparted similar beneficial effects in NPC1 neurons (Lee et al., 2014). Interestingly, while the cholesterol-lowering agent, 2-hydroxypropyl-β-cyclodextrin (HPβCD), further augmented the autophagic block that could be detrimental (Sarkar et al., 2013; Maetzel, Sarkar et al., 2014; Peake and Vance, 2012), the HPβCD analog called methyl-β-cyclodextrin (MβCD) improved the defective autophagic flux in NPC1 hiPSC-derived neurons (Dai et al., 2017).

In a nutshell, a block in autophagic flux due to impaired autophagosome maturation is a consistent phenotype across various NPC1 disease models including iPSC-derived neurons where autophagy inducers rescued the autophagy defect and improved neuronal survival. However, further studies in *Npc1* mutant mice are necessary to examine the *in vivo* efficacy of autophagy induction and a combination treatment strategy with cholesterol depletion.

1.8.2. Role of autophagy in infectious diseases

Besides the essential role of autophagy in cellular homeostasis linked to the clearance of aggregation-prone proteins and damaged mitochondria, autophagy also contributes to the innate defence mechanism by clearing intracellular pathogens. This selective removal of intracellular pathogens in host cells via autophagy is termed xenophagy (Sharma et al., 2018). The host immune cell-type that is primarily involved in this process is the macrophage. In many infectious diseases, macrophages are heavily involved in the first line of defence against invading pathogens. The first evidence of xenophagy was demonstrated through the studies involving *Mycobacterium tuberculosis (Mtb*), a bacterial pathogen causing tuberculosis (Gutierrez et al., 2004; Singh et al., 2006). Consequently, *Mtb* and other bacterial pathogens including *Salmonella* and *Listeria*, as well as virulent pathogens like HIV and Dengue, have been shown to manipulate autophagy to promote their own growth within the host organism (Jia et al., 2009; Kyei et al., 2009; Yoshikawa et al., 2009; Heaton and Randall, 2010). For instance, the manipulation of host cell autophagy by *Mtb* was important for *Mtb* survival in macrophages, as revealed by a genome-wide siRNA screen that aimed to identify the host factors necessary for *Mtb* survival (Kumar et al., 2010). However, recent studies have elucidated that *Mtb* selectively prevent xenophagy for their intracellular proliferation by disrupting the maturation of *Mtb*-containing autophagosomes while keeping the overall autophagic flux intact to ensure the survival of the host cells (Chandra et al., 2015).

Multiple proof-of-principle studies have shown that induction of autophagy could enhance pathogen clearance to prevent their survival and reduce their intracellular load. For example, rapamycin reduced the viral and bacterial load both *in vitro* and *in vivo* (Gutierrez et al., 2004; Donia et al., 2010). Furthermore, mTOR-independent autophagy inducers like SMER28, vitamin D3 and carbamazepine prevented bacterial survival and HIV replication (Floto et al., 2007; Yuk et al., 2009; Kumar et al., 2010; Campbell and Spector, 2011; Campbell and Spector, 2012; Schiebler et al., 2014). Carbamazepine also demonstrated its ability to reduce bacterial burden, improve lung pathology and stimulate adaptive immunity in mice infected with multidrug-resistant *Mtb* (Schiebler et al., 2014). Other compounds such as nortriptyline, nitazoxanide, flubendazole, Vitamin D, AZD0530 and Tat-Beclin have been shown to reduce the intracellular load of *Mtb,* HIV and other pathogens through activation of autophagy

(Sundaramurthy et al., 2013; Lam et al., 2012; Chauhan et al., 2015; Campbell and Spector, 2012; Chandra et al., 2016; Shoji-Kawata et al., 2013). Interestingly, trehalose, which has been shown to be beneficial in transgenic models of neurodegenerative disorders (Sarkar et al., 2006; Sarkar, 2013), also demonstrated efficiency in the activation of autophagy in human immortalised *Mtb*-infected macrophages that resulted in *Mtb* killing (Sharma et al., 2020). This study also suggested that trehalose was effective in facilitating xenophagy during HIV and *Mtb* co-infection by removing the HIV-mediated block in autophagy flux that resulted in reduction of *Mtb* survival (Sharma et al., 2020).

Despite the therapeutic potential of autophagy in infectious diseases including tuberculosis, this strategy has not been implemented in clinicals trials thus far; primarily due to lack of human-relevant data. As growing evidence points towards selective regulation of basal autophagy and xenophagy in host cells (Chandra et al., 2015; Sharma et al., 2018), it is important to elucidate any cell-specific regulation of these mechanisms by utilising biologically-relevant human cell-types like macrophages. This will have the potential to accelerate drug discovery applicable to patients and optimise existing therapeutic approaches to bacterial and viral infections. Thus far, there are no studies utilising hESC- or hiPSC-derived macrophages for studying xenophagy. A number of differentiation protocols have been established to obtain hiPSC-derived macrophages (Wilgenburg et al., 2013; Lachmann et al., 2015; Muffat et al., 2016; Amos et al., 2017; Takata et al., 2017). Recent studies have demonstrated that hiPSC-derived macrophages could be used as an infectious disease model to study the interaction between host cells and pathogens (Hong et al., 2018; Hale et al., 2015; Härtlova et al., 2018; Ye et al., 2014), and also serve as a drug discovery platform (Han et al., 2019).

1.9. The importance of human pluripotent stem cells (hPSCs) in biological studies

Human pluripotent stem cells (hPSCs) include human embryonic stem cells (hESCs), which are derived from an early human embryo, and human induced pluripotent stem cells (hiPSCs), which are the product of cellular reprogramming of somatic cells such as those obtained from patients. The hPSC-based model systems provide appropriate

experimental platforms for studying basic biology, disease mechanisms and drug discovery in a manner relevant to human biology.

1.9.1. Human pluripotent stem cells for studying basic biology and disease mechanisms

The hPSCs (i.e., hESCs and hiPSCs) are capable of both self-renewal and differentiation into any cell of embryonic origin (Thomson, 1998). Therefore, hPSCs offer an effectively indefinite source of differentiated physiologically-relevant (from hESCs) and disease-relevant (from hiPSCs) cells (Figure 1.7). This is crucial for studying basic biology in a manner relevant to humans, and in modelling human pathologies, as many cell-types are near impossible to isolate and culture, both technically and ethically, and have a limited proliferative capacity. Furthermore, readily available human cells avoid discrepancies due to evolutionary divergence between humans and animal models. Still, the utility of hPSCs in this context hinges on the refinement of reliable differentiation protocols into relevant cell identities. It might be for this reason that neurological and neurodegenerative diseases are at the forefront of disease modelling using hPSCs, as protocols for neuronal differentiation from hPSCs are relatively advanced (Shi et al., 2012, Seranova et al., 2020). Besides these, other types of cells for which differentiation protocols have been developed include cardiomyocytes (He et al., 2003), pancreatic beta cells (Assady et al., 2001), macrophages (Wilgenburg et al., 2013), hematopoietic cells (Kaufman et al., 2001), renal cells (Xia et al., 2013; Takasato et al., 2015) intestinal cells (Spence et al., 2010; McCracken et al., 2011), cells of the lung (McCauley et al., 2017; Jacob et al., 2017), and others. It is generally believed that hiPSCs hold similar potential to hESCs in their capacity to differentiate into various cell-types (Kim et al., 2010).

The hPSCs can also be subjected to genome engineering, such as with zinc finger nucleases (ZFNs), transcription activator-like effector nucleases (TALENs) or CRISPR (clustered regularly interspaced short palindromic repeats)/Cas9 systems (Chen and Knoepfler, 2016; Li et al., 2020; Geng et al., 2020; Vasileva et al., 2015). For instance, gene knockout or overexpression of reporter genes from the *AAVS1* (adeno-associated virus integration site 1) locus can be done in hESCs, and correction of disease-specific mutations to create isogenic controls can be done in patient-derived hiPSCs. The differentiation of hESCs and hiPSCs enables the establishment of

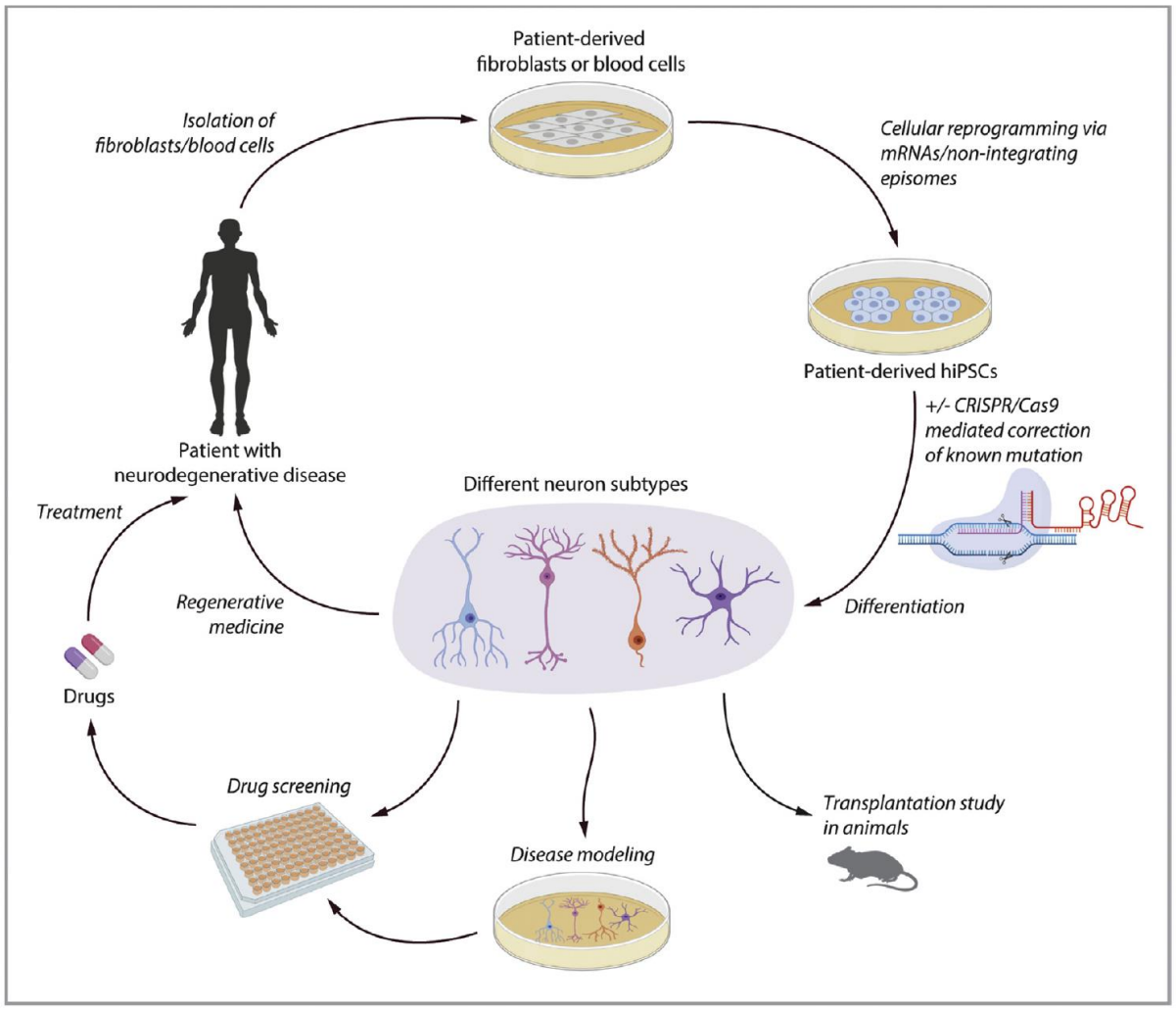


Figure 1.7. Cellular reprogramming for hiPSC generation and possible applications for hiPSC-based disease modelling and drug discovery.

A disease-affected patient serves as a source of easily obtained somatic cells which can subsequently be reprogrammed into human induced pluripotent stem cells (hiPSCs). Genetic editing technology such as CRISPR/Cas9 can be used to generate isogenic controls. hiPSCs are then differentiated into disease relevant cell-types, such as neurons for the modelling of neurodegenerative diseases. Thus, disease modelling may be performed on a platform with a genetic load which is identical to disease-bearing individuals. Such cells may be grown in two- or three-dimensional modelling conditions, engrafted into animals and subjected to high-throughput screening for drug discovery. Ultimately, new therapeutic agents may be discovered, and a personalised therapy plan may be used to benefit the individual patient. Derived cells may also be used for autologous transplantation after correction with genetic editing.

Figure reference: Seranova E. et al. Journal of Molecular Biology 432(8): 2754-2798 (2020).

workable *in vitro* platforms for studying gene function or biological processes in human cell-type-specific manner at a physiological level, or for studying disease mechanisms in specific disease-associated and disease-affected human cell-types.

Notwithstanding, while it is extremely useful to have established cultures of specific disease-affected cells, some phenotypes of a disease are not manifested in a two-dimensional culture system. Therefore, it is advantageous that more complex structures be utilised, ones in which the three-dimensional interactions between multiple cell subtypes are taken into account. This is partly being addressed by the development of three-dimensional organoid cultures, which replicate *in vivo* cell-cell interactions to some degree (Seranova et al., 2020). Some examples of diseases that have been studied using two- and three dimensional hiPSC-derived culture systems include developmental diseases such as autism spectrum disorder (ASD) (DeRosa et al., 2018, Nestor et al., 2015) neurodegenerative disorders such as PD (Fernández-Santiago et al., 2015) and AD (Lee et al., 2016), and lysosomal storage disorders like NPC1 disease (Maetzel, Sarkar et al., 2014), amongst many others. The study of infectious diseases has also been conducted with the use of hiPSC-derived intestinal and gastric organoids for *Helicobacter pylori, Salmonella* and *Clostridium difficile* (McCracken et al., 2014; Leslie et al., 2014; Paredes-Sabja et al., 2014), as well as hiPSC-derived monocytes (Ye et al., 2014), T cells and natural killer cells (Ni et al., 2010) for HIV infection. The host response to Zika and Dengue viruses has been investigated in hiPSC-derived macrophages (Lang et al., 2018).

1.9.2. Human pluripotent stem cells in drug discovery and drug screening

Understanding the molecular mechanisms underlying pathology is an important step in the development of targeted therapies. The hiPSC-derived disease models can serve as a more direct platform for drug discovery, as candidate drugs can be directly tested using patient-derived cells. Differentiated disease-relevant cells from large cohorts or from individual patients can be subjected to treatment with specific candidate drugs, or simultaneously with a large number of compounds using high-throughput screening (HTS) (Figure 1.7). Similarly, hESC-derived cell-types offer physiologically-relevant platforms to identify drugs that will be effective in the desired differentiated cells and also to ascertain cell-specific effects. In both cases, an

observable phenotype, or set of phenotypes, must be defined in order to evaluate the efficacy and potency of tested compounds in the setting of the specific disease model.

Numerous therapeutic agents have been tested in this way for multiple diseases, such as for various neurodegenerative disorders including AD (Bright et al., 2015), ALS (Burkhardt et al., 2013), NPC1 (Maetzel, Sarkar et al., 2014), and SMA (Naryshkin et al., 2014). In the case of HTS, the phenotype must be capable of being measured via automated analysis. This may not be suitable when the disease phenotype is difficult to quantify, or if a system which would allow automatic quantification would be extremely laborious to develop. HTS has the advantage of allowing testing of over one million compounds simultaneously without the need for prior knowledge about the drug mechanism. This allows the possibility of testing a large number of drugs, which have already been approved for use in humans for possible repositioning thereof in other diseases, thereby expediting clinical trials and new treatment options. Such systems have been employed in the study of AD (Xu et al., 2013), familial dysautonomia (Lee et al., 2012), and ALS (Barmada et al., 2014). Achieving rapid drug screening for patient-derived model systems could facilitate a breakthrough in personalised medicine, as the response to various drugs could be tested on individual patient cells. They also allow screening for drug toxicities on specific and possibly individual human tissues, most commonly hepatotoxicity (Takayama et al., 2018), cardiotoxicity (Blinova et al., 2018), and neurotoxicity (Ohara et al., 2017). Additionally, hiPSC-derived macrophages carrying a GBA mutation responsible for Gaucher disease have been utilised to validate hits from HTS that were capable of enhancing GBA activity and reverse disease phenotype (Aflaki et al., 2014).

While a number of autophagy modulators have been identified in immortalised cell lines, emerging reports suggest some of these compounds display cell-type specificity of efficacy and drug action (Sarkar et al., 2006; Chou et al., 2018; Sharma et al., 2020). For instance, some of the potent autophagy inducers discovered by HTS in HeLa cells did not show any efficacy in hiPSC-derived neuronal and hepatic cells of NPC1 disease (Kuo et al., 2015). Likewise, autophagy-inducing drugs like verapamil and SMER28 that could induce autophagy in hiPSC-derived neurons were ineffective in hiPSC-derived hepatic cells (Maetzel, Sarkar et al., 2014). Thus, it is pertinent to identify autophagy-modulating compounds in appropriate human cell-types that would

be effective in the target organs of patients. Therefore, there is a need to establish human cellular platforms to advance drug discovery for clinical translation.

1.10. Differentiation of hESCs into desired human cell-types

Since the first derivation of hESCs from *in vitro* fertilised human embryos in 1998 (Thomson, 1998), their use in drug discovery and stem cell therapy has been significantly increased over the past years. Due to the expression of pluripotency factors Nanog, Oct4, Sox2, SSEA4 that ensure their self renewal capability, hESCs are able to differentiate into all three embryonic germ layers and thus are virtually capable of producing any desirable cell-type for further studies. They are characterised by high levels of telomerase activity, the ability to proliferate in an undifferentiated state for months and the capability to form trophoblast for further derivation of endoderm, mesoderm and ectoderm (Hyslop et al., 2005; Hanna et al., 2010; Hiyama and Hiyama, 2007).

Ethical concerns about the fact that hESCs are derived from human embryos in the blastocyst stage are present in stem cell research, but the advantage of utilising human physiologically-relevant cellular platforms that can be differentiated into various somatic cell-types of interest is of tremendous advancement for biomedical research. The discovery of transcription factors OCT4, SOX2, KLF4 and c-MYC governing the cell fate had led to reprogramming of somatic cells back into pluripotency (Takahashi and Yamanaka, 2006; Takahashi et al., 2007). This resulted in the generation of patient-derived hiPSCs that are now widely used by researchers to study a range of diseases. However, the use of hESCs is more preferable than hiPSCs, because the hiPSCs could carry epigenetic alterations and background variations that may contribute to phenotypic cell-to-cell alterations (Soldner and Jaenisch, 2018).

As genome engineering can be utilised to edit genes in hESCs (Soldner and Jaenisch, 2018; Byrne et al., 2014), it is now possible to knockout an autophagy essential gene or to insert an autophagy reporter in the genome for generating hESC models with autophagy readouts. These have been recently established by Sarkar and colleagues (unpublished data) and have been utilised in this thesis study. Moreover, these hESC

models of autophagy can be differentiated into the desired somatic cell-types having identical genetic backgrounds, thus enabling the creation of isogenic cellular platforms. Such systems will enable the study of any human cell-specific regulation and therapeutic manipulation of autophagy. The differentiation of hESCs into neurons and macrophages, the desired cell-types generated in this thesis work, are discussed below.

1.10.1. Neuronal differentiation

From the moment the derivation of hESCs (Liu et al., 2017; Kilpinen et al., 2017) and later hiPSCs (Hara et al., 2006) was possible, there was a plethora of studies exploiting hPSCs to derive neuronal cells for experimentation. The differentiation of hPSCs into human neurons was employed to study multiple aspects of neural biology related to neurodegeneration, development and more. The hPSC-derived neurons can be exploited for multiple purposes, such as for understanding disease mechanisms in patient cells, the advancement of drug discovery or cell therapy applications (Miller et al., 2013; Vera et al., 2016). Autophagy has been also studied in hPSC-derived neurons in multiple human neuronal cell lines, contributing to our better understanding of this biological process in a physiologically relevant manner (Mertens et al., 2015; Mertens et al., 2018)

There are several differentiation protocols that have been developed in the last decade (Sterneckert et al., 2014; Soldner and Jaenisch, 2018; Jiménez-Moreno et al., 2017; Jungverdorben et al., 2017; Svendsen et al., 1997). The majority of them consists of two stages. Firstly, hESCs undergo a switching of the self-renewal state to neural induction. This usually includes the formation of spheroids cultured on non-adherent plates, which leads to the generation of neural precursors (NPs). The NPs then plated as a monolayer for expansion and further pushed to become terminally differentiated neurons. There are various growth factors used to direct this differentiation process.

There are two main signaling pathways that have been identified to play a crucial role in directed neural differentiation. The inhibition of both BMP and TGFβ contributes to significant enhancement of NP populations within hPSC culture (Pera et al., 2004; Gerrard et al., 2005). This has been achieved by several methods including small molecules and noggin-mediated suppression of BMP. The suppression of Lefty/Activin/TGFβ mediated by the small molecule SB431542 results in decreasing

the self-renewal capacity of hPSCs and promoting neural induction (Zhang et al., 2001). Variations of this dual signalling inhibition for neural differentiation are widely used by laboratories across the world. After the hPSCs have committed to the neuronal lineage and expressed markers representing the NP phenotype, it is possible to further direct the differentiation into specific cell-types such as neurons, astrocytes, microglia or even direct the cell into certain subtypes such as dopaminergic neurons. For the purpose of this project, a mixed population of neurons was generated that represents a physiologically-relevant culture. In this case, a mixed population of neurons refers to a population with subtypes of specific neurotransmitter release, such as GABAergic neurons, glutamatergic neurons, dopaminergic neurons, serotonergic neurons, and so on. This was achieved by applying the dual signaling inhibition protocol as previously described (Maetzel, Sarkar et al., 2014; Cohen et al., 2007).

1.10.2. Macrophage differentiation

There are few studies demonstrating the differentiation of hPSCs into macrophages (Wilgenburg et al., 2013; Haenseler et al., 2017; Ackermann et al., 2017; Lachmann et al., 2015; Takata et al., 2017; Shi et al., 2018). However, in comparison to the broad literature of differentiation methods for the hPSC-derived neuronal platforms, there are much fewer studies for generating hPSC-derived macrophages. The reason being that patient-derived macrophages can be obtained from patient blood samples, from which monocytes can be isolated and consequently cultured with appropriate growth factors to facilitate their terminal differentiation into macrophages. Another crucial element is the cost of the hPSC-derived macrophage culture, which is significantly higher than hPSC-derived neuronal culture. While the differentiation of macrophages from monocytes obtained from patient blood is possible *in vitro*, the resulting macrophages might have versatile physiological states that are influenced by the patient's genetic background. Moreover, large amounts of donor blood is required every time, hindering the scalability of such workflow. In addition, macrophages are refractory to genetic manipulation as they are capable of recognising foreign nucleic acids (Wilgenburg et al., 2013). Finally, primary human macrophages are not a convenient experimental platform because of their inability to be maintained in culture for more than a few days (Aggarwal et al., 2010). Because primary macrophages are difficult for genome engineering for making genetic models, and also present the issue of genetic variability in samples obtained from multiple individuals, genome engineered hESC-

derived macrophages serve as an ideal platform for drug discovery and other biological studies for the purpose of this thesis work. Alternative experimental systems include immortalised monocytic cell lines like THP-1 (Tsuchiya et al., 1980); however, they exhibit karyotypic abnormalities and are functionally immature (Odero et al., 2000, Berges et al., 2005).

The macrophage differentiation techniques have come a long way from co-culture of hiPSCs with OP9 mouse stromal cell monolayers (Choi et al., 2011; Senju et al., 2011) to EB-based protocols with serum-free, fully defined media (Karlsson et al., 2008; Wilgenburg et al., 2013; Lachmann et al., 2015). Most of the existing protocols utilise GM-CSF (granulocyte macrophage colony stimulating factor) or M-CSF (macrophage colony stimulating factor) to terminally differentiate myeloid progenitors, the so-called monocyte-like cells, into macrophages. Despite the fact that the existing protocols have been significantly optimised for yield and consistency, there are still pitfalls associated with high culture cost, lengthy time frames required to obtain the hPSC-derived macrophages, as well as considerations about the recapitulation of macrophage ontogeny in the resulting cells (Buchrieser et al., 2017). Studies have shown that the *in vitro* hematopoietic differentiation of hPSCs is more similar to *in vivo* primitive hematopoiesis than to definitive hematopoiesis (Vanhee et al., 2014), and this fact is something that should be kept in mind when hPSC-derived macrophages are utilised for biomedical studies. A way to validate findings from hPSC-derived macrophages is to compare them with human blood monocyte-derived macrophages. As differentiation protocols become more sophisticated, the refinement of differentiation into tissue specific subtypes, might solve this issue and provide an analogous final product of terminally differentiated macrophages that will serve as a superior platform for experimentation. This could be achieved through either co-culture with tissue specific cell-types such as neurons (Haenseler et al., 2017; Takata et al., 2017) and astrocytes (Pandya et al., 2017) for microglia production as an example, or cytokine treatment that would contribute to recapitulation of an environment that resembles organ specificity (Abud et al., 2017).

The cell-type specific investigation of autophagy regulation in macrophages is necessary for biomedical applications and drug discovery pertaining to xenophagy (clearance of pathogens) in infectious diseases. As there was a need to build an experimental platform in an appropriate human cellular context instead of immortalised

cell lines, this was done by establishing hESC-derived macrophages that were differentiated from hESCs genome engineered by Sarkar and colleagues to stably express the pH-sensitive autophagy reporter, mCherry-EGFP-LC3.

1.11. Aims and Hypotheses

There has been an exponential growth in the number of studies related to the role of autophagy in human health and diseases; thereby attributing this process to be of physiological and biomedical importance. However, *some of the core questions in the field include how impairment in autophagy causes cytotoxicity, and what are the potent autophagy inducers effective in the target organs of the patients*. This thesis work aims to develop hESC-based human cellular platforms for addressing these issues in a manner relevant to human biology. Such hESC models of autophagy are currently not available, and are expected to be of broad interest to the scientific community.

The aims and hypotheses of this thesis are:

Aim 1 (related to thesis Chapter 2): Establish autophagy-deficient human cellular platforms exhibiting cytotoxicity by utilising *ATG5*$^{-/-}$ hESCs.

Hypothesis 1 (related to Aim 1): Autophagy is vital for cellular survival and hence autophagy deficiency will increase cell death in these physiologically-relevant human cellular platforms.

Aim 2 (related to thesis Chapter 3): Investigate the mechanistic link between autophagy deficiency and cytotoxicity using hESC models of autophagy deficiency and hiPSC models with autophagy dysfunction.

Hypothesis 2 (related to Aim 2): Since autophagy maintains cellular homeostasis, the apoptotic phenotype due to autophagy deficiency might arise from a failure of its homeostatic functions, such as a metabolic defect because autophagy also promotes metabolic homeostasis.

Aim 3 (related to thesis Chapter 4): Establish autophagy reporter human cellular platform utilising mCherry-EGFP-LC3 hESCs for drug discovery in hESC-derived macrophages.

Hypothesis 3 (related to Aim 3): Since autophagy plays a major role in pathogen clearance, identifying potent autophagy inducers in immune cells like macrophages will be of biomedical importance.

Chapter 2

Establishment of autophagy-deficient human cellular platforms utilising hESCs

Chapter 2: Establishment of autophagy-deficient human cellular platforms utilising hESCs

2.1. Overview

The physiological relevance of experimental platforms used for fundamental science and drug discovery is gaining attention for elucidating human-relevant biology and subsequent translational research. Since cell-type specificity could unravel the precise biological mechanisms that govern human health and disease, the use of human embryonic stem cells (hESCs) as an experimental platform is advantageous for biomedical research. This is because these physiologically-relevant hESCs, upon differentiation to the desired cell-types, generate isogenic cellular platforms for comparison between the parental and the differentiated cell-types. In order to study the role of autophagy in cellular homeostasis, particularly how decline or malfunction of autophagy mediates cytotoxicity, an autophagy-deficient system was generated in hESCs. This was further utilised to generate autophagy-deficient neural precursors (NPs) and neurons that have the same genetic background as in the parental hESCs. Since autophagy has a major implication in neurodegeneration, this genetic hESC model of autophagy deficiency will enable investigating how loss of autophagy mediates neuronal cell death, and whether this neurotoxicity could be prevented by pharmacological treatments.

The objectives/milestones for this results chapter include:

(1) Establishment of hESC model with autophagy deficiency.
(2) Generation of autophagy-deficient neural precursors and neurons.
(3) Characterisation of cell death phenotype in these autophagy-deficient human cellular platforms.

2.2. Introduction to the existing autophagy knockout models and the need for a hESC-based experimental platform

Numerous studies of autophagy in knockout models demonstrate the importance of this process for development, survival and myriad physiological functions (see Chapter 1, Section 1.7). Mice with complete knockout of *Atg5* were not viable beyond 24 hours after birth (Kuma et al., 2004), and similar results were found with the knockout models

of *Atg16, Atg7, Atg3* and *Atg12* (Malhotra et al., 2015; Saitoh et al., 2008; Sou et al., 2008; Komatsu et al., 2005). However, when *Atg5* was re-expressed in the brains of *Atg5*-deficient mice, the pups were able to survive (Yoshii et al., 2017). On the other hand, conditional knockouts of autophagy genes in various organs make it possible to study the impact of autophagy, or lack thereof, in a tissue-specific manner (Mizushima and Levine, 2010; Kuma et al., 2017).

Despite the valuable *in vivo* data generated from mouse models, mice are physiologically distinct from humans. Thus, there is a need to create more physiologically-relevant models to study autophagy in the human system (Perlman, 2016). Using CRISPR/Cas9, an *ATG5* knockout human ovarian cancer stem cell line was generated in a recent study (Pagotto et al., 2017). Few other *ATG* gene knockouts were also made in HeLa cells (Mizushima and Levine, 2010; Kuma et al., 2017). However, these cellular systems being cancerous cell lines, and various mutations could be contributing to abnormal cell growth, it is desirable to create an improved human cellular model of autophagy that is of more physiological relevance to humans.

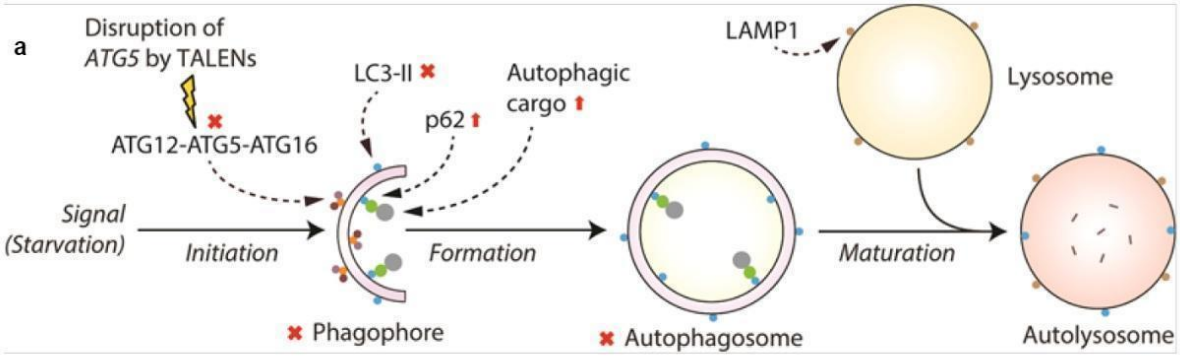
Human embryonic stem cells (hESCs) are one of the most physiologically-relevant cells derived from human embryos in the blastocyst stage. The hESCs can undergo self-renewal and are pluripotent, having the ability to be differentiated into various somatic cell types (Thomson, 1998) (see further details about the characteristics and utility of hESCs in Chapter 1, Section 1.9). Therefore, creating an autophagy-deficient hESC model will serve as a platform of high basic and biomedical relevance to study autophagy. Consequently, the aim of this chapter is to establish a hESC model with autophagy deficiency, differentiate them into the desired cell types, and further utilise these autophagy knockout, isogenic, human cellular platforms to investigate how loss of autophagy could lead to cell death. This study will not only elucidate how autophagy contributes to cellular homeostasis, but also identify potential therapeutic interventions to combat cytotoxicity in diseases associated with autophagy dysfunction.

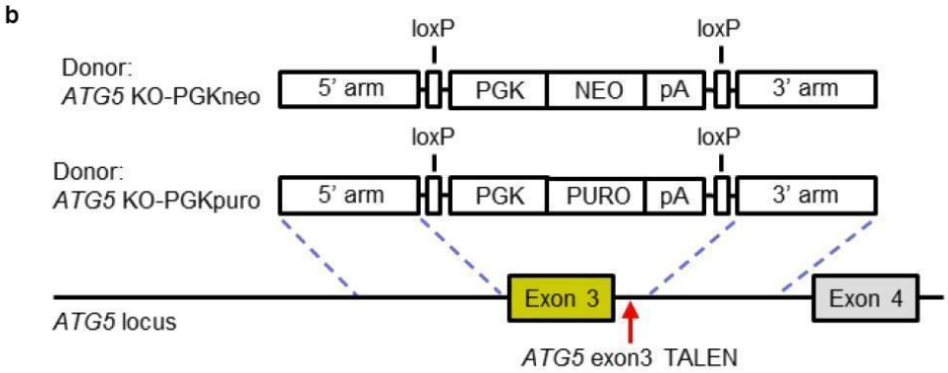
2.3. Results

2.3.1. Generation and characterisation of autophagy-deficient hESCs

Since there are no previous reports of an autophagy knockout system in hESCs, we chose to create this autophagy-deficient hESC model. This system will be of human physiological relevance, and will enable generation of isogenic cellular platforms to compare and study the cell type specific regulation and homeostatic function of autophagy. Loss of autophagy can be achieved by knockout of an essential autophagy-related (*ATG*) gene like *ATG5*, which encodes for a key protein required for autophagosome formation (Kuma et al., 2004) (Figure 2.1a). Previously, Sarkar and colleagues generated autophagy-deficient (*ATG5*$^{-/-}$) hESCs by knocking out exon 3 of the *ATG5* gene via genome engineering with transcription activator-like effector nucleases (TALENs) (Figure 2.1b). The TALEN technology employs engineered restriction enzymes made by fusing a TAL effector DNA-binding domain to a DNA-cleaving nuclease in order for the TALENs to target the specific DNA sequence of interest (Joung and Sander, 2012). The parental hESC line used was the WIBR3 hESC line that has been previously characterised and published (Lengner et al., 2010). The correctly targeted *ATG5*$^{-/-}$ clones were confirmed by Southern blot and Sanger sequencing (data not shown, performed previously by Sarkar and colleagues). Five homozygous (*ATG5*$^{-/-}$) and two heterozygous (*ATG5*$^{+/-}$) knockout clones were obtained (Figure 2.1c). This autophagy deficient hESC model will serve as an *in vitro* experimental platform to understand the role of autophagy in cellular homeostasis and identify any cell-specific effects in the isogenic hESC-derived cell types.

After the generation of autophagy-deficient hESCs, the pluripotency of some of these cell lines were examined in order to assess that loss of autophagy did not compromise this essential characteristic of pluripotent hESCs. Some of the major pluripotency markers in hESCs that were analysed include NANOG, POU5F1/OCT4, SOX2, SSEA4 and TRA-1-60 (Sperger et al., 2003). The *ATG5*$^{+/-}$ and multiple clones of *ATG5*$^{-/-}$ hESCs expressed these pluripotency markers that appeared comparable to the wild-type (*ATG5*$^{+/+}$) hESCs when evaluated by immunofluorescence staining (Figures 2.2a,b). Additionally, measurement of the relative mRNA expression levels of *NANOG*, *OCT4 (POU5F1)* and *SOX2* via qPCR also revealed that the expression of these pluripotency markers were not overtly different (Figures 2.2c,d).





c

Overview of parental and autophagy-deficient human embryonic stem cell (hESC) lines

WIBR3 hESC lines	*Genotype for ATG5 knockout*	*Autophagy status*	*No. of clones*	*Cell line designation with clone ID*
WIBR3 hESC *ATG5*$^{+/+}$	Wild-type	Yes	-	WIBR3
WIBR3 hESC *ATG5*$^{+/-}$	Heterozygous	Yes	2	WIBR3-ATG5$^{+/-}$ #1, #2
WIBR3 hESC *ATG5*$^{-/-}$	Homozygous	No	5	WIBR3-ATG5$^{-/-}$ #1, #3, #4, #5, #6

Figure 2.1. Schematic representation of the impact and the genome editing strategy of *ATG5* gene disruption, and the list of hESC lines obtained.

a, Schematic representation of the autophagy pathway indicating the consequences of *ATG5* gene deletion, such as loss of phagophore and autophagosome/LC3-II (denoted by red cross) and accumulation of autophagic cargo like p62 (denoted by red arrow).

b, Targeting strategy for deleting exon 3 in human *ATG5* gene by TALENs *(performed by Sovan Sarkar and colleagues)*.

c, List of parental and autophagy-deficient human embryonic stem cell (hESC) lines.

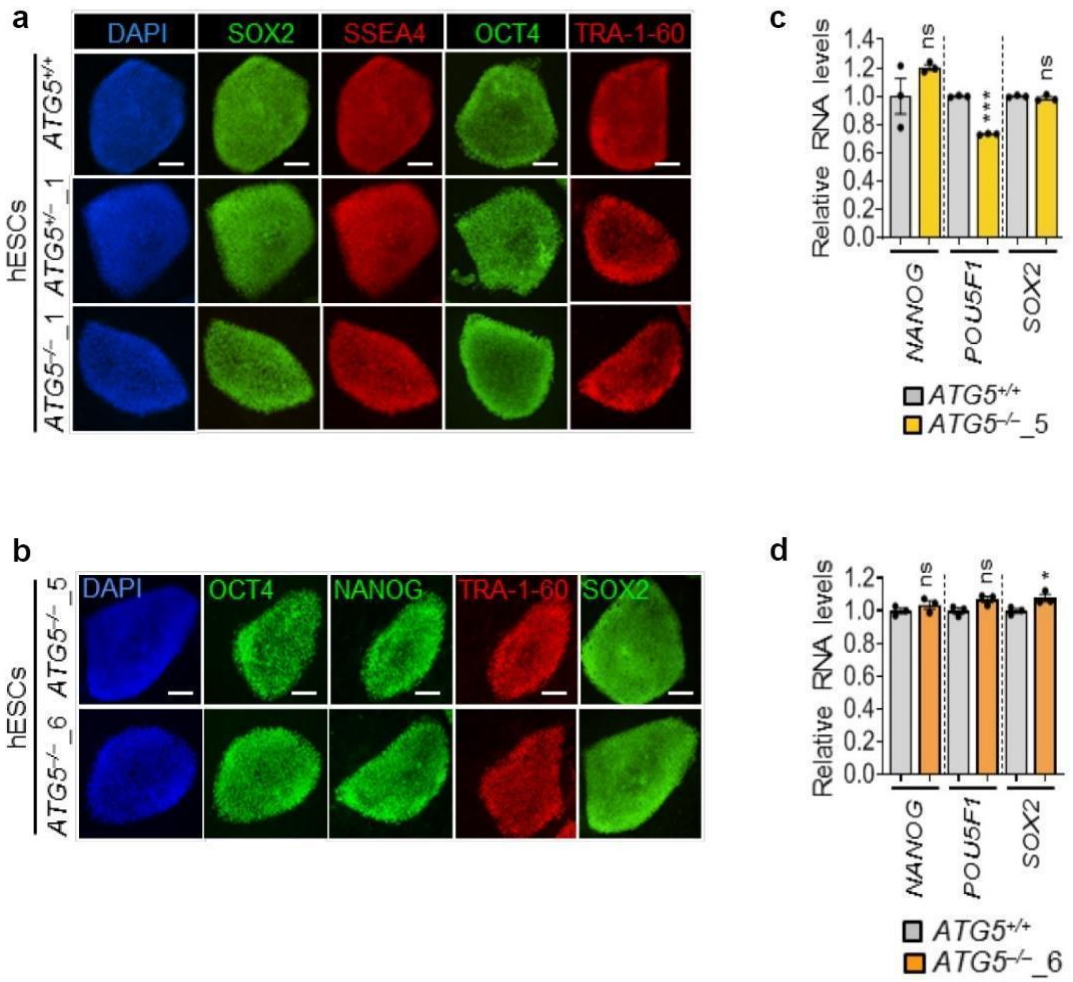


Figure 2.2. Characterisation of *ATG5*$^{-/-}$ hESCs for pluripotency.

a, b, Immunofluorescence analyses with anti-SOX2, anti-SSEA4, anti-OCT4 and anti-TRA-1-60 antibodies in *ATG5*$^{+/+}$, *ATG5*$^{+/-}$_1 and *ATG5*$^{-/-}$_1 hESCs (**a**) and with anti-OCT4, anti-NANOG, anti-TRA-1-60 and anti-SOX2 antibodies in *ATG5*$^{-/-}$_5 and *ATG5*$^{-/-}$_6 hESCs (**b**) that were stained with DAPI.

c, d, Quantitative RT-PCR (qPCR) expression analyses of human *NANOG*, *POU5F1* and *SOX2* genes in *ATG5*$^{+/+}$, *ATG5*$^{-/-}$_5 (**c**) and *ATG5*$^{-/-}$_6 (**d**) hESCs where data are shown relative to *GAPDH* expression.

Representative images (**a**, **b**) shown from one of 2 independent experiments. Graphical data denote mean ± s.e.m. (n = 3) where *P* values were calculated by unpaired two-tailed Student's *t*-test from 3 independent experiments (**c**, **d**). ***, $p<0.001$; *, $p<0.05$; ns, non-significant. Scale bar, 200 µm (**a, b**).

Although there was a small but significant decrease in OCT4 (*POU5F1*) mRNA expression levels in *ATG5*$^{-/-}$_5 (clone 5) hESCs compared to the *ATG5*$^{+/+}$ hESCs (Figure 2.2c), there were no significant reduction in the expression of other markers and also this difference did not seem to be compromising the self-renewal capacity of this cell line. This is evident by the proliferation and division rate of these cells, as well as their ability to differentiate into neural precursors and neurons that indicate of their commitment to the neuronal lineage (described later in Section 2.3.6). Thus, abrogation of autophagy does not seem to affect the pluripotency of these genome-edited hESCs.

2.3.2. Phenotypic characterisation of *ATG5*$^{-/-}$ hESCs for loss of autophagy

After confirming the pluripotency of *ATG5*$^{+/-}$ and *ATG5*$^{-/-}$ hESCs, partial or complete loss of autophagy was examined in these respective cell lines in comparison to the *ATG5*$^{+/+}$ hESCs under full growth medium (basal condition). Firstly, knockout of *ATG5* was assessed at a protein level by immunoblotting. Since the ATG5 protein normally exists in conjugation with ATG12 (Mizushima et al., 1998), immunoblotting analyses revealed complete or partial loss of the ATG5-ATG12 conjugate in *ATG5*$^{-/-}$_1 (clone 1) and *ATG5*$^{+/-}$_1 (clone 1) hESCs, respectively (Figure 2.3a). Other *ATG5*$^{-/-}$ clones (clones 3, 5 and 6) also displayed loss of the ATG5-ATG12 conjugate by immunoblotting (Figure 2.3b). Next, autophagy deficiency was examined under basal condition. The primary method to check this is via the absence of LC3-II levels, because LC3-II directly correlates with autophagosome number (Klionsky et al., 2016). While LC3-I is a cytosolic, the lipidated LC3-II form resides on the autophagosome membrane and thus serves as a specific marker for autophagic vesicles. Loss of autophagosomes was confirmed in *ATG5*$^{-/-}$_1 hESCs by absence of LC3-II levels and LC3^{+} puncta via immunoblotting and immunofluorescence, respectively, while *ATG5*$^{+/-}$_1 hESCs had less LC3-II levels and fewer LC3^{+} puncta compared to wild-type hESCs (Figures 2.3a,c). The absence of LC3-II levels were also confirmed in other *ATG5*$^{-/-}$ clones (clones 3, 5 and 6) by immunoblotting (Figure 2.3b).

Autophagy deficiency would lead to inhibition of autophagic flux that will prevent the degradation of autophagic cargo, leading to accumulation of these materials. Therefore, the levels of a specific autophagy substrate, such as p62/SQSTM1, was analysed that is routinely used as a marker to assess autophagic cargo clearance

(Bjørkøy et al., 2005; Pankiv et al., 2007). As expected, the levels of p62 were substantially increased in multiple *ATG5*$^{-/-}$ hESC lines compared to *ATG5*$^{+/+}$ hESCs (Figures 2.3a,b).

Since starvation is a physiological trigger of autophagy, autophagy deficiency in *ATG5*$^{-/-}$ hESCs were also analysed under starvation condition by culturing the cells in Hanks Balanced Salt Solution (HBSS). Starvation-induced autophagy occurs via inhibition of mTORC1 (Kamada et al., 2000). Suppression of the mTORC1 kinase activity is assessed by the phosphorylation status of its downstream target, p70 S6 kinase (S6K), and of S6 ribosomal protein (S6P) that is a target of S6K (Iiboshi et al., 1999, Kozma et al., 1990). The efficacy of HBSS treatment (starvation) in mediating mTORC1 inhibition was confirmed by substantial reduction of the phosphorylated S6K and S6P levels in *ATG5*$^{+/+}$, *ATG5*$^{+/-}$_1 and *ATG5*$^{-/-}$_1 hESC lines (Figure 2.3a). Notably, autophagy deficiency did not seem to affect mTORC1 activity because the phosphorylated S6K and S6P levels were comparable between *ATG5*$^{+/+}$ and *ATG5*$^{-/-}$ hESCs (Figure 2.3a). Expectedly, induction of autophagy by starvation occurred in *ATG5*$^{+/+}$ hESCs, as evident by increase in ATG5-ATG12 conjugate, LC3-II levels and LC3^{+} puncta under HBSS compared to full medium (FM); but this effect was not seen in *ATG5*$^{-/-}$ hESCs (Figures 2.3a-c). Likewise, p62 levels were decreased in wild-type hESCs, but not in *ATG5*$^{-/-}$ hESCs, when cultured in HBSS compared to FM (Figures 2.3a,b).

2.3.3. Nanoparticle-mediated *ATG5* mRNA delivery rescues autophagy deficiency

To further validate the genetic hESC model of autophagy deficiency, rescue of autophagy was studied by complementing with wild-type *ATG5*. Since it is difficult to attain a high transfection efficiency in hESCs, introduction of *ATG5* in *ATG5*$^{-/-}$ hESCs could be achieved by lipid nanoparticle (LNP)-mediated mRNA delivery that results in the expression of the functional protein in target cells (Yanez Arteta et al., 2018, Kowalski, Rudra, Miao and Anderson, 2019). As a negative control, *GFP* mRNA was used. Treatment with human *ATG5* mRNA containing LNPs, formulated with the ionizable lipid C12-200 (Kauffman et al., 2015), restored functional autophagic flux in multiple clones of *ATG5*$^{-/-}$ hESCs. This rescue effect by *ATG5* LNPs in *ATG5*$^{-/-}$ hESCs was evident from the generation of ATG5-ATG12 conjugate that enabled the

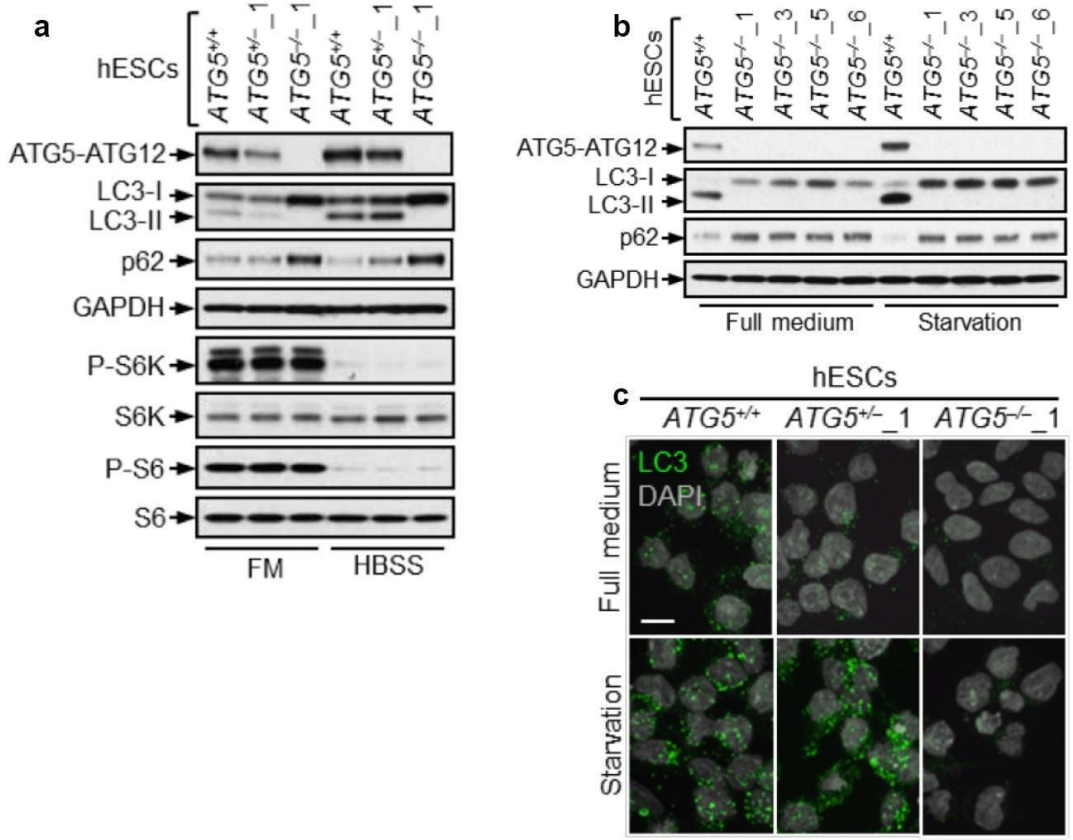


Figure 2.3. Characterisation of *ATG5*$^{-/-}$ hESCs for autophagy deficiency.

a, Immunoblotting analyses with anti-ATG5, anti-LC3, anti-p62, anti-GAPDH, anti-phospho-p70 S6 kinase (P-S6K; Thr^{389}), anti-p70 S6 kinase (S6K), anti-phospho-S6 ribosomal protein (P-S6P; Ser$^{235/236}$) and anti-S6 ribosomal protein (S6P) antibodies in *ATG5*$^{+/+}$, *ATG5*$^{+/-}$_1 and *ATG5*$^{-/-}$_1 hESCs, cultured in full growth medium (FM) or starvation condition (HBSS for 3 h).

b, Immunoblotting analyses with anti-ATG5, anti-LC3, anti-p62 and anti-GAPDH antibodies in *ATG5*$^{+/+}$ and multiple clones of *ATG5*$^{-/-}$ hESCs, cultured in full growth medium or starvation condition (HBSS for 3 h).

c, Immunofluorescence analysis with anti-LC3 antibody in *ATG5*$^{+/+}$, *ATG5*$^{+/-}$_1 and *ATG5*$^{-/-}$_1 hESCs, cultured either in full growth medium or starvation condition (HBSS for 3 h).

Representative immunoblot (**a**, **b**) shown from one of the 2 independent experiments. Representative images (**c**) shown from one of 2 independent experiments. Scale bar 100 µm (**c**).

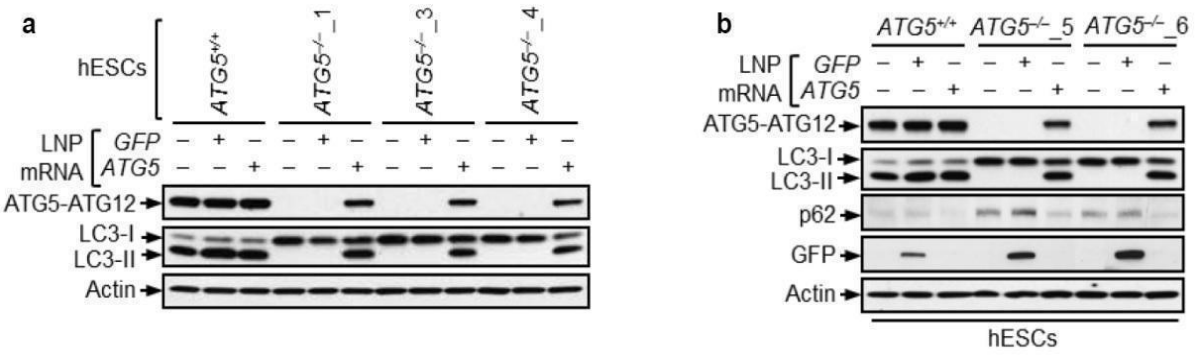


Figure 2.4. Rescue of functional autophagy in *ATG5*$^{-/-}$ hESCs via lipid nanoparticle-mediated *ATG5* mRNA delivery.

a, Immunoblotting analyses with anti-ATG5, anti-LC3 and anti-Tubulin antibodies in *ATG5*$^{+/+}$, *ATG5*$^{-/-}$_1, *ATG5*$^{-/-}$_3 and *ATG5*$^{-/-}$_4 hESCs, treated for 2 days with or without C12-200 lipid nanoparticle (LNP)-containing 2 µg of *GFP* or *ATG5* mRNA.

b, Immunoblotting analyses with anti-ATG5, anti-LC3, anti-p62, anti-GFP and anti-Actin antibodies in *ATG5*$^{+/+}$, *ATG5*$^{-/-}$_5 and *ATG5*$^{-/-}$_6 hESCs, treated for 2 days with or without C12-200 LNP-containing 2 µg of *GFP* or *ATG5* mRNA.

Representative immunoblot (**a**, **b**) shown from one of the 2 independent experiments.

formation of autophagosomes (LC3-II lipidation) and the clearance of p62; however, LNPs containing *GFP* mRNA did not have any effects (Figures 2.4a,b). These data further supported the autophagy-deficient hESC model established by *ATG5* knockout.

2.3.4. Increased cytotoxicity in autophagy-deficient hESCs

Having established the autophagy-deficient hESC model, the next important phenotype to assess is cell death. Multiple genetic studies have shown that tissue-specific abrogation of autophagy in normal mice has caused degeneration in the affected organs, suggesting that basal autophagy is essential for cellular and tissue homeostasis (Hara et al., 2006; Komatsu et al., 2006). However, it is not clear how loss or malfunction of autophagy disrupts cellular homeostasis and reduces cell viability. Thus, cell death was assessed in *ATG5*$^{-/-}$ hESCs because demonstrating this phenotype is pertinent for our objective of understanding how loss of autophagy affects cellular survival in human cells.

Cell death was measured by immunoblotting for cleaved caspase-3 and by CytoTox-Glo Cytotoxicity assay. The assessment of cleaved caspase-3 is a key parameter for apoptosis. Caspase-3 is activated by both caspase-8 and caspase-9, which respectively represent the intrinsic and extrinsic apoptosis pathways leading to cell death (Liu et al., 2017). Caspase-3 is activated when cleaved at an aspartate residue, and this active form is responsible for the degradation of various cytoplasmic proteins and DNA fragmentation (Woo et al., 1998). On the other hand, the CytoTox-Glo Cytotoxicity assay measures cell death protease secreted from dying cells. This assay measures the relative luminescence levels obtained after a luminogenic cell-impermeant peptide substrate generates a signal only from cells that undergo cytotoxic stress (Niles et al., 2009). Since cell death is a key phenotype for the research question, two detection methods were utilised to verify the reproducibility of results.

Two independent autophagy-deficient clones, such as *ATG5*$^{-/-}$_5 and *ATG5*$^{-/-}$_6 hESCs, were used for assessing cell death due to loss of autophagy in comparison to the wild-type *ATG5*$^{+/+}$ hESCs that has functional autophagy. Increased apoptosis was found in *ATG5*$^{-/-}$_5 and *ATG5*$^{-/-}$_6 hESCs, as evident from elevated levels of cleaved

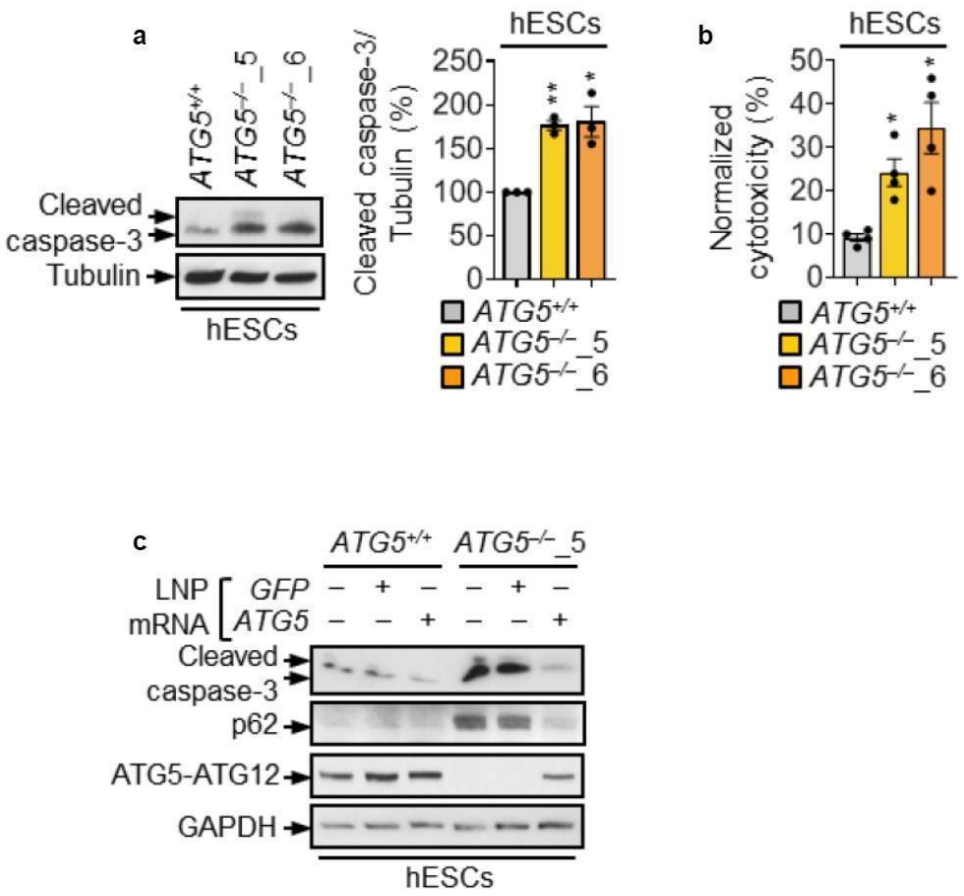


Figure 2.5. Autophagy-deficient hESCs exhibited increased cell death that could be rescued via lipid nanoparticle-mediated *ATG5* mRNA delivery.

a, Immunoblotting analysis with anti-cleaved caspase-3 and anti-Tubulin antibodies in *ATG5*$^{+/+}$, *ATG5*$^{-/-}$_5 and *ATG5*$^{-/-}$_6 hESCs.

b, Cytotoxicity assay in *ATG5*$^{+/+}$, *ATG5*$^{-/-}$_5 and *ATG5*$^{-/-}$_6 hESCs, where the data were normalised to total cell population.

c, Immunoblotting analyses with anti-cleaved caspase-3, anti-p62, anti-ATG5 and anti-GAPDH antibodies in *ATG5*$^{+/+}$ and *ATG5*$^{-/-}$_5 hESCs, treated for 2 days with or without C12-200 lipid nanoparticle (LNP)-containing 2 µg of *GFP* or *ATG5* mRNA.

Representative immunoblot shown from one of the 3 (**a**) or 2 (**c**) independent experiments. Graphical data (**a, b**) are mean ± s.e.m. (n = 3 or 4) where *P* values were calculated by unpaired two-tailed Student's *t*-test from 3 independent experiments. **, $p<0.01$; *, $p<0.05$.

caspase-3 by immunoblotting, as compared to *ATG5*$^{+/+}$ hESCs under normal growth conditions (Figure 2.5a). Similarly, increased cytotoxicity was observed in these autophagy-deficient hESCs via the luminescence-based CytoTox-Glo Cytotoxicity assay (Figure 2.5b). These data suggest that autophagy-deficient hESCs have increased cell death under basal condition in the absence of any external stressors.

To further determine whether loss of autophagy led to cell death in hESCs, *ATG5* was introduced in *ATG5*$^{-/-}$ cells via LNP-mediated mRNA delivery. Treatment with C12-200 LNPs containing *ATG5* mRNA, but not *GFP* mRNA, restored functional autophagic flux and rescued apoptosis in *ATG5*$^{-/-}$_5 hESCs. Immunoblotting analyses showed that *ATG5* LNPs led to generation of the ATG5 protein, restored autophagy and caused p62 clearance, and reduced cell death as observed from decreased levels of cleaved caspase-3 (Figure 2.5c). Collectively, these data suggest that autophagy deficiency compromises cell viability in hESCs.

2.3.5. Optimisation of neuronal differentiation from hESCs

Having established a genetic model of autophagy deficiency in hESCs that exhibit increased basal cell death, the next step was to generate a human neuronal model in order to investigate the role of autophagy in neuronal survival. The wild-type *ATG5*$^{+/+}$ and multiple clones of autophagy-deficient *ATG5*$^{-/-}$ hESCs were initially differentiated into neural precursors (NPs) via 'dual-SMAD inhibition method' followed by neuronal differentiation, as previously described (Maetzel, Sarkar et al., 2014; Cohen et al. 2007, Seranova et al., 2020) (Figure 2.6a) (see Chapter 1, Section 1.12).

A number of optimisation steps were undertaken while performing neuronal differentiation. The hESCs were initially differentiated into NPs that were further differentiated into neurons. Upon differentiation into NPs, the hESCs transition to a committed, multipotent neural lineage that can only differentiate into neuronal subtypes. Literature suggests that NPs can expand for at least 10 passages if maintained at a desired high density (Kozhich et al., 2013). Anecdotal evidence from cell culture observation suggests that NPs actively proliferate for up to 12-15 passages before losing their multipotent capacity and undergoing senescence. In order to accurately study any perturbations in the cellular processes and biological phenotypes between different cell lines, it is important to use a similar passage number such as

for the wild-type and autophagy-deficient cell lines. This applies to the experimentations at the NP level, and also when plating the NPs for terminal differentiation into neurons.

An additional parameter to consider for making the neuronal cultures is the initial seeding density of the NPs. This is important for neuronal differentiation because it affects the quality of the final neuronal population. When NPs are seeded too sparsely, their differentiation capability is compromised, usually leading to underdevelopment of neurons with short axons and a population that is unable to create neuronal networks. Additionally, this kind of cells largely do not stain positive for the neuronal markers such as TUJ1 or MAP2 (data not shown). On the other hand, when NPs are seeded too densely, the neuronal development appears to be closer to normal but there is a disproportionate number of astrocytic and microglial cells. This impacts on the purity of the neuronal population, thereby making this mixed population very difficult and inaccurate for certain experimental analyses at a population level. Moreover, different NP lines often show differential proliferation rates. Therefore, optimal seeding density of NPs for individual cell lines is essential to generate a near-homogenous population of neurons with similar density. For example, the cell numbers optimised for seeding in 1 well of a 6-well plate for the various NP lines for neuronal differentiation were 680000 for *ATG5*$^{+/+}$ NPs, 480000 for *ATG5*$^{-/-}$_5 NPs and 450000 for *ATG5*$^{-/-}$_6 NPs of passages 5-10. NPs of a lower passage would usually get utilised for expansion of the cell lines and subsequent cryopreservation.

Another point of consideration is the coating of cell culture plates. Human pluripotent stem cell (hPSC)-derived neuronal cells from different hPSC lines could achieve optimal growth with the use of distinct coating matrices that have their individual characteristics. For neuronal differentiation and culture in this study, Vitronectin, Matrigel and Poly-DL-ornithine (PDLO)/Laminin coating were tested. Neurons grown on PDLO/Laminin demonstrated superior attachment. Additionally, neuronal networks grown on Matrigel and Vitronectin appeared to form a more mixed population of cells including astrocytes and microglia. Thus, PDLO was selected for use in this study. PDLO is a basic polypeptide that provides optimal conditions for neuronal growth and prevents bacterial growth (Burblies et al., 2016). Interestingly, a study demonstrated improved firing activity in hiPSC-derived neuronal networks grown on PDLO/Laminin in comparison to other substrate coatings, showing synapse stabilisation and

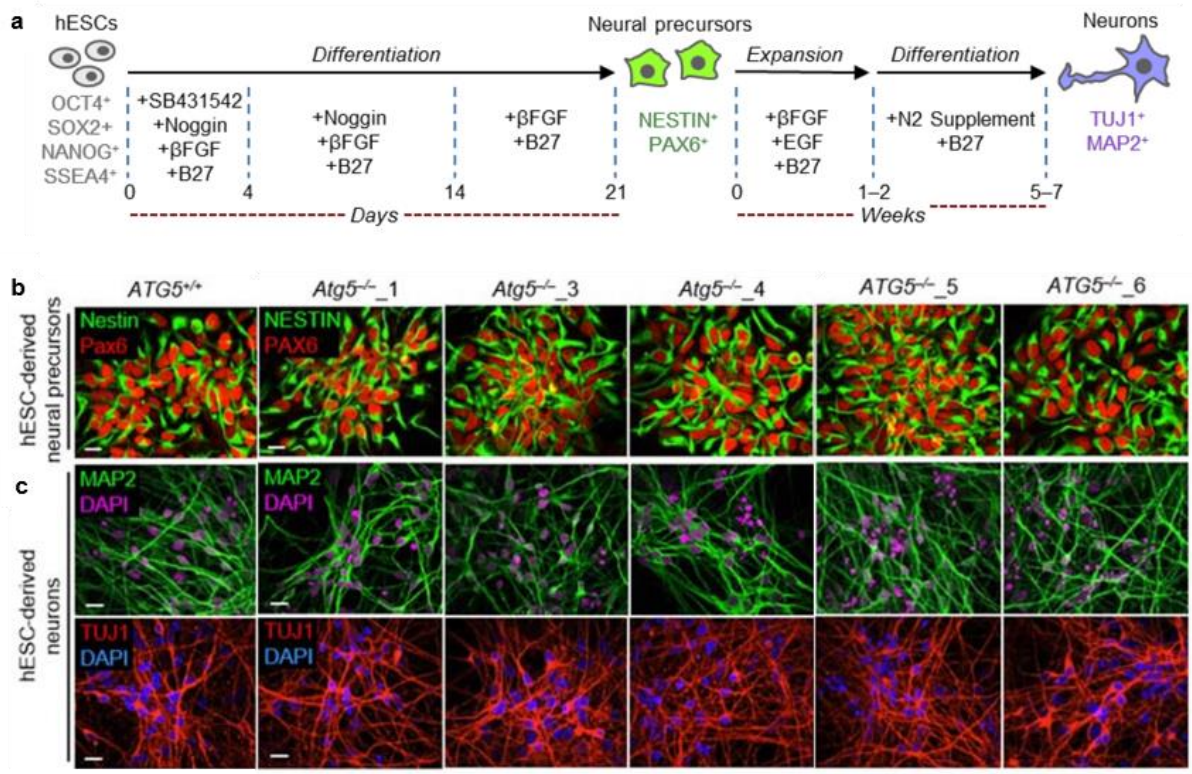


Figure 2.6. Generation and characterisation of autophagy-deficient hESC-derived neural precursors and neurons.

a, Schematic representation of the differentiation method of hESCs into neural precursors (NPs) and then to neurons, along with portrayal of cell type specific markers and the growth factors supplemented in the cell culture medium at each stage of the differentiation process.

b, Immunofluorescence analyses with anti-Nestin and anti-Pax6 antibodies in neural precursors (NPs) differentiated from *ATG5*$^{+/+}$ (wild-type), and *ATG5*$^{-/-}$_1, *ATG5*$^{-/-}$_3, *ATG5*$^{-/-}$_4, *ATG5*$^{-/-}$_5 and *ATG5*$^{-/-}$_6 (autophagy-deficient) hESCs.

c, Immunofluorescence analyses with anti-MAP2 and anti-TUJ1 antibodies in 4 weeks old neurons differentiated from *ATG5*$^{+/+}$, *ATG5*$^{-/-}$_1, *ATG5*$^{-/-}$_3, *ATG5*$^{-/-}$_4, *ATG5*$^{-/-}$_5 and *ATG5*$^{-/-}$_6 hESC-derived NPs.

Representative images (**b**, **c**) shown from one of 3 independent experiments. Scale bar, 100 µm (**b, c**).

favourable physiological neuronal maturation profile. This might be attributed to supplementary carbonyl groups contributing to negative charges, as well as the high molecular weight of ornithine molecules that provide additional binding sites for cell attachment (Amin et al., 2016).

2.3.6. Establishment and characterisation of hESC-derived neural precursors and neurons

Following the differentiation of wild-type and autophagy-deficient hESCs into neural precursors (NPs) and neurons, these hESC-derived cell-types were characterised by the expression of their lineage-specific markers. These include NESTIN and PAX6 for NPs, and MAP2 and TUJ1 for neurons. Immunofluorescence analyses with antibodies for these markers confirmed the cellular identity of NPs and neurons differentiated from *ATG5*$^{+/+}$ and multiple clones of *ATG5*$^{-/-}$ hESCs (Figures 2.6b,c). These cell type specific markers are routinely used to monitor the differentiation capacity and the cellular identity of hPSC-derived cells of neuronal lineage. PAX6 is a transcription factor that is essential for self-renewal and proliferation of neural stem cells (Curto et al., 2014), and NESTIN is a neuroepithelial stem cell protein and a cytoskeletal intermediate filament (Lendahl et al., 1990). Furthermore, SOX2 is a transcription factor expressed in both hESCs and NPs (but its expression is much higher in NPs compared to hESCs) that promotes neural ectodermal differentiation (Thomson et al., 2011). On the other hand, the neuron-specific class III beta-tubulin (TUJ1) and microtubule associated protein 2 (MAP2) are not expressed in NPs but are subsequently detected in terminally-differentiated neurons (Menezes and Luskin, 1994, Dehmelt and Halpain, 2004). TUJ1 is responsible for microtubule stability and neurite elongation once the neurons have formed their axons and dendrites (Ferreira and Caceres, 1992), while MAP2 regulates neuritic development and maintenance (Dehmelt and Halpain, 2004, Sánchez et al., 2000).

In addition to immunofluorescence assessment, immunoblotting analysis for these markers confirmed the expression of these proteins in *ATG5*$^{+/+}$ and multiple clones of *ATG5*$^{-/-}$ hESC-derived NPs (NESTIN, PAX6, SOX2) and neurons (MAP2, TUJ1) (Figures 2.7a-c). As a control non-expressing cell-type, hESCs were used in comparison to the NPs and neurons to demonstrate the cell-specific expression of PAX6 in NPs (Figure 2.7a), and MAP2 and TUJ1 in neurons (Figure 2.7c). Moreover,

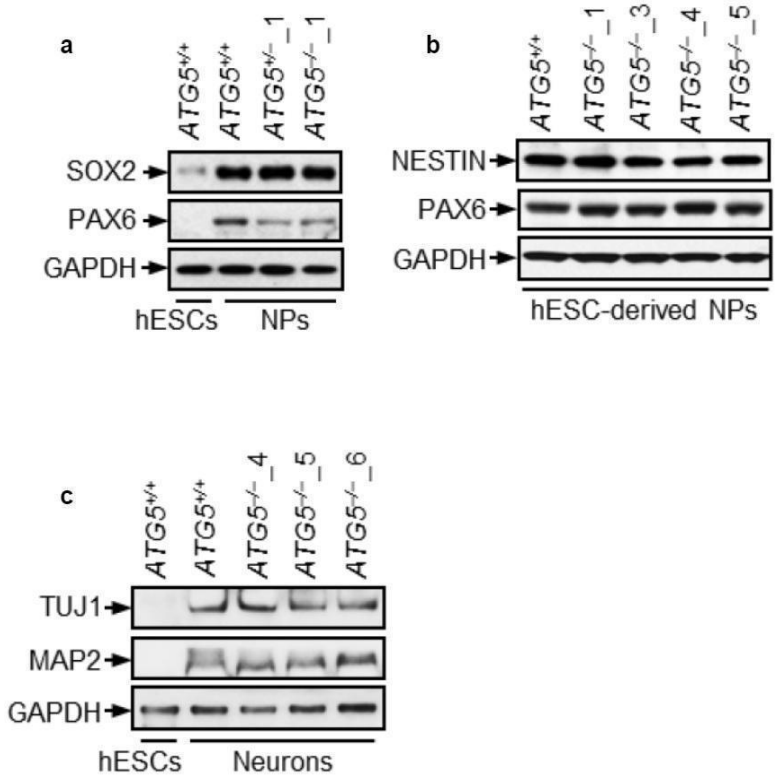


Figure 2.7. Characterisation of autophagy-deficient hESC-derived neural precursors and neurons via immunoblotting for cell specific markers.

a, b, Immunoblotting analyses with anti-SOX2, anti-PAX6, anti-NESTIN and anti-GAPDH antibodies in *ATG5*$^{+/+}$, *ATG5*$^{+/–}$_1 and *ATG5*$^{–/–}$_1 hESC-derived neural precursors (NPs) along with *ATG5*$^{+/+}$ hESCs (**a**), and in *ATG5*$^{+/+}$ and multiple clones of *ATG5*$^{–/–}$ hESC-derived NPs (**b**).

c, Immunoblotting analyses with anti-TUJ1, anti-MAP2 and anti-GAPDH antibodies in *ATG5*$^{+/+}$ and multiple clones of *ATG5*$^{–/–}$ hESC-derived neurons (4 weeks old) along with *ATG5*$^{+/+}$ hESCs.

Representative immunoblot shown from one of the 2 independent experiments.

SOX2 was expressed at a substantially higher level in NPs than in hESCs, as expected (Figure 2.7a). Overall, immunofluorescence and immunoblotting data do not show any obvious differences in the expression of these cell-specific markers between *ATG5*$^{+/+}$ and *ATG5*$^{-/-}$ NPs and neurons. These data suggest that abrogation of autophagy in hESCs did not overtly affect their differentiation potential into neuronal lineage.

2.3.7. Characterisation of *ATG5*$^{-/-}$ hESC-derived NPs and neurons for loss of autophagy.

After the characterisation of *ATG5*$^{+/+}$ and *ATG5*$^{-/-}$ hESC-derived NPs and neurons for cell-specific markers, loss of autophagy was next examined in *ATG5*$^{-/-}$ cells. This was done similar to the phenotypic analysis in *ATG5*$^{-/-}$ hESCs as described in the previous Section 2.3.2. Deletion of *ATG5* in NPs and neurons was confirmed by complete loss of the ATG5-ATG12 conjugate in multiple clones of *ATG5*$^{-/-}$ cells via immunoblotting (Figures 2.8a,c). Likewise, loss of autophagosomes was confirmed in these *ATG5*$^{-/-}$ hESC-derived cell-types under basal condition (full medium) by the absence of LC3-II levels (Figures 2.8a,c) and LC3^{+} puncta (Figures 2.8b,d) via immunoblotting and immunofluorescence, respectively. As a consequence of autophagy deficiency, the levels of the specific autophagy substrate, p62/SQSTM1, were substantially increased in multiple clones of *ATG5*$^{-/-}$ NPs and neurons (Figures 2.8a,c). In addition, induction of autophagy by starvation (with HBSS treatment) increased LC3^{+} puncta in *ATG5*$^{+/+}$ NPs, as compared to these cells under full medium, but no autophagosomes were observed in *ATG5*$^{-/-}$ NPs (Figure 2.8b). However, starvation treatment was difficult in neurons because of the fragile nature of these cells, especially under stress conditions where the *ATG5*$^{-/-}$ neurons were extremely prone to die and float away in the cell culture plates.

To further validate this autophagy-deficient human neuronal platform, human *ATG5* mRNA was introduced via lipid nanoparticles (LNPs) in *ATG5*$^{-/-}$ neurons (Figure 2.9a). Initial evaluation of C12-200 LNPs containing *GFP* mRNA indicated that these LNPs are efficient for mRNA delivery in hESC-derived neurons, as measured by GFP expression (Figure 2.9b). Similar to the rescue effects in *ATG5*$^{-/-}$ hESCs, C12-200 LNP-mediated delivery of human *ATG5* mRNA, but not *GFP* mRNA, restored functional autophagic flux in multiple clones of *ATG5*$^{-/-}$ neurons. This was evident from the effects of *ATG5* mRNA-encapsulated LNPs on the generation of ATG5-ATG12

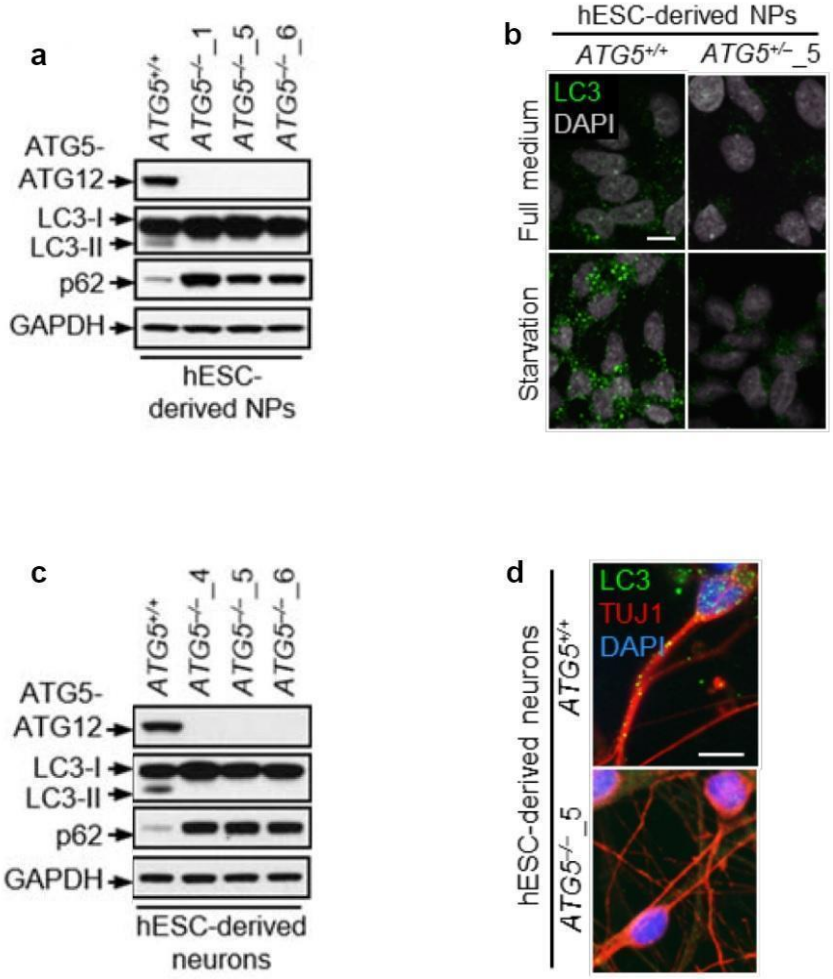


Figure 2.8. Phenotypic characterisation of *ATG5*$^{-/-}$ hESC-derived neural precursors and neurons for loss of autophagy.

a, Immunoblotting analyses with anti-ATG5, anti-LC3, anti-p62 and anti-GAPDH antibodies in *ATG5*$^{+/+}$ and multiple clones of *ATG5*$^{-/-}$ hESC-derived neural precursors (NPs).

b, Immunofluorescence analysis with anti-LC3 antibody in *ATG5*$^{+/+}$ and *ATG5*$^{-/-}$_5 hESC-derived NPs, cultured either in full growth medium or starvation condition (HBSS for 1 h).

c, Immunoblotting analyses with anti-ATG5, anti-LC3, anti-p62 and anti-GAPDH antibodies in *ATG5*$^{+/+}$ and multiple clones of *ATG5*$^{-/-}$ hESC-derived neurons (4 weeks old).

d, Immunofluorescence analysis with anti-LC3 antibody in *ATG5*$^{+/+}$ and *ATG5*$^{-/-}$_5 hESC-derived neurons (4 weeks old).

Representative immunoblot (**a**, **c**) shown from one of the 2 independent experiments. Representative images (**b**, **d**) shown from one of 2 independent experiments. Scale bar, 100 µm (**b**) or 10 µm (**d**).

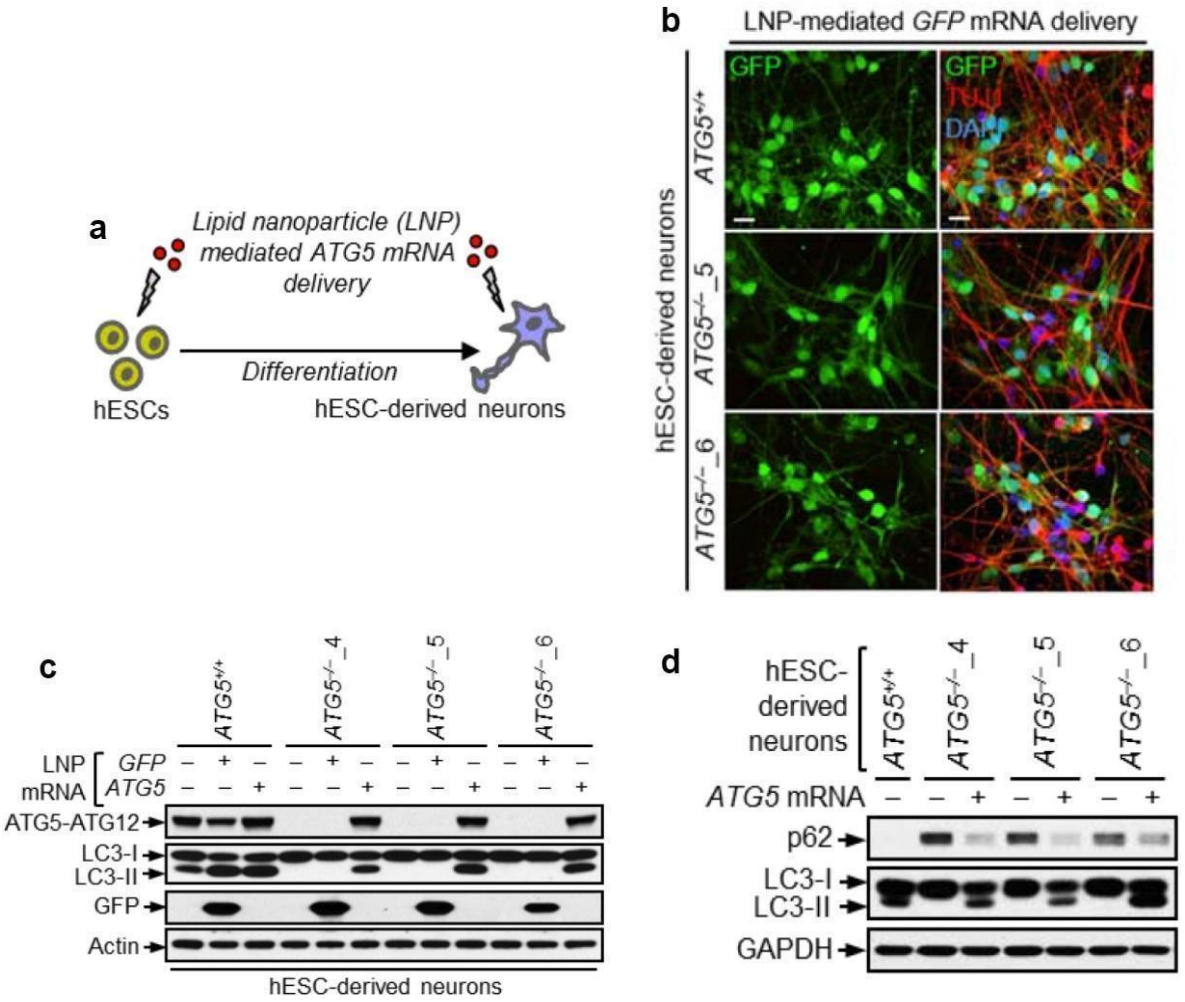


Figure 2.9. Lipid nanoparticle-mediated *ATG5* mRNA delivery in autophagy-deficient neurons restored functional autophagic flux.

a, Schematic representation of lipid nanoparticle (LNP)-mediated mRNA delivery in hESCs and hESC-derived neurons.

b, Fluorescence analysis of GFP expression in *ATG5*$^{+/+}$, *ATG5*$^{-/-}$_5 and *ATG5*$^{-/-}$_6 hESC-derived neurons (4 weeks old), treated for 6 days with C12-200 LNP-containing 2 µg of *GFP* mRNA and immunostained with anti-TUJ1 antibody.

c, Immunoblotting analyses with anti-ATG5, anti-LC3, anti-GFP and anti-Actin antibodies in ATG5$^{+/+}$ and multiple clones of ATG5$^{-/-}$ hESC-derived neurons (4 weeks old), treated for 4 days with or without C12-200 LNP-containing 2 µg/ml of *GFP* or *ATG5* mRNA.

d, Immunoblotting analysis with anti-p62, anti-LC3 and anti-GAPDH antibodies in *ATG5*$^{+/+}$, *ATG5*$^{-/-}$_4, *ATG5*$^{-/-}$_5 and *ATG5*$^{-/-}$_6 hESC-derived neurons (4 weeks old), treated for 6 days with or without C12-200 LNP-containing 2 µg of *ATG5* mRNA.

Representative immunoblot (**c**, **d**) shown from one of the 2 independent experiments. Representative images (**b**) shown from 1 experiment. Scale bar, 100 µm (**b**).

conjugate in *ATG5*$^{-/-}$ neurons, leading to the formation of LC3-II/autophagosomes and the consequent clearance of p62 (Figures 2.9c,d). However, *GFP* mRNA had no effects in *ATG5*$^{-/-}$ neurons on the generation of ATG5-ATG12 conjugate and LC3-II levels, as well as on p62 clearance (Figures 2.9c,d). These data further confirm the loss of autophagy phenotype in this autophagy-deficient human neuronal system.

2.3.8. Increased cytotoxicity in *ATG5*$^{-/-}$ hESC-derived NPs and neurons

To evaluate whether loss of autophagy in human neurons compromises cellular viability, cell death was analysed at population and single-cell levels. Similar to the apoptotic phenotype in autophagy-deficient hESCs, elevated levels of cleaved caspase-3 and increased cytotoxicity were seen in multiple clones of *ATG5*$^{-/-}$ hESC-derived NPs at population level analysis (Figures 2.10a,b). Although immunoblotting analysis showing higher cleaved caspase-3 levels suggest overall increased apoptosis in *ATG5*$^{-/-}$ NPs (Figure 2.10a), FACS analysis showed increase in early and intermediate apoptosis in *ATG5*$^{-/-}$ NPs compared to the wild-type NPs, and overall increased cell death after combining all the stages (Figure 2.10b). The discrimination between apoptosis stages was possible using two cell death markers simultaneously, FITC-Annexin V and Propidium Iodide (PI). The range of expression between the two markers was used to discriminate between live cells (PI$^-$/Annexin V$^-$), early apoptotic cells (PI$^-$/Annexin V$^+$), intermediate apoptotic cells (PI$^+$/Annexin V$^+$) and late apoptotic cells (PI$^+$/Annexin V$^-$).

ATG5$^{-/-}$ hESC-derived neurons (in two independent clones, *ATG5*$^{-/-}$_5 and *ATG5*$^{-/-}$_6) also exhibited elevation in cleaved caspase-3 levels, as seen by immunoblotting at basal level compared to wild-type neurons (Figure 2.11a). Increased cytotoxicity was observed by luminescence-based assay in *ATG5*$^{-/-}$ neuronal cells as early as 2 weeks of neuronal differentiation, and this was more substantial after 4 weeks (Figures 2.11b,c). These population level data indicate increased cell death in *ATG5*$^{-/-}$ neurons. Furthermore, cell death was analysed at a single cell level by TUNEL assay and DAPI-stained apoptotic nuclear morphology after immunostaining the neurons with TUJ1. The TUNEL assay is a sensitive detection method for fragmented DNA, which is an indication of apoptosis. Only nuclei of apoptotic cells are labelled with the TUNEL fluorophore and thus, quantification of TUNEL$^+$ nuclei provides a quantitative measure

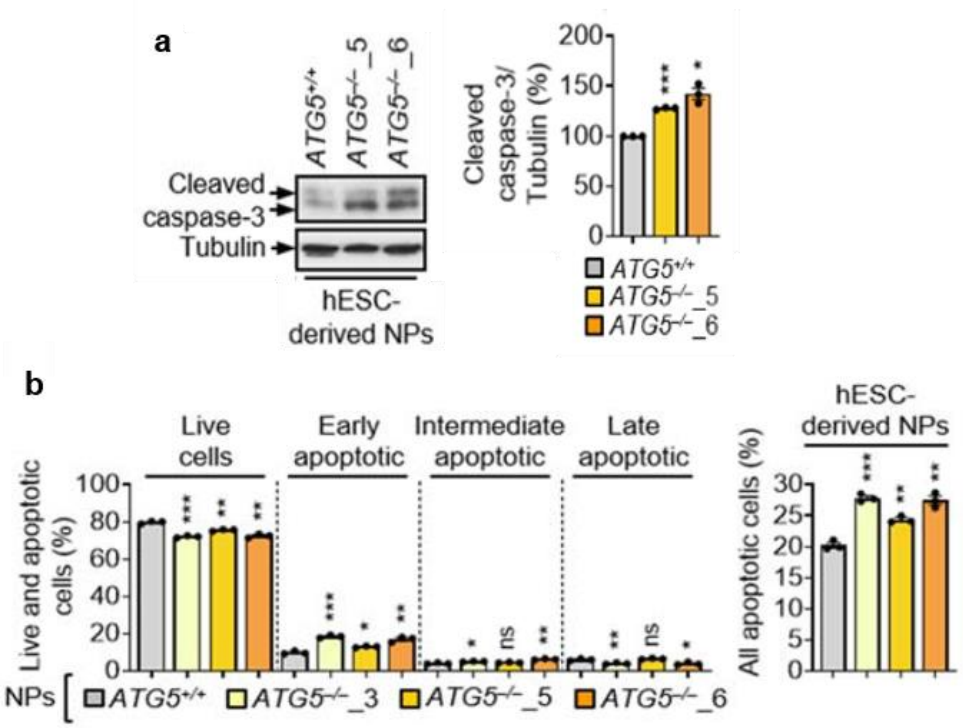


Figure 2.10. Increased cell death in autophagy-deficient hESC-derived neural precursors.

a, Immunoblotting analyses with anti-cleaved caspase-3 and anti-Tubulin antibodies in *ATG5*$^{+/+}$, *ATG5*$^{-/-}$_5 and *ATG5*$^{-/-}$_6 hESC-derived neural precursors (NPs).

b, Analyses of live and apoptotic (early, intermediate and late) cells with FITC-Annexin V and propidium iodide staining by FACS in *ATG5*$^{+/+}$ and multiple clones of *ATG5*$^{-/-}$ hESC-derived NPs.

Representative immunoblot (**a**) shown from one of 3 independent experiments. Graphical data (**a, b**) are mean ± s.e.m. (n = 3) from 3 independent experiments. *P* values were calculated by unpaired two-tailed Student's *t*-test (**a, b**). ***, p<0.001; **, p<0.01; *, p<0.05; ns, non-significant.

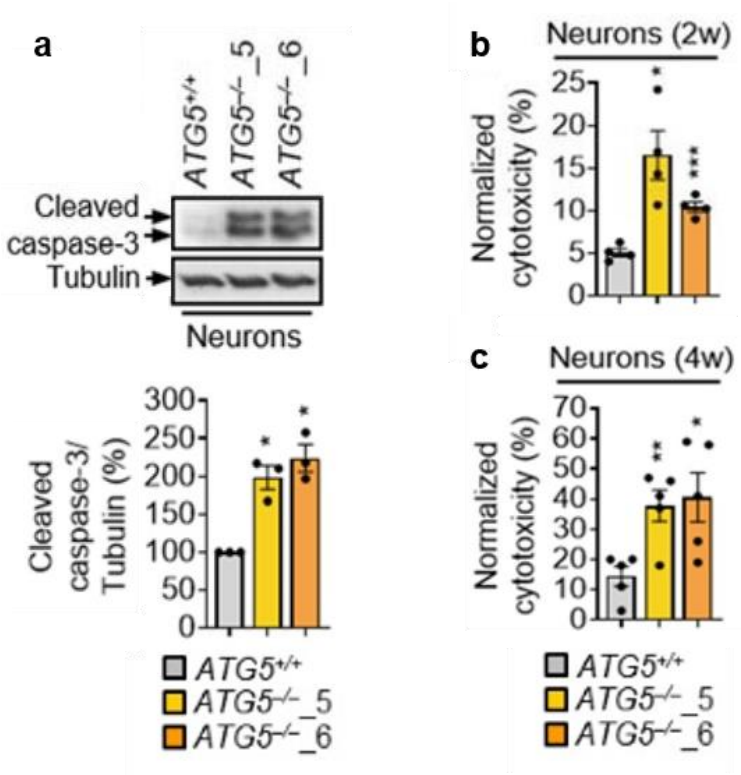


Figure 2.11. Increased cell death in autophagy-deficient hESC-derived neurons.

a, Immunoblotting analyses with anti-cleaved caspase-3 and anti-Tubulin antibodies in *ATG5*$^{+/+}$, *ATG5*$^{-/-}$_5 and *ATG5*$^{-/-}$_6 hESC-derived neurons (4 weeks old).

b, c, Cytotoxicity assay in *ATG5*$^{+/+}$, *ATG5*$^{-/-}$_5 and *ATG5*$^{-/-}$_6 hESC-derived neurons at 2 weeks or 4 weeks of neuronal differentiation.

Representative immunoblot (**a**) shown from one of 3 independent experiments. Graphical data (**a-c**) are mean ± s.e.m. (n = 3–5). *P* values were calculated by unpaired two-tailed Student's *t*-test (**a-c**) from 3 independent experiments. ***, p<0.001; **, p<0.01; *, p<0.05.

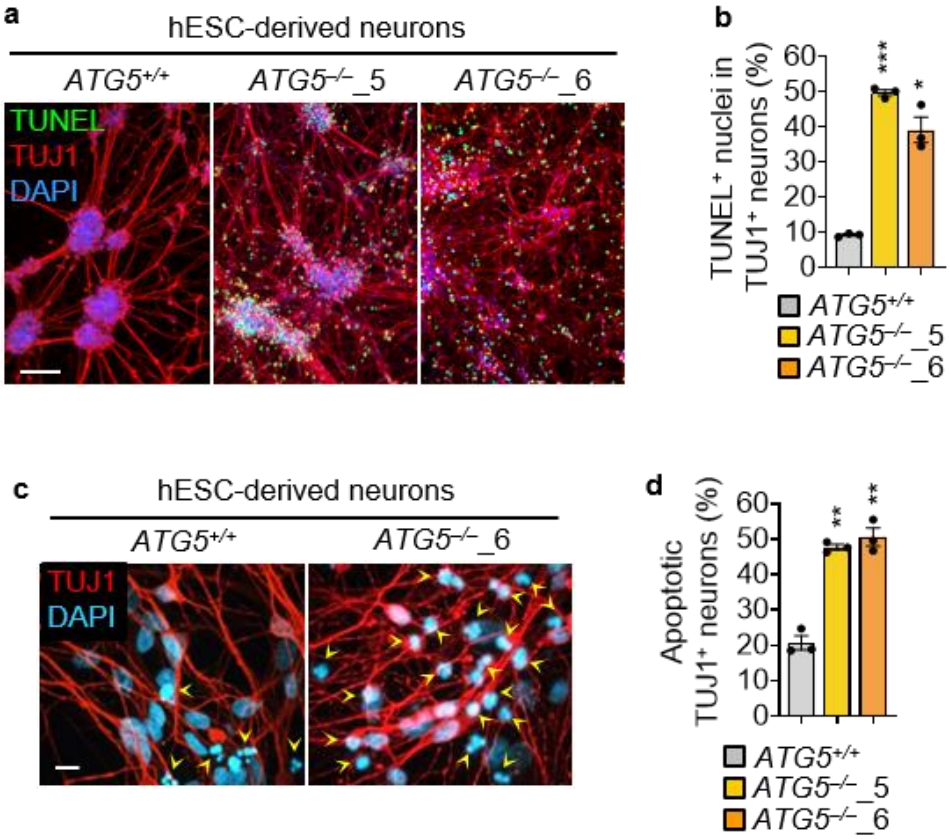


Figure 2.12. Increased apoptotic nuclei in autophagy-deficient hESC-derived neurons.

a, b, TUNEL staining in *ATG5*$^{+/+}$, *ATG5*$^{-/-}$_5 and *ATG5*$^{-/-}$_6 hESC-derived neurons (4 weeks old), immunostained with anti-TUJ1 antibody (**a**), where TUNEL^{+} nuclei were analysed in TUJ1^{+} cells (**b**).

c, d, Immunofluorescence analysis with anti-TUJ1 antibody along with DAPI staining (**c**) in *ATG5*$^{+/+}$, *ATG5*$^{-/-}$_5 and *ATG5*$^{-/-}$_6 hESC-derived neurons (4 weeks old), where apoptotic nuclear morphology was analysed in TUJ1^{+} cells (**d**).

Representative images (**a**, **c**) shown from one of 3 independent experiments. Graphical data (**b, d**) are mean ± s.e.m. (n = 3) where *P* values were calculated by unpaired two-tailed Student's *t*-test from 3 independent experiments. ***, $p<0.001$; **, $p<0.01$; *, $p<0.05$; ns, non-significant. Scale bar, 100 µm (**a, c**).

of cell death. *ATG5*$^{-/-}$ neurons displayed significantly more TUNEL^{+} nuclei compared to the wild-type *ATG5*$^{+/+}$ neurons (Figures 2.12a,b). Besides, apoptotic nuclear morphology was also assessed after DAPI staining (Kerr et al., 1972). Consistent with the TUNEL data, *ATG5*$^{-/-}$ neurons had significantly more apoptotic DAPI-stained nuclei compared to *ATG5*$^{+/+}$ neurons (Figures 2.12c,d). By confirming the cell death phenotype in *ATG5*$^{-/-}$ neurons via multiple methodologies, these data collectively suggest that autophagy deficiency reduces cell viability in human neurons.

2.4. Chapter summary

The focus of this chapter was to establish a genetic model of autophagy deficiency in hESCs and hESC-derived cell types, particularly in neurons, to investigate the role of autophagy in cellular homeostasis that has implications in human disease associated with defective autophagy. The pluripotency of autophagy-deficient *ATG5*$^{-/-}$ hESCs did not seem to be overtly affected after *ATG5* gene knockout. Moreover, these *ATG5*$^{-/-}$ hESCs could be differentiated into NPs and neurons, suggesting that their differentiation capability was not affected due to the loss of autophagy. The *ATG5*$^{-/-}$ hESCs, NPs and neurons expressed cell-specific markers comparable to that of their wild-type counterparts. Loss of autophagy was confirmed in all these *ATG5*$^{-/-}$ cells by multiple autophagy markers. Additionally, rescue of functional autophagic flux by introduction of *ATG5* mRNA via lipid nanoparticles further confirmed the genetic knockout system in this hESC-based model. Importantly, all these *ATG5*$^{-/-}$ cells exhibited higher basal cell death compared to the wild-type cells, as analysed via multiple methodologies. In a nutshell, hESC-based isogenic human cellular platforms with autophagy deficiency were established that will be utilised to investigate the role of autophagy in cellular homeostasis and viability.

Chapter 3

Metabolic and mitochondrial defects mediate cytotoxicity during autophagy deficiency

Chapter 3: Metabolic and mitochondrial defects mediate cytotoxicity during autophagy deficiency

3.1. Overview

In the previous chapter, once autophagy-deficient human cellular platforms were established, their cell death phenotype was confirmed as expected. The goal of this chapter is to investigate what cellular mechanisms underlying cell death are primarily affected due to autophagy deficiency. The *ATG5*$^{-/-}$ hESC and neuronal platforms would be advantageous for identifying any cell-specific or common perturbations, because they were generated via genome engineering from the same parental hESC (WIBR3) line, and therefore isogenic for having the same genetic background.

In this chapter, a metabolic defect was identified in autophagy-deficient cells via unbiased metabolic profiling. This was found to be due to NADH depletion, which in turn was found to cause mitochondrial depolarisation and oxidative stress, subsequently leading to cell death. This potential mechanism was supported by using NADH-boosting compounds that rescued the mitochondrial and cell death phenotypes. In order to further demonstrate the implication of the data arising from the genetic autophagy knockout model to a disease-relevant model, such as of neurodegeneration, hiPSC models of a neurodegenerative lipid storage disorder (NPC1 disease) was utilised where the NADH-boosting compounds were found to be cytoprotective.

The objectives/milestones of this results chapter include:

(1) An unbiased approach (metabolomics) to determine changes in biological pathways linked to cell death in autophagy-deficient cells
(2) Investigation of the cytotoxicity mechanism in *ATG5*$^{-/-}$ cells according to the perturbations from metabolic profiling (such as NADH depletion).
(3) Demonstration of rescue in cell death phenotype by pharmacological agents (by NADH-boosting compounds) in *ATG5*$^{-/-}$ neurons and in a clinically-relevant neuronal model of a neurodegenerative disease.

3.2. Introduction to the role of autophagy in metabolic homeostasis

As a catabolic pathway crucial for cellular functioning, autophagy is known to be involved in maintenance of metabolic homeostasis. Bulk degradation of cytoplasmic materials during non-selective autophagy following nutrient starvation releases a broad range of metabolites as breakdown products. For instance, the digestion of glycogen by autophagy releases glucose, which is used for glycolysis. The resulting pyruvate, after being converted to acetyl-CoA, is utilised by the tricarboxylic acid (TCA) cycle; the NADH generated through TCA cycle is utilised in oxidative phosphorylation. Otherwise, glucose is converted into substrates for anabolic synthesis. Alternatively, glucose via its conversion into glucose-6-phosphate is shunted to the oxidative pentose phosphate pathway to form ribulose-5-phosphate, which serves as a precursor for NAD and NADP (Rabinowitz and White, 2010). Additionally, the amino acids released from the breakdown of proteins can also be used as TCA cycle substrates and be later utilised for oxidative phosphorylation (Galluzzi et al., 2014). Because of this involvement of autophagy in the input of building blocks for TCA cycle and consequently oxidative phosphorylation utilisation, the interplay between autophagy and metabolism was next investigated.

Another role of autophagy in relation to aerobic metabolism is through the mitochondrial quality control. Selective clearance of damaged mitochondria by autophagy, termed mitophagy, is essential for the maintenance of mitochondrial health. Mitochondria are important cellular organelles that contribute to ATP production and regulate Ca^{2+} calcium availability (Lemasters, 2014). However, mitochondria can also contribute to the production of excess reactive oxygen species (ROS) when dysfunctional. ROS affects the cell in multiple ways, such as cellular membrane and DNA damage, as well as improper ATP production (Lemasters, 2014). Moreover, damaged mitochondria release pre-apoptotic molecules, leading to cell death (Wang and Youle, 2009). For these reasons, it is imperative to have tight mitochondrial quality control mechanisms in place, for which mitophagy plays a crucial part. Specialised mitophagy receptors tag dysfunctional mitochondria and capture them into autophagosomes to initiate their digestion via mitophagy. Constitutive basal autophagy occurs in all the cells for housekeeping functions including removal of excess or damaged organelles, but when there is an accumulation of damaged mitochondria, the levels of mitophagy are elevated. In metabolically active tissues

where mitochondrial function is required more, basal autophagy is also higher to ensure healthy mitochondrial population (McWilliams et al., 2018).

3.3. Results

3.3.1. Metabolic defects in autophagy-deficient hESCs and neurons

After generating and characterising *ATG5*$^{-/-}$ hESC-derived neurons, the major objective was to investigate what cellular mechanisms underlying neuronal cell death are primarily affected due to autophagy deficiency. Since autophagy promotes metabolic homeostasis by recycling cytoplasmic components and providing inputs to cellular anabolic processes (Lahiri et al., 2019; Rabinowitz and White, 2010), the apoptotic phenotypes of autophagy-deficient cells at basal state might arise from a metabolic failure (Altman and Rathmell, 2012). Although depletion of several metabolites, amino acids and nucleotides associated with loss of autophagy has been previously reported in immortalised cells and mouse models (Kuma et al., 2004; Mizushima et al., 2011; Fernie et al., 2004), the significance of this metabolic perturbation to cytotoxicity is not elucidated. To investigate whether any specific metabolic defect underlies cytotoxicity during autophagy deficiency, an unbiased metabolomics profiling via liquid chromatography–mass spectrometry (LC-MS) was performed in wild-type (*ATG5*$^{+/+}$) and autophagy-deficient (*ATG5*$^{-/-}$) hESCs and hESC-derived neurons.

Significant alterations of many metabolites related to glycolysis and TCA cycle, energy carriers such as ATP, ADP, NAD^+ and NADH, and various amino acids, were found in *ATG5*$^{-/-}$ cells compared to *ATG5*$^{+/+}$ cells (Figures 3.1a-d). Interestingly, *ATG5*$^{-/-}$ hESCs and neurons revealed differential metabolic perturbations (Figures 3.1c,d), likely due to cell-specific metabolic requirements to meet their energy demands. In fact, hESCs rely on glycolysis for energy production and pluripotency, but upon differentiation, switch to mitochondrial oxidative phosphorylation (OXPHOS) (Verdin, 2015). Indeed, differentiated cells like neurons having high energy demands are highly reliant on mitochondrial OXPHOS for ATP generation (Ying, 2008). Interestingly, glycolysis seems to be further downregulated in *ATG5*$^{-/-}$ neurons, and the majority of the amino acids were also depleted (Figure 3.1d). Moreover, the starting molecules of

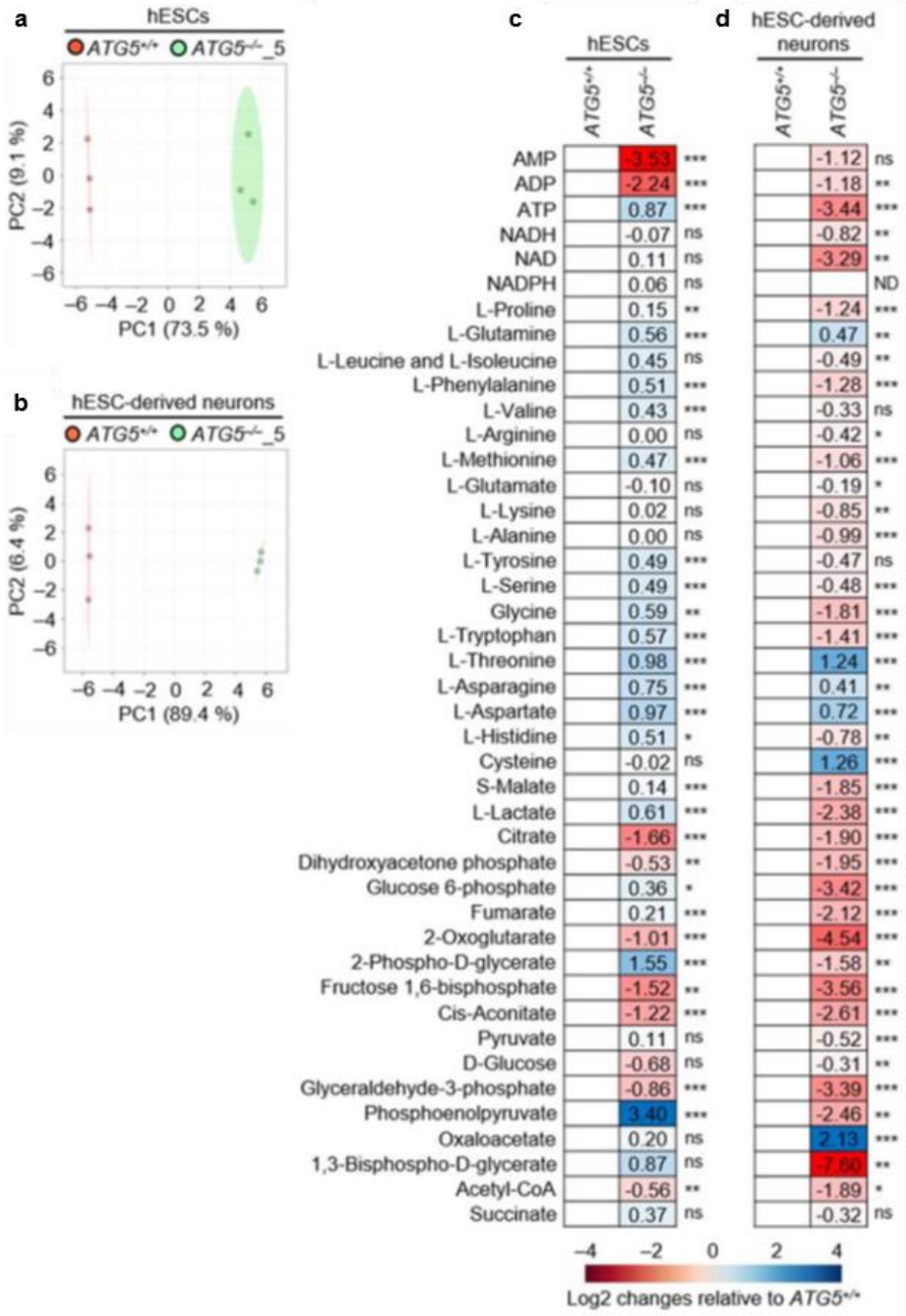


Figure 3.1. Autophagy-deficient hESCs and neurons have perturbed metabolic profiles.

a, b, Two-dimensional principal component analysis (PCA) scores plots of samples using metabolites in *ATG5*$^{+/+}$ and *ATG5*$^{-/-}$_5 hESCs (**a**) and hESC-derived neurons (3 weeks old) (**b**).

c, d, Metabolic profiling in *ATG5*$^{+/+}$ and *ATG5*$^{-/-}$_5 hESCs (**c**) and hESC-derived neurons (3 weeks old) (**d**), depicted as heatmaps of log2 (fold change) of *ATG5*$^{+/+}$ to *ATG5*$^{-/-}$ cells. *P* values were calculated by Student's *t*-test using Benjamini and Hochberg FDR method (n = 3) on 3 independent biological replicates.

LC-MS metabolomics was performed by Oliver Maddocks (University of Glasgow), and bioinformatics analysis was performed by Animesh Acharjee (University of Birmingham).

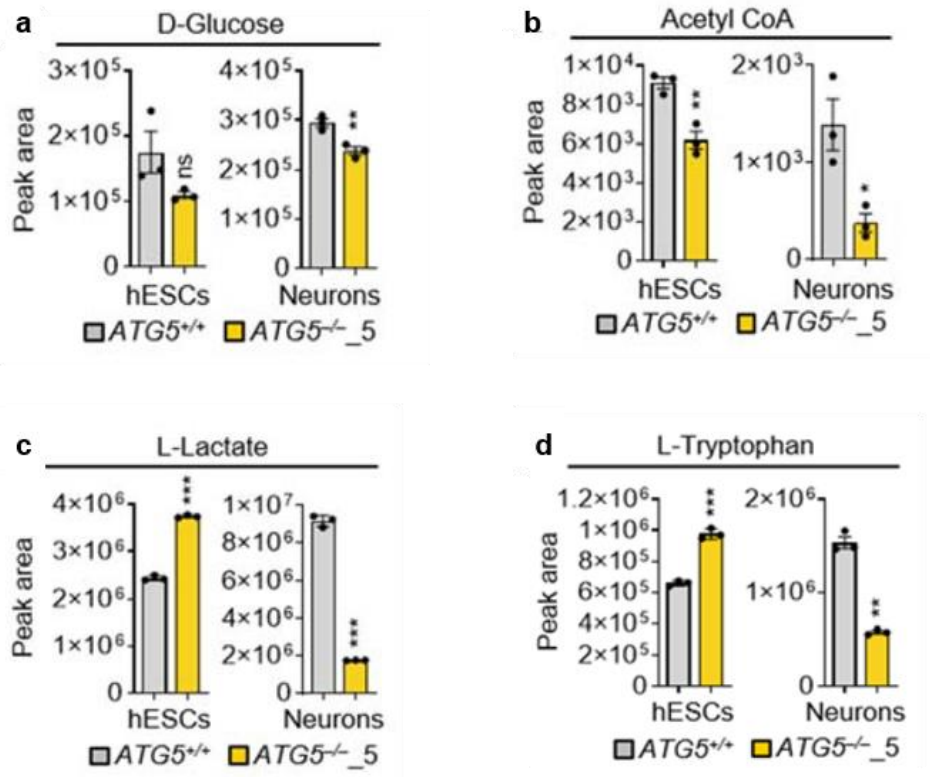


Figure 3.2. Perturbation of specific metabolites in autophagy-deficient hESCs and hESC-derived neurons.

a-d, Analyses of D-Glucose (**a**), acetyl CoA (**b**), L-Lactate (**c**) and L-Tryptophan (**d**) by LC-MS in *ATG5*$^{+/+}$ and *ATG5*$^{-/-}$_5 hESCs and hESC-derived neurons (3 weeks old).

Graphical data are mean ± s.e.m. (n = 3). *P* values were calculated by unpaired two-tailed Student's *t*-test on 3 independent biological replicates. ***, $p<0.001$; **, $p<0.01$; *, $p<0.05$; ns, non-significant.

glycolysis (glucose) and TCA cycle (acetyl-CoA) were reduced in both *ATG5*$^{-/-}$ hESCs and neurons (Figures 3.2a,b), suggesting that these metabolic pathways are affected.

3.3.2. Depletion of NADH is a common underlying perturbation in autophagy-deficient hESCs and neurons, and in other non-hESC model systems

Since cell death was observed in both *ATG5*$^{-/-}$ hESCs and neurons, one question is whether a common metabolic defect elicited due to autophagy deficiency. Amongst the common positively or negatively changed metabolites (Figures 3.3a,b), this study focused on those showing a reduction that include certain glycolytic and TCA cycle intermediates along with AMP, ADP and possibly NADH (Figure 3.3a). The overall yield from glycolysis and TCA cycle normally constitutes ATP and NADH, and lowering of these energy carriers could trigger energetic deficit (Youle and Narendra, 2010). Unbiased metabolomics data and more specific luminescence-based assay showed significant reduction of ATP levels in *ATG5*$^{-/-}$ neurons (Figures 3.1d and 3.4b); but surprisingly, ATP was significantly increased in *ATG5*$^{-/-}$ hESCs (Figures 3.1c and 3.4a). This could be possibly due to enhanced glycolysis in autophagy-deficient hESCs because lactate was increased and glucose was decreased, as revealed by LC-MS metabolomics (Figures 3.2a,c).

However, although unbiased metabolomics showed significant depletion of NADH in *ATG5*$^{-/-}$ neurons whereas its decrease in *ATG5*$^{-/-}$ hESCs was non-significant (Figures 3.1c,d), more specific colourimetric-based assay revealed significant depletion of NADH in both these *ATG5*$^{-/-}$ cell-types (Figure 3.4c). In contrast, NAD^+ (oxidised form) was significantly lower only in *ATG5*$^{-/-}$ neurons (Figure 3.4d), possibly due to shortage of substrates like the essential amino acid L-Tryptophan required for its *de novo* synthesis (Fang et al., 2017)(Figure 3.2d).

Therefore, depletion of NADH in autophagy-deficient hESCs and neurons could possibly be a common metabolic determinant of cell death. Moreover, our related collaborative study in non-hESC systems involving *in vitro* (immortalised MEFs, primary human fibroblasts) and *in vivo* (*Drosophila*, yeast) models of autophagy deficiency or dysfunction indicate NADH depletion as the primary cause for cell death (Sedlackova et al., 2020, BioRxiv https://doi.org/10.1101/2020.01.31.928424). Thus, the consequences of NADH depletion on cell death was next studied in the context of autophagy deficiency in hESCs and hESC-derived human neurons.

a Common negative changes in metabolites in *ATG5*$^{-/-}$ hESCs and hESC-derived neurons

Negative change in metabolites (ATG5$^{-/-}$ *to ATG5*$^{+/+}$ *)*	*hESCs*		*hESC-derived neurons*	
	Log2 (FC)	*Log10 (p adjusted)*	*Log2 (FC)*	*Log10 (p adjusted)*
AMP	-3.527	4.908	-1.124	0.684
ADP	-2.235	4.525	-1.176	2.316
NADH	-0.066	0.791	-0.818	2.170
L-Glutamate	-0.103	3.122	-0.193	1.498
Citrate	-1.663	3.831	-1.897	3.301
Dihydroxyacetone phosphate	-0.530	2.091	-1.949	4.674
2-Oxoglutarate	-1.007	5.094	-4.542	3.753
Fructose-1,6-bisphosphate	-1.523	2.685	-3.560	3.265
Cis-Aconitate	-1.219	3.250	-2.615	4.380
D-Glucose	-0.675	0.967	-0.308	2.086
Glyceraldehyde-3-phosphate	-0.860	4.642	-3.394	6.203
Acetyl CoA	-0.561	2.276	-1.888	1.665

b Common positive changes in metabolites in *ATG5*$^{-/-}$ hESCs and hESC-derived neurons

Positive change in metabolites (ATG5$^{-/-}$ *to ATG5*$^{+/+}$ *)*	*hESCs*		*hESC-derived neurons*	
	Log2 (FC)	*Log10 (p adjusted)*	*Log2 (FC)*	*Log10 (p adjusted)*
L-Glutamine	0.561	3.122	0.472	2.859
L-Threonine	0.979	5.384	1.238	4.242
L-Asparagine	0.746	3.788	0.411	2.321
L-Aspartate	0.966	5.219	0.722	3.656
Oxaloacetate	0.201	0.442	2.129	4.636

Figure 3.3. Common negative and positive changes in metabolites in autophagy-deficient hESCs and hESC-derived neurons.

a, b, List of common negative (**a**) and positive (**b**) changes in metabolites (log2 fold changes) in *ATG5*$^{+/+}$ and *ATG5*$^{-/-}$_5 hESCs and hESC-derived neurons (3 weeks old).

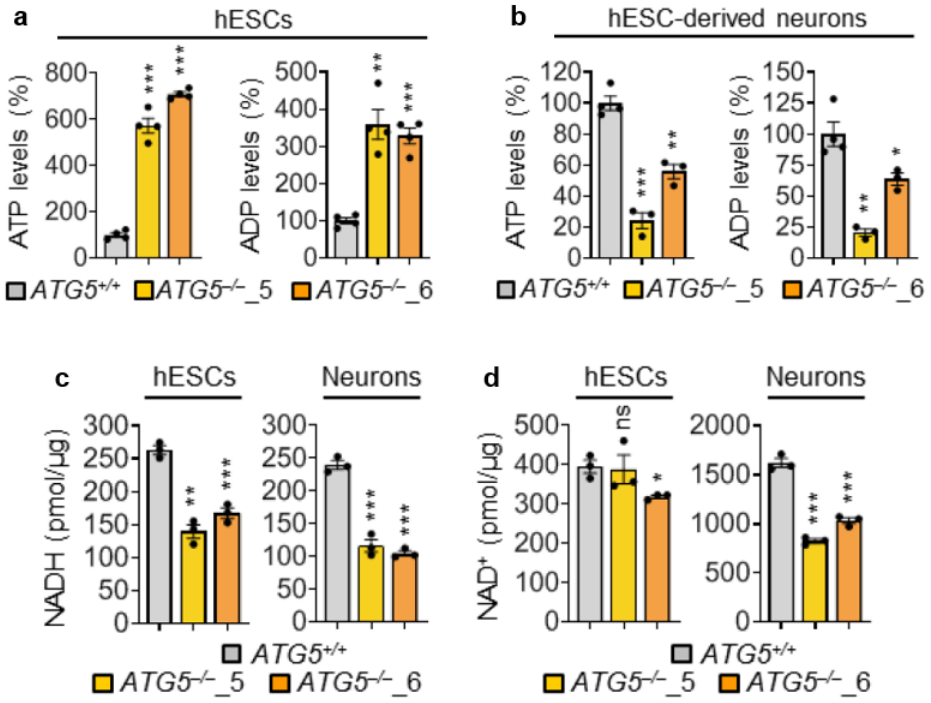


Figure 3.4. Alterations of the levels of energy carriers in autophagy-deficient hESCs and hESC-derived neurons.

a, b, Analyses of ATP and ADP levels in *ATG5*$^{+/+}$, *ATG5*$^{-/-}$_5 and *ATG5*$^{-/-}$_6 hESCs (**a**) and hESC-derived neurons (3 weeks old) (**b**) by colourimetric assay.

c, d, Analyses of NADH (**c**) and NAD$^+$ (**d**) levels in *ATG5*$^{+/+}$, *ATG5*$^{-/-}$_5 and *ATG5*$^{-/-}$_6 hESCs and hESC-derived neurons (3 weeks old) by colourimetric assay.

Graphical data are mean ± s.e.m. (n = 3 or 4). *P* values were calculated by unpaired two-tailed Student's *t*-test from 3 independent experiments. ***, $p<0.001$; **, $p<0.01$; *, $p<0.05$; ns, non-significant.

3.3.3. Autophagy-deficient hESCs and neurons exhibit mitochondrial depolarisation and elevation in ROS

The next goal is to study how depletion of NADH could mediate cytotoxicity in autophagy-deficient human cells. Oxidation of NADH mediates the generation of mitochondrial membrane potential (ΔΨm), in which the flow of electrons (donated by NADH) through the mitochondrial electron transport chain (ETC) together with the pumping of protons create an electrochemical proton gradient; which eventually drives ATP production by the mitochondrial F_0F_1-ATP synthase (Lautrup et al., 2019). Therefore, it is possible that depletion of NADH in autophagy-deficient cells could dissipate ΔΨm and mediate cytotoxicity. In order to test this hypothesis, ΔΨm was assessed by TMRE (tetramethylrhodamine, ethyl ester), a cell-permeant, cationic, red-orange fluorescent dye that gets readily sequestered by active mitochondria and thus serves as an indicator of mitochondrial polarisation (Farrelly et al., 2001). The ΔΨm was evaluated as the delta (Δ) fluorescence of TMRE, calculated by subtracting the basal fluorescence from the maximum fluorescence intensity after treatment of FCCP [carbonyl cyanide-4-(trifluoromethoxy)phenylhydrazone] (e Silva et al., 2019, Rosenstock et al., 2004). FCCP is a mitochondrial oxidative phosphorylation uncoupler, causing the disruption of ATP synthesis by transporting protons across the mitochondrial inner membranes. Using this standard TMRE assay, *ATG5*$^{-/-}$ hESCs and neurons displayed a significant reduction in ΔΨm compared to their wild-type counterparts (Figure 3.5a), suggesting that mitochondria are depolarised in these autophagy-deficient cells. Mitochondrial dysfunction is responsible for the production of ROS to a significant degree in mammalian cells (Murphy, 2008; Mailloux, 2015). ROS are oxygen-containing molecules that are highly reactive with nucleic acids, proteins and lipids (Kehrer, 1993), and excessive amounts of ROS can be damaging to the cells by triggering apoptosis (Matés and Sánchez-Jiménez, 2000; Fleury et al., 2002). Hence, ROS was measured in autophagy-deficient cells via CM-H_2DCFDA dye, which is a standard methodology. Mitochondrial depolarisation has been reported to be accompanied by a phenotype where increased ROS has been observed (Park, J., et al., 2011). Consistent with mitochondrial depolarisation, elevation in ROS levels was detected in *ATG5*$^{-/-}$ hESCs and neurons (Figure 3.5b). Together, these data reveal that mitochondrial depolarisation and increased ROS are associated with autophagy deficiency.

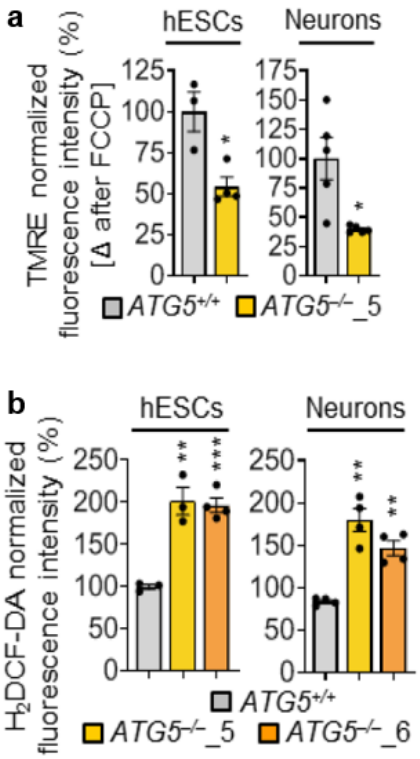


Figure 3.5. Mitochondrial depolarisation and elevation in ROS in autophagy-deficient hESCs and hESC-derived neurons.

a, Analysis of mitochondrial membrane potential (ΔΨm) by TMRE fluorescence intensity (measurement before or after FCCP treatment) in *ATG5*$^{+/+}$ and *ATG5*$^{-/-}$_5 hESCs and hESC-derived neurons (3 weeks old).

b, Analyses of reactive oxygen species (ROS) levels by H_2DCF-DA fluorescence intensity in *ATG5*$^{+/+}$, *ATG5*$^{-/-}$_5 and *ATG5*$^{-/-}$_6 hESCs and hESC-derived neurons (3 weeks old).

Graphical data are mean ± s.e.m. (n = 3–5). *P* values were calculated by unpaired two-tailed Student's *t*-test on 3 independent experiments. ***, $p<0.001$; **, $p<0.01$; *, $p<0.05$.

3.3.4. Autophagy-deficient hESCs and neurons are associated with mitochondrial fragmentation and impaired clearance of fragmented mitochondria

Further to observing mitochondrial dysfunction in autophagy-deficient cells, mitochondrial network integrity was studied by analysing mitochondrial rod length. This was measured by MitoTracker staining or by immunostaining for Tom20. Tom20 is part of the mitochondrial outer membrane translocase complex, which coordinates the import of most proteins into the mitochondria (Perry et al., 2008; Rapaport, 2005), wherein TOM20 functions as a primary receptor for mitochondrial precursor proteins (Hachiya et al., 1995). MitoTracker, a fluorescent dye that localises to mitochondria irrespective of ΔΨm and is retained after fixation; often used an additional assay to confirm the data on mitochondrial network obtained with TOM20 immunostaining.

Concomitant with increased ROS found in autophagy-deficient cells, mitochondrial fragmentation was observed in *ATG5*$^{-/-}$ hESCs and hESC-derived neurons via Tom20 immunofluorescence or MitoTracker staining, compared to the respective wild-type cell types (Figures 3.6a-f). This phenotype was also found in *ATG5*$^{-/-}$ hESC-derived neural precursors (NPs) (Figures 3.7a-d). The hESC-derived cell types were also immunostained with cell-specific markers, such as TUJ1 for neurons (Figures 3.6c,e) or NESTIN for NPs (Figure 3.7a), to confirm the cellular identity. Evidently, significant mitochondrial fragmentation was consistent across all the isogenic *ATG5*$^{-/-}$ cell types analysed, implicating that this phenotype is being affected by autophagy deficiency. As a consequence of mitochondrial depolarisation, damaged mitochondria are removed via mitophagy (Zhang et al., 2015), which is important for cellular homeostasis but crucial particularly for post-mitotic neurons. Due to lack of autophagy, it is expected that mitophagy will be suppressed in *ATG5*$^{-/-}$ cells. Although *ATG5*$^{-/-}$ neurons had increased mitochondrial load as seen by substantial elevation of Tom20 levels via immunoblotting, surprisingly *ATG5*$^{-/-}$ hESCs displayed no change in Tom20 levels compared to that of the wild-type cells (Figure 3.8a). This is possibly due to proliferation of hESCs, but not neurons, diluting the accumulating mitochondria in autophagy-deficient cells. Increased mitochondrial load in *ATG5*$^{-/-}$ neurons was further confirmed by immunostaining with anti-Tom20 and anti-TUJ1 antibodies where high Tom20 fluorescence intensity was observed (Figure 3.8b).

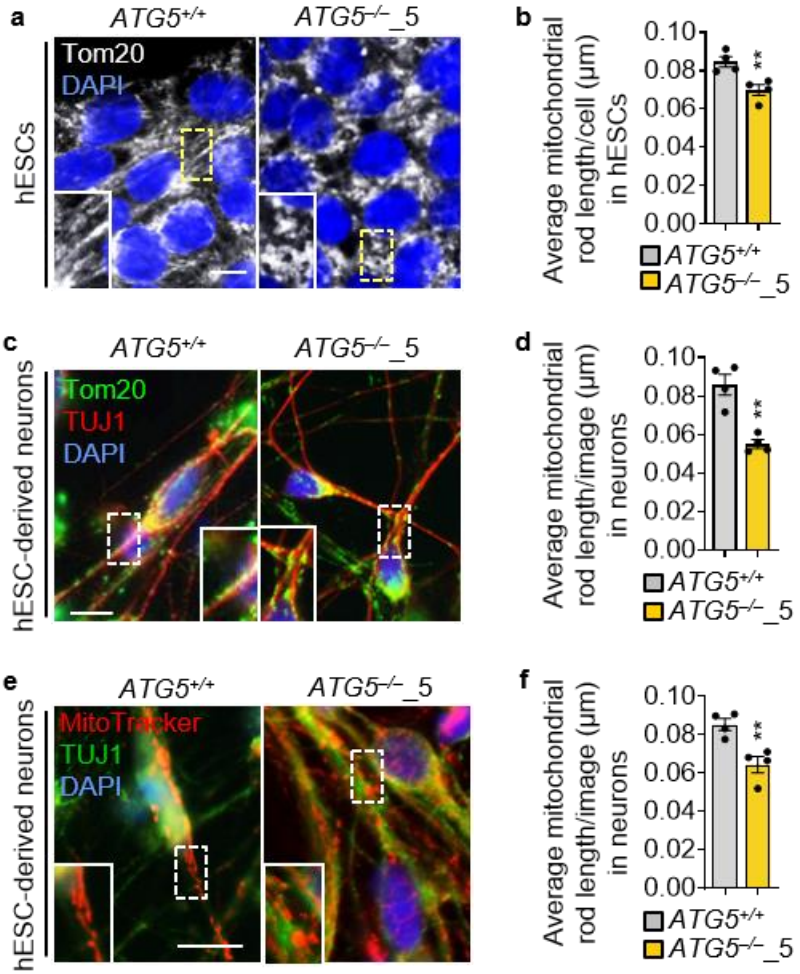


Figure 3.6. Increased mitochondrial fragmentation in autophagy-deficient hESCs and hESC-derived neurons.

a, b, Immunofluorescence with anti-Tom20 antibody (**a**) and analyses of average mitochondrial rod length per cell (**b**) in *ATG5*$^{+/+}$ and *ATG5*$^{-/-}$_5 hESCs.

c, d, Immunofluorescence with anti-Tom20 and anti-TUJ1 antibodies (**c**) and analyses of average mitochondrial rod length per image (**d**) in *ATG5*$^{+/+}$ and *ATG5*$^{-/-}$_5 hESC-derived neurons (3 weeks old).

e, f, MitoTracker staining together with TUJ1 immunostaining (**e**) and analysis of average mitochondrial rod length per image (**f**) in *ATG5*$^{+/+}$ and *ATG5*$^{-/-}$_5 hESC-derived neurons (3 weeks old).

Graphical data (**b, d, f**) are mean ± s.e.m. (n = 4). *P* values were calculated by unpaired two-tailed Student's *t*-test (**b, d, f**) from 3 independent experiments. **, $p<0.01$. Representative images (**a**, **c**, **e**) shown from one of 3 independent experiments. Scale bar, 10 µm (**a, c, e**).

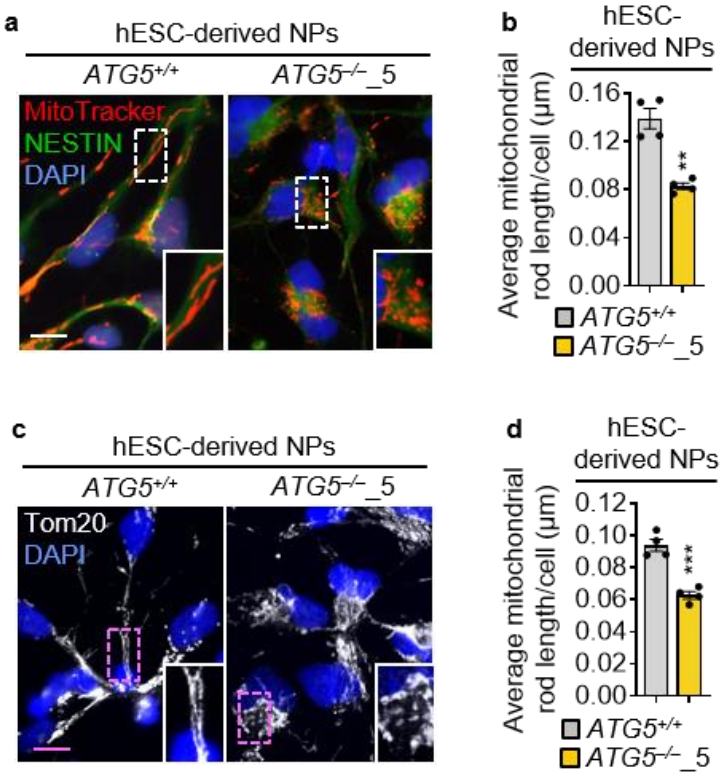


Figure 3.7. Increased mitochondrial fragmentation in autophagy-deficient hESC-derived neural precursors.

a, b, MitoTracker staining together with NESTIN immunostaining (**a**) and analysis of average mitochondrial rod length per cell (**b**) in *ATG5*$^{+/+}$ and *ATG5*$^{-/-}$_5 hESC-derived neural precursors (NPs).

c, d, Immunofluorescence with anti-Tom20 antibody (**c**) and analysis of average mitochondrial rod length per cell (**d**) in *ATG5*$^{+/+}$ and *ATG5*$^{-/-}$_5 hESC-derived NPs.

Graphical data (**b, d**) are mean ± s.e.m. (n = 4). *P* values were calculated by unpaired two-tailed Student's t-test (**b, d**) from 3 independent experiments. ***, p<0.001; **, p<0.01. Representative images (**a**, **c**) shown from one of 3 independent experiments. Scale bar, 10 µm (**a, c**).

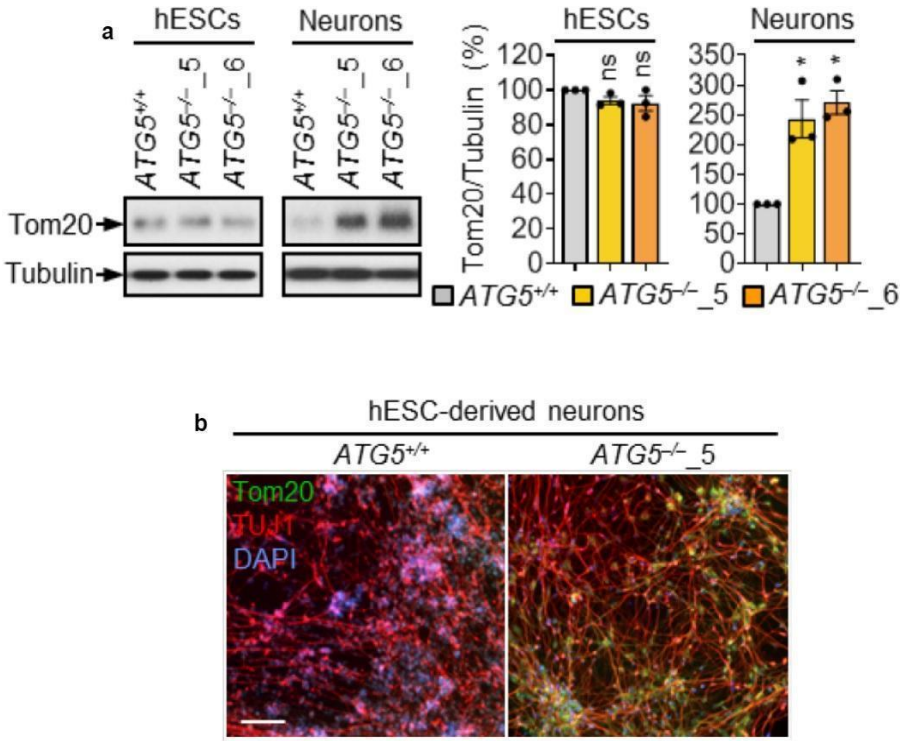


Figure 3.8. Impaired mitophagy in autophagy-deficient hESC-derived neurons.

a, Immunoblotting analyses with anti-Tom20 and anti-Tubulin antibodies in *ATG5*$^{+/+}$, *ATG5*$^{-/-}$_5 and *ATG5*$^{-/-}$_6 hESCs and hESC-derived neurons (3 weeks old).

b, Immunofluorescence analysis with anti-Tom20 and anti-TUJ1 antibodies in *ATG5*$^{+/+}$ and *ATG5*$^{-/-}$_5 hESC-derived neurons (3 weeks old).

Representative immunoblot (**a**) shown from one of 3 independent experiments. Graphical data (**a**) are mean ± s.e.m. (n = 3). *P* values were calculated by unpaired two-tailed Student's *t*-test from 3 independent experiments.*, $p<0.05$; ns, non-significant. Representative images (**b**) shown from 1 experiment. Scale bar, 100 µm (**b**).

3.3.5. NAD/NADH boosting compounds improve neuronal and mitochondrial phenotypes, and rescue cell death in autophagy-deficient neurons

Collectively, the data so far indicate that autophagy-deficient cells, which have a deficit in NADH and other metabolites, is associated with mitochondrial dysfunction and fragmentation along with elevation in ROS. Therefore, it is plausible that NADH depletion could link autophagy deficiency to cell death via mitochondrial depolarisation. To test this hypothesis, compounds that could boost NAD^+ and consequently NADH levels were utilised to study whether these pharmacological agents could prevent cell death in autophagy-deficient cells. A well-known strategy is supplementation with the NAD^+ precursor, nicotinamide (NAM) (Barrow et al., 2016). Additional means to elevate NADH include suppression of mitochondrial NADH consumption. This could be achieved with compounds such as CP2, which inhibits mitochondrial ETC complex I and prevents the use of NADH as a substrate (Ordonez et al., 2012); and I-BET 525762A (I-BET), previously shown to increase respiration through ETC complex II that consumes $FADH_2$ rather than NADH as a substrate (Hansen et al., 2018).

Initially, the effects of NAM, CP2 and I-BET in rescuing cell death in *ATG5*$^{-/-}$ hESCs and hESC-derived neurons was analysed by luminescence-based cytotoxicity assay, which measures the extracellular activity of a distinct dead-cell protease when it is released from membrane-compromised cells. As expected, untreated *ATG5*$^{-/-}$ cells had increased cytotoxicity compared to the untreated *ATG5*$^{+/+}$ cells (Figure 3.9a,b). All the NAD/NADH boosting agents significantly reduced cytotoxicity in both the *ATG5*$^{-/-}$ hESCs (Figure 3.9a) and hESC-derived neurons (Figure 3.9b). Furthermore, cell death was analysed in *ATG5*$^{-/-}$ neurons by measuring apoptotic nuclei via TUNEL assay together with immunostaining for the neuronal marker, TUJ1. Similar to the cytotoxicity data, the NAD/NADH boosting compounds significantly reduced apoptotic $TUNEL^+$ nuclei in $TUJ1^+$ *ATG5*$^{-/-}$ neurons (Figures 3.9c,d). These results suggest that boosting NAD/NADH levels in autophagy-deficient cells, which exhibit deficit in NADH and increase in cell death, improves cell viability.

Further to analysing cell death, neuronal phenotypes such as axonal length was also studied. Axonal health is related to good neuronal connectivity, and axonal loss often precedes somatic loss (Kordower et al., 2013). Axonal degeneration from injury differs

from the neuronal phenotypes related to apoptosis (Sagot et al., 1995; Deckwerth and Johnson, 1994). Axonal segmentation is one of the physical changes observed in neurodegeneration and is related to apoptosis (Kneynsberg et al., 2016). Interestingly, a significant reduction in axonal length was found in *ATG5*$^{-/-}$ neurons, compared to *ATG5*$^{+/+}$ neurons (Figures 3.10a,b); a phenotype compatible with increased cell death in autophagy-deficient neurons. Treatment of *ATG5*$^{-/-}$ neurons with NAD/NADH boosting compounds like NAM, CP2 and I-BET, which could rescue cell death (Figures 3.9b-d), also improved axonal length in autophagy-deficient neurons (Figures 3.10a,b). This could be indicative of recovery in neuronal health in autophagy-deficient neurons following their improvement in cell viability.

Next, the effects of NAD/NADH boosting treatments on the restoration of NADH levels and ΔΨm was assessed in order to study whether these changes were associated with the cytoprotective effects of the compounds. Indeed, NAM, CP2 and I-BET substantially increased NADH in *ATG5*$^{-/-}$ neurons (Figure 3.11a), in which NADH was depleted compared to the wild-type *ATG5*$^{+/+}$ neurons (Figures 3.1d, 3.4c and 3.11a). However, these compounds did not alter the ATP or ADP levels in *ATG5*$^{-/-}$ neurons (Figures 3.11b,c), which also had reduction in these energy carriers compared to the wild-type *ATG5*$^{+/+}$ neurons (Figures 3.1d, 3.4b and 3.11b,c); suggesting that the rescue of cell death in autophagy-deficient neurons was not due to ATP. Furthermore, mitochondria are depolarised in *ATG5*$^{-/-}$ neurons (Figures 3.5a and 3.11d). After treatment with NAM, CP2 and I-BET this mitochondrial depolarisation phenotype arising due to autophagy deficiency was significantly attenuated (Figure 3.11d). This suggests that increase in NADH levels is associated with the restoration of ΔΨm in autophagy-deficient neurons.

Overall, these data suggest that boosting cellular NADH levels in autophagy-deficient neurons is associated with improvement in cell viability and neuronal phenotypes by restoring ΔΨm. The data also implicate that the pharmacological agents boosting NAD/NADH levels could have potential biomedical applications to combat neurodegeneration in the context of neurodegenerative diseases associated with autophagy dysfunction.

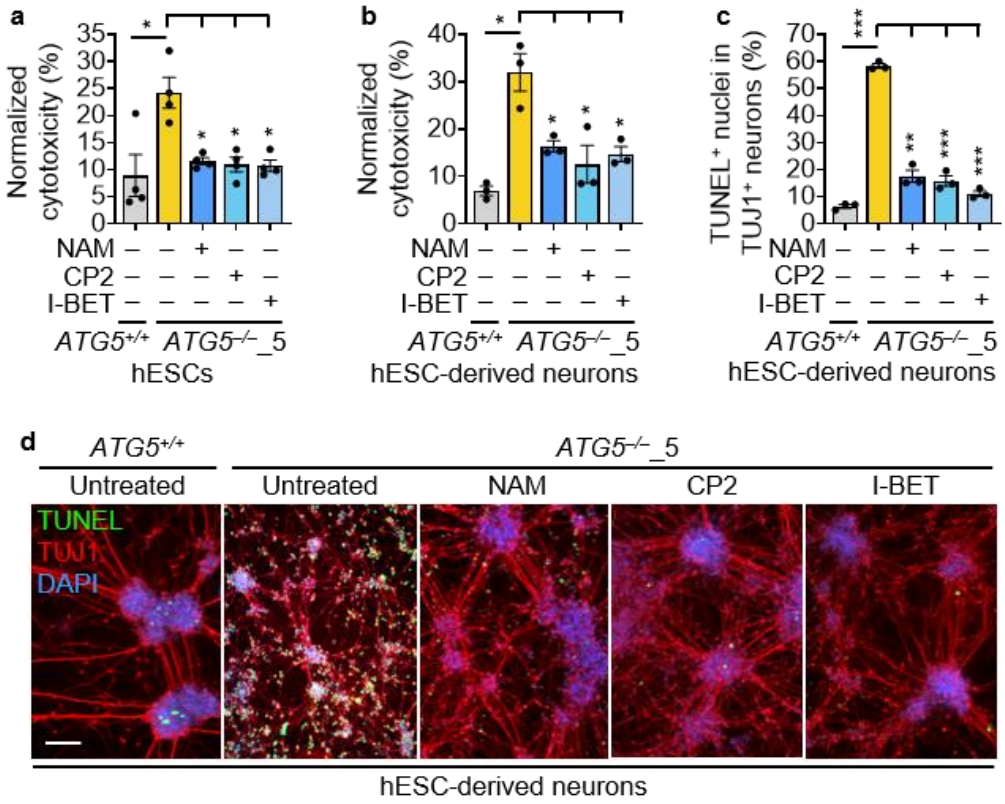


Figure 3.9. NAD/NADH boosting compounds rescued cell death in autophagy-deficient hESCs and hESC-derived neurons.

a, Cytotoxicity assay in *ATG5*$^{+/+}$ and *ATG5*$^{-/-}$_5 hESCs, where autophagy-deficient hESCs were treated with or without 1 mM nicotinamide (NAM), 1 µM CP2 and 500 nM I-BET 525762A (I-BET) for 2 days; *ATG5*$^{-/-}$ hESCs were replenished with compounds after 1 day.

b, Cytotoxicity assay in *ATG5*$^{+/+}$ and *ATG5*$^{-/-}$_5 hESC-derived neurons (3 weeks old), where autophagy-deficient neurons were treated with or without 1 mM nicotinamide (NAM), 1 µM CP2 and 500 nM I-BET 525762A (I-BET) for the last 6 days; *ATG5*$^{-/-}$ neurons were replenished with compounds at day 3.

c, d, TUNEL staining and immunofluorescence with anti-TUJ1 antibody along with DAPI staining (**d**) in *ATG5*$^{+/+}$ and *ATG5*$^{-/-}$_5 hESC-derived neurons (3 weeks old), where autophagy-deficient neurons were treated with or without NAM, CP2 and I-BET as in (**b**), and analysed for TUNEL^{+} apoptotic nuclei (**c**) in TUJ1^{+} neurons.

Graphical data (**a-c**) are mean ± s.e.m. (n = 3 or 4). *P* values were calculated by unpaired two-tailed Student's *t*-test (**a-c**) from 3 independent experiments. ***, $p<0.001$; **, $p<0.01$; *, $p<0.05$. Representative images (**d**) shown from one of 3 independent experiments. Scale bar, 100 µm (**d**).

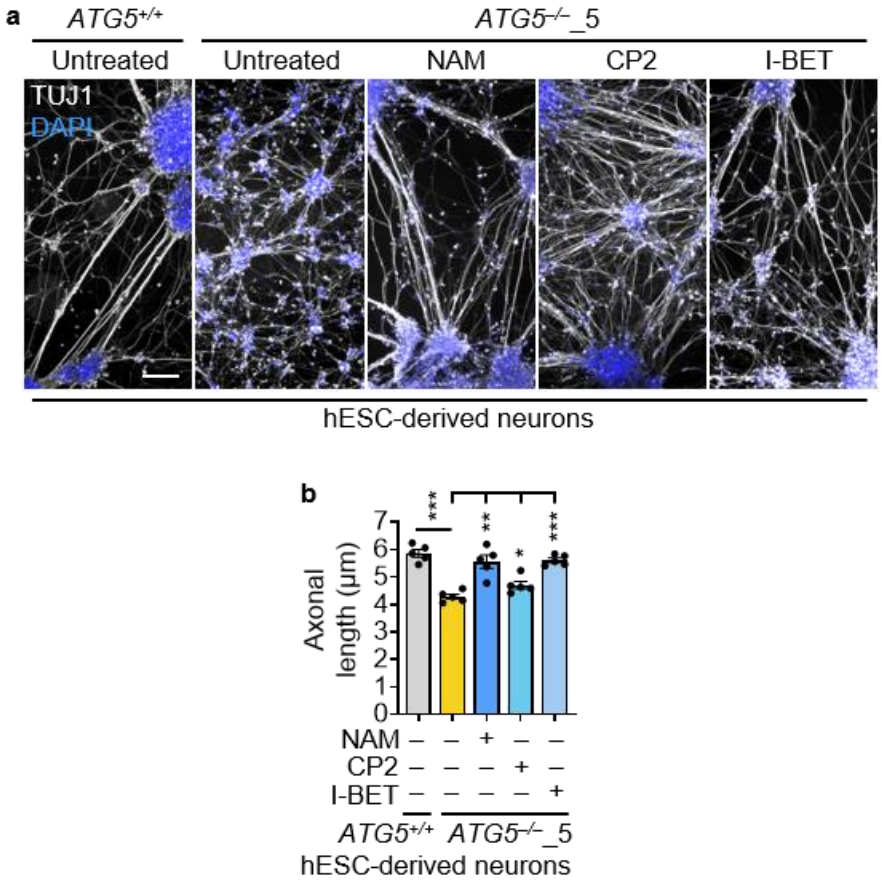


Figure 3.10. NAD/NADH boosting compounds improved axonal phenotype in autophagy-deficient hESC-derived neurons.

a, b, Analysis of axonal length (**b**) in *ATG5*$^{+/+}$ and *ATG5*$^{-/-}$_5 hESC-derived neurons (3 weeks old), where the autophagy-deficient neurons were treated with or without 1 mM NAM, 1 µM CP2 and 500 nM I-BET for the last 6 days (*ATG5*$^{-/-}$ neurons were replenished with compounds at day 3) and immunostained with anti-TUJ1 antibody (**a**).

Graphical data (**b**) are mean ± s.e.m. (n = 5). *P* values were calculated by unpaired two-tailed Student's *t*-test (**b**) from 3 independent experiments. ***, $p<0.001$; **, $p<0.01$; *, $p<0.05$. Representative images (**a**) shown from one of 3 independent experiments. Scale bar, 100 µm (**a**).

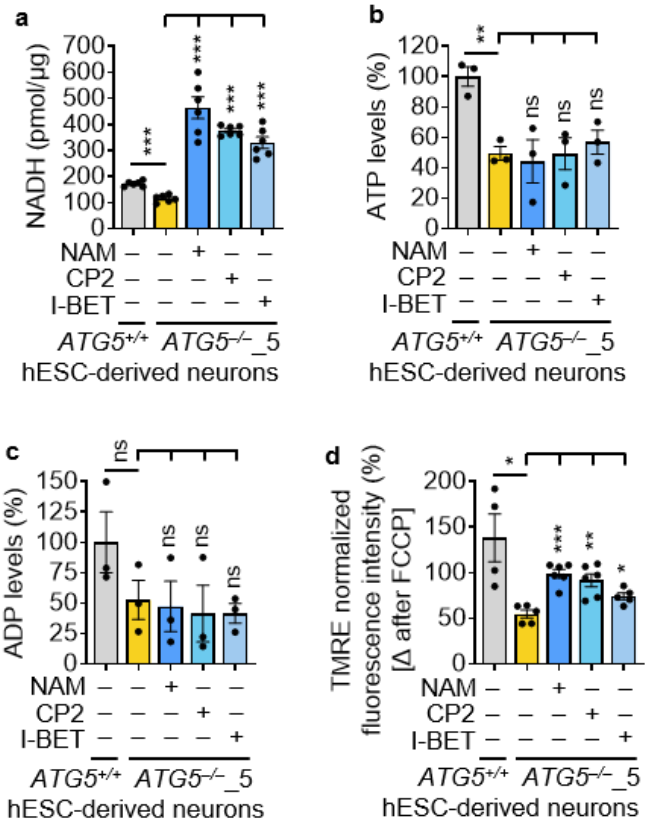


Figure 3.11. NAD/NADH boosting compounds increased cellular NADH levels and improved mitochondrial membrane potential in autophagy-deficient hESC-derived neurons without affected ATP/ADP levels.

a, Analysis of NADH levels in *ATG5*$^{+/+}$ and *ATG5*$^{-/-}$_5 hESC-derived neurons (3 weeks old), where autophagy-deficient neurons were treated with or without 1 mM NAM, 1 µM CP2 and 500 nM I-BET for the last 6 days (*ATG5*$^{-/-}$ neurons were replenished with compounds at day 3).

b, c, Analyses of ATP (**b**) and ADP (**c**) levels in *ATG5*$^{+/+}$ and *ATG5*$^{-/-}$_5 hESC-derived neurons (3 weeks old), where autophagy-deficient neurons were treated with or without NAM, CP2 and I-BET as in (**a**).

d, Analysis of TMRE fluorescence intensity (in FCCP treated cells) in *ATG5*$^{+/+}$ and *ATG5*$^{-/-}$_5 hESC-derived neurons (3 weeks old), where autophagy-deficient neurons were treated with or without NAM, CP2 and I-BET as in (**a**).

Graphical data (**a-d**) are mean ± s.e.m. (n = 3–6). *P* values were calculated by unpaired two-tailed Student's *t*-test (**a-d**) from 3 independent experiments. ***, $p<0.001$; **, $p<0.01$; *, $p<0.05$; ns, non-significant.

3.3.6. NAD/NADH boosting compounds improve cell viability in Niemann-Pick type C1 (NPC1) patient-derived disease-affected neurons

The final goal is to study whether the NAD/NADH boosting compounds, which were cytoprotective in the genetic neuronal model of autophagy deficiency, could also be effective in a neurodegenerative disease model associated with dysfunctional autophagy. For this aspect, patient-derived human induced pluripotent stem cell (hiPSC) models of Niemann-Pick type C1 (NPC1) disease (Maetzel, Sarkar et al., 2014), an early-onset neurodegenerative lysosomal storage disorder associated with cholesterol accumulation and autophagy defect (Sarkar et al., 2013) was utilised. Previously, Sarkar and colleagues demonstrated that the neurons generated from NPC1 patient-specific hiPSC lines exhibited impairment in autophagic flux, and importantly, increased cytotoxicity at basal condition (Maetzel, Sarkar et al., 2014). Moreover, mitochondrial fragmentation and dysfunction have been reported in NPC1 disease (Hansen et al., 2018; Schöndorf et al., 2018). Therefore, the NPC1 hiPSC-based neuronal platform provides a disease-affected, clinically-relevant experimental system to test the therapeutic benefits of NADH-boosting agents as per the line of this study.

Neural precursors (NPs) generated from a control and a NPC1 patient-derived hiPSC lines were used for neuronal differentiation (Figure 3.12a). Neurons were differentiated for 3 or 4 weeks and compound treatment was done for the last 6 days; after which the neurons were labelled by TUJ1 immunostaining and cell death was assessed by TUNEL assay. As described before (Maetzel, Sarkar et al., 2014), NPC1 neurons had substantial increase in cell death compared to the control neurons at basal condition without the application of any external stressors (Figures 3.12b,c). Cell death in NPC1 neurons appeared more after 4 weeks, compared to 3 weeks, of neuronal differentiation (Figures 3.12b,c), which is probably due to age-dependent neurodegeneration. Thus, this neuronal platform is appropriate to test the therapeutic efficacy of candidate drugs in preventing neuronal cell death. Similar to the beneficial effects seen in *ATG5*$^{-/-}$ neurons, the NAD/NADH boosting compounds, NAM, CP2 and I-BET, significantly reduced TUNEL^{+} apoptotic nuclei in TUJ1^{+} NPC1 hiPSC-derived neurons after 3 or 4 weeks of neuronal differentiation (Figures 3.12b,c). Therefore, boosting NADH levels could improve neuronal viability during autophagy dysfunction in the context of a neurodegenerative disease.

a Overview of control and NPC1 patient-derived hiPSC lines

hiPSC lines	*Cell line designation with clone ID*	*Mutation*	*Autophagic flux*
Con_#13 (Control)	WIBR-IPS-NPC1$^{1920delG/wt}$, clone #13	NPC1$^{1920delG/wt}$	Normal
NPC1-2_#26	WIBR-IPS-NPC1$^{P237S/I1061T}$, clone #26	NPC1$^{P237S/I1061T}$	Impaired/Blocked

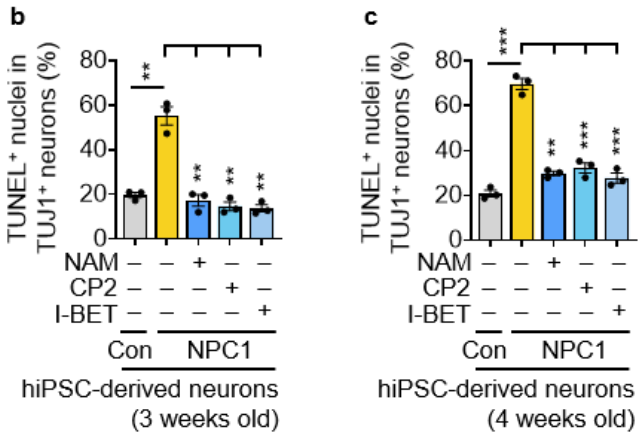


Figure 3.12. NAD/NADH boosting compounds improved cell viability in Niemann-Pick type C1 (NPC1) disease patient hiPSC-derived neurons.

a, Overview of control and NPC1 patient-derived hiPSC lines used in this study.

b, c, Analysis of TUNEL$^+$ apoptotic nuclei in control (Con) and NPC1 patient hiPSC-derived neurons after 3 weeks (**b**) or 4 weeks (**c**) of neuronal differentiation, where the NPC1 disease-affected neurons were treated with or without 1 mM NAM, 1 µM CP2 and 500 nM I-BET for the last 6 days (NPC1 neurons were replenished with compounds at day 3), and immunostained with anti-TUJ1 antibody.

Graphical data (**b, c**) are mean ± s.e.m. (n = 3). *P* values were calculated by unpaired two-tailed Student's *t*-test (**b, c**) from 3 independent experiments. ***, $p<0.001$; **, $p<0.01$.

3.4. Chapter summary

While defective autophagy has been reported in several neurodegenerative conditions (Menzies et al., 2017; Dong et al., 2014) it remains elusive how malfunction of this vital homeostatic process compromises neuronal survival. The results from this chapter suggest a metabolic defect underlying the cytotoxicity during autophagy deficiency. While unbiased metabolic profiling revealed gross perturbations in a number of metabolites including amino acids and nucleotides, the overall data point to the depletion of NADH and the consequent mitochondrial depolarisation as a potential mechanism that could be attributed to causing cytotoxicity during autophagy deficiency. These observations are supported by the results that pharmacologically boosting cellular NADH levels, such as with NAM, CP2 and I-BET, could improve ΔΨm and cell viability in *ATG5*$^{-/-}$ neurons. These treatments were also cytoprotective in NPC1 patient-derived, disease-affected neurons with dysfunctional autophagy. This study is consistent with another recent study by Sedlackova and colleagues in non-hESC based systems, where NADH depletion was found to be central in mediating the cytotoxicity in immortalised *Atg5*$^{-/-}$ mouse embryonic fibroblasts (MEFs), NPC1 patient-derived primary fibroblasts, and *Drosophila* and yeast models associated with autophagy deficiency or autophagy dysfunction (Sedlackova et al., 2020, BioRxiv https://doi.org/10.1101/2020.01.31.928424). Of biomedical relevance, this intervention could have therapeutic benefits in a range of age-related, neurodegenerative or lysosomal storage diseases linked to autophagy dysfunction.

Chapter 4

Establishment of autophagy reporter screening platform in human macrophages utilising hESCs

Chapter 4: Establishment of autophagy reporter screening platform in human macrophages utilising hESCs

4.1. Overview

Therapeutic exploitation of autophagy is steadily gaining interest as a treatment strategy for multiple diseases (Rubinsztein et al., 2012; Seranova et al., 2017; Palhegyi et al., 2019). Understanding the regulation of autophagy in a cell-specific manner will be clinically informative for therapeutic applications of autophagy modulators in the target organs affected in a vast range of diseases where autophagy is implicated. Moreover, in contrast to the use of immortalised, non-human or inappropriate cell-types, it is pertinent to determine the efficacy of autophagy modulation in the desired human cellular context because of cell-type-specific drug action (Kuo et al., 2015; Maetzel, Sarkar et al., 2014; Seranova et al., 2020). An autophagy reporter hESC-based platform was established that would enable the generation of isogenic human cell-types with autophagy readout to study cell-specific modulation of this process. The autophagy reporter system chosen for this purpose is the pH-sensitive mCherry-EGFP-LC3 reporter (Kimura et al., 2007), which could distinguish between autophagy inducers, inhibitors and blockers. The focus of this chapter is generation of macrophages, which are immune cells that act as the first line of defense for invading pathogens like bacteria and viruses. Stimulating autophagy in host cells like macrophages acts as a host-directed mechanism for enhancing the killing of pathogens; for instance, in the case of *Mycobacterium tuberculosis* associated with tuberculosis (TB) (Kim et al., 2019; Levine and Deretic, 2007; Sharma et al., 2018). Thus, autophagy reporter hESC-derived macrophages could be utilised for identifying potent or cell-specific autophagy inducers that have biomedical relevance in a range of infectious diseases including TB.

The objective/milestones for this results chapter include:

(1) Characterisation of autophagy reporter hESCs.

(2) Generation of autophagy reporter hESC-derived monocytes and macrophages.

(3) Characterisation of autophagy reporter human cellular platforms.

4.2. Introduction to the need for establishing autophagy reporter macrophage platform for identifying xenophagy inducers

Macrophages are the primary line of defence against invading pathogens to combat infection (Aderem, 2003). The autophagy process in these host immune cells contribute to intracellular pathogen clearance; a process termed xenophagy (Castrejón-Jiménez et al., 2015). The aim of establishing an autophagy reporter hESC-derived macrophage platform is for future studies related to how autophagy is regulated in human macrophages, and implementing this knowledge to discover novel, potent autophagy modulators that could be utilised in adjunctive therapies for infectious diseases.

Antibiotic resistance poses major challenge for multi- and extensively-drug-resistant species of *Mycobacterium tuberculosis (Mtb)* associated with TB (Palomino and Martin, 2014; Smith et al., 2012; Günther, 2014). Therefore, host-directed mechanisms like autophagy is an attractive alternative (Kim et al., 2019; Levine and Deretic, 2007; Sharma et al., 2018; Deretic, 2014). However, no treatment has been implemented by targeting autophagy, primarily due to lack of clinically-relevant human data. While the ability of some autophagy inducers to promote xenophagy is shown using immortalised, non-human or non-immune cells (Rubinsztein et al., 2015; Panda et al., 2019), their efficacy and drug action could be cell-type-specific (Kuo et al., 2015; Maetzel, Sarkar et al., 2014; Seranova et al., 2020). Thus, the key barrier to translation is lack of known potent autophagy inducers in physiologically-relevant human macrophages, and therefore, there is an urgent need to identify such cell-type-specific drugs that will provide new host-directed treatment strategy against multi-drug-resistant *Mtb*.

4.3. Results

4.3.1. Characterisation of autophagy reporter hESCs stably expressing mCherry-EGFP-LC3

To create an autophagy reporter hESC line (in WIBR3 hESC line), Sarkar and colleagues previously introduced the mCherry-EGFP-LC3 construct into the *AAVS1* (adeno-associated virus integration site 1) locus on chromosome 19 in the human genome by genome engineering with zinc finger nucleases (Figure 4.1a). This pH-sensitive, tandem fluorescent-tagged autophagy reporter enables assessment of autophagic flux by monitoring autophagosome turnover (Kimura et al., 2007). Using this reporter system, the autophagosomes emit both $mCherry^+$ and $EGFP^+$ signals ($mCherry^+/EGFP^+$; yellow puncta), whereas the acidic autolysosomes emit only the acid-stable $mCherry^+$ signal ($mCherry^+/EGFP^-$; red-only puncta) because the EGFP signal is acid-sensitive and gets quenched (Kimura et al., 2007) (Figure 4.1b).

The autophagy reporter hESCs stably expressing mCherry-EGFP-LC3 exhibited the mCherry and EGFP signals as visualised by fluorescence microscopy (Figure 4.2a). After generating mCherry-EGFP-LC3 hESCs, it was necessary to ensure that genome editing did not affect the stemness of these hESCs. To confirm this, pluripotency markers such as NANOG, POU5F1/OCT4, SOX2 and SSEA4 were assessed. Immunofluorescence analysis showed that mCherry-EGFP-LC3 hESCs were positive for all these pluripotency markers (Figure 4.2b). Furthermore, their gene expression in mCherry-EGFP-LC3 hESCs were also compared to that in the wild-type, parental WIBR3 hESCs via qPCR. While there was a subtle but significant reduction in RNA levels of *NANOG* and *POU5F1* in mCherry-EGFP-LC3 hESCs, no difference was found for *SOX2* in comparison to the wild-type hESCs (Figure 4.2c). Overall, it is likely that the pluripotency of autophagy reporter hESCs is not overtly different to their parental wild-type cells. Finally, expression of the mCherry-EGFP-LC3 construct at protein level was analysed in autophagy reporter hESC line via immunoblotting. In contrast to the wild-type hESCs where this reporter was absent, autophagy reporter hESCs displayed mCherry- and EGFP-tagged LC3-I and LC3-II bands at 78 kDa and 76 kDa, respectively (Figure 4.2d). Overall, these data confirm that autophagy reporter hESCs are pluripotent and express the mCherry-EGFP-LC3 reporter.

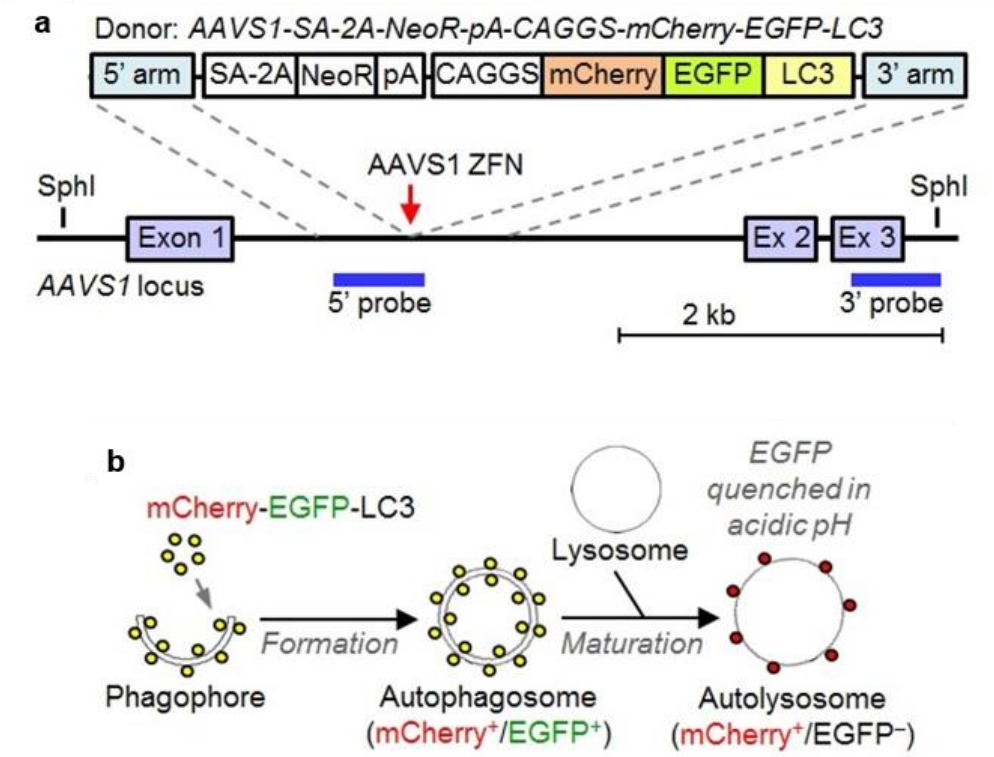


Figure 4.1. Schematic representation of the genome editing strategy in hESCs and the autophagy reporter readouts to monitor autophagosome turnover.

a, The autophagy reporter mCherry-EGFP-LC3 construct was targeted to the *AAVS1* locus via genome engineering with zinc finger nucleases (ZFNs); performed by Sovan Sarkar and colleagues. Probes for Southern blotting to confirm integration of the donor construct are indicated.

b, The mCherry-EGFP-LC3 construct is a pH-sensitive, tandem fluorescent-tagged autophagy reporter, wherein the autophagosome emits both $mCherry^{+}$ and $EGFP^{+}$ signals ($mCherry^{+}/EGFP^{+}$; yellow puncta), whereas the autolysosome emits only the acid-stable $mCherry^{+}$ signal ($mCherry^{+}/EGFP^{-}$; red-only puncta) because the EGFP signal is acid-sensitive and gets quenched in the acidic lysosomal environment.

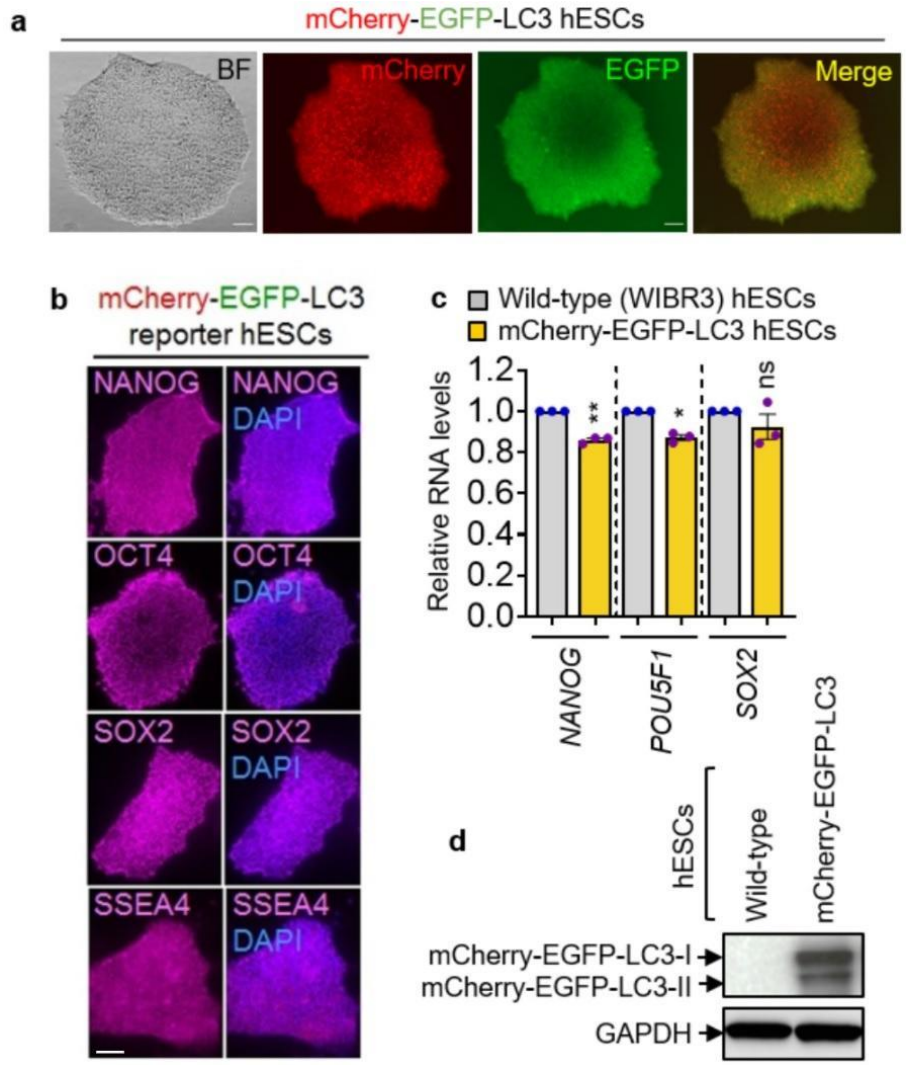


Figure 4.2. Phenotypic characterisation of mCherry-EGFP-hESCs.

a, Brightfield and fluorescent microscopy images of a mCherry-EGFP-LC3 colony expressing EGFP and mCherry signals.

b, Immunofluorescence analysis with anti-NANOG, anti-OCT4, anti-SOX2 and anti-SSEA4 antibodies in mCherry-EGFP-LC3 hESCs.

c, Quantitative RT-PCR (qPCR) expression analyses of human *NANOG*, *POU5F1* and *SOX2* genes in wild-type (parental WIBR3 line) and mCherry-EGFP-LC3 hESCs, where data are shown relative to *GAPDH* expression.

d, Immunoblotting analysis with anti-LC3 and anti-GAPDH antibodies in wild-type (parental WIBR3 line) and mCherry-EGFP-LC3 hESCs; immunoblot showing the higher molecular weight mCherry and EGFP-tagged LC3-I and LC3-II proteins in the autophagy reporter hESCs only.

Graphical data denote mean ± s.e.m. (n = 3) where *P* values were calculated by unpaired two-tailed Student's *t*-test (**c**) from 3 independent experiments. **, $p<0.01$; *, $p<0.05$; ns, non-significant. Representative images (**a**) shown from one of 2 independent experiments. Scale bar, 20 µm (**a**) and 50 µm (**b**).

The autophagy reporter hESC line was further characterised for perturbations of the autophagosome turnover readout when subjected to known pharmacological modulators of autophagy. These include the autophagy inducer, rapamycin, and the autophagy blocker, bafilomycin A_1. Rapamycin induces autophagy via inhibition of mTORC1 (Brown et al., 1994), while bafilomycin A_1 blocks autophagy by preventing lysosomal acidification and autophagosome–lysosome fusion (Yamamoto et al., 1998). Cells were either treated with dimethyl sulfoxide (DMSO; vehicle control), or with 200 nM rapamycin for 24 h or bafilomycin A_1 100 nM for 4 h. As expected, rapamycin enhanced autophagic flux as evident from the increase in autolysosomes ($mCherry^+/EGFP^-$ vesicles; red-only puncta indicated by red arrows in the merged panel) (Figure 4.3a); whereas bafilomycin A_1 blocked autophagic flux by preventing autophagosome maturation as evident from the accumulation of autophagosomes ($mCherry^+/EGFP^+$ vesicles; yellow puncta indicated by yellow arrows in the merged panel) (Figure 4.3a). Furthermore, mCherry-EGFP-LC3 hESCs were subjected to starvation-induced autophagy. Starvation is a physiological trigger of autophagy that acts via inhibition of mTORC1 (Klionsky et al., 2016). Cells were starved with Hank's Balanced Salt Solution (HBSS), which is routinely used in the field to stimulate autophagy (Klionsky et al., 2016). Indeed, culturing the hESCs in HBSS for 2 h significantly increased the numbers of autophagosomes and autolysosomes, as compared to the cells cultured in full growth medium (basal condition) (Figure 4.3b). These data suggest that the image-based readout of the autophagy reporter hESCs are sensitive to modulation of autophagy, and thus could be further developed as a screening platform.

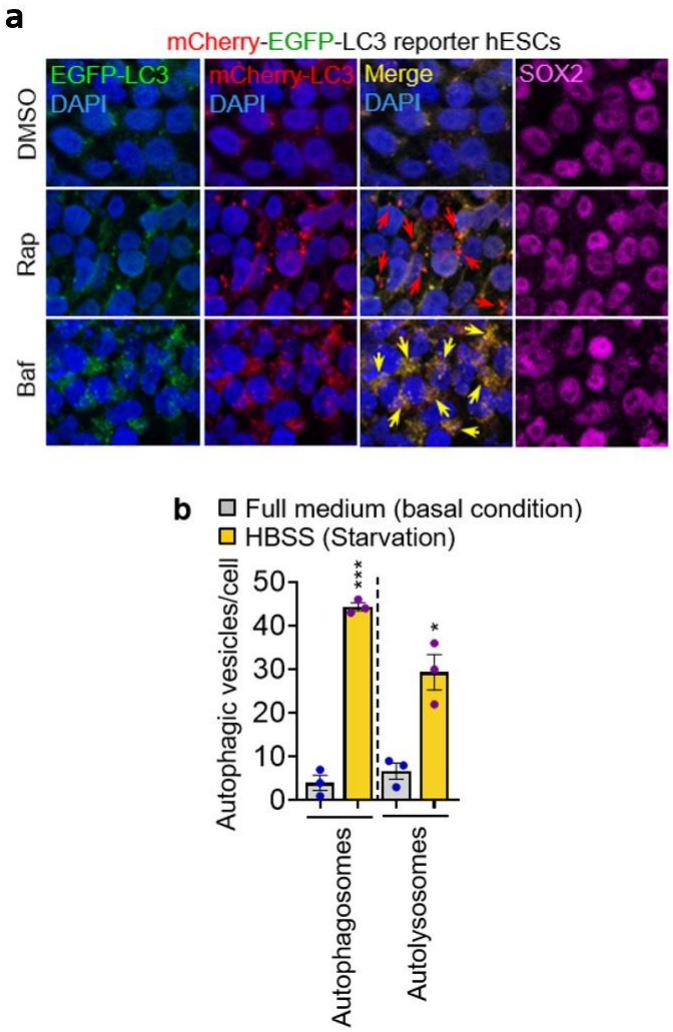


Figure 4.3. Perturbations of autophagosome turnover readout in mCherry-EGFP-LC3 hESCs by modulation of autophagy.

a, Fluorescence analysis of mCherry-EGFP-LC3 hESCs after treatment with DMSO (vehicle control), 200 nM rapamycin (Rap) for 24 h or 100 nM bafilomycin A_1 (Baf) for 4 h. The autophagosomes ($mCherry^+/EGFP^+$ puncta) and autolysosomes ($mCherry^+/EGFP^-$ puncta) are respectively shown by red or yellow arrows in the merged panel.

b, Quantification of autophagosomes and autolysosomes in mCherry-EGFP-LC3 hESCs, either cultured in full growth medium (basal condition) or subjected to starvation-induced autophagy by culturing in Hank's Balanced Salt Solution (HBSS) for 2 h.

Graphical data denote mean ± s.e.m. (n = 3) where *P* values were calculated by unpaired two-tailed Student's *t*-test (**b**) from 3 independent experiments. ***, $p<0.001$; *, $p<0.05$. Representative images (**a**) shown from one of 3 independent experiments.

4.3.2. Challenges and mitigations of generation of autophagy reporter hESC-derived macrophages

After verifying the functionality of the autophagy reporter cell line, the next step was to differentiate the hESCs into macrophages by defined culture conditions. Briefly, the protocol consists of the following stages: seeding hESCs as single cells to form embryoid bodies (EBs) in low attachment plates or AggreWells; collecting the EBs after 4 days and seeding them in T75 flasks or 6-well plates to form the so-called 'factories'; culturing the 'factories' for 4-5 weeks in X-VIVO 15 medium supplemented with IL3 and M-CSF for generating monocyte-like cells; after monocytopoiesis is initiated, harvesting the supernatant from the 'factories' once or twice a week and differentiating the monocytic cells into macrophages (Figure 4.4a). This protocol has been previously published and routinely used for generating macrophages from human pluripotent stem cells (Wilgenburg et al., 2013). There are two versions of the protocol described; the first method utilises low attachment plates to create EBs of various sizes, and the second method utilises microwell culture plates that allow for a homogeneous, pre-defined size of all the resulting EBs (Wilgenburg et al., 2013). An initial attempt was made for the first differentiation method using the low attachment plates, as they were cost-effective. However, the formation of EBs in this setting proved to be challenging because they were not uniform, and so the next stage of differentiation involving the seeding of EBs in T75 flasks or 6-well plates to form 'factories' proved unsuccessful. The amount of EBs that could successfully attach to adherent surface after seeding was insufficient, and this was possibly due to the difference in EB sizes that has been suggested to affect their development, attachment properties and differentiation capacity. Previously, the use of uniform, large sized EBs has been found to be more efficient for downstream differentiation applications (Wilgenburg et al., 2013). For these reasons, the differentiation protocol was switched to the second method using the microwell plates for uniform sized EBs. The microwells incorporated into the AggreWell plates produced EBs of similar size of approximately 800 μm in diameter. This method was successful for macrophage differentiation.

In addition to the above, a number of modifications were made to this differentiation method. The first change was made to overcome the hurdles of EB attachment to adherent surface after seeding into T75 flasks or 6-well plates for producing 'factories'. A range of coatings was tested to determine the best conditions for EB attachment

using matrigel, laminin, vitronectin and gelatin (data not shown). Surprisingly, the highest attachment rate with up to 100% was achieved with 0.2% gelatin. Other coatings like matrigel, laminin and vitronectin, which usually provide attachment of primary and hPSC-derived cells, were not so effective. Therefore, gelatin coating was utilised for the rest of the work described in this chapter. Furthermore, while the original protocol suggests keeping the EBs in microwells for 4 days (Wilgenburg et al., 2013), the EB formation period was experimented with and found to be most optimal for 7 days. The production of monocytic cells was enhanced when the EBs were cultured longer in AggreWells before transitioning to 'factories'.

An important modification made to the protocol was the inclusion of Quick-Tissue Mesoderm Booster, which is used to improve the differentiation capacity of various hiPSC lines. The treatment instructions suggest that the mesoderm booster can be applied when the differentiation protocol starts, with or without the growth factors used in the protocol. For macrophage differentiation, this means treating the EBs with mesoderm booster when initially putting them in the AggreWells, either in plain StemFlex medium or in StemFlex medium supplemented with BMP4, VEGF and SCF human recombinant growth factors. After trying both the options, treatment of the mesoderm booster in the presence of all the necessary growth factors was found to be more efficient, quicker and consistent in producing EBs (data not shown). Although the exact composition of the Quick-Tissue Mesoderm Booster is not publicly available, it appears to suppress the expression of pluripotency genes in hESCs; thereby augmenting their differentiation capacity and facilitating the switch from stemness to lineage commitment through the regulation of histone demethylase JMJD3 (Akiyama et al., 2016).

The above differentiation method and the modifications tested were carried out using the wild-type (parental WIBR3) hESC line, followed by the autophagy reporter (mCherry-EGFP-LC3) hESC line (Figure 4.4b). The modified protocol was adapted for all the macrophage differentiation experiments in this chapter. Confirmation of the cellular identity of hESC-derived monocytic cells and macrophages were done in the next step.

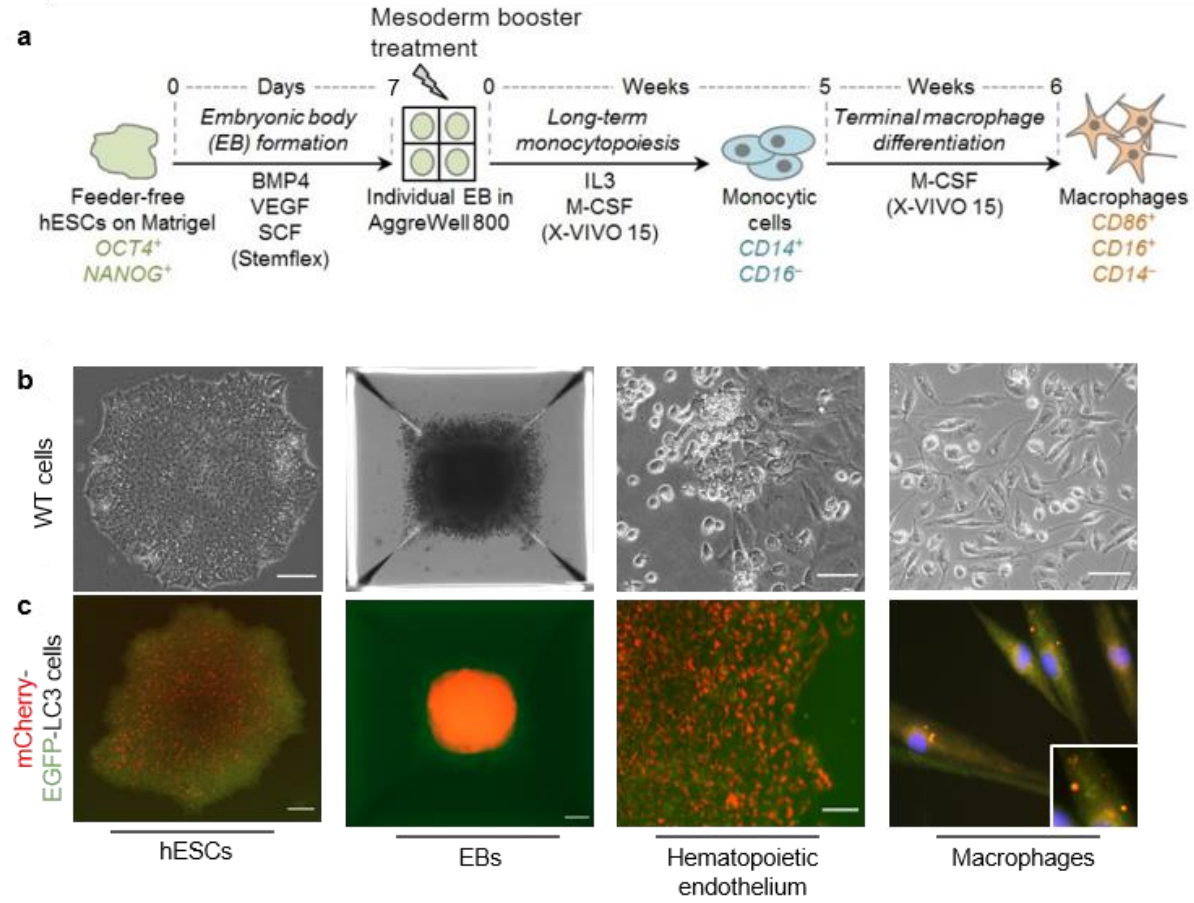


Figure 4.4. Differentiation of hESCs into macrophages via monocytic cells.

a, Schematic representation of the hESC differentiation method for generation of macrophages, indicating the growth factors, cytokines and speciality medium involved along with the timeline of the process.

b,c, Brightfield (**b**) and fluorescent (**c**) images of wild-type (WT) (**b**) and mCherry-EGFP-LC3 hESCs (**c**) showing different stages of the differentiation process: hESCs cultured on feeder-free basement membrane matrix; embryoid body (EB) formation in AggreWell; stroma from hematopoietic progenitors attached in “factory” for production of monocytic cells; macrophages.

Representative images (**b**, **c**) shown from one of 3 independent experiments. Scale bar, 20 µm (**b,c**).

4.3.3. Characterisation of cellular identity of hESC-derived monocytic cells

After the derivation of monocytic cells and macrophages from hESC, their cellular identities were determined. This was primarily carried out by analysing the expression of surface markers in hESC-derived monocytic cells and macrophages by antibody-based fluorescence activated cell sorting analysis (FACS). The gating strategy for FACS analysis (Figure 4.5) was done as follows. First, the cells were discriminated according to their size and granularity. The forward scatter was used to single out cells according to their relative size. The side scatter was used to discriminate the cells according to their optical granularity and complexity. The bigger the size of a cell, the bigger the cytoplasm, which allows more surface to scan for compartments. A big cell will be located on the high end of a side scatter with more cytoplasm and less nuclear area to scan. Next, a doublet discrimination was done using the pulse width and the forward scatter discrimination to ensure only the viable single leukocytes were selected for further analysis. Finally, the resulting cell population was plotted as a histogram versus cell count, and the data was presented in a logarithmic scale to evaluate the fluorescence intensity resulting from the antibody staining. For FACS analysis in mCherry-EGFP-LC3 hESC-derived monocytic cells and macrophages, UltraComp eBeads compensation beads were used to ensure the EGFP and mCherry signals do not bleed-through to the antibody staining channels.

Initially, characterisation of the wild-type (parental WIBR3) and the autophagy reporter (mCherry-EGFP-LC3) monocytic cells were done by FACS analysis of the surface markers such as CD14, CD16, CD86, CD11b, CD11c, MHC-II, CD206, CD163 and CD45 (Figures 4.6a-i and 4.7a-g). The aforementioned surface marker panel was chosen according to their properties described in Table 4.1.

Table 4.1. Monocyte and macrophage surface markers.

Antigen	*Function*	*Expression*
CD11b	Integrin receptor (active signaling receptor) Mediates cell-cell and cell-matrix adhesion Recruit leukocytes to inflammatory sites Promote cell activation	Expressed in monocytes and macrophages
CD11c	Integrin receptor (active signaling receptor) Mediate cell-cell and cell-matrix adhesion Recruit leukocytes to inflammatory sites Promote cell activation	Expressed in monocytes and macrophages

CD14	Surface antigen Mediates the innate immune response to bacterial LPS together with LPS binding protein (LBP)	Expressed more in monocytes than macrophages
CD16	Low affinity IgG receptor Expressed as 2 distinct forms CD16a and CD16b transmembrane proteins CD16b expressed specifically on neutrophils CD16 binds aggregated IgG which functions in phagocytosis and antibody-dependent cell mediated cytotoxicity (ADCC)	Expressed on surface of NK cells, activated monocytes and macrophages
CD45	A tyrosine phosphatase Critical for leukocytes functions Regulating signal transduction Cell activation associated with T cell, B cell and IL-2 receptors	Most abundant hematopoietic marker expressed on all leukocytes
CD68	Type I integral membrane protein Binds to tissue and organ specific lectins or selectins Also a scavenger receptor which function to clear debris, promote phagocytosis and mediate recruitment and activation of macrophages	Highly expressed by tissue macrophages and human monocytes
CD86	Ligand for CD28 antigen and cytotoxic T-lymphocyte associated protein 4 CD28 binding results in a co-stimulatory signal for T cell activation, induce high level expression of IL-2, impart resistance to apoptosis, enhance T cell cytotoxicity Cytotoxic T lymphocyte associated protein 4 binding negatively regulates T cell activation and diminished immune response	Expressed in antigen presenting cells (APCs) Marker for macrophages
CD163	Scavenger receptor Functions in the clearance and endocytosis of hemoglobin/haptoglobin complexes by macrophages, and protects tissues from free hemoglobin-mediated oxidative damage May also function as an innate immune sensor for bacteria and inducer of local inflammation Regulates cytokine production by macrophages	Exclusively expressed in monocytes and macrophages
CD206	Mannose receptor (MR) Type I membrane protein Pattern recognition receptor Recognises microbial carbohydrates with mannose, fucose, N-acetyl glucosamine, sulfated carbohydrate antigens and collagen Mediates endocytosis and phagocytosis Mediates macrophage activation and antigen presentation On lymphatic endothelial cells, it was found to be involved in leukocyte trafficking	Expressed on macrophages
MHCII	Involved in antigen presentation to T cells expressing CD3/TCR and CD4 proteins Main role of MHCII is to present processed antigens (derived from exogenous sources) to CD4+ T lymphocytes. Critical for initiation of antigen-specific immune response	Expressed in antigen presenting cells (APCs) Present on both monocytes and macrophages

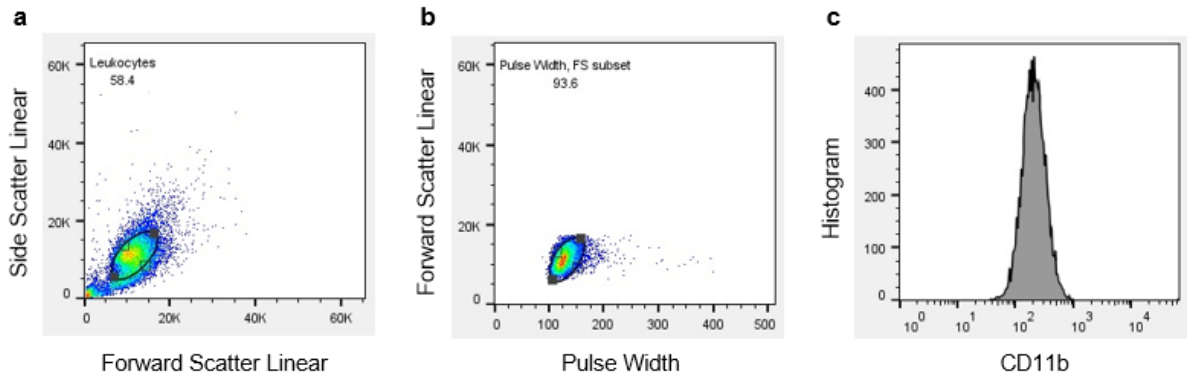


Figure 4.5. Gating strategy implemented for FACS analysis of cell surface markers.

a–c, Wild-type hESC-derived monocytic cells were discriminated according to their size (forward scatter) and granularity (side scatter) (**a**), and then the doublets were excluded by forward scatter and pulse width (**b**). Finally, the data was presented as histogram (cell count) versus the fluorescent channel analysed (**c**).

Primary human blood monocytes fall into two predominant categories: the classical $CD14^+/CD16^-$, and the non-classical $CD14^-/CD16^+$ (Sampath et al., 2018). Additionally, there might be small subsets where a range of intermediate expression of these markers are observed. As seen by FACS analysis in the context of both wild-type and autophagy reporter hESC-derived monocytic cells, the “factory” harvest consisted of cells that moderately expressed CD14 (Figures 4.6a and 4.7a) but were negative for CD16 (Figures 4.6b and 4.7b). These data indicate that the hESC-derived cells produced resemble more of the category of classical monocytic cells (Ziegler-Heitbrock et al., 2010).

Furthermore, there were expression of the surface markers CD86, CD11b, CD11c, CD163 and CD206 in both wild-type (Figures 4.6c-e,g,h) and autophagy reporter (Figures 4.7c-f) hESC-derived monocytic cells, as expected to be seen in monocytes. In addition, there was high expression of CD45 (Figures 4.6i and 4.7g), which is the most abundant hematopoietic marker expressed on the surface of all leukocytes (Ziegler-Heitbrock et al., 2010). When stained for MHC-II, the expression of this marker in the wild-type hESC-derived monocytic cells was negligible in rested state (Figure 4.6f). It is noteworthy that MHC-II is most abundantly expressed when cells have received an inflammatory stimulus (Sampath et al., 2018, Ziegler-Heitbrock et al., 2010).

Overall, both the wild-type and autophagy reporter hESC-derived monocytic cells displayed surface marker expression that are expected in primary monocytes, and these properties are consistent with the characterisation data demonstrated in human pluripotent stem cell-derived monocytic cells (Wilgenburg et al., 2013).

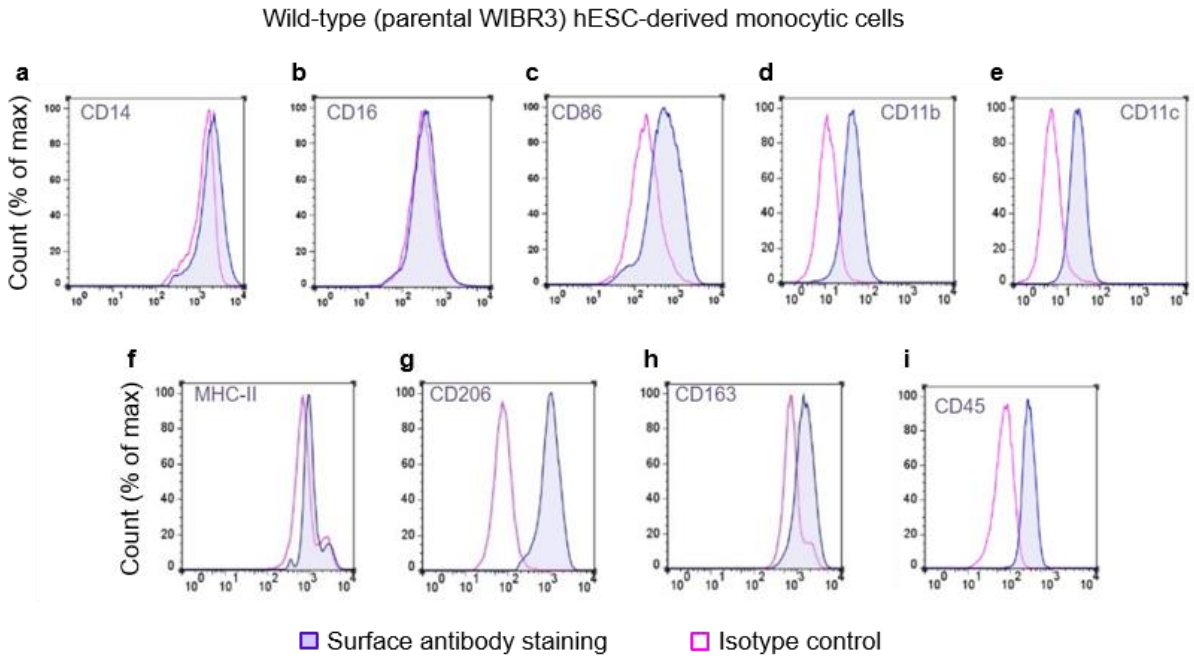


Figure 4.6. FACS analyses of surface markers in wild-type (parental WIBR3) hESC-derived monocytic cells.

a–i, Surface expression of CD14 (**a**), CD16 (**b**), CD86 (**c**), CD11b (**d**), CD11c (**e**), MHC-II (**f**), CD206 (**g**), CD163 (**h**) and CD45 (**i**) were measured by FACS in wild-type (parental WIBR3) hESC-derived monocytic cells. Histograms represent surface staining (shaded blue) compared to the isotype control (pink line). X-axis shows antibody staining, Y-axis shows cell count. For each sample, at least 10,000 cells were analysed.

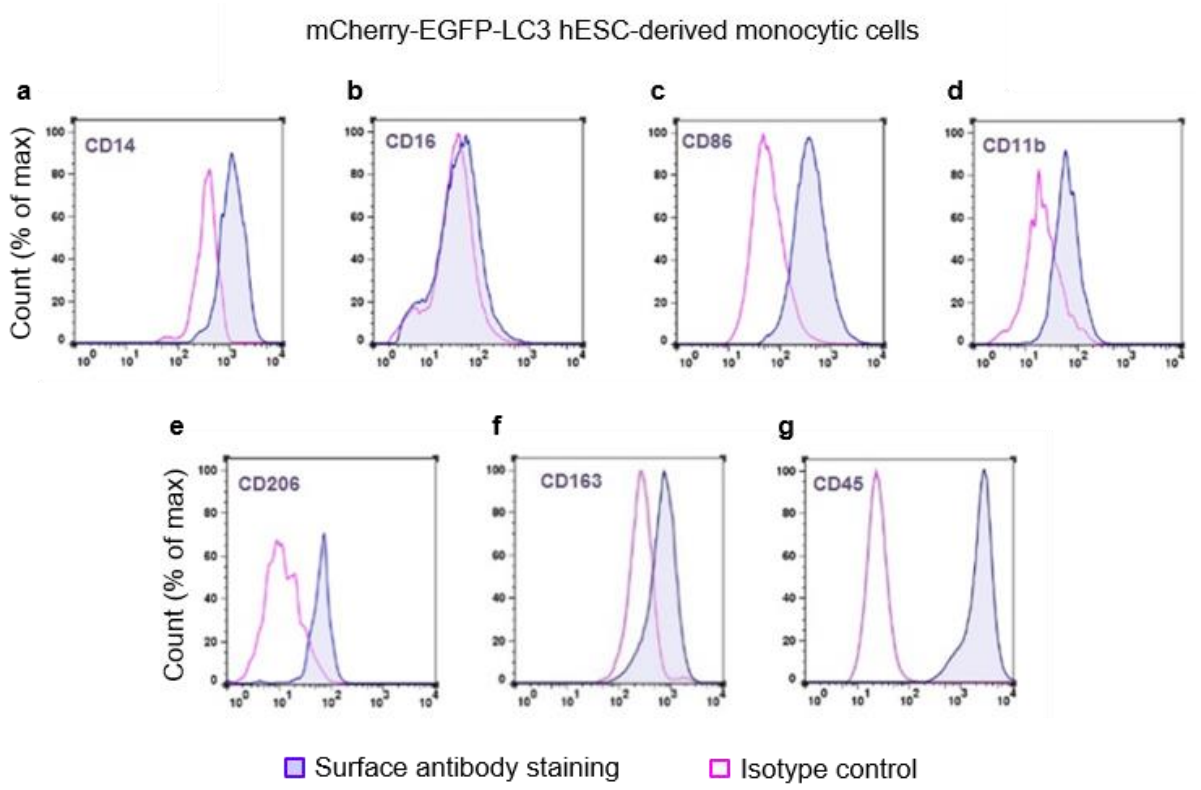


Figure 4.7. FACS analyses of surface markers in autophagy reporter (mCherry-EGFP-LC3) hESC-derived monocytic cells.

a–g, Surface expression of CD14 (**a**), CD16 (**b**), CD86 (**c**), CD11b (**d**), CD206 (**e**), CD163 (**f**) and CD45 (**g**) were measured by FACS in autophagy reporter (mCherry-EGFP-LC3) hESC-derived monocytic cells. Histograms represent surface staining (shaded blue) compared to the isotype control (pink line). X-axis shows antibody staining, Y-axis shows cell count. For each sample, at least 10,000 cells were analysed.

4.3.4. Characterisation of cellular identity and functionality of hESC-derived macrophages

Following the characterisation of wild-type and autophagy reporter hESC-derived monocytic cells, macrophages were generated and analysed for their cellular identity and functionality. First, the wild-type macrophages were characterised by FACS. Positive CD11b staining was detected in a percentage of wild-type macrophages, while the staining with CD206 and CD68 was identical with the isotype control (Figures 4.8a-c). These cells were not positive for CD68 as reported in literature in primary macrophages (Figure 4.8c). However, immunofluorescence analysis showed CD86 staining in the wild-type macrophages in unstimulated state (Figure 4.8d; left panel). CD86 is also a marker for macrophages and is expressed in antigen-presenting cells (Hughes et al., 2016; Gordon et al., 2014). Moreover, CD206 is not highly expressed in unstimulated macrophages (Gordon et al., 2014).

Functional characterisation was carried out by exposing these macrophages to inflammatory stimulus, such as interferon gamma (IFNγ). IFNγ is a cytokine, which falls into the category of an immune interferon, is produced by human lymphocytes when challenged with viral and bacterial infections (Shtrichman and Samuel, 2001). Immunofluorescence analysis after treatment with IFNγ (100 ng/mL for 24 h) showed that the wild-type hESC-derived macrophages expressed IBA1 (Figure 4.8d; right panel), which is a protein present in circulating macrophages when presented with inflammatory stimulus and microglia (Kanazawa et al., 2002). To further evaluate the inflammatory response, wild-type macrophages were treated with lipopolysaccharide (LPS). LPS resides on the outer membrane of gram-negative bacteria and serves as an inflammatory trigger (Chandler and Ernst, 2017). After LPS treatment for 24 h, the supernatant was collected for detecting the levels of cytokine secretion, such as IL-10, via enzyme-linked immunosorbent assay (ELISA). Wild-type macrophages stimulated with 20 or 40 ng/mL of LPS produced a gradually increasing amount of IL-10 in a dose-dependent manner (Figure 4.8e).

Next, the expression of surface markers in mCherry-EGFP-LC3 hESC-derived macrophages was evaluated by FACS. The autophagy reporter macrophages expressed CD86, CD11b, CD206 and CD45 (Figures 4.9c-e,g). CD45 expression was very strong and CD86 expression was higher in mCherry-EGFP-LC3 hESC-derived

macrophages than monocytes (Figures 4.7c,g and 4.9c,g), implying that the analysed cells had macrophage characteristics. However, very low expression of CD14 was detected, while the expression of CD16 and CD163 was non-detectable (Figures 4.9a,b,f). Notably, the expression of CD14 is usually more profound in primary monocytes than in primary macrophages (Gordon et al., 2014), which is what was also observed in the autophagy reporter hESC-derived cell-types (Figures 4.7a and 4.9a). Overall, the expression levels of these surface markers confirm the cellular identity of autophagy reporter macrophages; which also implicates that the integration of the autophagy reporter construct in hESCs did not interfere with their differentiation ability. Furthermore, CD86 staining was confirmed in these macrophages in an unstimulated state by immunofluorescence analysis (Figure 4.10a). Treatment of autophagy reporter macrophages with inflammatory stimulus like IFNγ (100 ng/mL for 24 h) caused expression of IBA1, which was detected by immunofluorescence analysis (Figure 4.10b). Interestingly, in contrast to the unstimulated cells stained for CD86, the stimulated macrophages positive for IBA1 appeared to be morphologically 'inflamed' (Figures 4.10a,b).

Further functional characterisation of the autophagy reporter macrophages was done by evaluating phagocytosis, i.e., the ability of macrophages to phagocytose external materials such as pathogens or cellular debris (Hirayama, Iida and Nakase, 2017). Phagocytosis assay was performed utilising necrotic Jurkat cells that were labelled with CellTracker Blue. The autophagy reporter macrophages were stimulated with 100 ng/mL IFNγ for 24 h prior to the exposure of necrotic Jurkat cells. The macrophages were labelled with DeepRed Cell Mask to contour the cytoplasm. The images of untreated and IFNγ-treated cells were acquired using the CellInsight CX5 High-Content Screening microscope, and pseudo colour was applied for visualisation. The necrotic Jurkat cells that were phagocytosed by macrophages and the ones that were not phagocytosed were indicated by respective colour-coded arrows (Figure 4.10c). As evident from the images, phagocytosis of necrotic cells was substantially more in IFNγ-treated activated macrophages (Figure 4.10c, pink arrows), indicating the functionality of hESC-derived macrophages.

Although the data presented here suggest successful generation of monocytic cells and macrophages from hESCs, further characterisation could be done in future for demonstrating their functional properties.

Attempts to analyse the TF-LC3 macrophages with regards to their ability to display the expected chages in $mCherry^+/EGFP^+$ (autophagosomes) and $mCherry^+/EGFP^-$ (autolysosomes) puncta when treated with appropriate autophagy modulators were made. Cells were treated with Bafilomycin A_1 (an autophagy blocker), Rapamycin (an mTOR dependent autophagy enhancer) and Trehalose (an mTOR independent autophagy enhancer). Both the autophagy enhancers have been reported to activate autophagy in human macrophages (Sharma et al., 2020). The reporter cell line behaved as expected with Bafilomycin A_1 by increasing the amount of $mCherry^+/EGFP^+$ puncta only, while the autophagy inducers increased both the $mCherry^+/EGFP^+$ and the $mCherry^+/EGFP^-$ puncta (as observed via fluorescence microscope; data not shown). The image acquisition and analysis was scheduled to take place with CellInsight CX5 high-content screening microscope, because the cells were plated in 96-well plates. Unfortunatly, due to technical issues with the microscope, this was not possible and thus no data were collected.

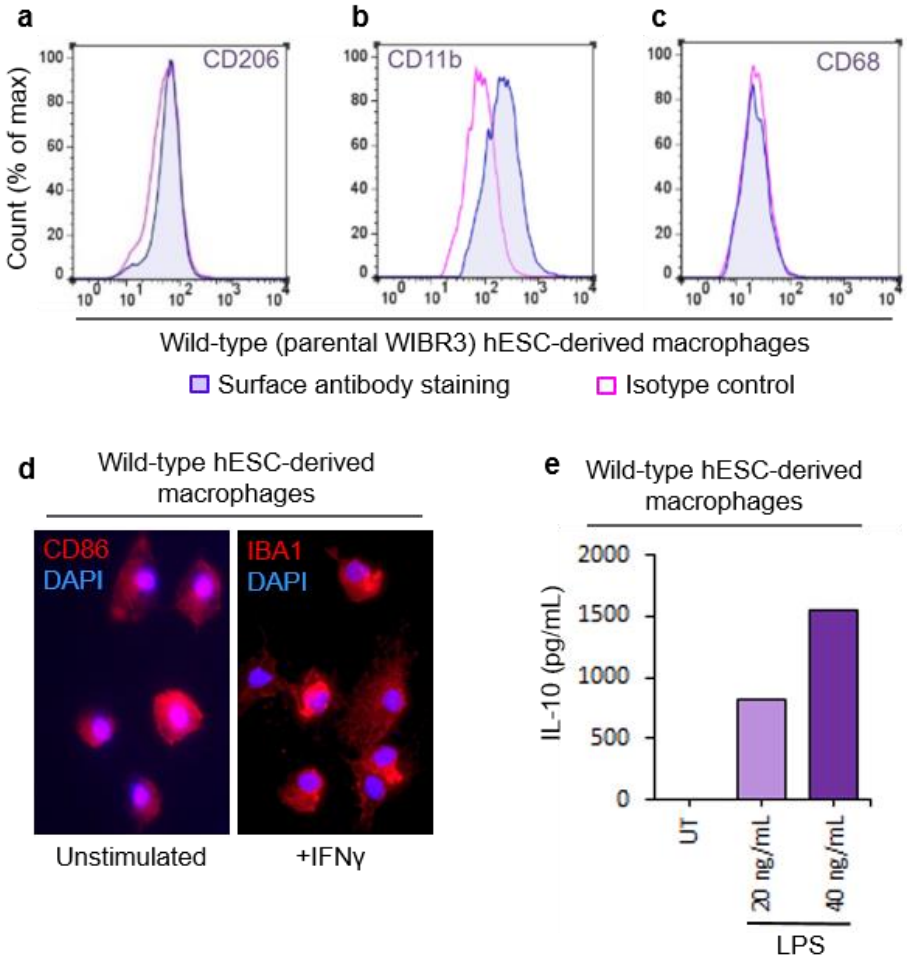


Figure 4.8. Characterisation of wild-type hESC-derived macrophages.

a–c, Surface expression of CD206 (**a**), CD11b (**b**) and CD68 (**c**) were measured by FACS in wild-type (parental WIBR3) hESC-derived macrophages. Histograms represent surface staining (shaded blue) compared to the isotype control (pink line). X-axis shows antibody staining, Y-axis shows cell count. For each sample, at least 10,000 cells were analysed.

d, Immunofluorescence analyses with anti-CD86 and anti-IBA1 antibodies in wild-type hESC-derived macrophages, either unstimulated or stimulated with 100 ng/mL IFNγ for 24 h as indicated.

e, Analysis of IL-10 cytokine secretion by enzyme-linked immunosorbent assay (ELISA) in wild-type hESC-derived macrophages after treatment with 20 or 40 ng/mL of lipopolysaccharide (LPS) for 24 h.

Representative images (**d**) and graphical data (**e**) are shown from 1 experiment.

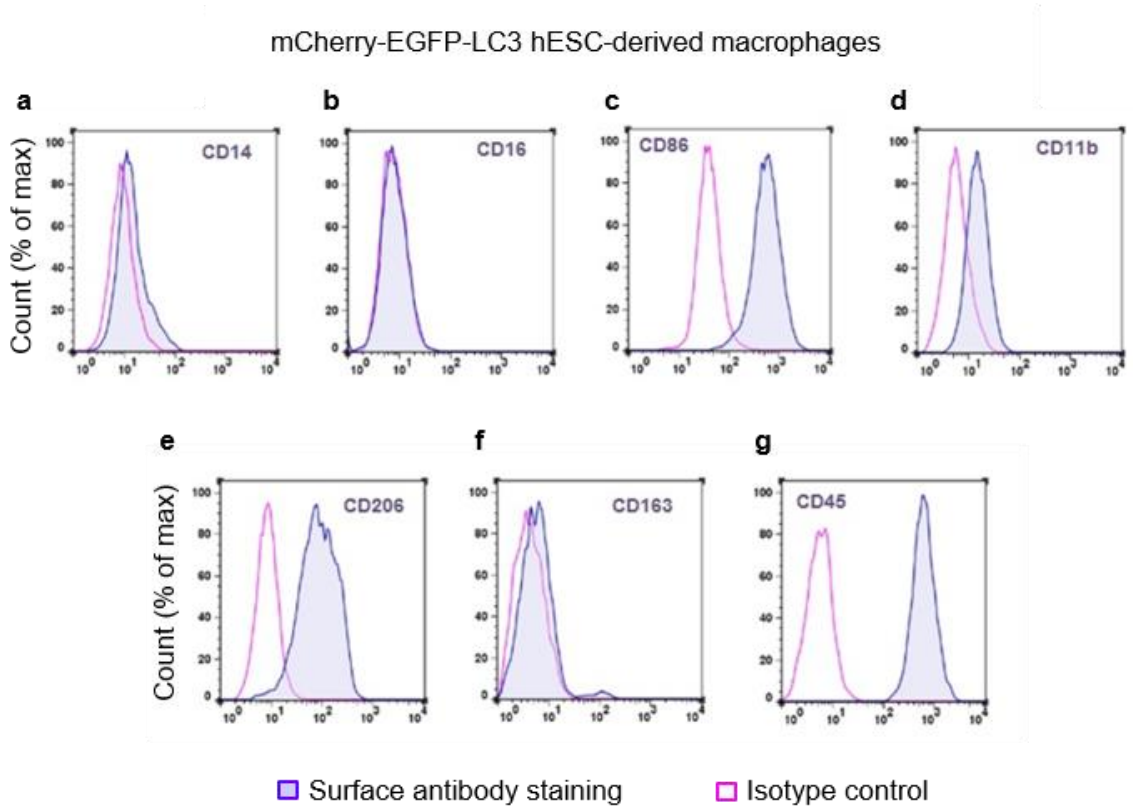


Figure 4.9. FACS analyses of surface markers in autophagy reporter (mCherry-EGFP-LC3) hESC-derived monocytic cells.

a–g, Surface expression of CD14 (**a**), CD16 (**b**), CD86 (**c**), CD11b (**d**), CD206 (**e**), CD163 (**f**) and CD45 (**g**) were measured by FACS in autophagy reporter (mCherry-EGFP-LC3) hESC-derived macrophages. Histograms represent surface staining (shaded blue) compared to the isotype control (pink line). X-axis shows antibody staining, Y-axis shows cell count. For each sample, at least 10,000 cells were analysed.

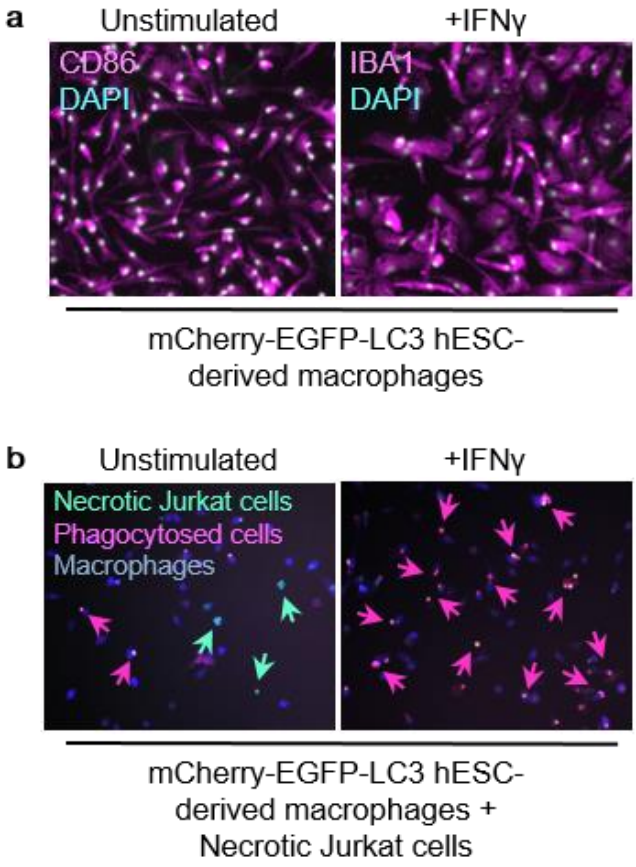


Figure 4.10. Functional characterisation of autophagy reporter hESC-derived macrophages.

a, Immunofluorescence analyses with anti-CD86 and anti-IBA1 antibodies in mCherry-EGFP-LC3 hESC-derived macrophages, either untreated or stimulated with 100 ng/mL IFNγ for 24 h.

b, mCherry-EGFP-LC3 hESC-derived macrophages, untreated or treated with 100 ng/mL IFNγ for 24 h, were exposed to necrotic Jurkat cells. The Jurkat cells and the macrophages were labelled with CellTracker Blue and DeepRed Cell Mask, respectively. Images were acquired using CellInsight CX5 High-Content Screening microscope, and pseudo colour was applied to visualise the phagocytosed (pink) and non-phagocytosed (light blue) necrotic Jurkat cells; indicated by respective colour-coded arrows.

Representative images are shown from one of 2 (**a**) or 1 (**b**) independent experiments.

4.4. Chapter summary

The goals of this chapter were to characterise autophagy reporter hESCs, and then to differentiate them for generating autophagy reporter macrophages. Initially, the mCherry-EGFP-LC3 hESCs, which were generated by Sarkar and colleagues, were confirmed for their pluripotency property. Thereafter, these autophagy reporter hESCs were first differentiated into monocytic cells and then to macrophages via defined culture conditions. The differentiation protocol, which has been previously published, was modified for better attachment and production of monocytic cells and macrophages. This method was tested for the differentiation of both wild-type (parental WIBR3) and autophagy reporter hESCs into human macrophages. All the hESC-derived cell-types were analysed for the expression of their surface markers, as well as examining some of the functional properties of the macrophages. The data demonstrate generation of monocytic cells and macrophages from hESCs, and that genome engineering in hESCs for stably incorporating the autophagy reporter in the genome did not affect their differentiation potential. Further analysis could be done in future for their molecular and functional characteristics.

The autophagy reporter human macrophage platform could be utilised for drug screening for identifying potent or tissue-specific autophagy modulators; which has been planned for future work in the laboratory of Dr Sovan Sarkar. The autophagy-inducing compounds stimulating macrophage autophagy could be utilised as candidate drugs for enhancing xenophagy and the killing of pathogens, and could be used as an adjunctive therapy in infectious diseases like tuberculosis as a host-directed therapy. The aspects related to pathogen biology will be undertaken in the future in collaboration with Dr Dhiraj Kumar at the International Centre for Genetic Engineering and Biotechnology in New Delhi, India.

Chapter 5

Discussions

Chapter 5: Discussions

5.1. Summary and significance of principal findings

5.1.1. Establishment of human embryonic stem cell (hESC) models of autophagy deficiency and autophagy reporter

In the scope of this thesis, isogenic human cellular platforms of autophagy deficiency (*ATG5*$^{-/-}$) and autophagy reporter (mCherry-EGFP-LC3) using hESC models were established and characterised. The autophagy-deficient hESCs were differentiated into neural precursors and neurons (in Chapters 2 and 3), while the autophagy reporter hESCs were differentiated into monocytic cells and macrophages (in Chapter 4). All the hESC-derived cell-types were further characterised for their cellular properties and autophagy phenotypes.

There are several advantages of hESC-based models to study autophagy. Firstly, hESCs are one of the most physiologically-relevant cell-types that can be subjected to genome editing (Soldner and Jaenisch, 2018; Byrne et al., 2014), as well as undergoing self-renewal and differentiation into the desired human cell-types that are otherwise not accessible or difficult to obtain (Thomson, 1998; Murry and Keller, 2008). hESCs are considered more relevant to undertaking research relevant to human biology, in comparison to immortalised cell lines or non-human cells (Keller, 2005). Moreover, primary cells are largely refractory to genome editing, and thus the hESC-derived cell-types that recapitulate many features of the corresponding primary cells provide a relevant experimental platform (Murry and Keller, 2008; Keller, 2005). Furthermore, the use of hESCs is more preferable than hiPSCs, because the latter could carry epigenetic alterations and background variations that may contribute to phenotypic cell-to-cell alterations (Soldner and Jaenisch, 2018). Secondly, both the autophagy-deficient and autophagy reporter hESC-based systems were generated from the same parental hESCs (WIBR3 hESCs) by genome engineering; thus making them isogenic with identical genetic background, except for the respective genes that were edited. Therefore, these systems can be employed for studying human cell-specific biological effects and drug discovery, and also makes them a powerful tool set for drug screening and validation for identifying novel small molecule autophagy modulators.

The hESC-based cellular platforms may also serve as a preclinical model for testing the efficacy of autophagy inducers before proceeding to clinical trials (Deb and Sarda, 2008; Guhr et al., 2018). For instance, the autophagy reporter human macrophage platform generated from hESCs will be utilised for drug screening with chemogenomics (drugs with known cellular targets) and marketed drug (FDA-approved drugs) libraries to identify the potent and/or cell-specific modulators of autophagy in this major immune cell-type. The candidate drugs augmenting macrophage autophagy will have therapeutic relevance for combating infections by promoting pathogen clearance (Kimmey and Stallings, 2016; Rubinsztein et al., 2015).

Similar research paradigm can be undertaken for other disease-relevant human cell-types that will have implications in diverse human diseases where stimulation of autophagy is beneficial (Rubinsztein et al., 2012; Galluzzi et al., 2017). There is a plethora of published protocols available for the differentiation of hESCs and hiPSCs into human cell-types of all the three germ layers. For instance, there are well-defined differentiation protocols describing the derivation of neurons (Chambers et al., 2009; Qi et al., 2017), hepatocytes (Touboul et al., 2009; Hay et al., 2008), pancreatic cells (D'Amour et al., 2006; Kroon et al., 2008), cardiomyocytes (Mummery et al., 2003; Kehat et al., 2001), amongst many others. Utilising the autophagy reporter hESC model, these cell-types can be generated with autophagy readout for image-based drug screening purposes. In a nutshell, the hESC models of autophagy are expected to have broad applications, and are not yet reported in the field.

5.1.2. Elucidation of a mechanistic link between autophagy deficiency and cell death using autophagy-deficient hESC model

Utilising the genetic hESC model of autophagy deficiency, the causal link between loss of autophagy and cytotoxicity was studied. Emphasis was given on the role of autophagy in maintaining neuronal homeostasis, given the major implications of autophagy dysfunction in contributing to the pathology of several neurodegenerative diseases (Seranova et al., 2020; Menzies et al., 2017; Nixon, 2013). *ATG5*$^{-/-}$ hESCs and hESC-derived neural precursors and neurons exhibited increased cell death, compared to their corresponding control (*ATG5*$^{+/+}$) cell-types, at basal state without the application of any external stressors. The neurotoxicity in *ATG5*$^{-/-}$ human neurons reinforces the notion that dysfunctional autophagy underlying neurodegenerative

disorders contributes to the disease pathology. The cell death phenotype in *ATG5*$^{-/-}$ cells is in agreement with the existing *in vivo* data wherein tissue-specific knockout of essential autophagy genes in normal mouse caused degeneration and/or dysfunction of the affected organs, such as brain (Hara et al., 2006; Komatsu et al., 2006), liver (Komatsu et al., 2007), muscle (Masiero et al., 2009) and heart (Nakai et al., 2007).

However, how loss or dysfunction of autophagy mediates cytotoxicity is not clear. By using metabolic profiling and biochemical approaches, a specific metabolic defect was identified to be causative of increased basal cell death in autophagy-deficient cells. Specifically, depletion of NADH was found to mediate cytotoxicity during autophagy deficiency via mitochondrial depolarisation and elevation in ROS. Boosting cellular NADH levels improved cell viability and mitochondrial membrane potential in *ATG5*$^{-/-}$ neurons. This intervention was also cytoprotective in a hiPSC-based model of NPC1 disease, which has been previously shown to be associated with autophagy and mitochondrial dysfunction (Maetzel, Sarkar et al., 2014; Ordonez et al., 2012). These findings elucidate a mechanistic link between autophagy deficiency and cytotoxicity that could be targeted for therapeutic interventions. This study also demonstrate proof-of-principle translation of the fundamental biology uncovered from a genetic model to imparting beneficial effects of biomedical relevance in a disease model.

5.2. Biomedical implications

Autophagy is implicated in diverse human pathological conditions including neurodegeneration and infection (Rubinsztein et al., 2015; Seranova et al., 2020; Levine and Deretic, 2007; Sharma et al., 2018). The output including the scientific data and knowledge, and the research tools, generated through this work has potential biomedical relevance for the treatment of human diseases.

5.2.1. Implications of NADH boosting compounds in neurodegenerative diseases associated with dysfunctional autophagy (related to Chapters 2 and 3)

Autophagy is critical for maintaining cellular homeostasis in post-mitotic cells like neurons (Stavoe and Holzbaur, 2019), whereas improper functioning of this process contributes to neuronal cell death (Menzies et al., 2014; Nixon, 2013). Genetic studies in mouse models demonstrated that brain-specific abrogation of basal autophagy causes neurodegeneration (Hara et al., 2006; Komatsu et al., 2006), implying that

basal autophagy is essential for neuronal homeostasis. Indeed, dysregulation of autophagy has been reported in myriad diseases including neurodegenerative and lysosomal storage disorders, where defective autophagy is implicated in disease pathology (Menzies et al., 2017; Nixon, 2013; Seranova et al., 2020; Seranova et al., 2017; Palhegyi et al., 2019; Sarkar, 2013). Of biomedical relevance, pharmacological induction of autophagy has beneficial effects in rescuing the disease pathology in transgenic models of a number of neurodegenerative disorders (Seranova et al., 2020; Sarkar, 2013; Levine et al., 2015; Boland et al., 2018; Rubinsztein et al., 2012). However, this therapeutic intervention relies on functional lysosomes so that autophagic flux could be restored by autophagy activation. Therefore, the autophagy induction strategy might not be effective in the context of certain neurodegenerative and lysosomal storage diseases if the functionality of lysosomes is compromised or due to the diverse nature of autophagy defects at multiple stages of the pathway (Seranova et al., 2020; Seranova et al., 2017).

Apart from diminished autophagic activity, ageing and neurodegenerative diseases are associated with lower NAD^+ levels (Lautrup et al., 2019; Hansen et al., 2018; Verdin, 2015). In these pathological contexts, supplementation with NAD^+ precursors is beneficial in animal and hiPSC models (Verdin, 2015; Schöndorf et al., 2018; Fang et al., 2017). The results from this study provided a new mechanistic link between loss of autophagy and cytotoxicity, mediated via NADH depletion, and also explained how pharmacologically boosting NAD^+/NADH levels can be neuroprotective in human neurons with autophagy deficiency or dysfunction. This approach was also found to be cytoprotective in a clinically-relevant model, such as NPC1 patient-derived neurons associated with defective autophagy. This intervention could have therapeutic relevance in a range of age-related, degenerative or lysosomal storage diseases linked to autophagy dysfunction (Seranova et al., 2020; Palhegyi et al., 2019; Seranova et al., 2017; Sarkar, 2013; Menzies et al., 2017; Nixon, 2013), where autophagy induction strategy might not be effective if lysosomal function is impaired. On the other hand, in the disease contexts where autophagy induction is beneficial, NADH-boosting agents could be used in addition to autophagy-inducing drugs for establishing a combinatorial treatment strategy.

5.2.2. Implications of autophagy reporter macrophage platforms for drug discovery for infectious diseases (related to Chapter 4)

Besides this essential role in maintaining cellular homeostasis, autophagy also contributes to innate defence mechanism by clearing invading pathogens within infected cells; a process termed xenophagy (Levine and Deretic, 2007; Deretic et al., 2013). In many infectious diseases, immune cells called macrophages provide the first line of defence against invading pathogens including bacteria and viruses (Stafford et al., 2002; Weiss and Schaible, 2015). However, these pathogens could manipulate host cell autophagy to evade their killing (Deretic et al., 2013; Sharma et al., 2018). Contrarily, multiple studies demonstrated that autophagy activation enhances pathogen clearance and killing; thus presenting a unique opportunity to combat infection (Kimmey and Stallings, 2016; Rubinsztein et al., 2015; Rubinsztein et al., 2012; Panda et al., 2019). This is pertinent for tuberculosis (TB), where stimulating autophagy facilitates clearance of the causative pathogen, *Mycobacterium tuberculosis (Mtb)* (Kim et al., 2019; Deretic, 2014). Since antibiotic resistance poses a major challenge for multi-drug resistant TB (Singh et al., 2019; Günther, 2014), host-directed mechanisms like autophagy are an attractive treatment alternative (Kim et al., 2019; Deretic, 2014). However, no treatment has been implemented by targeting autophagy, primarily due to lack of clinically-relevant human data. While the ability of some autophagy inducers to promote xenophagy is shown using immortalised, non-human or non-immune cells, their efficacy and drug action could be cell-type-specific (Rubinsztein et al., 2015; Panda et al., 2019; Seranova et al., 2020). Thus, the key barrier to translation is lack of known potent autophagy inducers in physiologically-relevant human macrophages, and therefore, there is an urgent need to identify such cell-type-specific drugs that will provide new host-directed treatment strategy against multi-drug-resistant *Mtb*.

This study has established autophagy reporter hESCs and hESC-derived human macrophage platforms. These *in vitro* generated macrophages recapitulated many features of primary macrophages, and thus present a physiologically-relevant experimental system for drug screening of xenophagy modulators. Moreover, the selectivity of autophagy in executing xenophagy without affecting the overall autophagic flux in host cells brings on the necessity to study potential fine-tuning mechanisms that can be deployed against a range of invading pathogens such as *Mtb,*

Salmonella and *HIV*, amongst others (Sharma et al., 2018; Chandra and Kumar, 2016). Furthermore, the autophagy reporter hESC-based system presents broad opportunities for making relevant human cell-types like neurons and hepatocytes for drug discovery programs in neurodegenerative or liver diseases associated with autophagy dysfunction (Rubinsztein et al., 2012; Galluzzi et al., 2017; Ueno and Komatsu, 2017; Sarkar, 2013).

5.3. Study limitations

5.3.1. Study limitations related to hESC-derived autophagy-deficient cellular platforms (related to Chapter 2)

One potential caveat is that the hESC- or hiPSC-derived human neurons are generated via *in vitro* differentiation, and thus are not the actual primary neurons. However, analyses of gene expression and functional properties including network formation demonstrated that these hPSC-derived neurons could resemble the characteristics of primary neurons, and that extended neuronal differentiation mimics human neural development (Nicholas et al., 2013; Hyvärinen et al., 2019; Weick, 2016; Kirwan et al., 2015). In general, multiple studies have validated the utility of hPSC-derived human neuronal platforms for studies related to neural development, disease modelling and drug screening in a manner relevant to human biology; thus providing a powerful tool for studying human neurodevelopment and neurodegeneration.

Another potential caveat include the possibility that autophagy deficiency would affect neuronal differentiation. However, this did not seem to be the case because autophagy deficient neurons could be generated from *ATG5*$^{-/-}$ hESCs. Although functional characterisation, such as measuring action potential of these neurons via long-term differentiation, was not undertaken, it seemed that short-term differentiation generated *ATG5*$^{-/-}$ neurons expressing the neuronal markers. Moreover, this work was done utilising two-dimensional culture conditions, and not in three-dimensional structure or in co-culture with other glial cells that recapitulates multiple aspects of the brain tissue (D'Aiuto et al., 2018; Frega et al., 2014; Roqué and Costa, 2017; Krencik et al., 2017). Nonetheless, the aim of this work was to generate autophagy-deficient human neurons as an in vitro experimental platform to study the role of autophagy in neuronal homeostasis and how loss of autophagy contributes to neurodegeneration.

In vitro differentiation of hPSCs usually generate up to 95% near-homogenous cell population of the desired cell-type (Saha and Jaenisch, 2009). To take this into account, many experiments were done by immunostaining the hPSC-derived cell-types, such as neural precursors, neurons, monocytic cells and macrophages, with lineage-specific markers to confirm their cellular identity. Furthermore, neuronal differentiation of multiple hESC lines often leads to variability of cell density of the neurons generated. Thus, it was important to normalise the experimental data to that of the cell number or loading control.

5.3.2. Study limitations related to the mechanistic link between autophagy deficiency and cell death (related to Chapter 3)

A mechanistic link between autophagy deficiency and cell death has been suggested due to a specific metabolic defect arising via NADH depletion, which results in mitochondrial depolarisation and oxidative stress to mediate cytotoxicity. Initially, unbiased metabolomics analyses revealed differential perturbations in *ATG5*$^{-/-}$ hESCs versus hESC-derived neurons. Although there were significant changes in glycolysis and TCA cycle intermediates, detailed analyses of these metabolic pathways were not performed due insufficient time, and will be considered to be undertaken in the future. Furthermore, apart from NADH, it is possible that there could also be other metabolites or amino acids contributing towards the cytotoxicity arising due to autophagy deficiency. Importantly, it is not mechanistically elucidated how loss of autophagy causes depletion of NADH. Moreover, although boosting NAD/NADH levels via pharmacological agents rescued the cell death in *ATG5*$^{-/-}$ hESCs and hESC-derived neurons, whether supplementation of other metabolites, nucleotides or amino acids will improve cellular viability was not examined. These aspects are pertinent to additionally understand how autophagy deficiency leads to cellular toxicity, and will be investigated in future follow-up studies.

Another aspect that requires further attention is the analysis of mitochondrial function. Firstly, it was difficult to measure mitochondrial respiration in hESC-derived neurons via Seahorse analysis due to technical limitations in differentiating and culturing the neuronal cells in speciality plates. Secondly, besides the measurement of mitochondrial $\Delta\Psi_m$, in-depth analyses of mitochondrial function including the activity of different ETC complexes were not done in *ATG5*$^{-/-}$ hESC-derived neurons. Similar

analyses could be done in NPC1 hiPSC-derived neurons, although mitochondrial defects have been reported in hESC-derived neurons with *NPC1* knockdown and in *Npc1* mutant mouse brain (Ordonez et al., 2012; Yu et al., 2005). Furthermore, additional dyes could have been utilised to measure mitochondrial $\Delta\Psi_m$ and ROS production (Dikalov and Harrison, 2014). For example, since the H_2DCF-DA probe used for measuring ROS is known to be oxidised by nanomolar concentrations of cytochrome c (Burkitt and Wardman, 2001), ROS production could be confirmed by HPLC-based method for detecting the oxidation of hydroethidine (Zielonka et al., 2019).

5.3.3. Study limitations related to hESC-derived autophagy reporter cellular platforms (related to Chapter 4)

There are few limitations related to the establishment of autophagy reporter cellular platforms in human macrophages differentiated from hESCs stably expressing mCherry-EGFP-LC3. The hESC-derived macrophages are not primary macrophages derived from human blood; rather, the former are *in vitro* derived cells. Nonetheless, the hESC- and hiPSC-derived macrophages expressed most of the surface markers, and also exhibited some of the physiological functions like phagocytosis and cytokine secretion (Gordon and Plüddemann, 2017). Even though there might be some differences in the expression of CD14, CD68 and CD163 in hPSC-derived macrophages, a number of studies have demonstrated that these cells largely recapitulate the surface marker expression profile and functional properties of primary macrophages (Karlsson et al., 2008; Wilgenburg et al., 2013; Härtlova et al., 2018; Lachmann et al., 2015).

It is important to consider that genome editing was possible in hESCs for generating the autophagy reporter human macrophages, which would have been difficult in primary macrophages because they are normally refractory to transfection (Warwick and Usachev, 2017). However, similar to the autophagy-deficient hESCs, there was a potential concern whether gene editing for inserting the mCherry-EGFP-LC3 construct in the *AAVS1* locus will affect the differentiation potential of hESCs into macrophages. Although there was a small but significant reduction in the expression of some of the pluripotency genes in autophagy reporter hESCs, their differentiation potential did not seem to be overtly affected because they could undergo differentiation into

macrophages via monocytic cells. During the differentiation process, there were some technical challenges that were successfully mitigated, such as those related to the production of similar-sized embryoid bodies, efficient generation of monocytic 'factories', and the differentiation of monocytic cells into macrophages in 96-well microplates for drug screening.

5.4. Future work

5.4.1. Further work for studying the role of autophagy in cell death (related to Chapters 2 and 3)

Employing the genetic hESC model of autophagy deficiency established through this work, the role of autophagy in cellular homeostasis was studied. Particularly, how loss of autophagy mediates cytotoxicity was elucidated, which was found to be via NADH depletion culminating in mitochondrial dysfunction and oxidative stress. The data opens up a new direction of research related to the role of autophagy in governing metabolic homeostasis, perturbation of which reduces cellular survival. There are a number of aspects in this study that could be further investigated in the future.

An unbiased metabolic profiling in this study revealed differential perturbations of glycolysis and TCA cycle metabolites, nucleotides and amino acids in *ATG5*$^{-/-}$ hESCs versus *ATG5*$^{-/-}$ hESC-derived neurons. This is possibly due to the cell-specific energy requirements of dividing hESCs and post-mitotic neurons. To further explore the data arising from metabolomics analysis, more experimental procedures could shed light into the metabolic status in these cells. The alterations in metabolites seen in the metabolomics data could be explained either by changes in its synthesis and/or utilisation. Thus, it is crucial to dissect why and how various metabolites are downregulated, and how this relates to increased cell death in autophagy-deficient cells. Although the respective starting molecules of glycolysis and TCA cycle, which are glucose and acetyl CoA, were decreased in *ATG5*$^{-/-}$ hESCs and neurons compared to the corresponding control (*ATG5*$^{+/+}$) cells, however, ATP was increased in *ATG5*$^{-/-}$ hESCs but decreased in *ATG5*$^{-/-}$ neurons. In-depth analysis of metabolic flux through these pathways should be undertaken in the future in autophagy-deficient cell-types via nuclear magnetic resonance (NMR) and mass spectrometry (MS)-based methods using stable isotope tracers (Allen and Young, 2020; Antoniewicz, 2015). The rate of glycolysis could also be simply measured by the amount of glucose uptake

versus lactate production. Additionally, the enzymes involved in the metabolic pathways affected could be analysed for their gene expression, protein level and enzymatic activity. Furthermore, since some of the nucleotides were perturbed in autophagy-deficient cells, the status of *de novo* and salvage pathways for nucleotide synthesis needs to be analysed in future (Fasullo and Endres, 2015; Mádrová et al., 2018).

Specifically in autophagy-deficient neurons, there seems to be metabolic collapse. Apart from various metabolites and energy carriers such as ATP, ADP, NAD^+ and NADH being significantly reduced in *ATG5*$^{-/-}$ neurons, the majority of the proteinogenic amino acids were also significantly decreased. This could also contribute to the cytotoxic effects arising from autophagy deficiency. For instance, reduction of NAD^+ in *ATG5*$^{-/-}$ neurons was possibly due to shortage of substrates like the essential amino acid, L-Tryptophan, which is required for its *de novo* synthesis (Verdin, 2015; Lautrup et al., 2019). It would be interesting to evaluate whether the supplementation of amino acids, such as L-Tryptophan or other amino acids that are depleted, would rescue the cell death phenotype in *ATG5*$^{-/-}$ neurons. Evaluating the effects by which an intervention is affecting the phenotype could clarify the importance of specific metabolic perturbations in autophagy-deficient cells.

Mitochondrial dysfunction is an important contributor to neurodegeneration (Burté, Carelli, Chinnery and Yu-Wai-Man, 2014; Bertholet et al., 2016), and this phenomenon in autophagy-deficient cells needs to be analysed in greater details. Firstly, mitochondrial respiration could be analysed by measuring oxygen consumption rates via Seahorse analysis in *ATG5*$^{-/-}$ hESCs and hESC-derived neurons (Eisner et al., 2018; Brand and Nicholls, 2011). These experiments should also be performed after the treatment with NADH-boosting agents in order to assess whether mitochondrial respiration is restored. Secondly, the measurement of mitochondrial $\Delta\Psi_m$ and ROS production could be analysed by additional dyes and methodologies (Dikalov and Harrison, 2014). In addition, the levels of SOD1 and SOD2 (superoxide dismutase 1 and 2) that converts the damaging superoxide radicals into hydrogen peroxide and molecular oxygen (Sea et al., 2014; Pias et al., 2003) should be evaluated to clarify their role in the cytotoxicity in *ATG5*$^{-/-}$ cells. Moreover, abrogation of autophagy by *ATG5* knockout likely prevented selective autophagy, which is normally dependent on cargo receptors and their ability to attach to a LIR motif during the autophagosome

formation. Indeed, mitophagy was found to be impaired in *ATG5*$^{-/-}$ neurons. Further investigation of various biomarkers related to mitophagy and mitochondrial homeostasis should be carried out. This would include mitochondrial fission and fusion. These events could be analysed through the levels of DRP1 (dynamin-related protein 1) and FIS1 (mitochondrial fission 1 protein) regulating mitochondrial fission, and OPA1 (dynamin-like 120 kDa protein) and Mitofusins regulating mitochondrial fusion (Scott and Youle, 2010; Westermann, 2010). Alterations in intracellular mitochondrial load due to impaired mitophagy in *ATG5*$^{-/-}$ cells could also be confirmed by measuring mitochondrial DNA copy number (Longchamps et al., 2020; O'Hara et al., 2019).

Detailed analysis of mitophagy and mitochondrial dysfunction could also be done in NPC1 patient hiPSC-derived neurons, although mitochondrial defects have been already reported in hESC-derived neurons with *NPC1* knockdown and in *Npc1* mutant mouse brain (Ordonez et al., 2012; Yu et al., 2005). Importantly, it is necessary to confirm that NADH is reduced in NPC1 hiPSC-derived neurons, and that the NADH-boosting compounds could rescue NADH levels and mitochondrial depolarisation for improving cell viability. Such data would strengthen the hypothesis that NADH depletion in neurodegenerative diseases associated with autophagy dysfunction is a critical determinant of neuronal cell death. Indeed, NADH levels were found to be reduced in 2 biological replicates (n = 2) of NPC1 patient hiPSC-derived neurons, compared to healthy control hiPSC-derived neurons (data not shown); however, this result needs to be confirmed in more biological replicates to obtain statistical relevance.

An important topic that warrants in-depth investigation is how NADH is depleted during autophagy deficiency. Unbiased multi-omics approaches, such as proteomics and transcriptomics, could be undertaken in *ATG5*$^{-/-}$ cells to identify any specific changes leading to NADH depletion. These cells could be also subjected to metabolomics after treatment with the NAD^+/NADH-boosting agents in order to confirm that restoration of NADH levels is a common denominator underlying their cytoprotective effects. Further confirmation of a role of NADH depletion causing cytotoxicity could be shown by using an inhibitor of nicotinamide phosphoribosyltransferase (NAMPT), which is involved in NAD biosynthesis (Hasmann and Schemainda, 2003). Apart from the shortage of L-Tryptophan in *ATG5*$^{-/-}$ neurons required for *de novo* NAD synthesis discussed above

(Verdin, 2015; Lautrup et al., 2019), further investigation is necessary to understand the role of enzymes that use NAD^+ as a cofactor and cleave it into ADP-ribose and nicotinamide (NAM) (Cantó et al., 2015); all of which will lead to depletion of NADH. Two main classes of such enzymes are sirtuins (SIRTs) and poly-ADP-ribose polymerases (PARPs), which are activated due to oxidative stress or DNA damage that could occur during autophagy deficiency (Hewitt and Korolchuk, 2017; Filomeni et al., 2014). While short-term activation of SIRTs and PARPs during stress response is beneficial for adaptation to metabolic or genetic abnormalities, uncontrolled NAD^+ cleavage could lead to depletion of NADH and contribute to cytotoxicity (Cantó et al., 2015). Furthermore, there is extensive literature that modulation of NAD^+ promotes longevity and healthy life span via regulation of sirtuins (Imai, 2009; Verdin, 2015; Imai and Guarente, 2016; Imai and Guarente, 2014). Therefore, it is important to assess any perturbations in the levels and activities of SIRTs and PARPs in *ATG5*$^{-/-}$ cells, and whether these changes are restored after boosting NAD^+/NADH levels via supplementation with NAM and nicotinamide riboside (NR).

Specifically, the enzymes SIRT1, PARP1 and PARP2 are competing for NAD^+. In the event of DNA damage, activation of PARP1 decreased the availability of NAD^+ for SIRT1 (Luna et al., 2013; Chung and Joe, 2014). PARP1 was also found to be increased by elevated ROS levels in neurons (Martire et al., 2013). On the other hand, SIRT1 was increased in PARP2 mutant mice (Bai et al., 2011), and NAD^+-dependent activation of SIRT3 prevented cell death (Brown et al., 2014). The anti-oxidant effects of SIRT3 could be attributed to its ability to activate SOD2 amongst other mechanisms. As SIRT3 is an NAD-dependent deacetylase located in the mitochondrial matrix, its levels should be assessed to interpret the calibration of NADH pools in *ATG5*$^{-/-}$ neurons. Moreover, PARPs may suppress sirtuin activity and SIRT1 regulates PGC-1α, a transcription factor that activates mitochondrial biogenesis (Rodgers et al., 2005). A further analysis of this elegant interplay between sirtuins and PARPs can clarify their role in depleting the NADH pools in autophagy-deficient cellular platforms. Taking all of these into consideration, the analysis of SIRT1, SIRT3, PARP1 and PARP2 in *ATG5*$^{-/-}$ cells would uncover up the mechanistic links between these molecular players.

The anabolic and catabolic effects of autophagy deficiency on NAD metabolism, and mRNA expression of the enzymes and their activity of some key rate-limiting steps

would provide more information of the physiological processes involved in the interplay of autophagy and NADH levels. It is noteworthy that changes in NAD^+ levels may be caused by both changes in its synthesis through *de novo* and/or salvage pathways, or by its degradation by various NADases (NAD^+ nucleosidase) such as CD38, PARPs and sirtuins (Bai et al., 2011; Bai and Cantó, 2012; Aksoy et al., 2006; Imai and Guarente, 2014). These aspects could be investigated in *ATG5*$^{-/-}$ cells along with the 'rescue' condition after boosting NAD^+/NADH levels with NAM and NR.

For biomedical applications, it is important to ascertain that the discoveries made in genetic models of autophagy deficiency are corroborated in neurodegenerative disease models associated with autophagy dysfunction. NPC1 disease model has been utilised in this study (Maetzel, Sarkar et al., 2014), where NADH-boosting agents improved cell viability. In future, depletion of NADH and improvement of cell viability by boosting NADH could be studied in multiple early-onset and late-onset neurodegenerative conditions. This would demonstrate the generalisability of the fundamental mechanism and biomedical relevance across several diseases wherein defective autophagy is a common contributor to the disease pathology. For instance, such studies could be initially carried out in patient-derived hiPSC models of a rare, childhood-onset neurodegenerative disorder called Wolfram syndrome (Barrett and Bundey, 1997), since the hiPSC lines are available in the laboratories of Dr. Sovan Sarkar and Prof. Timothy Barrett; and their research groups have found impairment of autophagy at the level of autophagosome formation in this disease context (unpublished data).

Overall, the outcome of this work has opened up multiple research directions for fundamental understanding or biomedical applications. Such a vast amount of work as suggested to be undertaken in the future was not feasible within the PhD timeframe, specifically because the nature of human stem cell culture work involving the generation of neurons is extremely time-consuming.

5.4.2. Further work for developing and utilising the autophagy reporter cellular platforms (related to Chapter 4)

In this study, autophagy reporter cellular platforms have been established using a hESC-based system. The goal was to generate a human macrophage screening platform expressing a tandem-fluorescent-tagged autophagy reporter that will be

utilised for studying xenophagy and identifying xenophagy modulators. A lot of characterisation of the autophagy reporter hESC-derived monocytic cells and macrophages has been done in this work. Despite this, further characterisation should be carried out to ensure that these *in vitro* derived cell-types exhibit the characteristics and functional properties of human blood-derived primary monocytes and macrophages (Wynn et al., 2013; Gordon and Plüddemann, 2017). Firstly, their ability to secrete iNOS (inducible nitric oxide synthase) and TNFα (tumor necrosis factor alpha) could be measured after an inflammatory stimulus like IFNγ in order to ascertain they are capable of chemokine secretion. Next, the levels of IL1, IL6, IL8, IL10, IL12 and other cytokines could be analysed via ELISA. The secretion of these pro-inflammatory and anti-inflammatory cytokines signifies an appropriate functionality of the macrophages and their proper response to infection (Arango Duque and Descoteaux, 2014). Finally, the phagocytic capability of hESC-derived macrophages should be evaluated, not only with necrotic Jurkat cells as done in this study, but also with various pathogens such as *Mtb* and *Salmonella*. These experiments will provide more support that the autophagy reporter hESC-derived macrophages are able to serve a physiologically-relevant cellular model for studying cell-specific autophagy regulation, xenophagy and drug screening.

The autophagy reporter macrophages would be utilised for drug screening to identify potent or cell-specific autophagy inducers, which will then be evaluated for their ability to promote pathogen clearance. To prepare for an image-based drug screen, the positive and negative controls (that are known autophagy inducers and blockers, respectively) should be determined in a dose-dependent manner in 96-well microplates using the CellInsight High-Content Screening (HCS) microscope and HCS Studio Cell Analysis software. The positive controls will include autophagy inducers such as rapamycin (induce autophagy via mTOR inhibition), and trehalose, carbamazepine and vitamin D (induce autophagy independently of mTOR); all of which are known to induce autophagy in macrophages (Sharma et al., 2020; Campbell and Spector, 2011; Schiebler et al., 2014; Gutierrez et al., 2004). The negative controls will include autophagy blockers such as bafilomycin A1 and chloroquine (Boya et al., 2005; Murakami et al., 1998). At least two drug screens could be initially undertaken in autophagy reporter hESC-derived macrophages using a chemogenomics drug library (comprising of compounds with known cellular targets) and a marketed drug

library (consisting of FDA-approved drugs); both of which have been procured from Dundee Drug Discovery Unit. The chemogenomics set will inform the regulation of autophagy in human macrophages, whereas the marketed drug set will inform about the FDA-approved drugs that could be repurposed for treating infectious diseases. The high-confidence hits will be characterised by secondary autophagy assays, followed by evaluation of their therapeutic efficacy in promoting xenophagy.

In general, the autophagy reporter hESC-based system will serve as a powerful tool to generate isogenic hESC-derived cell-types in order to undertake drug screening in a cell-specific manner. The autophagy reporter macrophages could also be utilised for xenophagy studies. For example, co-localisation between fluorescent-tagged pathogens with the autophagic compartments (autophagosomes and autolysosomes) will inform xenophagic flux in real time. In addition, autophagy-deficient macrophages could be generated from *ATG5*$^{-/-}$ hESCs. These platforms will be useful for investigating the dependency on autophagy for the clearance of a range of intracellular pathogens. In summary, both the autophagy reporter and autophagy-deficient systems are derived from the same parental hESCs, thereby providing state-of-the-art isogenic platforms for drug screening and validation.

Chapter 6

Materials and Methods

Chapter 6: Materials and Methods

6.1. Cell culture

6.1.1. Culture of human embryonic stem cells (hESCs) and human induced pluripotent stem cells

Human embryonic stem cells (WIBR3) and human induced pluripotent stem cells including control and NPC1 hiPSCs were obtained from Whitehead Institute, MIT, Boston, USA. All relevant ethical permissions can be presented upon request. Human embryonic stem cells (hESCs; WIBR3) (Lengner et al., 2010) including *ATG5*$^{+/+}$, *ATG5*$^{-/-}$ and mCherry-EGFP-LC3 hESC lines) and human induced pluripotent stem cells (hiPSCs) including control and NPC1 hiPSC lines (Maetzel, Sarkar et al., 2014) were cultured, as previously described (Lengner et al., 2010; Maetzel, Sarkar et al., 2014). Briefly, hESCs and hiPSCs were cultured on feeder layer of inactivated mouse embryonic fibroblasts (MEFs) in hESC medium consisting of DMEM/F12 (Gibco), 15% (v/v) fetal bovine serum (HyClone), 5% (v/v) KnockOut Serum Replacement (Gibco), 1% (v/v) L-glutamine (Gibco), 1% (v/v) non-essential amino acids (Gibco), 1% (v/v) Penicillin/Streptomycin (Gibco), 4 ng/mL human recombinant basic fibroblast growth factor (bFGF; R&D Systems) and 0.1 mM β-mercaptoethanol (Sigma-Aldrich). The hESCS and hiPSCs were also cultured feeder-free on Geltrex (Gibco) basement membrane matrix in StemFlex Basal Medium supplemented with StemFlex 10X Supplement (Gibco) and 1% (v/v) Penicillin/Streptomycin (Gibco), or on Matrigel (Stem Cell technologies) basement membrane matrix in mTeSR1 medium supplemented with mTeSR1 5X supplement (Stem Cell Technologies) and 1% (v/v) Penicillin/Streptomycin (Gibco). The hESCs and hiPSCs were maintained on feeders or feeder-free in a humidified incubator with 5% CO_2 and 5% O_2 at 37 °C. For starvation-induced autophagy, hESCs were cultured in Hank's Balanced Salt Solution (Gibco) for 3 h.

6.1.2. Human pluripotent stem cell culture: challenges and considerations

Human pluripotent stem cells (hPSCs; comprising of hESCs and hiPSCs) require continuous daily cell culture. Previously, the standard process was to co-culture hPSCs in a feeder layer of inactivated mouse embryonic fibroblasts (iMEFs). The iMEFs secrete various growth factors such as Activin A (Beattie et al., 2005) and thus

contribute to the maintenance of stemness in hPSCs for over 20 passages. The culture medium is changed daily with specialised hESC medium containing HyClone FBS and growth factors such as bFGF. The daily feeding is necessary as the half-life of bFGF is approximately 18 h, and it is crucial to maintain a high level of growth factors to maintain the hESCs in undifferentiated state. The hESCs are cryopreserved in HyClone FBS-containing cryomedium, and need to be revived back onto a feeder layer. More recently, more sophisticated culture methods were established, replacing the feeder layer of iMEFs with a basement membrane containing extracellular proteins and growth factors termed extracellular matrix (ECM), which maintains the pluripotency of hPSCs. Various ready-to-use commercial ECMs, such as Matrigel or Geltrex, are efficient for culturing hPSCs and require less time investment than the iMEFs generation and maintenance. In addition, a feeder-free culture ensures that only hPSCs are being analysed when cells are harvested from wells for population-level analysis such as for gene expression and immunoblotting. For these reasons, the hESC cell lines used in this study were primarily cultured feeder-free with fully-defined, xeno-free stem cell culture medium. When hPSCs are cultured on an ECM, the complementing media are optimised for prolonged feeding intervals. This results from the chemical structure of the growth factors contained in the media, with the most crucial optimised component being the beta Fibroblast Growth Factor (bFGF), which remains stable at 37 °C for over 40 hours and thus allowing for a flexible feeding schedule. The feeder-free medium, mTeSR and StemFlex, used in this study both contain thermostable growth factors including bFGF.

6.2. Differentiation of hESCs and hiPSCs into neural precursors and terminally differentiated neurons

Differentiation into neural precursor cells (NPs) and terminally differentiated neurons was performed, as previously described (Maetzel, Sarkar et al., 2014; Sarkar et al., 2007). This was carried out for *ATG5*$^{+/+}$ and *ATG5*$^{-/-}$ hESC lines, and the Control and NPC1 hiPSC lines. Briefly, hESC or hiPSC colonies were collected using 1.5 mg/mL collagenase type IV (Thermo Fisher Scientific), separated from the MEF feeder cells by gravity and cultured in non-adherent suspension culture dishes (Corning) in NP medium (NPM) comprising of DMEM -F12 containing B27, 1% (v/v) L-Glutamine, 1% (v/v) nonessential amino acids and 1% (v/v) Penicillin/Streptomycin (all from Thermo

Fisher Scientific) supplemented with 50 ng/ml human recombinant Noggin (Peprotech) and 10 μM SB431542 (Stemgent) for the first 4 days. NPM supplemented with Noggin and 20 ng/ml bFGF (R&D Systems) was used sequentially in the next 2 days (days 6-7), and NPM supplemented with only bFGF were used sequentially in the following 7 days (days 7-14) for further NP differentiation. At day 14, NPs clusters were dissociated and plated onto 100 μg/ml poly-L-ornithine (Sigma-Aldrich) and 14 μg/ml laminin (Sigma-Aldrich) pre-coated culture dishes in N2B27 medium comprising of DMEM -F12 containing N2, B27, 1% (v/v) L-Glutamine, 1% (v/v) nonessential amino acids and 1% (v/v) Penicillin/Streptomycin (all from Thermo Fisher Scientific) supplemented with 20 ng/ml bFGF (R&D systems) and 20ng/ml EGF (R&D systems). After 7 days in culture, neural rosette-bearing cultures were dissociated using StemPro Accutase (Thermo Fisher Scientific) and subsequently expanded on poly-L-ornithine and laminin coated cell culture dishes at the density of ~1.5×10^6 cells per well (of 6-well plate) in N2B27 medium supplemented with bFGF and EGF. Proliferating NPs were passaged up to 4 times before induction of terminal differentiation into neurons by growth factor withdrawal in N2B27 medium. Differentiated neurons were used for analysis 3-4 weeks after differentiation.

6.3. Differentiation of hESCs into monocytic cells and macrophages

The hESCs were differentiated into macrophages utilising the previously described protocol via embryoid body (EB) formation (Wilgenburg et al., 2013; Karlsson et al., 2008). This was carried out for wild-type (WIBR3) and mCherry-EGFP-LC3 hESC lines. Briefly, hESCs were cultured until colonies reached approximately 70% confluency, after which the hESC colonies were broken down into single cells for plating the cells into Aggrewells 800 (Stem Cell Technologies). This initial step of differentiation was modified while putting the cells in the Aggrewells 800 by adding the Mesoderm Booster reagent (Elixirgen Scientific) in EB medium at 1:10 ratio, and then replacing with EB medium after 4 h. Cells were seeded at approximately 4×10^6 per Aggrewell to form 300 EBs of around 2×10^4 cells/EB. Cells were maintained in 2 mL of EB medium comprising of mTeSR1 or StemFlex medium supplemented with 50 ng/mL BMP4 (Gibco), 20 ng/mL SCF (Peprotech), 50 ng/mL VEGF (Peprotech) with daily media change. After 7 days, the EBs were collected and plated into adherent 6-well plates or T75 flasks (for the generation of monocytic cell ‘factories’) in X-VIVO 15

medium (Lonza) supplemented with 25 ng/mL IL-3 (Invitrogen) and 100 ng/mL M-CSF (Invitrogen), 1% (v/v) Penicillin/Streptomycin, 2 mM Glutamax (Gibco) and 50 µM of 2-mercaptoethanol. 50% of the media was changed once a week. After 4-5 weeks, the 'factories' started producing monocytes. For generation of macrophages, the monocytic cells were harvested along with the supernatant, centrifuged for 5 min at 300 x g, resuspended in X-VIVO 15 medium supplemented with 100 ng/mL M-CSF, 1% (v/v) Penicillin/Streptomycin and 2 mM Glutamax, and cultured for 7 days with media change every 3-4 days. Macrophages were also generated from hiPSC-derived monocytic cell 'factories' obtained from the laboratory of Prof. Robin May (University of Birmingham, UK).

6.4. Lipid nanoparticle mediated mRNA delivery

Lipid nanoparticles (LNPs) were provided by and made in the laboratory of Daniel Anderson at the Koch Institute in MIT, USA. C12-200 (prepared as previously described (Love et al., 2010); courtesy of Alnylam Pharmaceuticals, Cambridge, MA) was mixed together with 1,2-dioleoyl-sn-glycero-3-phosphoethanolamine (DOPE; Avanti Polar Lipids, Alabaster, AL), cholesterol (Sigma), and 1,2-dimyristoyl-snglycero- 3-phosphoethanolamine-N-[methoxy(polyethylene glycol)-2000] (ammonium salt) (PEG; Avanti) at a 50:20:20:10 weight ratio in ethanol. Then, an aqueous phase containing human ATG5 or GFP mRNA (TriLink Biotechnologies, San Diego, CA) in 10 mM citrate buffer was prepared. Syringe pumps were used to mix the ethanol and aqueous phases at a 1:3 ratio, as previously described (Kauffman et al., 2015), to generate C12-200 lipid nanoparticles (LNPs), which were then dialyzed against 1x PBS in a 20k MWCO cassette at 4 °C for 2 h. The mRNA concentration was quantified using a modified Quant-iT RiboGreen RNA Assay (Invitrogen), as previously described (Heyes, Palmer, Bremner and MacLachlan, 2005). Cells (hESCs and hESC-derived neurons) were treated with 2 µg/ml C12-200 LNP-encapsulated human *ATG5* or *GFP* mRNA, for 4 days with replenishment on day 2, or as indicated in the figure legends.

6.5. Compounds and treatment

Compounds used for boosting cellular NAD/NADH levels in *ATG5*$^{-/-}$ hESCs and in neurons derived from *ATG5*$^{-/-}$ hESCs or NPC1 hiPSCs are as follows: 1mM

Nicotinamide (NAM) (Sigma-Aldrich), 1 µM CP2 (synthesised previously) (Zhang et al., 2015) and 500 nM I-BET 525762A (I-BET) (Med Chem Express). Treatment of NAD/NADH boosting compounds was done in *ATG5*$^{-/-}$ hESCs for 2 days with replenishment on day 1, and in *ATG5*$^{-/-}$ hESC- and NPC1 hiPSC-derived neurons for 6 days with replenishment on day 3. Autophagy-modulating compounds used in mCherry-EGFP-LC3 hESCs are as follows: 200 nM Rapamycin (autophagy inducer) and 40 nM Bafilomycin A_1 (autophagy blocker) (both from Enzo Life Sciences). mCherry-EGFP-LC3 hESCs were treated with Rapamycin for 24 h for inducing autophagy, and with Bafilomycin A_1 for 4 h for blocking autophagy.

6.6. Analysis of autophagic vesicles by mCherry-EGFP-LC3 reporter

Autophagic vesicles can be quantified using the pH–sensitive, tandem fluorescent-tagged mRFP-GFP-LC3 reporter (Kimura et al., 2007). mCherry-EGFP-LC3 hESC line was subjected to starvation-induced autophagy by HBSS for 2 h, after which the cells were fixed with 4% formaldehyde and mounted on ProLong Gold antifade reagent with DAPI prior to fluorescence image analysis. Analysis was done for the number of autophagosomes that have both mCherry and EGFP signals (mCherry$^+$/EGFP$^+$), and for autolysosomes that emit only acid-stable mCherry signal (mCherry$^+$/EGFP$^-$) because the acid-labile EGFP signal is quenched in the acidic lysosomal environment. Autolysosomes were quantified by subtracting the EGFP spot count from the mCherry spot count, while the autophagosomes were quantified by the EGFP spot count only. Images were taken with Perkin Elmer UltraView spinning disk confocal system (Perkin Elmer) as described in Section 6.9. Quantification of mCherry$^+$ and EGFP$^+$ vesicles was done using the Analyze Particle plugin in ImageJ software (NIH), as described previously (Sarkar et al., 2013).

6.7. Immunoblotting analysis

Cell lysates were subjected to immunoblot analysis, as previously described (Seranova et al., 2019; Sarkar et al., 2013). Cell pellets were lysed on ice in 2X Lysis Buffer comprising of 20 mM Tris-HCl pH 6.8, 137 mM NaCl, 1 mM EGTA, 1% (v/v) Triton X-100, 10% (v/v) glycerol and 25X Protease Inhibitor Cocktail (all from Sigma-Aldrich) (buffer made to 1X) for 30 min, boiled for 5-10 min at 100 °C. Protein concentration of the lysates was measured by Bio-Rad Protein Assay (Bio-Rad), and

equal amounts of protein (15-40 µg) per sample were subjected to SDS–PAGE and immunoblot analysis, as previously described (Seranova et al., 2019). The blots were then incubated in Blocking Buffer [6% (w/v) non-fat milk powder in PBS-Tween 20) for 1 h at room temperature. For cleaved caspase-3 immunoblotting, cells were lysed with RIPA Lysis Buffer comprising of 50 mM Tris-HCl pH8, 150 mM NaCl, 1 mM EDTA, 0.5% (w/v) deoxycholate, 1% (v/v) IGEPAL (all from Sigma-Aldrich), 0.1% (w/v) SDS (Bio-Rad) and Complete Protease Inhibitor Cocktail (Roche), sonicated and centrifuged at 14000 rpm for 30 min at 4 °C. The samples were subjected to SDS–PAGE on a 16.5% (v/v) gel, immunoblot analysis on nitrocellulose membrane, then membrane was blocked in 1% (v/v) Glutaraldehyde solution (VWR Life Science) in TBS for 30 min and in Blocking Buffer [6% (w/v) non-fat milk powder in PBS-Tween 20] for 1 h at room temperature. All the blots were incubated overnight in primary antibodies (Table 6.1) at 4 °C on a shaker platform. The immunoblots were then probed with the relevant secondary antibodies (Table 6.1) for 1 h at room temperature on a shaker platform, and visualised using Amersham ECL Western Blotting Detection Reagent (GE Healthcare). Densitometry analyses on immunoblots were performed using ImageJ v1.48 (NIH), as previously described (Seranova et al., 2019, Sarkar et al., 2013). The data were expressed as a percentage of the control condition that is set to 100%.

Table 6.1. List of primary and secondary antibodies for immunoblotting analysis

Antigen	*Source*	*Catalogue number*	*Dilution*
Primary antibodies			
Actin	Sigma-Aldrich	MABT1333	1:4000
ATG5	NanoTools	0262-100/ATG5-7C6	1:400
Cleaved caspase-3$^{(Asp175)}$	Cell Signaling Technology	9661	1:1000
GAPDH	Sigma-Aldrich	G8795	1:5000
GFP	Clontech	632375	1:5000
LC3B	Novus Biologicals	NB100-2220	1:2000
MAP2	Invitrogen	PA5-17646	1:5000
NESTIN	BioLegend	656802	1:2000
p62	BD Biosciences	610832	1:1000
p70 S6 kinase	Cell Signaling Technology	9202	1:1000
PAX6	BioLegend	901301	1:2000
Phospho-p70 S6 kinase$^{(Thr389)}$	Cell Signaling Technology	9206	1:1000
Phospho-S6 ribosomal protein $^{(Ser235/236)}$	Cell Signaling Technology	2211	1:4000
S6 ribosomal protein	Cell Signaling Technology	2217	1:4000
SOX2	R&D Systems	AF2018	1:500
Tom20	Santa Cruz Biotechnology	sc-17764	1:5000
Tubulin	Sigma-Aldrich	T6793	1:5000
TUJ1 (TUBB3)	BioLegend	801201	1:5000
Secondary antibodies			
Goat anti-mouse IgG, H&L chain specific peroxidase conjugate	Calbiochem	401253	1:10000

Goat anti-rabbit IgG, H&L chain specific peroxidase conjugate	Calbiochem	401393	1:10000
Rabbit anti-goat IgG, H&L chain specific peroxidase conjugate	Calbiochem	401515	1:10000

6.8. Immunofluorescence analysis

Immunofluorescence analysis was performed in hESCs and hESC-derived cell-types (such as neural precursors, neurons and macrophages), as previously described (Maetzel, Sarkar et al., 2014; Seranova et al., 2019; Sarkar et al., 2013) in 12-well plates or 24-well plates, where cells were cultured on coverslips. Briefly, cells were washed in PBS, fixed with 4% (v/v) formaldehyde (Thermo Fisher Scientific) at room temperature (RT) for 15 min, permeabilised with 0.5% (v/v) Triton X-100 (Sigma-Aldrich) for 10 min (for all primary antibodies except LC3 antibody) or with pre-chilled methanol for 5 min (for LC3 antibody), again washed in PBS and incubated with Blocking Buffer, comprising of 5% (v/v) goat or donkey serum (Sigma-Aldrich) in PBS, for 1 h at RT on a shaker platform. Cells were then incubated overnight with primary antibodies (Table 6.2) at 4 °C followed by incubation with relevant secondary antibodies (Table 6.2) for 1 h at RT, during which the cells were washed multiple times with PBS after the applications of primary and secondary antibodies. For 12-well plates, the volume of all reagents was 200 µL and for 24-well plates was 100 µL per well. The coverslips were mounted on glass slides with ProLong Gold antifade reagent with DAPI (Invitrogen).

Table 6.2. List of primary and secondary antibodies for immunofluorescence

Antigen	*Source*	*Catalogue number*	*Dilution*
Primary antibodies			
CD86	Abcam	Ab53004	1:500
IBA1	Abcam	Ab5076	1:500
LC3B	NanoTools	0231-100/LC3-5F10	1:200
MAP2	Invitrogen	PA5-17646	1:200
NANOG	R&D Systems	SC009	1:100
NESTIN	BioLegend	656802	1:100
OCT-3/4	R&D Systems	SC009	1:100
PAX6	BioLegend	901301	1:100
SOX2	R&D Systems	SC009	1:100
SSEA4	R&D Systems	SC009	1:100
Tom20	Santa Cruz Biotechnology	sc-17764	1:100
TRA-1-60	R&D Systems	MAB4770	1:100
TUJ1 (TUBB3)	BioLegend	801201	1:200
Secondary antibodies			
Donkey anti-goat IgG (H+L) Alexa fluor 647	Invitrogen	A-32849	1:1000
Donkey anti-mouse IgG (H+L) Alexa Fluor 594	Invitrogen	A-32744	1:1000
Goat anti-mouse IgG (H+L), Alexa Fluor 488	Invitrogen	A-11001	1:1000
Goat anti-mouse IgG (H+L), Alexa Fluor 594	Invitrogen	A-11005	1:1000

Goat anti-rabbit IgG (H+L), Alexa Fluor 488	Invitrogen	A-11008	1:1000
Goat anti-rabbit IgG (H+L), Alexa Fluor 594	Invitrogen	A-11012	1:1000
Goat anti-rabbit IgG (H+L) Alexa Fluor 647	Invitrogen	A-32733	1:1000
Donkey anti-goat IgG (H+L), Alexa Fluor 488	Invitrogen	A-11055	1:1000

6.9. Image acquisition of fixed cells

Fluorescence images of fixed cells were acquired using EVOS FL Cell Imaging System (Thermo Fisher Scientific) with AMG 10x Plan FL and AMG 40x Plan FL lens, Leica DM6000 B (Leica Microsystems) with Leica DFC 350 FX R2 camera and with HC PL APO 40x/1.25 or HC PL APO 100x/1.40 oil immersion lens with Leica Application Suite X software (Leica Microsystems), or with Perkin Elmer UltraView spinning disk confocal system (Perkin Elmer) with an Orca-ER cooled–CCD camera (Hamamatsu) on a Zeiss Axiovert 200 (Carl Zeiss Inc.) with 63x 1.4NA plan-apochromat oil immersion lens using Volocity v6.1 software (Improvision). For each experiment, the exposure of the control samples was established as a baseline first, and then images of control and treated or knockout/reporter cells were taken. Images were taken at a non-saturating threshold.

6.10. Gene expression analysis

Total RNA was extracted using Trizol (Ambion) followed by DNase treatment using the RNase-free DNase set (Qiagen). Reverse transcription PCR (RT-PCR) was performed using M-MLV Reverse Transcriptase (Promega) and quantitative PCR (qPCR) was performed using the CFX Connect Real-Time System (Bio-Rad), as previously described (Hummon et al., 2007). 25 µM of primers (Table 6.3) (Sigma-Aldrich) were used in SYBR Green mastermix (Applied Biosystems) that was added to 5 ng of cDNA in white, 96-well plates with round bottom (Bio-Rad). Results were analysed using $2^{-\Delta\Delta Ct}$ method and were normalised to the expression of the housekeeping gene *GAPDH*.

Table 6.3. List of primers for qPCR

Gene	*Species*	*Primer*	*Sequence*
NANOG	Human	*NANOG* Forward	TGTGTACTCAATGATAGATT
		NANOG Reverse	GTCTTCACCTGTTTGTAG
POU5F1	Human	*POU5F1* Forward	TCTATTTGGGAAGGTATTC
		POU5F1 Reverse	TTGCATATCTCCTGAAGA
SOX2	Human	*SOX2* Forward	CGGACAGCGAACTGGAGG
		SOX2 Reverse	CTGTTTCTTACTCTCCTCTTTTGC
GAPDH	Human	*GAPDH* Forward	TCGACAGTCAGCCGCATCTTCTTT

	GAPDH Reverse	ACCAAATCCGTTGACCTT

6.11. Cell death analysis

6.11.1. TUNEL assay for apoptotic cells

Cells were stained with Click-iT Plus TUNEL Assay for in situ apoptosis detection, Alexa Fluor 488 dye (Invitrogen), according to the manufacturer's protocol. In brief, cells (hESC-derived neurons and hiPSC-derived neurons) were cultured in 24-well plates, on coverslips coated with poly-L-ornithine and laminin as described in 6.2. Cells were fixed with 4% (v/v) formaldehyde (Thermo Fisher Scientific) for 15 min and permeabilised with 0.25% (v/v) Triton X-100 (Sigma-Aldrich) for 20 min at room temperature, then washed with deionised water. Cells were incubated at 37 °C for 10 min in TdT reaction buffer, followed by incubation with TdT reaction mixture containing TdT reaction buffer, EdUTP, TdT enzyme for 60 min at 37 °C, washed with 3% (w/v) BSA, and finally incubated with Click-iT Plus TUNEL reaction cocktail for 30 min at 37 °C followed by washes with 3% BSA. For detection of TUNEL$^+$ apoptotic nuclei in specifically in neurons, cells with subjected to immunofluorescence by blocking with 3% (w/v) BSA (in PBS) followed by incubation with TUJ1 antibody (in 3% BSA in PBS) overnight at 4°C, and thereafter incubated with Alexa Fluor 594 secondary antibody for 1 h at room temperature. The volume of each reagent was 125 µL per well. Coverslips were mounted on glass slides with ProLong Gold antifade reagent with DAPI (Invitrogen). The quantification of TUNEL$^+$ apoptotic nuclei in TUJ1$^+$ neuronal cells was performed via fluorescence microscopy, as previously described (Seranova et al., 2019). The percentage of TUNEL$^+$ nuclei was calculated from the total number of TUJ1$^+$ cells analysed (~200 cells per sample were analysed).

6.11.2. Cytotoxicity assay

Cytotoxicity was measured with CytoTox-Glo Cytotoxicity Assay (Promega) as per manufacturer's protocol. In brief, cells (hESCs and hESC-derived neurons) were cultured as described in 6.2 in white, 96 well plates with transparent bottom (Perkin Elmer). Cells were incubated with CytoTox-Glo Assay Reagent (comprising of Assay Buffer and AAF-Glo Substrate) for 15 min at room temperature in the dark, then luminescence was measured using EnSpire Multimode plate reader (Perkin Elmer) and the readings obtained were attributed to the overall cytotoxicity per well. To

calculate the total number of cells/well, cells were further incubated with Lysis Reagent (comprising of Assay Buffer and Digitonin) for 30 min at room temperature in the dark, after which luminescence was measured again. The volume of each reagent mixture was 100 µL per well. Cytotoxicity data was normalised to the total cell number by dividing the overall cytotoxicity per well (first reading) to the total number of cells per well (second reading) and expressed as a percentage.

6.11.3. FACS analysis of live and apoptotic cells

Analysis of live and apoptotic cells was performed with FITC Annexin V Apoptosis Detection Kit I (BD Biosciences) according to manufacturer's protocol and as previously described (Sarkar et al., 2013). In brief, cells (hESC-derived neural precursors) were cultured as previously described in 6.2 in 6-well plates. Cells were washed with cold PBS, resuspended in 1X Binding Buffer, incubated with FITC Annexin V and propidium iodide for 15 min at room temperature in the dark, followed by analysis via flow cytometry (100000 cells were analysed per sample) using BD LSRFortessa cell analyser (BD Biosciences) and BD FACSDiva v8.0 and FlowJo v7.6.5 software (BD Biosciences). Cells were first selected from the overall population by side scatter area (SSC-A) versus forward scatter area (FSC-A) to eliminate cell debris. To further exclude doublets, cells were discriminated by plotting the side scatter area (SSC-A) versus side scatter width (SSC-W) and the forward scatter area (FSC-A) versus forward scatter width (FSC-W). The resulting cell population was gated into two parameter density plot [Y axis = propidium iodide (PE), X axis = FITC Annexin V (FITC)], and discriminated into 4 sections of live cells (propidium iodide$^-$/FITC Annexin V$^-$), early apoptosis (propidium iodide$^-$/FITC Annexin V$^+$), intermediate apoptosis (propidium iodide$^+$/FITC Annexin V$^+$) or late apoptosis (propidium iodide$^+$/FITC Annexin V$^-$).

6.11.4. DAPI staining for apoptotic nuclear morphology

For analysing apoptotic nuclei morphology by DAPI staining in hESC-derived neurons, the percentage of apoptotic nuclei was calculated from the total number of TUJ1$^+$ cells analysed (~150-200 cells per sample were analysed) (Sarkar et al., 2007; Sarkar et al., 2009).

6.12. NAD^+ and NADH measurements

NAD^+ and NADH measurements were done using NAD/NADH Quantitation Colourimetric Kit (BioVision) according to manufacturer's instructions. Briefly, cells (hESCs and hESC-derived neurons) were washed with cold PBS, then lysed with NADH/NAD Extraction Buffer and immediately freeze-thawed twice on dry ice, centrifuged at 14000 rpm for 5 min at 4 °C. Half of the supernatant was incubated at 60 °C for 30 min to decompose the NAD and detect the NADH. Both halves of the supernatants were then cooled on ice, transferred into a 96-well plate, followed by incubation in Reaction Mix comprising of NAD Cycling Buffer and NAD Cycling Enzyme Mix for 5 min at room temperature. Then NADH Developer was added to each well and the reaction was left to cycle for 1-2 h at room temperature. Measurements of optical density (OD) at 450 nm using the EnSpire Multimode plate reader (Perkin Elmer) were performed every 20-30 min to detect the saturating OD, then normalised to protein concentration via Bio-Rad Protein Assay to measure the pmol/µg of NAD^+ and NADH.

6.13. ATP and ADP measurements

Measurements of ATP and ADP were done using ApoSENSOR ADP/ATP Ratio Bioluminescent Assay Kit (BioVision) according to manufacturer's instructions. Briefly, a Reaction Mix containing Nucleotide Releasing Buffer (NBR) and ATP monitoring enzyme was added in the wells of a white-walled 96-well plate and kept in room temperature for a few hours to burn residual ATP levels. Cells (hESCs and hESC-derived neurons) cultured in another 96-well plate were incubated with NBR 5 min at room temperature to release the ATP, and then the supernatant was transferred to the appropriate wells of the white-walled 96-well plate. Luminescence was measured using EnSpire Multimode plate reader (Perkin Elmer) for determining ATP levels, and again measured after adding ADP Converting Enzyme for determining ADP levels, after which data were normalised to protein concentration via Bio-Rad Protein Assay.

6.14. Mitochondrial ΔΨm and ROS measurements

Measurements of mitochondrial membrane potential (ΔΨm) and reactive oxygen species (ROS) were performed as previously described (e Silva et al., 2019). Briefly, cells (hESCs and hESC-derived neurons) were loaded with Microscopy Medium

comprising of 120 mM NaCl, 3.5 KCl, 0.4 mM KH_2PO_4, 5 mM $NaHCO_3$, 1.2 mM $NaSO_4$, 20 mM HEPES and 15 mM glucose in dH_2O adjusted to pH 7.4 and supplemented with 1 mM $CaCl_2$ (all from Sigma-Aldrich), and incubated with 500 nM TMRE (for mitochondrial ΔΨm measurement; Invitrogen) and 20 µM CM-H_2DCFDA (for ROS measurement; Invitrogen) for 1 h at 37 ºC. The fluorescence of TMRE and CM-H_2DCFDA was acquired using EnSpire Multimode plate reader (Perkin Elmer) for a period of 5 min to get basal fluorescence, and again for TMRE for another 5 min after the addition of 10 µM FCCP (fluorocarbonyl cyanide phenylhydrazone) to obtain maximum fluorescence. The baseline fluorescence was calculated as the mean of the last 10 reading points before the addition of FCCP (for TMRE and CM-H_2DCFDA), and the delta (Δ) fluorescence was calculated by subtracting the basal fluorescence from the maximum fluorescence intensity after FCCP treatment (for TMRE only). Data were obtained as relative fluorescence units, normalised to protein concentration via Bio-Rad Protein Assay, and expressed as a percentage of the control condition.

6.15. MitoTracker staining and mitochondrial rod length analysis

MitoTracker Red CMXRos (Invitrogen) was used to label mitochondria as per manufacturer's protocol. Briefly, cells (hESCs and hESC-derived NPs and neurons) were cultured in 24-well plates on coverslips as previously described in Section 6.2. Cells were incubated with 100 nM MitoTracker Red CMXRos for 45 min at 37 °C, after which the cells were either fixed and imaged for analysis or subjected to immunofluorescence with cell-specific markers. Mitochondrial rod/branch length analysis (after MitoTracker staining or immunofluorescence with Tom20 antibody) was made as previously described (Valente et al., 2017). In brief, measurement of mitochondrial rod/branch length was done per cell for hESCs and NPs (~40 cells per sample and 5-50 fragments per cell were analysed) and per field of view for neurons (~4 images per sample and 200-4000 fragments per image were analysed) using the Analyse Skeleton plugin from the Mitochondrial Network Analysis (MiNA) toolset in ImageJ v1.41 (NIH).

6.16. Axonal length measurement in neurons

Cells (hESC-derived neurons) were grown in 12-well plates on coverslips as previously described in Section 6.2. Cells were immunostained with the neuronal

marker, such as TUJ1, were imaged and analysed for axonal length (~5 images per sample and 1000-1500 lines per image were analysed) using the Analyse Skeleton plugin in the ImageJ v1.41 (NIH).

6.17. Metabolomics

6.17.1. LC-MS-based metabolomics

Liquid chromatography–mass spectrometry (LC-MS)-based metabolomics was performed, broadly as previously described (Maddocks et al., 2016) on hESCs and hESC-derived neurons. Briefly, cells were washed with cold PBS and lysed on ice at 2 x 10^6 cells/ml concentration in Metabolite Extraction Buffer comprising of 30% (v/v) acetonitrile (Sigma-Aldrich), 50% (v/v) methanol (Fisher Scientific) and 20% (v/v) Milli-Q water. Samples were vortexed for 45 s, centrifuged at 13000 rpm for 5 min at 4 °C, and the supernatants subjected to LC-MS using a 3-point calibration curve with universally-labelled carbon-13/nitrogen-15 amino acids for quantification. LC-MS platform consisting of Accela 600 LC system and Exactive mass spectrometer (Thermo Scientific) was used to analyse the samples. For separation of the metabolites, Sequant ZIC-pHILIC column (4.6 mm x 150 mm, 5 µm; Merck) was used with the mobile phase mixed by A = 20 mM ammonium carbonate in water and B = acetonitrile. A gradient program starting at 20% of A and linearly increasing to 80% at 30 min was used, followed by washing (92% of A for 5 min) and re-equilibration (20% of A for 10 min), and the total run time of the method was 45 min. The LC stream was desolvated and ionised in the HESI probe. The Exactive mass spectrometer was operated in full scan mode over a mass range of 70-1200 m/z at a resolution of 50000 with polarity switching. The LC-MS raw data was converted into mzML files via ProteoWizard and imported to MZMine 2.10 for peak extraction and sample alignment. A house-made database integrating KEGG, HMDB and LIPID MAPS was used for the assignment of the LC-MS signals by searching the accurate mass, and the metabolites were confirmed by running their commercial standards. Lastly, peak areas were used for comparative quantification.

6.17.2. Metabolomics data analysis

Multivariate statistical analysis on MS-based metabolomics was performed using MetaboAnalyst 4.0. We first normalised each of the metabolite peaks by auto-scaling

(mean-centred and divided by SD of each variable) and then applied principal component analysis (PCA). Metabolite fold change was calculated relative to *ATG5*$^{+/+}$ (wild-type) cells, and then converted to Log2 values. Each metabolite was plotted on a heatmap. Statistical significance was determined using the Student's *t*-test with *P* value corrected with Benjamini and Hochberg (BH) false discovery rate (FDR) method.

6.18. Fluorescence Activated Cell Sorting (FACS)

The wild-type and mCherry-EGFP-LC3 hESC-derived monocytic cells and macrophages were characterised for the cell lineage markers by fluorescence-activated cell sorting (FACS). The macrophages were dissociated using accutase (Stem Cell Technologies), centrifuged (300 x g) for 5 min at 21 °C, resuspended in ice-cold FACS Buffer consisting of 1.5% (v/v) Fetal Bovine Serum (heat-inactivated, S. American, Gibco) in PBS, and collected into 5 ml falcon round-bottom polystyrene tubes. The monocytic cells were harvested from the "factory", filtered via 40 µm cell strainer, centrifuged (400 x g) for 5 min at 21 °C, and also resuspended in FACS Buffer. The respective monocytic cell and macrophage suspensions were then incubated in the dark for 20 min on ice with primary antibodies (Table 6.4) (1:25 dilutions; except 1:100 for CD45 after performing titration curve) for multiple cell surface-specific expressing markers and compensation beads, and centrifuged (400 x g) for 5 min at 4°C. The cells were fixed using 4% (v/v) formaldehyde for 20 min, diluted with 1X PBS, centrifuged again (400 x g) for 5 min at 4°C, resuspended in 450 µL of PBS, and mixed thoroughly to prevent cell clumping, and analysed by CyAn ADP Analyser (Beckman Coulter) or CytoFLEX Flow Cytometer (Beckman Coulter). The FACS data were analysed by FlowJo software. Compensation from UltraComp eBeads Compensation Beads (Invitrogen) was applied using the FlowJo v10 software. Cells were first selected from the overall population by side scatter linear (SS Lin) versus forward scatter linear (FS Lin). The resulting population was discriminated by FS Lin versus Pulse width to avoid debris, and finally, the antibody's fluorescent channel was gated against cell count to visualise the staining. The histograms denote surface antibody staining and isotype control as indicated in the figures.

Table 6.4. List of primary antibodies and isotype controls for FACS

Antigen	*Dilution*	*Source*	*Catalogue number*
CD11b	1:25	Tonbo Biosciences	75-0112
Isotype Control for CD11b	1:100	Tonbo Biosciences	75-4031-U100

CD11c	1:25	Tonbo Biosciences	75-0116
Isotype Control for CD11c	1:100	Tonbo Biosciences	75-4714-U100
CD14	1:25	Invitrogen	15-0149-42
Isotype Control for CD14	1:100	BioLegend	400126
CD16	1:25	BioLegend	302011
Isotype Control for CD16	1:66	BioLegend	562946
CD45	1:100	Tonbo Biosciences	60-9459-ST05
Isotype Control for CD45	1:100	BioLegend	304058
CD68	1:25	BioLegend	333821
Isotype Control for CD68	1:100	BioLegend	400328
CD86	1:25	BioLegend	305425
Isotype Control for CD86	1:100	BioLegend	400342
CD163	1:25	BioLegend	333621
Isotype Control for CD163	1:100	BioLegend	400127
CD206	1:25	BioLegend	321109
Isotype Control for CD206	1:100	BioLegend	400119
MHC II	1:25	BioLegend	307617
Isotype Control for MHC II	1:100	BioLegend	400229

6.19. Enzyme-linked immunosorbent assay (ELISA)

ELISA was done in hESC-derived macrophages. ELISA 96 well plates were coated overnight with 4 µg/mL of TNFα (BD Biosciences) and IL10 (R&D Systems) at room temperature (in PBS). After disposing the liquid, the plate was incubated with blocking buffer consisting of 1% (v/v) BSA in PBS for 2 h, and then 50 µL of the sample was added to each well and incubated at room temperature (RT) for 2 h. Optical density curves were used at 2000 pg/mL as the highest value of the curve and serial dilution was implemented. After the sample incubation, 3 washes with 0.05% (v/v) Tween-20 in PBS was performed and the detection antibody was added in all the wells in 50 µL of blocking buffer. Afterwards, 3 more PBS washes were performed, and biotinylated detection antibodies were added to all the wells. Then, streptavidin-conjugated HRP was added to 50 µL of blocking buffer and the plate was incubated for 30 min in RT. After 3 more washes with PBS, HRP substrate with 3,3',5,5'-tetramethylbenzidine (TMB) was added and the reaction was stopped using sulphuric acid. The plate was then read at 450 nM using the Multimode Plate Reader (Perkin Elmer).

6.20. Phagocytosis assay

Monocytic cells derived from hESCs were harvested from the ‘factories’ and seeded at 60000 cells per well in a 96-well black plate with transparent bottom (Thermo Fisher Scientific). Cells were then differentiated into macrophages for 7 days, and the culture medium was changed to macrophage medium supplemented with 100U/mL iFNγ

(Gibco) for 24 h. iFNγ supplemented medium was removed and replaced with 100 µL per well of the macrophage medium. Jurkat T cells, stained with CellTracker Blue (Thermo Fisher Scientific) and heat-killed at 60 ºC, were added at 100000 cells per well and incubated at 37 ºC for 3-4 h. Medium was removed, cells were washed twice with PBS and cells were stained with Cell Mask Deep Red (Thermo Fisher Scientific) in macrophage medium. After 10 min incubation at 37 ºC, cells were washed once with PBS and 100 µL/well of macrophage medium was added before immediate imaging with CX5 CellInsight microscope (Thermo Fisher Scientific). Cells can be fixed with 4% (v/v) paraformaldehyde if re-imaging is necessary or for further staining.

6.21. Statistical analyses

Quantification of data is described under various sections of experimental procedures as appropriate. Graphical data are shown by column graph scatter dot plot (mean ± s.e.m.) using Prism 8.3.1 software (GraphPad). Statistical significance on all graphical data was determined using unpaired two-tailed Student's *t*-test using Prism 8.3.1 software (GraphPad) from multiple biological replicates (n number = 3 or more as indicated) in 3 independent or representative experiments. For metabolomics data analysis, statistical significance was determined by Student's *t*-test using Benjamini and Hochberg FDR method. ***, $p<0.001$; **, $p<0.01$; *, $p<0.05$; ns, non-significant.

References

References

Abud, E., Ramirez, R., Martinez, E., Healy, L., Nguyen, C., Newman, S., Yeromin, A., Scarfone, V., Marsh, S., Fimbres, C., Caraway, C., Fote, G., Madany, A., Agrawal, A., Kayed, R., Gylys, K., Cahalan, M., Cummings, B., Antel, J., Mortazavi, A., Carson, M., Poon, W. and Blurton-Jones, M., 2017. iPSC-Derived Human Microglia-like Cells to Study Neurological Diseases. *Neuron*, 94(2), pp.278-293.e9.

Ackermann, M., Kuhn, A., Kunkiel, J., Merkert, S., Martin, U., Moritz, T. and Lachmann, N., 2017. Ex vivo Generation of Genetically Modified Macrophages from Human Induced Pluripotent Stem Cells. *Transfusion Medicine and Hemotherapy*, 44(3), pp.135-142.

Aderem, A., 2003. Phagocytosis and the Inflammatory Response. *The Journal of Infectious Diseases*, 187(s2), pp.S340-S345.

Aflaki, E., Stubblefield, B., Maniwang, E., Lopez, G., Moaven, N., Goldin, E., Marugan, J., Patnaik, S., Dutra, A., Southall, N., Zheng, W., Tayebi, N. and Sidransky, E., 2014. Macrophage Models of Gaucher Disease for Evaluating Disease Pathogenesis and Candidate Drugs. *Science Translational Medicine*, 6(240), pp.240ra73-240ra73.

Aggarwal, R., Pompili, V.J. and Das, H., 2010. Genetic modification of ex-vivo expanded stem cells for clinical application. *Frontiers in Bioscience*, 15(1), p.854.

Akiyama, T., Wakabayashi, S., Soma, A., Sato, S., Nakatake, Y., Oda, M., Murakami, M., Sakota, M., Chikazawa-Nohtomi, N., Ko, S. and Ko, M., 2016. Transient ectopic expression of the histone demethylase JMJD3 accelerates the differentiation of human pluripotent stem cells. *Development*, 143(20), pp.3674-3685.

Aksoy, P., White, T., Thompson, M. and Chini, E., 2006. Regulation of intracellular levels of NAD: A novel role for CD38. *Biochemical and Biophysical Research Communications*, 345(4), pp.1386-1392.

Allen, D. and Young, J., 2020. Tracing metabolic flux through time and space with isotope labeling experiments. *Current Opinion in Biotechnology*, 64, pp.92-100.

Amin, H., Maccione, A., Marinaro, F., Zordan, S., Nieus, T. and Berdondini, L., 2016. Electrical Responses and Spontaneous Activity of Human iPS-Derived Neuronal Networks Characterized for 3-month Culture with 4096-Electrode Arrays. *Frontiers in Neuroscience*, 10.

Amos, P., Fung, S., Case, A., Kifelew, J., Osnis, L., Smith, C., Green, K., Naydenov, A., Aloi, M., Hubbard, J., Ramakrishnan, A., Garden, G. and Jayadev, S., 2017. Modulation of Hematopoietic Lineage Specification Impacts TREM2 Expression in Microglia-Like Cells Derived From Human Stem Cells. *ASN Neuro*, 9(4), p.175909141771661.

Antoniewicz, M., 2015. Methods and advances in metabolic flux analysis: a mini-review. *Journal of Industrial Microbiology & Biotechnology*, 42(3), pp.317-325.

Arango Duque, G. and Descoteaux, A., 2014. Macrophage Cytokines: Involvement in Immunity and Infectious Diseases. *Frontiers in Immunology*, 5.

Assady, S., Maor, G., Amit, M., Itskovitz-Eldor, J., Skorecki, K. and Tzukerman, M., 2001. Insulin Production by Human Embryonic Stem Cells. *Diabetes*, 50(8), pp.1691-1697.

Axe, E., Walker, S., Manifava, M., Chandra, P., Roderick, H., Habermann, A., Griffiths, G. and Ktistakis, N., 2008. Autophagosome formation from membrane compartments enriched in phosphatidylinositol 3-phosphate and dynamically connected to the endoplasmic reticulum. *Journal of Cell Biology*, 182(4), pp.685-701.

Bai, P. and Cantó, C., 2012. The Role of PARP-1 and PARP-2 Enzymes in Metabolic Regulation and Disease. *Cell Metabolism*, 16(3), pp.290-295.

Bai, P., Canto, C., Brunyánszki, A., Huber, A., Szántó, M., Cen, Y., Yamamoto, H., Houten, S., Kiss, B., Oudart, H., Gergely, P., Menissier-de Murcia, J., Schreiber, V., Sauve, A. and Auwerx, J., 2011. PARP-2 Regulates SIRT1 Expression and Whole-Body Energy Expenditure. *Cell Metabolism*, 13(4), pp.450-460.

Bai, P., Cantó, C., Oudart, H., Brunyánszki, A., Cen, Y., Thomas, C., Yamamoto, H., Huber, A., Kiss, B., Houtkooper, R., Schoonjans, K., Schreiber, V., Sauve, A., Menissier-de Murcia, J. and Auwerx, J., 2011. PARP-1 Inhibition Increases

Mitochondrial Metabolism through SIRT1 Activation. *Cell Metabolism*, 13(4), pp.461-468.

Barmada, S., Serio, A., Arjun, A., Bilican, B., Daub, A., Ando, D., Tsvetkov, A., Pleiss, M., Li, X., Peisach, D., Shaw, C., Chandran, S. and Finkbeiner, S., 2014. Autophagy induction enhances TDP43 turnover and survival in neuronal ALS models. *Nature Chemical Biology*, 10(8), pp.677-685.

Barrett, T. and Bundey, S., 1997. Wolfram (DIDMOAD) syndrome. *Journal of Medical Genetics*, 34(10), pp.838-841.

Barrow, J., Balsa, E., Verdeguer, F., Tavares, C., Soustek, M., Hollingsworth, L., Jedrychowski, M., Vogel, R., Paulo, J., Smeitink, J., Gygi, S., Doench, J., Root, D. and Puigserver, P., 2016. Bromodomain Inhibitors Correct Bioenergetic Deficiency Caused by Mitochondrial Disease Complex I Mutations. *Molecular Cell*, 64(1), pp.163-175.

Beattie, G., Lopez, A., Bucay, N., Hinton, A., Firpo, M., King, C. and Hayek, A., 2005. Activin A Maintains Pluripotency of Human Embryonic Stem Cells in the Absence of Feeder Layers. *Stem Cells*, 23(4), pp.489-495.

Berger, Z., Ravikumar, B., Menzies, F., Oroz, L., Underwood, B., Pangalos, M., Schmitt, I., Wullner, U., Evert, B., O'Kane, C. and Rubinsztein, D., 2005. Rapamycin alleviates toxicity of different aggregate-prone proteins. *Human Molecular Genetics*, 15(3), pp.433-442.

Berges, C., Naujokat, C., Tinapp, S., Wieczorek, H., Höh, A., Sadeghi, M., Opelz, G. and Daniel, V., 2005. A cell line model for the differentiation of human dendritic cells. *Biochemical and Biophysical Research Communications*, 333(3), pp.896-907.

Bertholet, A., Delerue, T., Millet, A., Moulis, M., David, C., Daloyau, M., Arnauné-Pelloquin, L., Davezac, N., Mils, V., Miquel, M., Rojo, M. and Belenguer, P., 2016. Mitochondrial fusion/fission dynamics in neurodegeneration and neuronal plasticity. *Neurobiology of Disease*, 90, pp.3-19.

Bjørkøy, G., Lamark, T., Brech, A., Outzen, H., Perander, M., Øvervatn, A., Stenmark, H. and Johansen, T., 2005. p62/SQSTM1 forms protein aggregates degraded by

autophagy and has a protective effect on huntingtin-induced cell death. *Journal of Cell Biology*, 171(4), pp.603-614.

Blinova, K., Dang, Q., Millard, D., Smith, G., Pierson, J., Guo, L., Brock, M., Lu, H., Kraushaar, U., Zeng, H., Shi, H., Zhang, X., Sawada, K., Osada, T., Kanda, Y., Sekino, Y., Pang, L., Feaster, T., Kettenhofen, R., Stockbridge, N., Strauss, D. and Gintant, G., 2018. International Multisite Study of Human-Induced Pluripotent Stem Cell-Derived Cardiomyocytes for Drug Proarrhythmic Potential Assessment. *Cell Reports*, 24(13), pp.3582-3592.

Blommaart, E., Luiken, J., Blommaart, P., van Woerkom, G. and Meijer, A., 1995. Phosphorylation of Ribosomal Protein S6 Is Inhibitory for Autophagy in Isolated Rat Hepatocytes. *Journal of Biological Chemistry*, 270(5), pp.2320-2326.

Boland, B., Yu, W., Corti, O., Mollereau, B., Henriques, A., Bezard, E., Pastores, G., Rubinsztein, D., Nixon, R., Duchen, M., Mallucci, G., Kroemer, G., Levine, B., Eskelinen, E., Mochel, F., Spedding, M., Louis, C., Martin, O. and Millan, M., 2018. Promoting the clearance of neurotoxic proteins in neurodegenerative disorders of ageing. *Nature Reviews Drug Discovery*, 17(9), pp.660-688.

Boya, P., González-Polo, R., Casares, N., Perfettini, J., Dessen, P., Larochette, N., Métivier, D., Meley, D., Souquere, S., Yoshimori, T., Pierron, G., Codogno, P. and Kroemer, G., 2005. Inhibition of Macroautophagy Triggers Apoptosis. *Molecular and Cellular Biology*, 25(3), pp.1025-1040.

Brand, M. and Nicholls, D., 2011. Assessing mitochondrial dysfunction in cells. *Biochemical Journal*, 435(2), pp.297-312.

Bright, J., Hussain, S., Dang, V., Wright, S., Cooper, B., Byun, T., Ramos, C., Singh, A., Parry, G., Stagliano, N. and Griswold-Prenner, I., 2015. Human secreted tau increases amyloid-beta production. *Neurobiology of Aging*, 36(2), pp.693-709.

Brown, A., Patel, S., Ward, C., Lorenz, A., Ortiz, M., DuRoss, A., Wieghardt, F., Esch, A., Otten, E., Heiser, L., Korolchuk, V., Sun, C., Sarkar, S. and Sahay, G., 2016. PEG-lipid micelles enable cholesterol efflux in Niemann-Pick Type C1 disease-based lysosomal storage disorder. *Scientific Reports*, 6(1).

Brown, E., Albers, M., Bum Shin, T., ichikawa, K., Keith, C., Lane, W. and Schreiber, S., 1994. A mammalian protein targeted by G1-arresting rapamycin–receptor complex. *Nature*, 369(6483), pp.756-758.

Brown, K., Maqsood, S., Huang, J., Pan, Y., Harkcom, W., Li, W., Sauve, A., Verdin, E. and Jaffrey, S., 2014. Activation of SIRT3 by the NAD+ Precursor Nicotinamide Riboside Protects from Noise-Induced Hearing Loss. *Cell Metabolism*, 20(6), pp.1059-1068.

Buchrieser, J., James, W. and Moore, M., 2017. Human Induced Pluripotent Stem Cell-Derived Macrophages Share Ontogeny with MYB -Independent Tissue-Resident Macrophages. *Stem Cell Reports*, 8(2), pp.334-345.

Burblies, N., Schulze, J., Schwarz, H., Kranz, K., Motz, D., Vogt, C., Lenarz, T., Warnecke, A. and Behrens, P., 2016. Coatings of Different Carbon Nanotubes on Platinum Electrodes for Neuronal Devices: Preparation, Cytocompatibility and Interaction with Spiral Ganglion Cells. *PLOS ONE*, 11(7), p.e0158571.

Burkhardt, M., Martinez, F., Wright, S., Ramos, C., Volfson, D., Mason, M., Garnes, J., Dang, V., Lievers, J., Shoukat-Mumtaz, U., Martinez, R., Gai, H., Blake, R., Vaisberg, E., Grskovic, M., Johnson, C., Irion, S., Bright, J., Cooper, B., Nguyen, L., Griswold-Prenner, I. and Javaherian, A., 2013. A cellular model for sporadic ALS using patient-derived induced pluripotent stem cells. *Molecular and Cellular Neuroscience*, 56, pp.355-364.

Burkitt, M. and Wardman, P., 2001. Cytochrome c Is a Potent Catalyst of Dichlorofluorescin Oxidation: Implications for the Role of Reactive Oxygen Species in Apoptosis. *Biochemical and Biophysical Research Communications*, 282(1), pp.329-333.

Burté, F., Carelli, V., Chinnery, P. and Yu-Wai-Man, P., 2014. Disturbed mitochondrial dynamics and neurodegenerative disorders. *Nature Reviews Neurology*, 11(1), pp.11-24.

Buzzai, M., Jones, R., Amaravadi, R., Lum, J., DeBerardinis, R., Zhao, F., Viollet, B. and Thompson, C., 2007. Systemic Treatment with the Antidiabetic Drug Metformin

Selectively Impairs p53-Deficient Tumor Cell Growth. *Cancer Research*, 67(14), pp.6745-6752.

Byrne, S., Mali, P. and Church, G., 2014. Genome Editing in Human Stem Cells. *Methods in Enzymology*, pp.119-138.

Campbell, G. and Spector, S., 2011. Hormonally Active Vitamin D3 (1α,25-Dihydroxycholecalciferol) Triggers Autophagy in Human Macrophages That Inhibits HIV-1 Infection. *Journal of Biological Chemistry*, 286(21), pp.18890-18902.

Campbell, G. and Spector, S., 2012. Vitamin D Inhibits Human Immunodeficiency Virus Type 1 and Mycobacterium tuberculosis Infection in Macrophages through the Induction of Autophagy. *PLoS Pathogens*, 8(5), p.e1002689.

Cantó, C., Menzies, K. and Auwerx, J., 2015. NAD+ Metabolism and the Control of Energy Homeostasis: A Balancing Act between Mitochondria and the Nucleus. *Cell Metabolism*, 22(1), pp.31-53.

Cao, Y., Espinola, J., Fossale, E., Massey, A., Cuervo, A., MacDonald, M. and Cotman, S., 2006. Autophagy Is Disrupted in a Knock-in Mouse Model of Juvenile Neuronal Ceroid Lipofuscinosis. *Journal of Biological Chemistry*, 281(29), pp.20483-20493.

Castrejón-Jiménez, N., Leyva-Paredes, K., Hernández-González, J., Luna-Herrera, J. and García-Pérez, B., 2015. The role of autophagy in bacterial infections. *BioScience Trends*, 9(3), pp.149-159.

Chambers, S., Fasano, C., Papapetrou, E., Tomishima, M., Sadelain, M. and Studer, L., 2009. Highly efficient neural conversion of human ES and iPS cells by dual inhibition of SMAD signaling. *Nature Biotechnology*, 27(3), pp.275-280.

Chan, E., Kir, S. and Tooze, S., 2007. siRNA Screening of the Kinome Identifies ULK1 as a Multidomain Modulator of Autophagy. *Journal of Biological Chemistry*, 282(35), pp.25464-25474.

Chandler, C. and Ernst, R., 2017. Bacterial lipids: powerful modifiers of the innate immune response. *F1000Research*, 6, p.1334.

Chandra, P. and Kumar, D., 2016. Selective autophagy gets more selective: Uncoupling of autophagy flux and xenophagy flux inMycobacterium tuberculosis-infected macrophages. *Autophagy*, 12(3), pp.608-609.

Chandra, P., Ghanwat, S., Matta, S., Yadav, S., Mehta, M., Siddiqui, Z., Singh, A. and Kumar, D., 2015. Mycobacterium tuberculosis Inhibits RAB7 Recruitment to Selectively Modulate Autophagy Flux in Macrophages. *Scientific Reports*, 5(1).

Chandra, P., Rajmani, R., Verma, G., Bhavesh, N. and Kumar, D., 2016. Targeting Drug-Sensitive and -Resistant Strains of Mycobacterium tuberculosis by Inhibition of Src Family Kinases Lowers Disease Burden and Pathology. *mSphere*, 1(2).

Chauhan, S., Ahmed, Z., Bradfute, S., Arko-Mensah, J., Mandell, M., Won Choi, S., Kimura, T., Blanchet, F., Waller, A., Mudd, M., Jiang, S., Sklar, L., Timmins, G., Maphis, N., Bhaskar, K., Piguet, V. and Deretic, V., 2015. Pharmaceutical screen identifies novel target processes for activation of autophagy with a broad translational potential. *Nature Communications*, 6(1).

Chen, D., Fan, W., Lu, Y., Ding, X., Chen, S. and Zhong, Q., 2012. A Mammalian Autophagosome Maturation Mechanism Mediated by TECPR1 and the Atg12-Atg5 Conjugate. *Molecular Cell*, 45(5), pp.629-641.

Chen, K. and Knoepfler, P., 2016. To CRISPR and beyond: the evolution of genome editing in stem cells. *Regenerative Medicine*, 11(8), pp.801-816.

Choi, K., Vodyanik, M. and Slukvin, I., 2011. Hematopoietic differentiation and production of mature myeloid cells from human pluripotent stem cells. *Nature Protocols*, 6(3), pp.296-313.

Chou, L., Cheng, Y., Hsieh, C., Lin, C., Yang, H., Chen, Y., Hung, C., Tian, Y., Yang, C. and Chang, M., 2018. Effect of Trehalose Supplementation on Autophagy and Cystogenesis in a Mouse Model of Polycystic Kidney Disease. *Nutrients*, 11(1), p.42.

Chung, H. and Joe, Y., 2014. Antagonistic crosstalk between SIRT1, PARP-1, and -2 in the regulation of chronic inflammation associated with aging and metabolic diseases. *Integrative Medicine Research*, 3(4), pp.198-203.

Cohen, M., Itsykson, P. and E. Reubinoff, B., 2007. Neural Differentiation of Human ES Cells. *Current Protocols in Cell Biology*, 36(1), pp.23.7.1-23.7.20.

Cortes, C., Qin, K., Cook, J., Solanki, A. and Mastrianni, J., 2012. Rapamycin Delays Disease Onset and Prevents PrP Plaque Deposition in a Mouse Model of Gerstmann-Straussler-Scheinker Disease. *Journal of Neuroscience*, 32(36), pp.12396-12405.

Curto, G., Nieto-Estévez, V., Hurtado-Chong, A., Valero, J., Gómez, C., Alonso, J., Weruaga, E. and Vicario-Abejón, C., 2014. Pax6 Is Essential for the Maintenance and Multi-Lineage Differentiation of Neural Stem Cells, and for Neuronal Incorporation into the Adult Olfactory Bulb. *Stem Cells and Development*, 23(23), pp.2813-2830.

Cuyvers, E., van der Zee, J., Bettens, K., Engelborghs, S., Vandenbulcke, M., Robberecht, C., Dillen, L., Merlin, C., Geerts, N., Graff, C., Thonberg, H., Chiang, H., Pastor, P., Ortega-Cubero, S., Pastor, M., Diehl-Schmid, J., Alexopoulos, P., Benussi, L., Ghidoni, R., Binetti, G., Nacmias, B., Sorbi, S., Sanchez-Valle, R., Lladó, A., Gelpi, E., Almeida, M., Santana, I., Clarimon, J., Lleó, A., Fortea, J., de Mendonça, A., Martins, M., Borroni, B., Padovani, A., Matěj, R., Rohan, Z., Ruiz, A., Frisoni, G., Fabrizi, G., Vandenberghe, R., De Deyn, P., Van Broeckhoven, C. and Sleegers, K., 2015. Genetic variability in SQSTM1 and risk of early-onset Alzheimer dementia: a European early-onset dementia consortium study. *Neurobiology of Aging*, 36(5), pp.2005.e15-2005.e22.

D'Aiuto, L., Naciri, J., Radio, N., Tekur, S., Clayton, D., Apodaca, G., Di Maio, R., Zhi, Y., Dimitrion, P., Piazza, P., Demers, M., Wood, J., Chu, C., Callio, J., McClain, L., Yolken, R., McNulty, J., Kinchington, P., Bloom, D. and Nimgaonkar, V., 2018. Generation of three-dimensional human neuronal cultures: application to modeling CNS viral infections. *Stem Cell Research & Therapy*, 9(1).

Dai, S., Dulcey, A., Hu, X., Wassif, C., Porter, F., Austin, C., Ory, D., Marugan, J. and Zheng, W., 2017. Methyl-β-cyclodextrin restores impaired autophagy flux in Niemann-Pick C1-deficient cells through activation of AMPK. *Autophagy*, 13(8), pp.1435-1451.

D'Amour, K., Bang, A., Eliazer, S., Kelly, O., Agulnick, A., Smart, N., Moorman, M., Kroon, E., Carpenter, M. and Baetge, E., 2006. Production of pancreatic hormone–

expressing endocrine cells from human embryonic stem cells. *Nature Biotechnology*, 24(11), pp.1392-1401.

Deb, K. and Sarda, K., 2008. Human embryonic stem cells: preclinical perspectives. *Journal of Translational Medicine*, 6(1).

DeBosch, B., Heitmeier, M., Mayer, A., Higgins, C., Crowley, J., Kraft, T., Chi, M., Newberry, E., Chen, Z., Finck, B., Davidson, N., Yarasheski, K., Hruz, P. and Moley, K., 2016. Trehalose inhibits solute carrier 2A (SLC2A) proteins to induce autophagy and prevent hepatic steatosis. *Science Signaling*, 9(416), pp.ra21-ra21.

Deckwerth, T. and Johnson, E., 1994. Neurites Can Remain Viable after Destruction of the Neuronal Soma by Programmed Cell Death (Apoptosis). *Developmental Biology*, 165(1), pp.63-72.

Dehmelt, L. and Halpain, S., 2004. *Genome Biology*, 6(1), p.204.

DeJesus, R., Moretti, F., McAllister, G., Wang, Z., Bergman, P., Liu, S., Frias, E., Alford, J., Reece-Hoyes, J., Lindeman, A., Kelliher, J., Russ, C., Knehr, J., Carbone, W., Beibel, M., Roma, G., Ng, A., Tallarico, J., Porter, J., Xavier, R., Mickanin, C., Murphy, L., Hoffman, G. and Nyfeler, B., 2016. Functional CRISPR screening identifies the ufmylation pathway as a regulator of SQSTM1/p62. *eLife*, 5.

Deretic, V., 2014. Autophagy in Tuberculosis. *Cold Spring Harbor Perspectives in Medicine*, 4(11), pp.a018481-a018481.

Deretic, V., Saitoh, T. and Akira, S., 2013. Autophagy in infection, inflammation and immunity. *Nature Reviews Immunology*, 13(10), pp.722-737.

DeRosa, B., El Hokayem, J., Artimovich, E., Garcia-Serje, C., Phillips, A., Van Booven, D., Nestor, J., Wang, L., Cuccaro, M., Vance, J., Pericak-Vance, M., Cukier, H., Nestor, M. and Dykxhoorn, D., 2018. Convergent Pathways in Idiopathic Autism Revealed by Time Course Transcriptomic Analysis of Patient-Derived Neurons. *Scientific Reports*, 8(1).

Di Malta, C., Cinque, L. and Settembre, C., 2019. Transcriptional Regulation of Autophagy: Mechanisms and Diseases. *Frontiers in Cell and Developmental Biology*, 7.

Diao, J., Liu, R., Rong, Y., Zhao, M., Zhang, J., Lai, Y., Zhou, Q., Wilz, L., Li, J., Vivona, S., Pfuetzner, R., Brunger, A. and Zhong, Q., 2015. ATG14 promotes membrane tethering and fusion of autophagosomes to endolysosomes. *Nature*, 520(7548), pp.563-566.

Dikalov, S. and Harrison, D., 2014. Methods for Detection of Mitochondrial and Cellular Reactive Oxygen Species. *Antioxidants & Redox Signaling*, 20(2), pp.372-382.

Dong, Y., Love, K., Dorkin, J., Sirirungruang, S., Zhang, Y., Chen, D., Bogorad, R., Yin, H., Chen, Y., Vegas, A., Alabi, C., Sahay, G., Olejnik, K., Wang, W., Schroeder, A., Lytton-Jean, A., Siegwart, D., Akinc, A., Barnes, C., Barros, S., Carioto, M., Fitzgerald, K., Hettinger, J., Kumar, V., Novobrantseva, T., Qin, J., Querbes, W., Koteliansky, V., Langer, R. and Anderson, D., 2014. Lipopeptide nanoparticles for potent and selective siRNA delivery in rodents and nonhuman primates. *Proceedings of the National Academy of Sciences*, 111(11), pp.3955-3960.

Donia, M., McCubrey, J., Bendtzen, K. and Nicoletti, F., 2010. Potential use of rapamycin in HIV infection. *British Journal of Clinical Pharmacology*, 70(6), pp.784-793.

Dooley, H., Razi, M., Polson, H., Girardin, S., Wilson, M. and Tooze, S., 2014. WIPI2 Links LC3 Conjugation with PI3P, Autophagosome Formation, and Pathogen Clearance by Recruiting Atg12–5-16L1. *Molecular Cell*, 55(2), pp.238-252.

e Silva, L., Brito, M., Yuzawa, J. and Rosenstock, T., 2019. Mitochondrial Dysfunction and Changes in High-Energy Compounds in Different Cellular Models Associated to Hypoxia: Implication to Schizophrenia. *Scientific Reports*, 9(1).

Egan, D., Chun, M., Vamos, M., Zou, H., Rong, J., Miller, C., Lou, H., Raveendra-Panickar, D., Yang, C., Sheffler, D., Teriete, P., Asara, J., Turk, B., Cosford, N. and Shaw, R., 2015. Small Molecule Inhibition of the Autophagy Kinase ULK1 and Identification of ULK1 Substrates. *Molecular Cell*, 59(2), pp.285-297.

Egan, D., Shackelford, D., Mihaylova, M., Gelino, S., Kohnz, R., Mair, W., Vasquez, D., Joshi, A., Gwinn, D., Taylor, R., Asara, J., Fitzpatrick, J., Dillin, A., Viollet, B., Kundu, M., Hansen, M. and Shaw, R., 2010. Phosphorylation of ULK1 (hATG1) by AMP-Activated Protein Kinase Connects Energy Sensing to Mitophagy. *Science*, 331(6016), pp.456-461.

Eisner, V., Picard, M. and Hajnóczky, G., 2018. Mitochondrial dynamics in adaptive and maladaptive cellular stress responses. *Nature Cell Biology*, 20(7), pp.755-765.

Fang, E., Lautrup, S., Hou, Y., Demarest, T., Croteau, D., Mattson, M. and Bohr, V., 2017. NAD + in Aging: Molecular Mechanisms and Translational Implications. *Trends in Molecular Medicine*, 23(10), pp.899-916.

Farrelly, E., Amaral, M., Marshall, L. and Huang, S., 2001. A High-Throughput Assay for Mitochondrial Membrane Potential in Permeabilized Yeast Cells. *Analytical Biochemistry*, 293(2), pp.269-276.

Fasullo, M. and Endres, L., 2015. Nucleotide Salvage Deficiencies, DNA Damage and Neurodegeneration. *International Journal of Molecular Sciences*, 16(12), pp.9431-9449.

Felbor, U., Kessler, B., Mothes, W., Goebel, H., Ploegh, H., Bronson, R. and Olsen, B., 2002. Neuronal loss and brain atrophy in mice lacking cathepsins B and L. *Proceedings of the National Academy of Sciences*, 99(12), pp.7883-7888.

Feng, Y., He, D., Yao, Z. and Klionsky, D., 2013. The machinery of macroautophagy. *Cell Research*, 24(1), pp.24-41.

Fernández, Á. and López-Otín, C., 2015. The functional and pathologic relevance of autophagy proteases. *Journal of Clinical Investigation*, 125(1), pp.33-41.

Fernández-Santiago, R., Carballo-Carbajal, I., Castellano, G., Torrent, R., Richaud, Y., Sánchez-Danés, A., Vilarrasa-Blasi, R., Sánchez-Pla, A., Mosquera, J., Soriano, J., López-Barneo, J., Canals, J., Alberch, J., Raya, Á., Vila, M., Consiglio, A., Martín-Subero, J., Ezquerra, M. and Tolosa, E., 2015. Aberrant epigenome in iPSC -derived dopaminergic neurons from Parkinson's disease patients. *EMBO Molecular Medicine*, 7(12), pp.1529-1546.

Fernie, A., Carrari, F. and Sweetlove, L., 2004. Respiratory metabolism: glycolysis, the TCA cycle and mitochondrial electron transport. *Current Opinion in Plant Biology*, 7(3), pp.254-261.

Ferreira, A. and Caceres, A., 1992. Expression of the Class III β-tubulin isotype in developing neurons in culture. *Journal of Neuroscience Research*, 32(4), pp.516-529.

Filimonenko, M., Isakson, P., Finley, K., Anderson, M., Jeong, H., Melia, T., Bartlett, B., Myers, K., Birkeland, H., Lamark, T., Krainc, D., Brech, A., Stenmark, H., Simonsen, A. and Yamamoto, A., 2010. The Selective Macroautophagic Degradation of Aggregated Proteins Requires the PI3P-Binding Protein Alfy. *Molecular Cell*, 38(2), pp.265-279.

Filomeni, G., De Zio, D. and Cecconi, F., 2014. Oxidative stress and autophagy: the clash between damage and metabolic needs. *Cell Death & Differentiation*, 22(3), pp.377-388.

Fleury, C., Mignotte, B. and Vayssière, J., 2002. Mitochondrial reactive oxygen species in cell death signaling. *Biochimie*, 84(2-3), pp.131-141.

Floto, R., Sarkar, S., Perlstein, E., Kampmann, B., Schreiber, S. and Rubinsztein, D., 2007. Small Molecule Enhancers of Rapamycin-Induced TOR Inhibition Promote Autophagy, Reduce Toxicity in Huntington's Disease Models and Enhance Killing of Mycobacteria by Macrophages. *Autophagy*, 3(6), pp.620-622.

Fornai, F., Longone, P., Cafaro, L., Kastsiuchenka, O., Ferrucci, M., Manca, M., Lazzeri, G., Spalloni, A., Bellio, N., Lenzi, P., Modugno, N., Siciliano, G., Isidoro, C., Murri, L., Ruggieri, S. and Paparelli, A., 2008. Lithium delays progression of amyotrophic lateral sclerosis. *Proceedings of the National Academy of Sciences*, 105(6), pp.2052-2057.

Franco, L., Nair, V., Scharn, C., Xavier, R., Torrealba, J., Shiloh, M. and Levine, B., 2017. The Ubiquitin Ligase Smurf1 Functions in Selective Autophagy of Mycobacterium tuberculosis and Anti-tuberculous Host Defense. *Cell Host & Microbe*, 21(1), pp.59-72.

Frega, M., Tedesco, M., Massobrio, P., Pesce, M. and Martinoia, S., 2014. Network dynamics of 3D engineered neuronal cultures: a new experimental model for in-vitro electrophysiology. *Scientific Reports*, 4(1).

Galluzzi, L., Bravo-San Pedro, J., Levine, B., Green, D. and Kroemer, G., 2017. Pharmacological modulation of autophagy: therapeutic potential and persisting obstacles. *Nature Reviews Drug Discovery*, 16(7), pp.487-511.

Galluzzi, L., Pietrocola, F., Levine, B. and Kroemer, G., 2014. Metabolic Control of Autophagy. *Cell*, 159(6), pp.1263-1276.

Ganley, I., Wong, P., Gammoh, N. and Jiang, X., 2011. Distinct Autophagosomal-Lysosomal Fusion Mechanism Revealed by Thapsigargin-Induced Autophagy Arrest. *Molecular Cell*, 42(6), pp.731-743.

Gatica, D., Lahiri, V. and Klionsky, D., 2018. Cargo recognition and degradation by selective autophagy. *Nature Cell Biology*, 20(3), pp.233-242.

Geng, B., Choi, K., Wang, S., Chen, P., Pan, X., Dong, N., Ko, J. and Zhu, H., 2020. A simple, quick, and efficient CRISPR/Cas9 genome editing method for human induced pluripotent stem cells. *Acta Pharmacologica Sinica*,.

Geng, J. and Klionsky, D., 2008. The Atg8 and Atg12 ubiquitin-like conjugation systems in macroautophagy. *EMBO reports*, 9(9), pp.859-864.

Gerrard, L., Rodgers, L. and Cui, W., 2005. Differentiation of Human Embryonic Stem Cells to Neural Lineages in Adherent Culture by Blocking Bone Morphogenetic Protein Signaling. *Stem Cells*, 23(9), pp.1234-1241.

Gordon, S. and Plüddemann, A., 2017. Tissue macrophages: heterogeneity and functions. *BMC Biology*, 15(1).

Gordon, S., Plüddemann, A. and Martinez Estrada, F., 2014. Macrophage heterogeneity in tissues: phenotypic diversity and functions. *Immunological Reviews*, 262(1), pp.36-55.

Guhr, A., Kobold, S., Seltmann, S., Seiler Wulczyn, A., Kurtz, A. and Löser, P., 2018. Recent Trends in Research with Human Pluripotent Stem Cells: Impact of Research

and Use of Cell Lines in Experimental Research and Clinical Trials. *Stem Cell Reports*, 11(2), pp.485-496.

Günther, G., 2014. Multidrug-resistant and extensively drug-resistant tuberculosis: a review of current concepts and future challenges. *Clinical Medicine*, 14(3), pp.279-285.

Guo, H., Zhao, M., Qiu, X., Deis, J., Huang, H., Tang, Q. and Chen, X., 2016. Niemann-Pick type C2 deficiency impairs autophagy-lysosomal activity, mitochondrial function, and TLR signaling in adipocytes. *Journal of Lipid Research*, 57(9), pp.1644-1658.

Gutierrez, M., Munafo, D.B., Beron W. and Colombo M.I., 2004. Rab7 is required for the normal progression of the autophagic pathway in mammalian cells. *Journal of Cell Science*, 117(13), pp.2687-2697.

Gutierrez, M., Master, S., Singh, S., Taylor, G., Colombo, M. and Deretic, V., 2004. Autophagy Is a Defense Mechanism Inhibiting BCG and Mycobacterium tuberculosis Survival in Infected Macrophages. *Cell*, 119(6), pp.753-766.

Gwinn, D., Shackelford, D., Egan, D., Mihaylova, M., Mery, A., Vasquez, D., Turk, B. and Shaw, R., 2008. AMPK Phosphorylation of Raptor Mediates a Metabolic Checkpoint. *Molecular Cell*, 30(2), pp.214-226.

Hachiya, N., Mihara, K., Suda, K., Horst, M., Schatz, G. and Lithgow, T., 1995. Reconstitution of the initial steps of mitochondrial protein import. *Nature*, 376(6542), pp.705-709.

Haenseler, W., Sansom, S., Buchrieser, J., Newey, S., Moore, C., Nicholls, F., Chintawar, S., Schnell, C., Antel, J., Allen, N., Cader, M., Wade-Martins, R., James, W. and Cowley, S., 2017. A Highly Efficient Human Pluripotent Stem Cell Microglia Model Displays a Neuronal-Co-culture-Specific Expression Profile and Inflammatory Response. *Stem Cell Reports*, 8(6), pp.1727-1742.

Hale, C., Cheng, Q., Ortuno, D., Huang, M., Nojima, D., Kassner, P., Wang, S., Ollmann, M. and Carlisle, H., 2016. Identification of modulators of autophagic flux in an image-based high content siRNA screen. *Autophagy*, 12(4), pp.713-726.

Hale, C., Yeung, A., Goulding, D., Pickard, D., Alasoo, K., Powrie, F., Dougan, G. and Mukhopadhyay, S., 2015. Induced Pluripotent Stem Cell Derived Macrophages as a Cellular System to Study Salmonella and Other Pathogens. *PLOS ONE*, 10(5), p.e0124307.

Han, H., Seo, H., Jo, H., Han, H., Falcão, V., Delorme, V., Heo, J., Shum, D., Choi, J., Lee, J., Lee, S., Heo, H., Hong, S., Park, M., Thimmulappa, R. and Kim, J., 2019. Drug Discovery Platform Targeting M. tuberculosis with Human Embryonic Stem Cell-Derived Macrophages. *Stem Cell Reports*, 13(6), pp.980-991.

Hanna, J., Cheng, A., Saha, K., Kim, J., Lengner, C., Soldner, F., Cassady, J., Muffat, J., Carey, B. and Jaenisch, R., 2010. Human embryonic stem cells with biological and epigenetic characteristics similar to those of mouse ESCs. *Proceedings of the National Academy of Sciences*, 107(20), pp.9222-9227.

Hansen, M., Rubinsztein, D. and Walker, D., 2018. Autophagy as a promoter of longevity: insights from model organisms. *Nature Reviews Molecular Cell Biology*, 19(9), pp.579-593.

Hara, T., Nakamura, K., Matsui, M., Yamamoto, A., Nakahara, Y., Suzuki-Migishima, R., Yokoyama, M., Mishima, K., Saito, I., Okano, H. and Mizushima, N., 2006. Suppression of basal autophagy in neural cells causes neurodegenerative disease in mice. *Nature*, 441(7095), pp.885-889.

Härtlova, A., Herbst, S., Peltier, J., Rodgers, A., Bilkei-Gorzo, O., Fearns, A., Dill, B., Lee, H., Flynn, R., Cowley, S., Davies, P., Lewis, P., Ganley, I., Martinez, J., Alessi, D., Reith, A., Trost, M. and Gutierrez, M., 2018. LRRK2 is a negative regulator of Mycobacterium tuberculosis phagosome maturation in macrophages. *The EMBO Journal*, 37(12).

Hasmann, M. and Schemainda, I., 2003. FK866, a highly specific noncompetitive inhibitor of nicotinamide phosphoribosyltransferase, represents a novel mechanism for induction of tumor cell apoptosis. *Cancer Research*, 1;63(21), pp.7436-42.

Hay, D., Fletcher, J., Payne, C., Terrace, J., Gallagher, R., Snoeys, J., Black, J., Wojtacha, D., Samuel, K., Hannoun, Z., Pryde, A., Filippi, C., Currie, I., Forbes, S.,

Ross, J., Newsome, P. and Iredale, J., 2008. Highly efficient differentiation of hESCs to functional hepatic endoderm requires ActivinA and Wnt3a signaling. *Proceedings of the National Academy of Sciences*, 105(34), pp.12301-12306.

He, J., Ma, Y., Lee, Y., Thomson, J. and Kamp, T., 2003. Human Embryonic Stem Cells Develop Into Multiple Types of Cardiac Myocytes. *Circulation Research*, 93(1), pp.32-39.

Heaton, N. and Randall, G., 2010. Dengue Virus-Induced Autophagy Regulates Lipid Metabolism. *Cell Host & Microbe*, 8(5), pp.422-432.

Hewitt, G. and Korolchuk, V., 2017. Repair, Reuse, Recycle: The Expanding Role of Autophagy in Genome Maintenance. *Trends in Cell Biology*, 27(5), pp.340-351.

Heyes, J., Palmer, L., Bremner, K. and MacLachlan, I., 2005. Cationic lipid saturation influences intracellular delivery of encapsulated nucleic acids. *Journal of Controlled Release*, 107(2), pp.276-287.

Hirayama, D., Iida, T. and Nakase, H., 2017. The Phagocytic Function of Macrophage-Enforcing Innate Immunity and Tissue Homeostasis. *International Journal of Molecular Sciences*, 19(1), p.92.

Hiyama, E. and Hiyama, K., 2007. Telomere and telomerase in stem cells. *British Journal of Cancer*, 96(7), pp.1020-1024.

Hong, D., Ding, J., Li, O., He, Q., Ke, M., Zhu, M., Liu, L., Ou, W., He, Y. and Wu, Y., 2018. Human-induced pluripotent stem cell-derived macrophages and their immunological function in response to tuberculosis infection. *Stem Cell Research & Therapy*, 9(1).

Hughes, C., Benson, R., Bedaj, M. and Maffia, P., 2016. Antigen-Presenting Cells and Antigen Presentation in Tertiary Lymphoid Organs. *Frontiers in Immunology*, 7.

Hummon, A., Lim, S., Difilippantonio, M. and Ried, T., 2007. Isolation and solubilization of proteins after TRIzol® extraction of RNA and DNA from patient material following prolonged storage. *BioTechniques*, 42(4), pp.467-472.

Hyslop, L., Armstrong, L., Stojkovic, M. and Lako, M., 2005. Human embryonic stem cells: biology and clinical implications. *Expert Reviews in Molecular Medicine*, 7(19).

Hyvärinen, T., Hyysalo, A., Kapucu, F., Aarnos, L., Vinogradov, A., Eglen, S., Ylä-Outinen, L. and Narkilahti, S., 2019. Functional characterisation of human pluripotent stem cell-derived cortical networks differentiated on laminin-521 substrate: comparison to rat cortical cultures. *Scientific Reports*, 9(1).

Ichimura, Y., Kirisako, T., Takao, T., Satomi, Y., Shimonishi, Y., Ishihara, N., Mizushima, N., Tanida, I., Kominami, E., Ohsumi, M., Noda, T. and Ohsumi, Y., 2000. A ubiquitin-like system mediates protein lipidation. *Nature*, 408(6811), pp.488-492.

Iiboshi, Y., Papst, P., Kawasome, H., Hosoi, H., Abraham, R., Houghton, P. and Terada, N., 1999. Amino Acid-dependent Control of p70s6k. *Journal of Biological Chemistry*, 274(2), pp.1092-1099.

Imai, S. and Guarente, L., 2014. NAD+ and sirtuins in aging and disease. *Trends in Cell Biology*, 24(8), pp.464-471.

Imai, S. and Guarente, L., 2016. It takes two to tango: NAD+ and sirtuins in aging/longevity control. *npj Aging and Mechanisms of Disease*, 2(1).

Imai, S., 2009. The NAD World: A New Systemic Regulatory Network for Metabolism and Aging—Sirt1, Systemic NAD Biosynthesis, and Their Importance. *Cell Biochemistry and Biophysics*, 53(2), pp.65-74.

Inoki, K., Zhu, T. and Guan, K., 2003. TSC2 Mediates Cellular Energy Response to Control Cell Growth and Survival. *Cell*, 115(5), pp.577-590.

Itakura, E., Kishi-Itakura, C. and Mizushima, N., 2012. The Hairpin-type Tail-Anchored SNARE Syntaxin 17 Targets to Autophagosomes for Fusion with Endosomes/Lysosomes. *Cell*, 151(6), pp.1256-1269.

Jacob, A., Morley, M., Hawkins, F., McCauley, K., Jean, J., Heins, H., Na, C., Weaver, T., Vedaie, M., Hurley, K., Hinds, A., Russo, S., Kook, S., Zacharias, W., Ochs, M., Traber, K., Quinton, L., Crane, A., Davis, B., White, F., Wambach, J., Whitsett, J., Cole, F., Morrisey, E., Guttentag, S., Beers, M. and Kotton, D., 2017. Differentiation of

Human Pluripotent Stem Cells into Functional Lung Alveolar Epithelial Cells. *Cell Stem Cell*, 21(4), pp.472-488.e10.

Jager, S., Bucci, C., Tanida, I., Ueno, T., Kominami, E., Saftig, P. and Eskelinen, E.L., 2004. Role for Rab7 in maturation of late autophagic vacuoles. *Journal of Cell Science*, 117(20), pp.4837-4848.

Jia, K., Thomas, C., Akbar, M., Sun, Q., Adams-Huet, B., Gilpin, C. and Levine, B., 2009. Autophagy genes protect against Salmonella typhimurium infection and mediate insulin signaling-regulated pathogen resistance. *Proceedings of the National Academy of Sciences*, 106(34), pp.14564-14569.

Jiang, P. and Mizushima, N., 2013. Autophagy and human diseases. *Cell Research*, 24(1), pp.69-79.

Jiang, S., Wells, C. and Roach, P., 2011. Starch-binding domain-containing protein 1 (Stbd1) and glycogen metabolism: Identification of the Atg8 family interacting motif (AIM) in Stbd1 required for interaction with GABARAPL1. *Biochemical and Biophysical Research Communications*, 413(3), pp.420-425.

Jiang, T., Yu, J., Zhu, X., Zhang, Q., Cao, L., Wang, H., Tan, M., Gao, Q., Qin, H., Zhang, Y. and Tan, L., 2014. Temsirolimus attenuates tauopathy in vitro and in vivo by targeting tau hyperphosphorylation and autophagic clearance. *Neuropharmacology*, 85, pp.121-130.

Jiménez-Moreno, N., Stathakos, P., Caldwell, M. and Lane, J., 2017. Induced Pluripotent Stem Cell Neuronal Models for the Study of Autophagy Pathways in Human Neurodegenerative Disease. *Cells*, 6(3), p.24.

Jin, S., 2006. Autophagy, Mitochondrial Quality Control, and Oncogenesis. *Autophagy*, 2(2), pp.80-84.

Johansen, T. and Lamark, T., 2020. Selective Autophagy: ATG8 Family Proteins, LIR Motifs and Cargo Receptors. *Journal of Molecular Biology*, 432(1), pp.80-103.

Jordens, I., Fernandez-Borja, M., Marsman, M., Dusseljee, S., Janssen, L., Calafat, J., Janssen, H., Wubbolts, R. and Neefjes, J., 2001. The Rab7 effector protein RILP

controls lysosomal transport by inducing the recruitment of dynein-dynactin motors. *Current Biology*, 11(21), pp.1680-1685.

Joung, J. and Sander, J., 2012. TALENs: a widely applicable technology for targeted genome editing. *Nature Reviews Molecular Cell Biology*, 14(1), pp.49-55.

Jungverdorben, J., Till, A. and Brüstle, O., 2017. Induced pluripotent stem cell-based modeling of neurodegenerative diseases: a focus on autophagy. *Journal of Molecular Medicine*, 95(7), pp.705-718.

Kabeya, Y., Mizushima, N., Ueno, T., Yamamoto, A., Kirisako, T., Noda, T., Kominami, E., Ohsumi, Y. and Yoshimori, T., 2000. LC3, a mammalian homologue of yeast Apg8p, is localized in autophagosome membranes after processing. *The EMBO Journal*, 19(21), pp.5720-5728.

Kabeya, Y., Mizushima, N., Yamamoto, A., Oshitani-Okamoto, S., Ohsumi, Y. and Yoshimori, T., 2004. LC3, GABARAP and GATE16 localize to autophagosomal membrane depending on form-II formation. *Journal of Cell Science*, 117(13), pp.2805-2812.

Kaizuka, T., Morishita, H., Hama, Y., Tsukamoto, S., Matsui, T., Toyota, Y., Kodama, A., Ishihara, T., Mizushima, T. and Mizushima, N., 2016. An Autophagic Flux Probe that Releases an Internal Control. *Molecular Cell*, 64(4), pp.835-849.

Kamada, Y., Funakoshi, T., Shintani, T., Nagano, K., Ohsumi, M. and Ohsumi, Y., 2000. Tor-Mediated Induction of Autophagy via an Apg1 Protein Kinase Complex. *Journal of Cell Biology*, 150(6), pp.1507-1513.

Kanazawa, H., Ohsawa, K., Sasaki, Y., Kohsaka, S. and Imai, Y., 2002. Macrophage/Microglia-specific Protein Iba1 Enhances Membrane Ruffling and Rac Activation via Phospholipase C-γ-dependent Pathway. *Journal of Biological Chemistry*, 277(22), pp.20026-20032.

Karanasios, E., Stapleton, E., Manifava, M., Kaizuka, T., Mizushima, N., Walker, S. and Ktistakis, N., 2013. Dynamic association of the ULK1 complex with omegasomes during autophagy induction. *Journal of Cell Science*, 126(22), pp.5224-5238.

Karanasios, E., Walker, S., Okkenhaug, H., Manifava, M., Hummel, E., Zimmermann, H., Ahmed, Q., Domart, M., Collinson, L. and Ktistakis, N., 2016. Autophagy initiation by ULK complex assembly on ER tubulovesicular regions marked by ATG9 vesicles. *Nature Communications*, 7(1).

Karlsson, K., Cowley, S., Martinez, F., Shaw, M., Minger, S. and James, W., 2008. Homogeneous monocytes and macrophages from human embryonic stem cells following coculture-free differentiation in M-CSF and IL-3. *Experimental Hematology*, 36(9), pp.1167-1175.

Karten, B., Peake, K. and Vance, J., 2009. Mechanisms and consequences of impaired lipid trafficking in Niemann–Pick type C1-deficient mammalian cells. *Biochimica et Biophysica Acta (BBA) - Molecular and Cell Biology of Lipids*, 1791(7), pp.659-670.

Kauffman, K., Dorkin, J., Yang, J., Heartlein, M., DeRosa, F., Mir, F., Fenton, O. and Anderson, D., 2015. Optimisation of Lipid Nanoparticle Formulations for mRNA Delivery in Vivo with Fractional Factorial and Definitive Screening Designs. *Nano Letters*, 15(11), pp.7300-7306.

Kaufman, D., Hanson, E., Lewis, R., Auerbach, R. and Thomson, J., 2001. Hematopoietic colony-forming cells derived from human embryonic stem cells. *Proceedings of the National Academy of Sciences*, 98(19), pp.10716-10721.

Kehat, I., Kenyagin-Karsenti, D., Snir, M., Segev, H., Amit, M., Gepstein, A., Livne, E., Binah, O., Itskovitz-Eldor, J. and Gepstein, L., 2001. Human embryonic stem cells can differentiate into myocytes with structural and functional properties of cardiomyocytes. *Journal of Clinical Investigation*, 108(3), pp.407-414.

Kehrer, J., 1993. Free Radicals as Mediators of Tissue Injury and Disease. *Critical Reviews in Toxicology*, 23(1), pp.21-48.

Keller, G., 2005. Embryonic stem cell differentiation: emergence of a new era in biology and medicine. *Genes & Development*, 19(10), pp.1129-1155.

Kerr, J., Wyllie, A. and Currie, A., 1972. Apoptosis: A Basic Biological Phenomenon with Wideranging Implications in Tissue Kinetics. *British Journal of Cancer*, 26(4), pp.239-257.

Khaminets, A., Behl, C. and Dikic, I., 2016. Ubiquitin-Dependent And Independent Signals In Selective Autophagy. *Trends in Cell Biology*, 26(1), pp.6-16.

Kilpinen, H., Goncalves, A., Leha, A., Afzal, V., Alasoo, K., Ashford, S., Bala, S., Bensaddek, D., Casale, F., Culley, O., Danecek, P., Faulconbridge, A., Harrison, P., Kathuria, A., McCarthy, D., McCarthy, S., Meleckyte, R., Memari, Y., Moens, N., Soares, F., Mann, A., Streeter, I., Agu, C., Alderton, A., Nelson, R., Harper, S., Patel, M., White, A., Patel, S., Clarke, L., Halai, R., Kirton, C., Kolb-Kokocinski, A., Beales, P., Birney, E., Danovi, D., Lamond, A., Ouwehand, W., Vallier, L., Watt, F., Durbin, R., Stegle, O. and Gaffney, D., 2017. Common genetic variation drives molecular heterogeneity in human iPSCs. *Nature*, 546(7658), pp.370-375.

Kim, J., Kim, Y., Fang, C., Russell, R., Kim, J., Fan, W., Liu, R., Zhong, Q. and Guan, K., 2013. Differential Regulation of Distinct Vps34 Complexes by AMPK in Nutrient Stress and Autophagy. *Cell*, 152(1-2), pp.290-303.

Kim, J., Kundu, M., Viollet, B. and Guan, K., 2011. AMPK and mTOR regulate autophagy through direct phosphorylation of Ulk1. *Nature Cell Biology*, 13(2), pp.132-141.

Kim, K., Doi, A., Wen, B., Ng, K., Zhao, R., Cahan, P., Kim, J., Aryee, M., Ji, H., Ehrlich, L., Yabuuchi, A., Takeuchi, A., Cunniff, K., Hongguang, H., Mckinney-Freeman, S., Naveiras, O., Yoon, T., Irizarry, R., Jung, N., Seita, J., Hanna, J., Murakami, P., Jaenisch, R., Weissleder, R., Orkin, S., Weissman, I., Feinberg, A. and Daley, G., 2010. Epigenetic memory in induced pluripotent stem cells. *Nature*, 467(7313), pp.285-290.

Kim, K., Mutter, R., Cao, C., Albert, J., Freeman, M., Hallahan, D. and Lu, B., 2006. Autophagy for Cancer Therapy through Inhibition of Pro-apoptotic Proteins and Mammalian Target of Rapamycin Signaling. *Journal of Biological Chemistry*, 281(48), pp.36883-36890.

Kim, Y., Silwal, P., Kim, S., Yoshimori, T. and Jo, E., 2019. Autophagy-activating strategies to promote innate defense against mycobacteria. *Experimental & Molecular Medicine*, 51(12), pp.1-10.

Kimmey, J. and Stallings, C., 2016. Bacterial Pathogens versus Autophagy: Implications for Therapeutic Interventions. *Trends in Molecular Medicine*, 22(12), pp.1060-1076.

Kimura, S., Noda, T. and Yoshimori, T., 2007. Dissection of the Autophagosome Maturation Process by a Novel Reporter Protein, Tandem Fluorescent-Tagged LC3. *Autophagy*, 3(5), pp.452-460.

Kirkin, V., Lamark, T., Sou, Y., Bjørkøy, G., Nunn, J., Bruun, J., Shvets, E., McEwan, D., Clausen, T., Wild, P., Bilusic, I., Theurillat, J., Øvervatn, A., Ishii, T., Elazar, Z., Komatsu, M., Dikic, I. and Johansen, T., 2009. A Role for NBR1 in Autophagosomal Degradation of Ubiquitinated Substrates. *Molecular Cell*, 33(4), pp.505-516.

Kirkin, V., McEwan, D., Novak, I. and Dikic, I., 2009. A Role for Ubiquitin in Selective Autophagy. *Molecular Cell*, 34(3), pp.259-269.

Kirwan, P., Turner-Bridger, B., Peter, M., Momoh, A., Arambepola, D., Robinson, H. and Livesey, F., 2015. Development and function of human cerebral cortex neural networks from pluripotent stem cells in vitro. *Development*, 142(18), pp.3178-3187.

Klionsky, D., Abdelmohsen, K., Abe, A., Abedin, M., Abeliovich, H., Acevedo Arozena, A., Adachi, H., Adams, C., Adams, P., Adeli, K., Adhihetty, P., Adler, S., Agam, G., Agarwal, R., Aghi, M., Agnello, M., Agostinis, P., Aguilar, P., Aguirre-Ghiso, J., Airoldi, E., Ait-Si-Ali, S., Akematsu, T., Akporiaye, E., Al-Rubeai, M., Albaiceta, G., Albanese, C., Albani, D., Albert, M., Aldudo, J., Algül, H., Alirezaei, M., Alloza, I., Almasan, A., Almonte-Beceril, M., Alnemri, E., Alonso, C., Altan-Bonnet, N., Altieri, D., Alvarez, S., Alvarez-Erviti, L., Alves, S., Amadoro, G., Amano, A., Amantini, C., Ambrosio, S., Amelio, I., Amer, A., Amessou, M., Amon, A., An, Z., Anania, F., Andersen, S., Andley, U., Andreadi, C., Andrieu-Abadie, N., Anel, A., Ann, D., Anoopkumar-Dukie, S., Antonioli, M., Aoki, H., Apostolova, N., Aquila, S., Aquilano, K., Araki, K., Arama, E., Aranda, A., Araya, J., Arcaro, A., Arias, E., Arimoto, H., Ariosa, A., Armstrong, J., Arnould, T., Arsov, I., Asanuma, K., Askanas, V., Asselin, E., Atarashi, R., Atherton,

S., Atkin, J., Attardi, L., Auberger, P., Auburger, G., Aurelian, L., Autelli, R., Avagliano, L., Avantaggiati, M., Avrahami, L., Awale, S., Azad, N., Bachetti, T., Backer, J., Bae, D., Bae, J., Bae, O., Bae, S., Baehrecke, E., Baek, S., Baghdiguian, S., Bagniewska-Zadworna, A., Bai, H., Bai, J., Bai, X., Bailly, Y., Balaji, K., Balduini, W., Ballabio, A., Balzan, R., Banerjee, R., Bánhegyi, G., Bao, H., Barbeau, B., Barrachina, M., Barreiro, E., Bartel, B., Bartolomé, A., Bassham, D., Bassi, M., Bast, R., Basu, A., Batista, M., Batoko, H., Battino, M., Bauckman, K., Baumgarner, B., Bayer, K., Beale, R., Beaulieu, J., Beck, G., Becker, C., Beckham, J., Bédard, P., Bednarski, P., Begley, T., Behl, C., Behrends, C., Behrens, G., Behrns, K., Bejarano, E., Belaid, A., Belleudi, F., Bénard, G., Berchem, G., Bergamaschi, D., Bergami, M., Berkhout, B., Berliocchi, L., Bernard, A., Bernard, M., Bernassola, F., Bertolotti, A., Bess, A., Besteiro, S., Bettuzzi, S., Bhalla, S., Bhattacharyya, S., Bhutia, S., Biagosch, C., Bianchi, M., Biard-Piechaczyk, M., Billes, V., Bincoletto, C., Bingol, B., Bird, S., Bitoun, M., Bjedov, I., Blackstone, C., Blanc, L., Blanco, G., Blomhoff, H., Boada-Romero, E., Böckler, S., Boes, M., Boesze-Battaglia, K., Boise, L., Bolino, A., Boman, A., Bonaldo, P., Bordi, M., Bosch, J., Botana, L., Botti, J., Bou, G., Bouché, M., Bouchecareilh, M., Boucher, M., Boulton, M., Bouret, S., Boya, P., Boyer-Guittaut, M., Bozhkov, P., Brady, N., Braga, V., Brancolini, C., Braus, G., Bravo-San Pedro, J., Brennan, L., Bresnick, E., Brest, P., Bridges, D., Bringer, M., Brini, M., Brito, G., Brodin, B., Brookes, P., Brown, E., Brown, K., Broxmeyer, H., Bruhat, A., Brum, P., Brumell, J., Brunetti-Pierri, N., Bryson-Richardson, R., Buch, S., Buchan, A., Budak, H., Bulavin, D., Bultman, S., Bultynck, G., Bumbasirevic, V., Burelle, Y., Burke, R., Burmeister, M., Bütikofer, P., Caberlotto, L., Cadwell, K., Cahova, M., Cai, D., Cai, J., Cai, Q., Calatayud, S., Camougrand, N., Campanella, M., Campbell, G., Campbell, M., Campello, S., Candau, R., Caniggia, I., Cantoni, L., Cao, L., Caplan, A., Caraglia, M., Cardinali, C., Cardoso, S., Carew, J., Carleton, L., Carlin, C., Carloni, S., Carlsson, S., Carmona-Gutierrez, D., Carneiro, L., Carnevali, O., Carra, S., Carrier, A., Carroll, B., Casas, C., Casas, J., Cassinelli, G., Castets, P., Castro-Obregon, S., Cavallini, G., Ceccherini, I., Cecconi, F., Cederbaum, A., Ceña, V., Cenci, S., Cerella, C., Cervia, D., Cetrullo, S., Chaachouay, H., Chae, H., Chagin, A., Chai, C., Chakrabarti, G., Chamilos, G., Chan, E., Chan, M., Chandra, D., Chandra, P., Chang, C., Chang, R., Chang, T., Chatham, J., Chatterjee, S., Chauhan, S., Che, Y., Cheetham, M., Cheluvappa, R., Chen, C., Chen, G., Chen, G., Chen, G., Chen, H., Chen, J., Chen, J., Chen, M., Chen, M., Chen, P., Chen, Q., Chen, Q., Chen, S., Chen, S., Chen, S., Chen, W., Chen, W., Chen, W., Chen, W., Chen, X.,

Chen, Y., Chen, Y., Chen, Y., Chen, Y., Chen, Y., Chen, Y., Chen, Y., Chen, Y., Chen, Z., Chen, Z., Cheng, A., Cheng, C., Cheng, H., Cheong, H., Cherry, S., Chesney, J., Cheung, C., Chevet, E., Chi, H., Chi, S., Chiacchiera, F., Chiang, H., Chiarelli, R., Chiariello, M., Chieppa, M., Chin, L., Chiong, M., Chiu, G., Cho, D., Cho, S., Cho, W., Cho, Y., Cho, Y., Choi, A., Choi, E., Choi, E., Choi, J., Choi, M., Choi, S., Chou, T., Chouaib, S., Choubey, D., Choubey, V., Chow, K., Chowdhury, K., Chu, C., Chuang, T., Chun, T., Chung, H., Chung, T., Chung, Y., Chwae, Y., Cianfanelli, V., Ciarcia, R., Ciechomska, I., Ciriolo, M., Cirone, M., Claerhout, S., Clague, M., Clària, J., Clarke, P., Clarke, R., Clementi, E., Cleyrat, C., Cnop, M., Coccia, E., Cocco, T., Codogno, P., Coers, J., Cohen, E., Colecchia, D., Coletto, L., Coll, N., Colucci-Guyon, E., Comincini, S., Condello, M., Cook, K., Coombs, G., Cooper, C., Cooper, J., Coppens, I., Corasaniti, M., Corazzari, M., Corbalan, R., Corcelle-Termeau, E., Cordero, M., Corral-Ramos, C., Corti, O., Cossarizza, A., Costelli, P., Costes, S., Cotman, S., Coto-Montes, A., Cottet, S., Couve, E., Covey, L., Cowart, L., Cox, J., Coxon, F., Coyne, C., Cragg, M., Craven, R., Crepaldi, T., Crespo, J., Criollo, A., Crippa, V., Cruz, M., Cuervo, A., Cuezva, J., Cui, T., Cutillas, P., Czaja, M., Czyzyk-Krzeska, M., Dagda, R., Dahmen, U., Dai, C., Dai, W., Dai, Y., Dalby, K., Dalla Valle, L., Dalmasso, G., D'Amelio, M., Damme, M., Darfeuille-Michaud, A., Dargemont, C., Darley-Usmar, V., Dasarathy, S., Dasgupta, B., Dash, S., Dass, C., Davey, H., Davids, L., Dávila, D., Davis, R., Dawson, T., Dawson, V., Daza, P., de Belleroche, J., de Figueiredo, P., de Figueiredo, R., de la Fuente, J., De Martino, L., De Matteis, A., De Meyer, G., De Milito, A., De Santi, M., de Souza, W., De Tata, V., De Zio, D., Debnath, J., Dechant, R., Decuypere, J., Deegan, S., Dehay, B., Del Bello, B., Del Re, D., Delage-Mourroux, R., Delbridge, L., Deldicque, L., Delorme-Axford, E., Deng, Y., Dengjel, J., Denizot, M., Dent, P., Der, C., Deretic, V., Derrien, B., Deutsch, E., Devarenne, T., Devenish, R., Di Bartolomeo, S., Di Daniele, N., Di Domenico, F., Di Nardo, A., Di Paola, S., Di Pietro, A., Di Renzo, L., DiAntonio, A., Díaz-Araya, G., Díaz-Laviada, I., Diaz-Meco, M., Diaz-Nido, J., Dickey, C., Dickson, R., Diederich, M., Digard, P., Dikic, I., Dinesh-Kumar, S., Ding, C., Ding, W., Ding, Z., Dini, L., Distler, J., Diwan, A., Djavaheri-Mergny, M., Dmytruk, K., Dobson, R., Doetsch, V., Dokladny, K., Dokudovskaya, S., Donadelli, M., Dong, X., Dong, X., Dong, Z., Donohue, T., Doran, K., D'Orazi, G., Dorn, G., Dosenko, V., Dridi, S., Drucker, L., Du, J., Du, L., Du, L., du Toit, A., Dua, P., Duan, L., Duann, P., Dubey, V., Duchen, M., Duchosal, M., Duez, H., Dugail, I., Dumit, V., Duncan, M., Dunlop, E., Dunn, W., Dupont, N., Dupuis, L., Durán, R., Durcan, T.,

Duvezin-Caubet, S., Duvvuri, U., Eapen, V., Ebrahimi-Fakhari, D., Echard, A., Eckhart, L., Edelstein, C., Edinger, A., Eichinger, L., Eisenberg, T., Eisenberg-Lerner, A., Eissa, N., El-Deiry, W., El-Khoury, V., Elazar, Z., Eldar-Finkelman, H., Elliott, C., Emanuele, E., Emmenegger, U., Engedal, N., Engelbrecht, A., Engelender, S., Enserink, J., Erdmann, R., Erenpreisa, J., Eri, R., Eriksen, J., Erman, A., Escalante, R., Eskelinen, E., Espert, L., Esteban-Martínez, L., Evans, T., Fabri, M., Fabrias, G., Fabrizi, C., Facchiano, A., Færgeman, N., Faggioni, A., Fairlie, W., Fan, C., Fan, D., Fan, J., Fang, S., Fanto, M., Fanzani, A., Farkas, T., Faure, M., Favier, F., Fearnhead, H., Federici, M., Fei, E., Felizardo, T., Feng, H., Feng, Y., Feng, Y., Ferguson, T., Fernández, Á., Fernandez-Barrena, M., Fernandez-Checa, J., Fernández-López, A., Fernandez-Zapico, M., Feron, O., Ferraro, E., Ferreira-Halder, C., Fesus, L., Feuer, R., Fiesel, F., Filippi-Chiela, E., Filomeni, G., Fimia, G., Fingert, J., Finkbeiner, S., Finkel, T., Fiorito, F., Fisher, P., Flajolet, M., Flamigni, F., Florey, O., Florio, S., Floto, R., Folini, M., Follo, C., Fon, E., Fornai, F., Fortunato, F., Fraldi, A., Franco, R., Francois, A., François, A., Frankel, L., Fraser, I., Frey, N., Freyssenet, D., Frezza, C., Friedman, S., Frigo, D., Fu, D., Fuentes, J., Fueyo, J., Fujitani, Y., Fujiwara, Y., Fujiya, M., Fukuda, M., Fulda, S., Fusco, C., Gabryel, B., Gaestel, M., Gailly, P., Gajewska, M., Galadari, S., Galili, G., Galindo, I., Galindo, M., Galliciotti, G., Galluzzi, L., Galluzzi, L., Galy, V., Gammoh, N., Gandy, S., Ganesan, A., Ganesan, S., Ganley, I., Gannagé, M., Gao, F., Gao, F., Gao, J., García Nannig, L., García Véscovi, E., Garcia-Macía, M., Garcia-Ruiz, C., Garg, A., Garg, P., Gargini, R., Gassen, N., Gatica, D., Gatti, E., Gavard, J., Gavathiotis, E., Ge, L., Ge, P., Ge, S., Gean, P., Gelmetti, V., Genazzani, A., Geng, J., Genschik, P., Gerner, L., Gestwicki, J., Gewirtz, D., Ghavami, S., Ghigo, E., Ghosh, D., Giammarioli, A., Giampieri, F., Giampietri, C., Giatromanolaki, A., Gibbings, D., Gibellini, L., Gibson, S., Ginet, V., Giordano, A., Giorgini, F., Giovannetti, E., Girardin, S., Gispert, S., Giuliano, S., Gladson, C., Glavic, A., Gleave, M., Godefroy, N., Gogal, R., Gokulan, K., Goldman, G., Goletti, D., Goligorsky, M., Gomes, A., Gomes, L., Gomez, H., Gomez-Manzano, C., Gómez-Sánchez, R., Gonçalves, D., Goncu, E., Gong, Q., Gongora, C., Gonzalez, C., Gonzalez-Alegre, P., Gonzalez-Cabo, P., González-Polo, R., Goping, I., Gorbea, C., Gorbunov, N., Goring, D., Gorman, A., Gorski, S., Goruppi, S., Goto-Yamada, S., Gotor, C., Gottlieb, R., Gozes, I., Gozuacik, D., Graba, Y., Graef, M., Granato, G., Grant, G., Grant, S., Gravina, G., Green, D., Greenhough, A., Greenwood, M., Grimaldi, B., Gros, F., Grose, C., Groulx, J., Gruber, F., Grumati, P., Grune, T., Guan, J., Guan, K., Guerra, B., Guillen, C., Gulshan, K.,

Gunst, J., Guo, C., Guo, L., Guo, M., Guo, W., Guo, X., Gust, A., Gustafsson, Å., Gutierrez, E., Gutierrez, M., Gwak, H., Haas, A., Haber, J., Hadano, S., Hagedorn, M., Hahn, D., Halayko, A., Hamacher-Brady, A., Hamada, K., Hamai, A., Hamann, A., Hamasaki, M., Hamer, I., Hamid, Q., Hammond, E., Han, F., Han, W., Handa, J., Hanover, J., Hansen, M., Harada, M., Harhaji-Trajkovic, L., Harper, J., Harrath, A., Harris, A., Harris, J., Hasler, U., Hasselblatt, P., Hasui, K., Hawley, R., Hawley, T., He, C., He, C., He, F., He, G., He, R., He, X., He, Y., He, Y., Heath, J., Hébert, M., Heinzen, R., Helgason, G., Hensel, M., Henske, E., Her, C., Herman, P., Hernández, A., Hernandez, C., Hernández-Tiedra, S., Hetz, C., Hiesinger, P., Higaki, K., Hilfiker, S., Hill, B., Hill, J., Hill, W., Hino, K., Hofius, D., Hofman, P., Höglinger, G., Höhfeld, J., Holz, M., Hong, Y., Hood, D., Hoozemans, J., Hoppe, T., Hsu, C., Hsu, C., Hsu, L., Hu, D., Hu, G., Hu, H., Hu, H., Hu, M., Hu, Y., Hu, Z., Hua, F., Hua, Y., Huang, C., Huang, H., Huang, K., Huang, K., Huang, S., Huang, S., Huang, W., Huang, Y., Huang, Y., Huang, Y., Huber, T., Huebbe, P., Huh, W., Hulmi, J., Hur, G., Hurley, J., Husak, Z., Hussain, S., Hussain, S., Hwang, J., Hwang, S., Hwang, T., Ichihara, A., Imai, Y., Imbriano, C., Inomata, M., Into, T., Iovane, V., Iovanna, J., Iozzo, R., Ip, N., Irazoqui, J., Iribarren, P., Isaka, Y., Isakovic, A., Ischiropoulos, H., Isenberg, J., Ishaq, M., Ishida, H., Ishii, I., Ishmael, J., Isidoro, C., Isobe, K., Isono, E., Issazadeh-Navikas, S., Itahana, K., Itakura, E., Ivanov, A., Iyer, A., Izquierdo, J., Izumi, Y., Izzo, V., Jäättelä, M., Jaber, N., Jackson, D., Jackson, W., Jacob, T., Jacques, T., Jagannath, C., Jain, A., Jana, N., Jang, B., Jani, A., Janji, B., Jannig, P., Jansson, P., Jean, S., Jendrach, M., Jeon, J., Jessen, N., Jeung, E., Jia, K., Jia, L., Jiang, H., Jiang, H., Jiang, L., Jiang, T., Jiang, X., Jiang, X., Jiang, X., Jiang, Y., Jiang, Y., Jiménez, A., Jin, C., Jin, H., Jin, L., Jin, M., Jin, S., Jinwal, U., Jo, E., Johansen, T., Johnson, D., Johnson, G., Johnson, J., Jonasch, E., Jones, C., Joosten, L., Jordan, J., Joseph, A., Joseph, B., Joubert, A., Ju, D., Ju, J., Juan, H., Juenemann, K., Juhász, G., Jung, H., Jung, J., Jung, Y., Jungbluth, H., Justice, M., Jutten, B., Kaakoush, N., Kaarniranta, K., Kaasik, A., Kabuta, T., Kaeffer, B., Kågedal, K., Kahana, A., Kajimura, S., Kakhlon, O., Kalia, M., Kalvakolanu, D., Kamada, Y., Kambas, K., Kaminskyy, V., Kampinga, H., Kandouz, M., Kang, C., Kang, R., Kang, T., Kanki, T., Kanneganti, T., Kanno, H., Kanthasamy, A., Kantorow, M., Kaparakis-Liaskos, M., Kapuy, O., Karantza, V., Karim, M., Karmakar, P., Kaser, A., Kaushik, S., Kawula, T., Kaynar, A., Ke, P., Ke, Z., Kehrl, J., Keller, K., Kemper, J., Kenworthy, A., Kepp, O., Kern, A., Kesari, S., Kessel, D., Ketteler, R., Kettelhut, I., Khambu, B., Khan, M., Khandelwal, V., Khare, S., Kiang, J.,

Kiger, A., Kihara, A., Kim, A., Kim, C., Kim, D., Kim, D., Kim, E., Kim, H., Kim, H., Kim, J., Kim, J., Kim, J., Kim, J., Kim, K., Kim, M., Kim, M., Kim, P., Kim, S., Kim, S., Kim, Y., Kim, Y., Kimchi, A., Kimmelman, A., Kimura, T., King, J., Kirkegaard, K., Kirkin, V., Kirshenbaum, L., Kishi, S., Kitajima, Y., Kitamoto, K., Kitaoka, Y., Kitazato, K., Kley, R., Klimecki, W., Klinkenberg, M., Klucken, J., Knævelsrud, H., Knecht, E., Knuppertz, L., Ko, J., Kobayashi, S., Koch, J., Koechlin-Ramonatxo, C., Koenig, U., Koh, Y., Köhler, K., Kohlwein, S., Koike, M., Komatsu, M., Kominami, E., Kong, D., Kong, H., Konstantakou, E., Kopp, B., Korcsmaros, T., Korhonen, L., Korolchuk, V., Koshkina, N., Kou, Y., Koukourakis, M., Koumenis, C., Kovács, A., Kovács, T., Kovacs, W., Koya, D., Kraft, C., Krainc, D., Kramer, H., Kravic-Stevovic, T., Krek, W., Kretz-Remy, C., Krick, R., Krishnamurthy, M., Kriston-Vizi, J., Kroemer, G., Kruer, M., Kruger, R., Ktistakis, N., Kuchitsu, K., Kuhn, C., Kumar, A., Kumar, A., Kumar, A., Kumar, D., Kumar, D., Kumar, R., Kumar, S., Kundu, M., Kung, H., Kuno, A., Kuo, S., Kuret, J., Kurz, T., Kwok, T., Kwon, T., Kwon, Y., Kyrmizi, I., La Spada, A., Lafont, F., Lahm, T., Lakkaraju, A., Lam, T., Lamark, T., Lancel, S., Landowski, T., Lane, D., Lane, J., Lanzi, C., Lapaquette, P., Lapierre, L., Laporte, J., Laukkarinen, J., Laurie, G., Lavandero, S., Lavie, L., LaVoie, M., Law, B., Law, H., Law, K., Layfield, R., Lazo, P., Le Cam, L., Le Roch, K., Le Stunff, H., Leardkamolkarn, V., Lecuit, M., Lee, B., Lee, C., Lee, E., Lee, G., Lee, H., Lee, H., Lee, J., Lee, J., Lee, J., Lee, J., Lee, M., Lee, M., Lee, P., Lee, S., Lee, S., Lee, S., Lee, S., Lee, S., Lee, S., Lee, S., Lee, S., Lee, S., Lee, Y., Lee, Y., Lee, Y., Leeuwenburgh, C., Lefort, S., Legouis, R., Lei, J., Lei, Q., Leib, D., Leibowitz, G., Lekli, I., Lemaire, S., Lemasters, J., Lemberg, M., Lemoine, A., Leng, S., Lenz, G., Lenzi, P., Lerman, L., Lettieri Barbato, D., Leu, J., Leung, H., Levine, B., Lewis, P., Lezoualc'h, F., Li, C., Li, F., Li, F., Li, J., Li, K., Li, L., Li, M., Li, M., Li, Q., Li, R., Li, S., Li, W., Li, W., Li, X., Li, Y., Lian, J., Liang, C., Liang, Q., Liao, Y., Liberal, J., Liberski, P., Lie, P., Lieberman, A., Lim, H., Lim, K., Lim, K., Lima, R., Lin, C., Lin, C., Lin, F., Lin, F., Lin, F., Lin, K., Lin, K., Lin, P., Lin, T., Lin, W., Lin, Y., Lin, Y., Linden, R., Lindholm, D., Lindqvist, L., Lingor, P., Linkermann, A., Liotta, L., Lipinski, M., Lira, V., Lisanti, M., Liton, P., Liu, B., Liu, C., Liu, C., Liu, F., Liu, H., Liu, J., Liu, J., Liu, J., Liu, K., Liu, L., Liu, L., Liu, Q., Liu, R., Liu, S., Liu, S., Liu, W., Liu, X., Liu, X., Liu, X., Liu, X., Liu, X., Liu, X., Liu, Y., Liu, Y., Liu, Z., Liu, Z., Liuzzi, J., Lizard, G., Ljujic, M., Lodhi, I., Logue, S., Lokeshwar, B., Long, Y., Lonial, S., Loos, B., López-Otín, C., López-Vicario, C., Lorente, M., Lorenzi, P., Lõrincz, P., Los, M., Lotze, M., Lovat, P., Lu, B., Lu, B., Lu, J., Lu, Q., Lu, S., Lu, S., Lu, Y., Luciano, F., Luckhart, S., Lucocq, J.,

Ludovico, P., Lugea, A., Lukacs, N., Lum, J., Lund, A., Luo, H., Luo, J., Luo, S., Luparello, C., Lyons, T., Ma, J., Ma, Y., Ma, Y., Ma, Z., Machado, J., Machado-Santelli, G., Macian, F., MacIntosh, G., MacKeigan, J., Macleod, K., MacMicking, J., MacMillan-Crow, L., Madeo, F., Madesh, M., Madrigal-Matute, J., Maeda, A., Maeda, T., Maegawa, G., Maellaro, E., Maes, H., Magariños, M., Maiese, K., Maiti, T., Maiuri, L., Maiuri, M., Maki, C., Malli, R., Malorni, W., Maloyan, A., Mami-Chouaib, F., Man, N., Mancias, J., Mandelkow, E., Mandell, M., Manfredi, A., Manié, S., Manzoni, C., Mao, K., Mao, Z., Mao, Z., Marambaud, P., Marconi, A., Marelja, Z., Marfe, G., Margeta, M., Margittai, E., Mari, M., Mariani, F., Marin, C., Marinelli, S., Mariño, G., Markovic, I., Marquez, R., Martelli, A., Martens, S., Martin, K., Martin, S., Martin, S., Martin-Acebes, M., Martín-Sanz, P., Martinand-Mari, C., Martinet, W., Martinez, J., Martinez-Lopez, N., Martinez-Outschoorn, U., Martínez-Velázquez, M., Martinez-Vicente, M., Martins, W., Mashima, H., Mastrianni, J., Matarese, G., Matarrese, P., Mateo, R., Matoba, S., Matsumoto, N., Matsushita, T., Matsuura, A., Matsuzawa, T., Mattson, M., Matus, S., Maugeri, N., Mauvezin, C., Mayer, A., Maysinger, D., Mazzolini, G., McBrayer, M., McCall, K., McCormick, C., McInerney, G., McIver, S., McKenna, S., McMahon, J., McNeish, I., Mechta-Grigoriou, F., Medema, J., Medina, D., Megyeri, K., Mehrpour, M., Mehta, J., Mei, Y., Meier, U., Meijer, A., Meléndez, A., Melino, G., Melino, S., de Melo, E., Mena, M., Meneghini, M., Menendez, J., Menezes, R., Meng, L., Meng, L., Meng, S., Menghini, R., Menko, A., Menna-Barreto, R., Menon, M., Meraz-Ríos, M., Merla, G., Merlini, L., Merlot, A., Meryk, A., Meschini, S., Meyer, J., Mi, M., Miao, C., Micale, L., Michaeli, S., Michiels, C., Migliaccio, A., Mihailidou, A., Mijaljica, D., Mikoshiba, K., Milan, E., Miller-Fleming, L., Mills, G., Mills, I., Minakaki, G., Minassian, B., Ming, X., Minibayeva, F., Minina, E., Mintern, J., Minucci, S., Miranda-Vizuete, A., Mitchell, C., Miyamoto, S., Miyazawa, K., Mizushima, N., Mnich, K., Mograbi, B., Mohseni, S., Moita, L., Molinari, M., Molinari, M., Møller, A., Mollereau, B., Mollinedo, F., Mongillo, M., Monick, M., Montagnaro, S., Montell, C., Moore, D., Moore, M., Mora-Rodriguez, R., Moreira, P., Morel, E., Morelli, M., Moreno, S., Morgan, M., Moris, A., Moriyasu, Y., Morrison, J., Morrison, L., Morselli, E., Moscat, J., Moseley, P., Mostowy, S., Motori, E., Mottet, D., Mottram, J., Moussa, C., Mpakou, V., Mukhtar, H., Mulcahy Levy, J., Muller, S., Muñoz-Moreno, R., Muñoz-Pinedo, C., Münz, C., Murphy, M., Murray, J., Murthy, A., Mysorekar, I., Nabi, I., Nabissi, M., Nader, G., Nagahara, Y., Nagai, Y., Nagata, K., Nagelkerke, A., Nagy, P., Naidu, S., Nair, S., Nakano, H., Nakatogawa, H., Nanjundan, M., Napolitano, G., Naqvi, N., Nardacci, R., Narendra,

D., Narita, M., Nascimbeni, A., Natarajan, R., Navegantes, L., Nawrocki, S., Nazarko, T., Nazarko, V., Neill, T., Neri, L., Netea, M., Netea-Maier, R., Neves, B., Ney, P., Nezis, I., Nguyen, H., Nguyen, H., Nicot, A., Nilsen, H., Nilsson, P., Nishimura, M., Nishino, I., Niso-Santano, M., Niu, H., Nixon, R., Njar, V., Noda, T., Noegel, A., Nolte, E., Norberg, E., Norga, K., Noureini, S., Notomi, S., Notterpek, L., Nowikovsky, K., Nukina, N., Nürnberger, T., O'Donnell, V., O'Donovan, T., O'Dwyer, P., Oehme, I., Oeste, C., Ogawa, M., Ogretmen, B., Ogura, Y., Oh, Y., Ohmuraya, M., Ohshima, T., Ojha, R., Okamoto, K., Okazaki, T., Oliver, F., Ollinger, K., Olsson, S., Orban, D., Ordonez, P., Orhon, I., Orosz, L., O'Rourke, E., Orozco, H., Ortega, A., Ortona, E., Osellame, L., Oshima, J., Oshima, S., Osiewacz, H., Otomo, T., Otsu, K., Ou, J., Outeiro, T., Ouyang, D., Ouyang, H., Overholtzer, M., Ozbun, M., Ozdinler, P., Ozpolat, B., Pacelli, C., Paganetti, P., Page, G., Pages, G., Pagnini, U., Pajak, B., Pak, S., Pakos-Zebrucka, K., Pakpour, N., Palková, Z., Palladino, F., Pallauf, K., Pallet, N., Palmieri, M., Paludan, S., Palumbo, C., Palumbo, S., Pampliega, O., Pan, H., Pan, W., Panaretakis, T., Pandey, A., Pantazopoulou, A., Papackova, Z., Papademetrio, D., Papassideri, I., Papini, A., Parajuli, N., Pardo, J., Parekh, V., Parenti, G., Park, J., Park, J., Park, O., Parker, R., Parlato, R., Parys, J., Parzych, K., Pasquet, J., Pasquier, B., Pasumarthi, K., Patschan, D., Patterson, C., Pattingre, S., Pattison, S., Pause, A., Pavenstädt, H., Pavone, F., Pedrozo, Z., Peña, F., Peñalva, M., Pende, M., Peng, J., Penna, F., Penninger, J., Pensalfini, A., Pepe, S., Pereira, G., Pereira, P., Pérez-de la Cruz, V., Pérez-Pérez, M., Pérez-Rodríguez, D., Pérez-Sala, D., Perier, C., Perl, A., Perlmutter, D., Perrotta, I., Pervaiz, S., Pesonen, M., Pessin, J., Peters, G., Petersen, M., Petrache, I., Petrof, B., Petrovski, G., Phang, J., Piacentini, M., Pierdominici, M., Pierre, P., Pierrefite-Carle, V., Pietrocola, F., Pimentel-Muiños, F., Pinar, M., Pineda, B., Pinkas-Kramarski, R., Pinti, M., Pinton, P., Piperdi, B., Piret, J., Platanias, L., Platta, H., Plowey, E., Pöggeler, S., Poirot, M., Polčic, P., Poletti, A., Poon, A., Popelka, H., Popova, B., Poprawa, I., Poulose, S., Poulton, J., Powers, S., Powers, T., Pozuelo-Rubio, M., Prak, K., Prange, R., Prescott, M., Priault, M., Prince, S., Proia, R., Proikas-Cezanne, T., Prokisch, H., Promponas, V., Przyklenk, K., Puertollano, R., Pugazhenthi, S., Puglielli, L., Pujol, A., Puyal, J., Pyeon, D., Qi, X., Qian, W., Qin, Z., Qiu, Y., Qu, Z., Quadrilatero, J., Quinn, F., Raben, N., Rabinowich, H., Radogna, F., Ragusa, M., Rahmani, M., Raina, K., Ramanadham, S., Ramesh, R., Rami, A., Randall-Demllo, S., Randow, F., Rao, H., Rao, V., Rasmussen, B., Rasse, T., Ratovitski, E., Rautou, P., Ray, S., Razani, B., Reed, B., Reggiori, F., Rehm, M.,

Reichert, A., Rein, T., Reiner, D., Reits, E., Ren, J., Ren, X., Renna, M., Reusch, J., Revuelta, J., Reyes, L., Rezaie, A., Richards, R., Richardson, D., Richetta, C., Riehle, M., Rihn, B., Rikihisa, Y., Riley, B., Rimbach, G., Rippo, M., Ritis, K., Rizzi, F., Rizzo, E., Roach, P., Robbins, J., Roberge, M., Roca, G., Roccheri, M., Rocha, S., Rodrigues, C., Rodríguez, C., de Cordoba, S., Rodriguez-Muela, N., Roelofs, J., Rogov, V., Rohn, T., Rohrer, B., Romanelli, D., Romani, L., Romano, P., Roncero, M., Rosa, J., Rosello, A., Rosen, K., Rosenstiel, P., Rost-Roszkowska, M., Roth, K., Roué, G., Rouis, M., Rouschop, K., Ruan, D., Ruano, D., Rubinsztein, D., Rucker, E., Rudich, A., Rudolf, E., Rudolf, R., Ruegg, M., Ruiz-Roldan, C., Ruparelia, A., Rusmini, P., Russ, D., Russo, G., Russo, G., Russo, R., Rusten, T., Ryabovol, V., Ryan, K., Ryter, S., Sabatini, D., Sacher, M., Sachse, C., Sack, M., Sadoshima, J., Saftig, P., Sagi-Eisenberg, R., Sahni, S., Saikumar, P., Saito, T., Saitoh, T., Sakakura, K., Sakoh-Nakatogawa, M., Sakuraba, Y., Salazar-Roa, M., Salomoni, P., Saluja, A., Salvaterra, P., Salvioli, R., Samali, A., Sanchez, A., Sánchez-Alcázar, J., Sanchez-Prieto, R., Sandri, M., Sanjuan, M., Santaguida, S., Santambrogio, L., Santoni, G., dos Santos, C., Saran, S., Sardiello, M., Sargent, G., Sarkar, P., Sarkar, S., Sarrias, M., Sarwal, M., Sasakawa, C., Sasaki, M., Sass, M., Sato, K., Sato, M., Satriano, J., Savaraj, N., Saveljeva, S., Schaefer, L., Schaible, U., Scharl, M., Schatzl, H., Schekman, R., Scheper, W., Schiavi, A., Schipper, H., Schmeisser, H., Schmidt, J., Schmitz, I., Schneider, B., Schneider, E., Schneider, J., Schon, E., Schönenberger, M., Schönthal, A., Schorderet, D., Schröder, B., Schuck, S., Schulze, R., Schwarten, M., Schwarz, T., Sciarretta, S., Scotto, K., Scovassi, A., Screaton, R., Screen, M., Seca, H., Sedej, S., Segatori, L., Segev, N., Seglen, P., Seguí-Simarro, J., Segura-Aguilar, J., Seki, E., Seiliez, I., Sell, C., Semenkovich, C., Semenza, G., Sen, U., Serra, A., Serrano-Puebla, A., Sesaki, H., Setoguchi, T., Settembre, C., Shacka, J., Shajahan-Haq, A., Shapiro, I., Sharma, S., She, H., Shen, C., Shen, C., Shen, H., Shen, S., Shen, W., Sheng, R., Sheng, X., Sheng, Z., Shepherd, T., Shi, J., Shi, Q., Shi, Q., Shi, Y., Shibutani, S., Shibuya, K., Shidoji, Y., Shieh, J., Shih, C., Shimada, Y., Shimizu, S., Shin, D., Shinohara, M., Shintani, M., Shintani, T., Shioi, T., Shirabe, K., Shiri-Sverdlov, R., Shirihai, O., Shore, G., Shu, C., Shukla, D., Sibirny, A., Sica, V., Sigurdson, C., Sigurdsson, E., Sijwali, P., Sikorska, B., Silveira, W., Silvente-Poirot, S., Silverman, G., Simak, J., Simmet, T., Simon, A., Simon, H., Simone, C., Simons, M., Simonsen, A., Singh, R., Singh, S., Singh, S., Sinha, D., Sinha, S., Sinicrope, F., Sirko, A., Sirohi, K., Sishi, B., Sittler, A., Siu, P., Sivridis, E., Skwarska, A., Slack, R.,

Slaninová, I., Slavov, N., Smaili, S., Smalley, K., Smith, D., Soenen, S., Soleimanpour, S., Solhaug, A., Somasundaram, K., Son, J., Sonawane, A., Song, C., Song, F., Song, H., Song, J., Song, W., Soo, K., Sood, A., Soong, T., Soontornniyomkij, V., Sorice, M., Sotgia, F., Soto-Pantoja, D., Sotthibundhu, A., Sousa, M., Spaink, H., Span, P., Spang, A., Sparks, J., Speck, P., Spector, S., Spies, C., Springer, W., Clair, D., Stacchiotti, A., Staels, B., Stang, M., Starczynowski, D., Starokadomskyy, P., Steegborn, C., Steele, J., Stefanis, L., Steffan, J., Stellrecht, C., Stenmark, H., Stepkowski, T., Stern, S., Stevens, C., Stockwell, B., Stoka, V., Storchova, Z., Stork, B., Stratoulias, V., Stravopodis, D., Strnad, P., Strohecker, A., Ström, A., Stromhaug, P., Stulik, J., Su, Y., Su, Z., Subauste, C., Subramaniam, S., Sue, C., Suh, S., Sui, X., Sukseree, S., Sulzer, D., Sun, F., Sun, J., Sun, J., Sun, S., Sun, Y., Sun, Y., Sun, Y., Sundaramoorthy, V., Sung, J., Suzuki, H., Suzuki, K., Suzuki, N., Suzuki, T., Suzuki, Y., Swanson, M., Swanton, C., Swärd, K., Swarup, G., Sweeney, S., Sylvester, P., Szatmari, Z., Szegezdi, E., Szlosarek, P., Taegtmeyer, H., Tafani, M., Taillebourg, E., Tait, S., Takacs-Vellai, K., Takahashi, Y., Takáts, S., Takemura, G., Takigawa, N., Talbot, N., Tamagno, E., Tamburini, J., Tan, C., Tan, L., Tan, M., Tan, M., Tan, Y., Tanaka, K., Tanaka, M., Tang, D., Tang, D., Tang, G., Tanida, I., Tanji, K., Tannous, B., Tapia, J., Tasset-Cuevas, I., Tatar, M., Tavassoly, I., Tavernarakis, N., Taylor, A., Taylor, G., Taylor, G., Taylor, J., Taylor, M., Tchetina, E., Tee, A., Teixeira-Clerc, F., Telang, S., Tencomnao, T., Teng, B., Teng, R., Terro, F., Tettamanti, G., Theiss, A., Theron, A., Thomas, K., Thomé, M., Thomes, P., Thorburn, A., Thorner, J., Thum, T., Thumm, M., Thurston, T., Tian, L., Till, A., Ting, J., Titorenko, V., Toker, L., Toldo, S., Tooze, S., Topisirovic, I., Torgersen, M., Torosantucci, L., Torriglia, A., Torrisi, M., Tournier, C., Towns, R., Trajkovic, V., Travassos, L., Triola, G., Tripathi, D., Trisciuoglio, D., Troncoso, R., Trougakos, I., Truttmann, A., Tsai, K., Tschan, M., Tseng, Y., Tsukuba, T., Tsung, A., Tsvetkov, A., Tu, S., Tuan, H., Tucci, M., Tumbarello, D., Turk, B., Turk, V., Turner, R., Tveita, A., Tyagi, S., Ubukata, M., Uchiyama, Y., Udelnow, A., Ueno, T., Umekawa, M., Umemiya-Shirafuji, R., Underwood, B., Ungermann, C., Ureshino, R., Ushioda, R., Uversky, V., Uzcátegui, N., Vaccari, T., Vaccaro, M., Váchová, L., Vakifahmetoglu-Norberg, H., Valdor, R., Valente, E., Vallette, F., Valverde, A., Van den Berghe, G., Van Den Bosch, L., van den Brink, G., van der Goot, F., van der Klei, I., van der Laan, L., van Doorn, W., van Egmond, M., van Golen, K., Van Kaer, L., van Lookeren Campagne, M., Vandenabeele, P., Vandenberghe, W., Vanhorebeek, I., Varela-Nieto, I.,

Vasconcelos, M., Vasko, R., Vavvas, D., Vega-Naredo, I., Velasco, G., Velentzas, A., Velentzas, P., Vellai, T., Vellenga, E., Vendelbo, M., Venkatachalam, K., Ventura, N., Ventura, S., Veras, P., Verdier, M., Vertessy, B., Viale, A., Vidal, M., Vieira, H., Vierstra, R., Vigneswaran, N., Vij, N., Vila, M., Villar, M., Villar, V., Villarroya, J., Vindis, C., Viola, G., Viscomi, M., Vitale, G., Vogl, D., Voitsekhovskaja, O., von Haefen, C., von Schwarzenberg, K., Voth, D., Vouret-Craviari, V., Vuori, K., Vyas, J., Waeber, C., Walker, C., Walker, M., Walter, J., Wan, L., Wan, X., Wang, B., Wang, C., Wang, C., Wang, C., Wang, C., Wang, C., Wang, D., Wang, F., Wang, F., Wang, G., Wang, H., Wang, H., Wang, H., Wang, H., Wang, H., Wang, J., Wang, J., Wang, M., Wang, M., Wang, P., Wang, P., Wang, R., Wang, S., Wang, T., Wang, X., Wang, X., Wang, X., Wang, X., Wang, X., Wang, Y., Wang, Y., Wang, Y., Wang, Y., Wang, Y., Wang, Y., Wang, Y., Wang, Y., Wang, Z., Wappner, P., Ward, C., Ward, D., Warnes, G., Watada, H., Watanabe, Y., Watase, K., Weaver, T., Weekes, C., Wei, J., Weide, T., Weihl, C., Weindl, G., Weis, S., Wen, L., Wen, X., Wen, Y., Westermann, B., Weyand, C., White, A., White, E., Whitton, J., Whitworth, A., Wiels, J., Wild, F., Wildenberg, M., Wileman, T., Wilkinson, D., Wilkinson, S., Willbold, D., Williams, C., Williams, K., Williamson, P., Winklhofer, K., Witkin, S., Wohlgemuth, S., Wollert, T., Wolvetang, E., Wong, E., Wong, G., Wong, R., Wong, V., Woodcock, E., Wright, K., Wu, C., Wu, D., Wu, G., Wu, J., Wu, J., Wu, M., Wu, M., Wu, S., Wu, W., Wu, Y., Wu, Z., Xavier, C., Xavier, R., Xia, G., Xia, T., Xia, W., Xia, Y., Xiao, H., Xiao, J., Xiao, S., Xiao, W., Xie, C., Xie, Z., Xie, Z., Xilouri, M., Xiong, Y., Xu, C., Xu, C., Xu, F., Xu, H., Xu, H., Xu, J., Xu, J., Xu, J., Xu, L., Xu, X., Xu, Y., Xu, Y., Xu, Z., Xu, Z., Xue, Y., Yamada, T., Yamamoto, A., Yamanaka, K., Yamashina, S., Yamashiro, S., Yan, B., Yan, B., Yan, X., Yan, Z., Yanagi, Y., Yang, D., Yang, J., Yang, L., Yang, M., Yang, P., Yang, P., Yang, Q., Yang, W., Yang, W., Yang, X., Yang, Y., Yang, Y., Yang, Z., Yang, Z., Yao, M., Yao, P., Yao, X., Yao, Z., Yao, Z., Yasui, L., Ye, M., Yedvobnick, B., Yeganeh, B., Yeh, E., Yeyati, P., Yi, F., Yi, L., Yin, X., Yip, C., Yoo, Y., Yoo, Y., Yoon, S., Yoshida, K., Yoshimori, T., Young, K., Yu, H., Yu, J., Yu, J., Yu, J., Yu, L., Yu, W., Yu, X., Yu, Z., Yuan, J., Yuan, Z., Yue, B., Yue, J., Yue, Z., Zacks, D., Zacksenhaus, E., Zaffaroni, N., Zaglia, T., Zakeri, Z., Zecchini, V., Zeng, J., Zeng, M., Zeng, Q., Zervos, A., Zhang, D., Zhang, F., Zhang, G., Zhang, G., Zhang, H., Zhang, H., Zhang, H., Zhang, H., Zhang, J., Zhang, J., Zhang, J., Zhang, J., Zhang, J., Zhang, L., Zhang, L., Zhang, L., Zhang, L., Zhang, M., Zhang, X., Zhang, X., Zhang, Y., Zhang, Y., Zhang, Y., Zhang, Y., Zhang, Y., Zhao, M., Zhao, W., Zhao, X., Zhao, Y., Zhao, Y., Zhao, Y., Zhao, Y., Zhao, Z.,

Zhao, Z., Zheng, D., Zheng, X., Zheng, X., Zhivotovsky, B., Zhong, Q., Zhou, G., Zhou, G., Zhou, H., Zhou, S., Zhou, X., Zhu, H., Zhu, H., Zhu, W., Zhu, W., Zhu, X., Zhu, Y., Zhuang, S., Zhuang, X., Ziparo, E., Zois, C., Zoladek, T., Zong, W., Zorzano, A. and Zughaier, S., 2016. Guidelines for the use and interpretation of assays for monitoring autophagy (3rd edition). *Autophagy*, 12(1), pp.1-222.

Klionsky, D., Cregg, J., Dunn, W., Emr, S., Sakai, Y., Sandoval, I., Sibirny, A., Subramani, S., Thumm, M., Veenhuis, M. and Ohsumi, Y., 2003. A Unified Nomenclature for Yeast Autophagy-Related Genes. *Developmental Cell*, 5(4), pp.539-545.

Kneynsberg, A., Collier, T., Manfredsson, F. and Kanaan, N., 2016. Quantitative and semi-quantitative measurements of axonal degeneration in tissue and primary neuron cultures. *Journal of Neuroscience Methods*, 266, pp.32-41.

Koike, M., Shibata, M., Waguri, S., Yoshimura, K., Tanida, I., Kominami, E., Gotow, T., Peters, C., von Figura, K., Mizushima, N., Saftig, P. and Uchiyama, Y., 2005. Participation of Autophagy in Storage of Lysosomes in Neurons from Mouse Models of Neuronal Ceroid-Lipofuscinoses (Batten Disease). *The American Journal of Pathology*, 167(6), pp.1713-1728.

Komatsu, M., Kurokawa, H., Waguri, S., Taguchi, K., Kobayashi, A., Ichimura, Y., Sou, Y., Ueno, I., Sakamoto, A., Tong, K., Kim, M., Nishito, Y., Iemura, S., Natsume, T., Ueno, T., Kominami, E., Motohashi, H., Tanaka, K. and Yamamoto, M., 2010. The selective autophagy substrate p62 activates the stress responsive transcription factor Nrf2 through inactivation of Keap1. *Nature Cell Biology*, 12(3), pp.213-223.

Komatsu, M., Waguri, S., Chiba, T., Murata, S., Iwata, J., Tanida, I., Ueno, T., Koike, M., Uchiyama, Y., Kominami, E. and Tanaka, K., 2006. Loss of autophagy in the central nervous system causes neurodegeneration in mice. *Nature*, 441(7095), pp.880-884.

Komatsu, M., Waguri, S., Koike, M., Sou, Y., Ueno, T., Hara, T., Mizushima, N., Iwata, J., Ezaki, J., Murata, S., Hamazaki, J., Nishito, Y., Iemura, S., Natsume, T., Yanagawa, T., Uwayama, J., Warabi, E., Yoshida, H., Ishii, T., Kobayashi, A., Yamamoto, M., Yue, Z., Uchiyama, Y., Kominami, E. and Tanaka, K., 2007. Homeostatic Levels of p62

Control Cytoplasmic Inclusion Body Formation in Autophagy-Deficient Mice. *Cell*, 131(6), pp.1149-1163.

Komatsu, M., Waguri, S., Ueno, T., Iwata, J., Murata, S., Tanida, I., Ezaki, J., Mizushima, N., Ohsumi, Y., Uchiyama, Y., Kominami, E., Tanaka, K. and Chiba, T., 2005. Impairment of starvation-induced and constitutive autophagy in Atg7-deficient mice. *Journal of Cell Biology*, 169(3), pp.425-434.

Korac, J., Schaeffer, V., Kovacevic, I., Clement, A., Jungblut, B., Behl, C., Terzic, J. and Dikic, I., 2012. Ubiquitin-independent function of optineurin in autophagic clearance of protein aggregates. *Journal of Cell Science*, 126(2), pp.580-592.

Kordower, J., Olanow, C., Dodiya, H., Chu, Y., Beach, T., Adler, C., Halliday, G. and Bartus, R., 2013. Disease duration and the integrity of the nigrostriatal system in Parkinson's disease. *Brain*, 136(8), pp.2419-2431.

Kowalski, P., Rudra, A., Miao, L. and Anderson, D., 2019. Delivering the Messenger: Advances in Technologies for Therapeutic mRNA Delivery. *Molecular Therapy*, 27(4), pp.710-728.

Kozhich, O., Hamilton, R.S., and Mallon, B.S., 2013. Standardized Generation and Differentiation of Neural Precursor Cells from Human Pluripotent Stem Cells. *Stem Cell Reviews and Reports*, 9(4), pp. 531-536.

Kozma, S., Ferrari, S., Bassand, P., Siegmann, M., Totty, N. and Thomas, G., 1990. Cloning of the mitogen-activated S6 kinase from rat liver reveals an enzyme of the second messenger subfamily. *Proceedings of the National Academy of Sciences*, 87(19), pp.7365-7369.

Krainc, D., 2010. Clearance of Mutant Proteins as a Therapeutic Target in Neurodegenerative Diseases. *Archives of Neurology*, 67(4).

Krencik, R., Seo, K., van Asperen, J., Basu, N., Cvetkovic, C., Barlas, S., Chen, R., Ludwig, C., Wang, C., Ward, M., Gan, L., Horner, P., Rowitch, D. and Ullian, E., 2017. Systematic Three-Dimensional Coculture Rapidly Recapitulates Interactions between Human Neurons and Astrocytes. *Stem Cell Reports*, 9(6), pp.1745-1753.

Kroon, E., Martinson, L., Kadoya, K., Bang, A., Kelly, O., Eliazer, S., Young, H., Richardson, M., Smart, N., Cunningham, J., Agulnick, A., D'Amour, K., Carpenter, M. and Baetge, E., 2008. Pancreatic endoderm derived from human embryonic stem cells generates glucose-responsive insulin-secreting cells in vivo. *Nature Biotechnology*, 26(4), pp.443-452.

Kuma, A., Hatano, M., Matsui, M., Yamamoto, A., Nakaya, H., Yoshimori, T., Ohsumi, Y., Tokuhisa, T. and Mizushima, N., 2004. The role of autophagy during the early neonatal starvation period. *Nature*, 432(7020), pp.1032-1036.

Kuma, A., Komatsu, M. and Mizushima, N., 2017. Autophagy-monitoring and autophagy-deficient mice. *Autophagy*, 13(10), pp.1619-1628.

Kumar, D., Nath, L., Kamal, M., Varshney, A., Jain, A., Singh, S. and Rao, K., 2010. Genome-wide Analysis of the Host Intracellular Network that Regulates Survival of Mycobacterium tuberculosis. *Cell*, 140(5), pp.731-743.

Kuo, S., Castoreno, A., Aldrich, L., Lassen, K., Goel, G., Dančík, V., Kuballa, P., Latorre, I., Conway, K., Sarkar, S., Maetzel, D., Jaenisch, R., Clemons, P., Schreiber, S., Shamji, A. and Xavier, R., 2015. Small-molecule enhancers of autophagy modulate cellular disease phenotypes suggested by human genetics. *Proceedings of the National Academy of Sciences*, 112(31), pp.E4281-E4287.

Kwon, H., Abi-Mosleh, L., Wang, M., Deisenhofer, J., Goldstein, J., Brown, M. and Infante, R., 2009. Structure of N-Terminal Domain of NPC1 Reveals Distinct Subdomains for Binding and Transfer of Cholesterol. *Cell*, 137(7), pp.1213-1224.

Kyei, G., Dinkins, C., Davis, A., Roberts, E., Singh, S., Dong, C., Wu, L., Kominami, E., Ueno, T., Yamamoto, A., Federico, M., Panganiban, A., Vergne, I. and Deretic, V., 2009. Autophagy pathway intersects with HIV-1 biosynthesis and regulates viral yields in macrophages. *Journal of Cell Biology*, 186(2), pp.255-268.

Lachmann, N., Ackermann, M., Frenzel, E., Liebhaber, S., Brennig, S., Happle, C., Hoffmann, D., Klimenkova, O., Lüttge, D., Buchegger, T., Kühnel, M., Schambach, A., Janciauskiene, S., Figueiredo, C., Hansen, G., Skokowa, J. and Moritz, T., 2015. Large-Scale Hematopoietic Differentiation of Human Induced Pluripotent Stem Cells

Provides Granulocytes or Macrophages for Cell Replacement Therapies. *Stem Cell Reports*, 4(2), pp.282-296.

Lahiri, V., Hawkins, W. and Klionsky, D., 2019. Watch What You (Self-) Eat: Autophagic Mechanisms that Modulate Metabolism. *Cell Metabolism*, 29(4), pp.803-826.

Lam, K., Zheng, X., Forestieri, R., Balgi, A., Nodwell, M., Vollett, S., Anderson, H., Andersen, R., Av-Gay, Y. and Roberge, M., 2012. Nitazoxanide Stimulates Autophagy and Inhibits mTORC1 Signaling and Intracellular Proliferation of Mycobacterium tuberculosis. *PLoS Pathogens*, 8(5), p.e1002691.

Lang, J., Cheng, Y., Rolfe, A., Hammack, C., Vera, D., Kyle, K., Wang, J., Meissner, T., Ren, Y., Cowan, C. and Tang, H., 2018. An hPSC-Derived Tissue-Resident Macrophage Model Reveals Differential Responses of Macrophages to ZIKV and DENV Infection. *Stem Cell Reports*, 11(2), pp.348-362.

Larsen, K., Lamark, T., Øvervatn, A., Harneshaug, I., Johansen, T. and Bjørkøy, G., 2010. A reporter cell system to monitor autophagy based on p62/SQSTM1. *Autophagy*, 6(6), pp.784-793.

Lautrup, S., Sinclair, D., Mattson, M. and Fang, E., 2019. NAD+ in Brain Aging and Neurodegenerative Disorders. *Cell Metabolism*, 30(4), pp.630-655.

Lee, G., Ramirez, C., Kim, H., Zeltner, N., Liu, B., Radu, C., Bhinder, B., Kim, Y., Choi, I., Mukherjee-Clavin, B., Djaballah, H. and Studer, L., 2012. Large-scale screening using familial dysautonomia induced pluripotent stem cells identifies compounds that rescue IKBKAP expression. *Nature Biotechnology*, 30(12), pp.1244-1248.

Lee, H., Lee, J., Park, M., Hong, Y., Marti, H., Kim, H., Okada, Y., Otsu, M., Seo, E., Park, J., Bae, J., Okino, N., He, X., Schuchman, E., Bae, J. and Jin, H., 2014. Pathological roles of the VEGF/SphK pathway in Niemann–Pick type C neurons. *Nature Communications*, 5(1).

Lee, H., Velazquez Sanchez, C., Chen, M., Morin, P., Wells, J., Hanlon, E. and Xia, W., 2016. Three Dimensional Human Neuro-Spheroid Model of Alzheimer's Disease

Based on Differentiated Induced Pluripotent Stem Cells. *PLOS ONE*, 11(9), p.e0163072.

Lemasters, J., 2014. Variants of mitochondrial autophagy: Types 1 and 2 mitophagy and micromitophagy (Type 3). *Redox Biology*, 2, pp.749-754.

Lendahl, U., Zimmerman, L. and McKay, R., 1990. CNS stem cells express a new class of intermediate filament protein. *Cell*, 60(4), pp.585-595.

Lengner, C., Gimelbrant, A., Erwin, J., Cheng, A., Guenther, M., Welstead, G., Alagappan, R., Frampton, G., Xu, P., Muffat, J., Santagata, S., Powers, D., Barrett, C., Young, R., Lee, J., Jaenisch, R. and Mitalipova, M., 2010. Derivation of Pre-X Inactivation Human Embryonic Stem Cells under Physiological Oxygen Concentrations. *Cell*, 141(5), pp.872-883.

Leslie, J., Huang, S., Opp, J., Nagy, M., Kobayashi, M., Young, V. and Spence, J., 2014. Persistence and Toxin Production by Clostridium difficile within Human Intestinal Organoids Result in Disruption of Epithelial Paracellular Barrier Function. *Infection and Immunity*, 83(1), pp.138-145.

Levine, B. and Deretic, V., 2007. Unveiling the roles of autophagy in innate and adaptive immunity. *Nature Reviews Immunology*, 7(10), pp.767-777.

Levine, B. and Kroemer, G., 2008. Autophagy in the Pathogenesis of Disease. *Cell*, 132(1), pp.27-42.

Levine, B., Packer, M. and Codogno, P., 2015. Development of autophagy inducers in clinical medicine. *Journal of Clinical Investigation*, 125(1), pp.14-24.

Li, H., Yang, Y., Hong, W., Huang, M., Wu, M. and Zhao, X., 2020. Applications of genome editing technology in the targeted therapy of human diseases: mechanisms, advances and prospects. *Signal Transduction and Targeted Therapy*, 5(1).

Li, L., Zhang, S., Zhang, X., Li, T., Tang, Y., Liu, H., Yang, W. and Le, W., 2013. Autophagy Enhancer Carbamazepine Alleviates Memory Deficits and Cerebral Amyloid-β Pathology in a Mouse Model of Alzheimer's Disease. *Current Alzheimer Research*, 10(4), pp.433-441.

Liang, C., Lee, J., Inn, K., Gack, M., Li, Q., Roberts, E., Vergne, I., Deretic, V., Feng, P., Akazawa, C. and Jung, J., 2008. Beclin1-binding UVRAG targets the class C Vps complex to coordinate autophagosome maturation and endocytic trafficking. *Nature Cell Biology*, 10(7), pp.776-787.

Liu, L., Feng, D., Chen, G., Chen, M., Zheng, Q., Song, P., Ma, Q., Zhu, C., Wang, R., Qi, W., Huang, L., Xue, P., Li, B., Wang, X., Jin, H., Wang, J., Yang, F., Liu, P., Zhu, Y., Sui, S. and Chen, Q., 2012. Mitochondrial outer-membrane protein FUNDC1 mediates hypoxia-induced mitophagy in mammalian cells. *Nature Cell Biology*, 14(2), pp.177-185.

Liu, P., Hu, Y., Kang, B., Tseng, Y., Wu, P., Liang, C., Hou, Y., Fu, T., Liou, H., Hsieh, I., Ger, L. and Shu, C., 2017. Expression levels of cleaved caspase-3 and caspase-3 in tumorigenesis and prognosis of oral tongue squamous cell carcinoma. *PLOS ONE*, 12(7), p.e0180620.

Liu, X., Nefzger, C., Rossello, F., Chen, J., Knaupp, A., Firas, J., Ford, E., Pflueger, J., Paynter, J., Chy, H., O'Brien, C., Huang, C., Mishra, K., Hodgson-Garms, M., Jansz, N., Williams, S., Blewitt, M., Nilsson, S., Schittenhelm, R., Laslett, A., Lister, R. and Polo, J., 2017. Comprehensive characterisation of distinct states of human naive pluripotency generated by reprogramming. *Nature Methods*, 14(11), pp.1055-1062.

Lloyd-Evans, E., Morgan, A., He, X., Smith, D., Elliot-Smith, E., Sillence, D., Churchill, G., Schuchman, E., Galione, A. and Platt, F., 2008. Niemann-Pick disease type C1 is a sphingosine storage disease that causes deregulation of lysosomal calcium. *Nature Medicine*, 14(11), pp.1247-1255.

Loftus, S.K., Morris, J.A., Carstea, E.D., Gu, J.Z., Brown, A., Ellison, J., Ohno, K., Rosenfeld, M.A., Tagle, D.A., Pentchev and P.G., Pavan, W.J. 1997. Murine Model of Niemann-Pick C Disease: Mutation in a Cholesterol Homeostasis Gene. *Science* 277 (5323), 232–235.

Longchamps, R., Castellani, C., Yang, S., Newcomb, C., Sumpter, J., Lane, J., Grove, M., Guallar, E., Pankratz, N., Taylor, K., Rotter, J., Boerwinkle, E. and Arking, D., 2020. Evaluation of mitochondrial DNA copy number estimation techniques. *PLOS ONE*, 15(1), p.e0228166.

Love, K., Mahon, K., Levins, C., Whitehead, K., Querbes, W., Dorkin, J., Qin, J., Cantley, W., Qin, L., Racie, T., Frank-Kamenetsky, M., Yip, K., Alvarez, R., Sah, D., de Fougerolles, A., Fitzgerald, K., Koteliansky, V., Akinc, A., Langer, R. and Anderson, D., 2010. Lipid-like materials for low-dose, in vivo gene silencing. *Proceedings of the National Academy of Sciences*, 107(5), pp.1864-1869.

Lu, K., Psakhye, I. and Jentsch, S., 2014. A new class of ubiquitin-Atg8 receptors involved in selective autophagy and polyQ protein clearance. *Autophagy*, 10(12), pp.2381-2382.

Lum, J., Bauer, D., Kong, M., Harris, M., Li, C., Lindsten, T. and Thompson, C., 2005. Growth Factor Regulation of Autophagy and Cell Survival in the Absence of Apoptosis. *Cell*, 120(2), pp.237-248.

Luna, A., Aladjem, M. and Kohn, K., 2013. SIRT1/PARP1 crosstalk: connecting DNA damage and metabolism. *Genome Integrity*, 4(1), p.6.

Maddocks, O., Labuschagne, C., Adams, P. and Vousden, K., 2016. Serine Metabolism Supports the Methionine Cycle and DNA/RNA Methylation through De Novo ATP Synthesis in Cancer Cells. *Molecular Cell*, 61(2), pp.210-221.

Madeo, F., Eisenberg, T., Büttner, S., Ruckenstuhl, C. and Kroemer, G., 2010. Spermidine: A novel autophagy inducer and longevity elixir. *Autophagy*, 6(1), pp.160-162.

Mádrová, L., Krijt, M., Barešová, V., Václavík, J., Friedecký, D., Dobešová, D., Součková, O., Škopová, V., Adam, T. and Zikánová, M., 2018. Mass spectrometric analysis of purine de novo biosynthesis intermediates. *PLOS ONE*, 13(12), p.e0208947.

Maetzel, D., Sarkar, S., Wang, H., Abi-Mosleh, L., Xu, P., Cheng, A., Gao, Q., Mitalipova, M. and Jaenisch, R., 2014. Genetic and Chemical Correction of Cholesterol Accumulation and Impaired Autophagy in Hepatic and Neural Cells Derived from Niemann-Pick Type C Patient-Specific iPS Cells. *Stem Cell Reports*, 2(6), pp.866-880.

Mailloux, R., 2015. Teaching the fundamentals of electron transfer reactions in mitochondria and the production and detection of reactive oxygen species. *Redox Biology*, 4, pp.381-398.

Malhotra, R., Warne, J., Salas, E., Xu, A. and Debnath, J., 2015. Loss of Atg12, but not Atg5, in pro-opiomelanocortin neurons exacerbates diet-induced obesity. *Autophagy*, 11(1), pp.145–154.

Malik, S., Orhon, I., Morselli, E., Criollo, A., Shen, S., Mariño, G., BenYounes, A., Bénit, P., Rustin, P., Maiuri, M. and Kroemer, G., 2011. BH3 mimetics activate multiple pro-autophagic pathways. *Oncogene*, 30(37), pp.3918-3929.

Mandell, M., Jain, A., Arko-Mensah, J., Chauhan, S., Kimura, T., Dinkins, C., Silvestri, G., Münch, J., Kirchhoff, F., Simonsen, A., Wei, Y., Levine, B., Johansen, T. and Deretic, V., 2014. TRIM Proteins Regulate Autophagy and Can Target Autophagic Substrates by Direct Recognition. *Developmental Cell*, 30(4), pp.394-409.

Maria Fimia, G., Stoykova, A., Romagnoli, A., Giunta, L., Di Bartolomeo, S., Nardacci, R., Corazzari, M., Fuoco, C., Ucar, A., Schwartz, P., Gruss, P., Piacentini, M., Chowdhury, K. and Cecconi, F., 2007. Ambra1 regulates autophagy and development of the nervous system. *Nature*, 447(7148), pp.1121-1125.

Mariño, G., Madeo, F. and Kroemer, G., 2011. Autophagy for tissue homeostasis and neuroprotection. *Current Opinion in Cell Biology*, 23(2), pp.198-206.

Mariño, G., Salvador-Montoliu, N., Fueyo, A., Knecht, E., Mizushima, N. and López-Otín, C., 2007. Tissue-specific Autophagy Alterations and Increased Tumorigenesis in Mice Deficient in Atg4C/Autophagin-3. *Journal of Biological Chemistry*, 282(25), pp.18573-18583.

Martire, S., Fuso, A., Rotili, D., Tempera, I., Giordano, C., De Zottis, I., Muzi, A., Vernole, P., Graziani, G., Lococo, E., Faraldi, M., Maras, B., Scarpa, S., Mosca, L. and d'Erme, M., 2013. PARP-1 Modulates Amyloid Beta Peptide-Induced Neuronal Damage. *PLoS ONE*, 8(9), p.e72169.

Masiero, E., Agatea, L., Mammucari, C., Blaauw, B., Loro, E., Komatsu, M., Metzger, D., Reggiani, C., Schiaffino, S. and Sandri, M., 2009. Autophagy Is Required to Maintain Muscle Mass. *Cell Metabolism*, 10(6), pp.507-515.

Matés, J. and Sánchez-Jiménez, F., 2000. Role of reactive oxygen species in apoptosis: implications for cancer therapy. *The International Journal of Biochemistry & Cell Biology*, 32(2), pp.157-170.

Matsunaga, K., Saitoh, T., Tabata, K., Omori, H., Satoh, T., Kurotori, N., Maejima, I., Shirahama-Noda, K., Ichimura, T., Isobe, T., Akira, S., Noda, T. and Yoshimori, T., 2009. Two Beclin 1-binding proteins, Atg14L and Rubicon, reciprocally regulate autophagy at different stages. *Nature Cell Biology*, 11(4), pp.385-396.

McCauley, K., Hawkins, F., Serra, M., Thomas, D., Jacob, A. and Kotton, D., 2017. Efficient Derivation of Functional Human Airway Epithelium from Pluripotent Stem Cells via Temporal Regulation of Wnt Signaling. *Cell Stem Cell*, 20(6), pp.844-857.e6.

McCracken, K., Catá, E., Crawford, C., Sinagoga, K., Schumacher, M., Rockich, B., Tsai, Y., Mayhew, C., Spence, J., Zavros, Y. and Wells, J., 2014. Modelling human development and disease in pluripotent stem-cell-derived gastric organoids. *Nature*, 516(7531), pp.400-404.

McCracken, K., Howell, J., Wells, J. and Spence, J., 2011. Generating human intestinal tissue from pluripotent stem cells in vitro. *Nature Protocols*, 6(12), pp.1920-1928.

McEwan, D., Popovic, D., Gubas, A., Terawaki, S., Suzuki, H., Stadel, D., Coxon, F., Miranda de Stegmann, D., Bhogaraju, S., Maddi, K., Kirchof, A., Gatti, E., Helfrich, M., Wakatsuki, S., Behrends, C., Pierre, P. and Dikic, I., 2015. PLEKHM1 Regulates Autophagosome-Lysosome Fusion through HOPS Complex and LC3/GABARAP Proteins. *Molecular Cell*, 57(1), pp.39-54.

McWilliams, T., Prescott, A., Montava-Garriga, L., Ball, G., Singh, F., Barini, E., Muqit, M., Brooks, S. and Ganley, I., 2018. Basal Mitophagy Occurs Independently of PINK1 in Mouse Tissues of High Metabolic Demand. *Cell Metabolism*, 27(2), pp.439-449.e5.

Medina, D., Di Paola, S., Peluso, I., Armani, A., De Stefani, D., Venditti, R., Montefusco, S., Scotto-Rosato, A., Prezioso, C., Forrester, A., Settembre, C., Wang, W., Gao, Q., Xu, H., Sandri, M., Rizzuto, R., De Matteis, M. and Ballabio, A., 2015. Lysosomal calcium signalling regulates autophagy through calcineurin and TFEB. *Nature Cell Biology*, 17(3), pp.288-299.

Meijer, A., Lorin, S., Blommaart, E. and Codogno, P., 2014. Regulation of autophagy by amino acids and MTOR-dependent signal transduction. *Amino Acids*, 47(10), pp.2037-2063.

Meley, D., Bauvy, C., Houben-Weerts, J., Dubbelhuis, P., Helmond, M., Codogno, P. and Meijer, A., 2006. AMP-activated Protein Kinase and the Regulation of Autophagic Proteolysis. *Journal of Biological Chemistry*, 281(46), pp.34870-34879.

Menezes, J. and Luskin, M., 1994. Expression of neuron-specific tubulin defines a novel population in the proliferative layers of the developing telencephalon. *The Journal of Neuroscience*, 14(9), pp.5399-5416.

Menzies, F., Fleming, A., Caricasole, A., Bento, C., Andrews, S., Ashkenazi, A., Füllgrabe, J., Jackson, A., Jimenez Sanchez, M., Karabiyik, C., Licitra, F., Lopez Ramirez, A., Pavel, M., Puri, C., Renna, M., Ricketts, T., Schlotawa, L., Vicinanza, M., Won, H., Zhu, Y., Skidmore, J. and Rubinsztein, D., 2017. Autophagy and Neurodegeneration: Pathogenic Mechanisms and Therapeutic Opportunities. *Neuron*, 93(5), pp.1015-1034.

Menzies, F., Huebener, J., Renna, M., Bonin, M., Riess, O. and Rubinsztein, D., 2009. Autophagy induction reduces mutant ataxin-3 levels and toxicity in a mouse model of spinocerebellar ataxia type 3. *Brain*, 133(1), pp.93-104.

Mercer, T., Gubas, A. and Tooze, S., 2018. A molecular perspective of mammalian autophagosome biogenesis. *Journal of Biological Chemistry*, 293(15), pp.5386-5395.

Mertens, J., Paquola, A., Ku, M., Hatch, E., Böhnke, L., Ladjevardi, S., McGrath, S., Campbell, B., Lee, H., Herdy, J., Gonçalves, J., Toda, T., Kim, Y., Winkler, J., Yao, J., Hetzer, M. and Gage, F., 2015. Directly Reprogrammed Human Neurons Retain

Aging-Associated Transcriptomic Signatures and Reveal Age-Related Nucleocytoplasmic Defects. *Cell Stem Cell*, 17(6), pp.705-718.

Mertens, J., Reid, D., Lau, S., Kim, Y. and Gage, F., 2018. Aging in a Dish: iPSC-Derived and Directly Induced Neurons for Studying Brain Aging and Age-Related Neurodegenerative Diseases. *Annual Review of Genetics*, 52(1), pp.271-293.

Miller, J., Ganat, Y., Kishinevsky, S., Bowman, R., Liu, B., Tu, E., Mandal, P., Vera, E., Shim, J., Kriks, S., Taldone, T., Fusaki, N., Tomishima, M., Krainc, D., Milner, T., Rossi, D. and Studer, L., 2013. Human iPSC-Based Modeling of Late-Onset Disease via Progerin-Induced Aging. *Cell Stem Cell*, 13(6), pp.691-705.

Mizushima, N. and Levine, B., 2010. Autophagy in mammalian development and differentiation. *Nature Cell Biology*, 12(9), pp.823-830.

Mizushima, N., 2018. A brief history of autophagy from cell biology to physiology and disease. *Nature Cell Biology*, 20(5), pp.521-527.

Mizushima, N., Levine, B., Cuervo, A. and Klionsky, D., 2008. Autophagy fights disease through cellular self-digestion. *Nature*, 451(7182), pp.1069-1075.

Mizushima, N., Noda, T., Yoshimori, T., Tanaka, Y., Ishii, T., George, M., Klionsky, D., Ohsumi, M. and Ohsumi, Y., 1998. A protein conjugation system essential for autophagy. *Nature*, 395(6700), pp.395-398.

Mizushima, N., Yoshimori, T. and Ohsumi, Y., 2011. The Role of Atg Proteins in Autophagosome Formation. *Annual Review of Cell and Developmental Biology*, 27(1), pp.107-132.

Morselli, E., Maiuri, M., Markaki, M., Megalou, E., Pasparaki, A., Palikaras, K., Criollo, A., Galluzzi, L., Malik, S., Vitale, I., Michaud, M., Madeo, F., Tavernarakis, N. and Kroemer, G., 2010. Caloric restriction and resveratrol promote longevity through the Sirtuin-1-dependent induction of autophagy. *Cell Death & Disease*, 1(1), pp.e10-e10.

Muffat, J., Li, Y., Yuan, B., Mitalipova, M., Omer, A., Corcoran, S., Bakiasi, G., Tsai, L., Aubourg, P., Ransohoff, R. and Jaenisch, R., 2016. Efficient derivation of microglia-like cells from human pluripotent stem cells. *Nature Medicine*, 22(11), pp.1358-1367.

Mummery, C., Ward-van Oostwaard, D., Doevendans, P., Spijker, R., van den Brink, S., Hassink, R., van der Heyden, M., Opthof, T., Pera, M., de la Riviere, A., Passier, R. and Tertoolen, L., 2003. Differentiation of Human Embryonic Stem Cells to Cardiomyocytes. *Circulation*, 107(21), pp.2733-2740.

Murakami, N., Oyama, F., Gu, Y., McLennan, I., Nonaka, I. and Ihara, Y., 1998. Accumulation of Tau in Autophagic Vacuoles in Chloroquine Myopathy. *Journal of Neuropathology and Experimental Neurology*, 57(7), pp.664-673.

Murphy, M.P., 2008. How mitochondria produce reactive oxygen species. *Biochemical Journal*, 417(1), pp.1-13.

Murry, C. and Keller, G., 2008. Differentiation of Embryonic Stem Cells to Clinically Relevant Populations: Lessons from Embryonic Development. *Cell*, 132(4), pp.661-680.

Nakai, A., Yamaguchi, O., Takeda, T., Higuchi, Y., Hikoso, S., Taniike, M., Omiya, S., Mizote, I., Matsumura, Y., Asahi, M., Nishida, K., Hori, M., Mizushima, N. and Otsu, K., 2007. The role of autophagy in cardiomyocytes in the basal state and in response to hemodynamic stress. *Nature Medicine*, 13(5), pp.619-624.

Nakamura, S. and Yoshimori, T., 2017. New insights into autophagosome–lysosome fusion. *Journal of Cell Science*, 130(7), pp.1209-1216.

Naryshkin, N., Weetall, M., Dakka, A., Narasimhan, J., Zhao, X., Feng, Z., Ling, K., Karp, G., Qi, H., Woll, M., Chen, G., Zhang, N., Gabbeta, V., Vazirani, P., Bhattacharyya, A., Furia, B., Risher, N., Sheedy, J., Kong, R., Ma, J., Turpoff, A., Lee, C., Zhang, X., Moon, Y., Trifillis, P., Welch, E., Colacino, J., Babiak, J., Almstead, N., Peltz, S., Eng, L., Chen, K., Mull, J., Lynes, M., Rubin, L., Fontoura, P., Santarelli, L., Haehnke, D., McCarthy, K., Schmucki, R., Ebeling, M., Sivaramakrishnan, M., Ko, C., Paushkin, S., Ratni, H., Gerlach, I., Ghosh, A. and Metzger, F., 2014. SMN2 splicing modifiers improve motor function and longevity in mice with spinal muscular atrophy. *Science*, 345(6197), pp.688-693.

Naureckiene, S., 2000. Identification of HE1 as the Second Gene of Niemann-Pick C Disease. *Science*, 290(5500), pp.2298-2301.

Nazio, F., Strappazzon, F., Antonioli, M., Bielli, P., Cianfanelli, V., Bordi, M., Gretzmeier, C., Dengjel, J., Piacentini, M., Fimia, G. and Cecconi, F., 2013. mTOR inhibits autophagy by controlling ULK1 ubiquitylation, self-association and function through AMBRA1 and TRAF6. *Nature Cell Biology*, 15(4), pp.406-416.

N'Diaye, E., Kajihara, K., Hsieh, I., Morisaki, H., Debnath, J. and Brown, E., 2009. PLIC proteins or ubiquilins regulate autophagy-dependent cell survival during nutrient starvation. *EMBO reports*, 10(2), pp.173-179.

Nestor, M., Phillips, A., Artimovich, E., Nestor, J., Hussman, J. and Blatt, G., 2015. Human Inducible Pluripotent Stem Cells and Autism Spectrum Disorder: Emerging Technologies. *Autism Research*, 9(5), pp.513-535.

Nguyen, T., Padman, B., Usher, J., Oorschot, V., Ramm, G. and Lazarou, M., 2016. Atg8 family LC3/GABARAP proteins are crucial for autophagosome–lysosome fusion but not autophagosome formation during PINK1/Parkin mitophagy and starvation. *Journal of Cell Biology*, 215(6), pp.857-874.

Ni, Z., Knorr, D., Clouser, C., Hexum, M., Southern, P., Mansky, L., Park, I. and Kaufman, D., 2010. Human Pluripotent Stem Cells Produce Natural Killer Cells That Mediate Anti-HIV-1 Activity by Utilising Diverse Cellular Mechanisms. *Journal of Virology*, 85(1), pp.43-50.

Nicholas, C., Chen, J., Tang, Y., Southwell, D., Chalmers, N., Vogt, D., Arnold, C., Chen, Y., Stanley, E., Elefanty, A., Sasai, Y., Alvarez-Buylla, A., Rubenstein, J. and Kriegstein, A., 2013. Functional Maturation of hPSC-Derived Forebrain Interneurons Requires an Extended Timeline and Mimics Human Neural Development. *Cell Stem Cell*, 12(5), pp.573-586.

Niles, A., Moravec, R. and Riss, T., 2009. In Vitro Viability and Cytotoxicity Testing and Same-Well Multi-Parametric Combinations for High Throughput Screening. *Current Chemical Genomics*, 3, pp.33-41.

Nixon, R., 2013. The role of autophagy in neurodegenerative disease. *Nature Medicine*, 19(8), pp.983-997.

Odero, M., Zeleznik-Le, N., Chinwalla, V. and Rowley, J., 2000. Cytogenetic and molecular analysis of the acute monocytic leukemia cell line THP-1 with anMLL-AF9 translocation. *Genes, Chromosomes and Cancer*, 29(4), pp.333-338.

Ohara, R., Imamura, K., Morii, F., Egawa, N., Tsukita, K., Enami, T., Shibukawa, R., Mizuno, T., Nakagawa, M. and Inoue, H., 2017. Modeling Drug-Induced Neuropathy Using Human iPSCs for Predictive Toxicology. *Clinical Pharmacology & Therapeutics*, 101(6), pp.754-762.

O'Hara, R., Tedone, E., Ludlow, A., Huang, E., Arosio, B., Mari, D. and Shay, J., 2019. Quantitative mitochondrial DNA copy number determination using droplet digital PCR with single-cell resolution. *Genome Research*, 29(11), pp.1878-1888.

Ordonez, M., Roberts, E., Kidwell, C., Yuan, S., Plaisted, W. and Goldstein, L., 2012. Disruption and therapeutic rescue of autophagy in a human neuronal model of Niemann Pick type C1. *Human Molecular Genetics*, 21(12), pp.2651-2662.

Ozcelik, S., Fraser, G., Castets, P., Schaeffer, V., Skachokova, Z., Breu, K., Clavaguera, F., Sinnreich, M., Kappos, L., Goedert, M., Tolnay, M. and Winkler, D., 2013. Rapamycin Attenuates the Progression of Tau Pathology in P301S Tau Transgenic Mice. *PLoS ONE*, 8(5), p.e62459.

Pagotto, A., Pilotto, G., Mazzoldi, E., Nicoletto, M., Frezzini, S., Pastò, A. and Amadori, A., 2017. Autophagy inhibition reduces chemoresistance and tumorigenic potential of human ovarian cancer stem cells. *Cell Death & Disease*, 8(7), pp.e2943-e2943.

Palhegyi, A., Seranova, E., Dimova, S., Hoque, S. and Sarkar, S., 2019. Biomedical Implications of Autophagy in Macromolecule Storage Disorders. *Frontiers in Cell and Developmental Biology*, 7.

Pallottini, V., Pfrieger, F.W., 2020. Understanding and Treating Niemann–Pick Type C Disease: Models Matter. *International Journal of Molecular Sciences* 21 (23), 8979.

Palmieri, M., Pal, R., Nelvagal, H., Lotfi, P., Stinnett, G., Seymour, M., Chaudhury, A., Bajaj, L., Bondar, V., Bremner, L., Saleem, U., Tse, D., Sanagasetti, D., Wu, S., Neilson, J., Pereira, F., Pautler, R., Rodney, G., Cooper, J. and Sardiello, M., 2017.

mTORC1-independent TFEB activation via Akt inhibition promotes cellular clearance in neurodegenerative storage diseases. *Nature Communications*, 8(1).

Palomino, J. and Martin, A., 2014. Drug Resistance Mechanisms in Mycobacterium tuberculosis. *Antibiotics*, 3(3), pp.317-340.

Pampaloni, F., Mayer, B., Kabat Vel-Job, K., Ansari, N., Hötte, K., Kögel, D. and Stelzer, E., 2017. A Novel Cellular Spheroid-Based Autophagy Screen Applying Live Fluorescence Microscopy Identifies Nonactin as a Strong Inducer of Autophagosomal Turnover. *SLAS DISCOVERY: Advancing the Science of Drug Discovery*, 22(5), pp.558-570.

Panda, P., Fahrner, A., Vats, S., Seranova, E., Sharma, V., Chipara, M., Desai, P., Torresi, J., Rosenstock, T., Kumar, D. and Sarkar, S., 2019. Chemical Screening Approaches Enabling Drug Discovery of Autophagy Modulators for Biomedical Applications in Human Diseases. *Frontiers in Cell and Developmental Biology*, 7.

Pandya, H., Shen, M., Ichikawa, D., Sedlock, A., Choi, Y., Johnson, K., Kim, G., Brown, M., Elkahloun, A., Maric, D., Sweeney, C., Gossa, S., Malech, H., McGavern, D. and Park, J., 2017. Differentiation of human and murine induced pluripotent stem cells to microglia-like cells. *Nature Neuroscience*, 20(5), pp.753-759.

Pankiv, S., Alemu, E., Brech, A., Bruun, J., Lamark, T., Øvervatn, A., Bjørkøy, G. and Johansen, T., 2010. FYCO1 is a Rab7 effector that binds to LC3 and PI3P to mediate microtubule plus end–directed vesicle transport. *Journal of Cell Biology*, 188(2), pp.253-269.

Pankiv, S., Clausen, T., Lamark, T., Brech, A., Bruun, J., Outzen, H., Øvervatn, A., Bjørkøy, G. and Johansen, T., 2007. p62/SQSTM1 Binds Directly to Atg8/LC3 to Facilitate Degradation of Ubiquitinated Protein Aggregates by Autophagy. *Journal of Biological Chemistry*, 282(33), pp.24131-24145.

Paredes-Sabja, D., Shen, A. and Sorg, J., 2014. Clostridium difficile spore biology: sporulation, germination, and spore structural proteins. *Trends in Microbiology*, 22(7), pp.406-416.

Park, D., Jeong, H., Lee, M., Koh, A., Kwon, O., Yang, Y., Noh, J., Suh, P., Park, H. and Ryu, S., 2016. Resveratrol induces autophagy by directly inhibiting mTOR through ATP competition. *Scientific Reports*, 6(1).

Park, J., Lee, J., and Choi, C., 2011. Mitochondrial Network Determines Intracellular ROS Dynamics and Sensitivity to Oxidative Stress through Switching Inter-Mitochondrial Messengers. *PloS ONE*, 6(8), e23211.

Patterson, M., Hendriksz, C., Walterfang, M., Sedel, F., Vanier, M. and Wijburg, F., 2012. Recommendations for the diagnosis and management of Niemann–Pick disease type C: An update. *Molecular Genetics and Metabolism*, 106(3), pp.330-344.

Peake, K. and Vance, J., 2012. Normalization of Cholesterol Homeostasis by 2-Hydroxypropyl-β-cyclodextrin in Neurons and Glia from Niemann-Pick C1 (NPC1)-deficient Mice. *Journal of Biological Chemistry*, 287(12), pp.9290-9298.

Pera, M., Andrade, J., Houssami, S., Reubinoff, B., Trounson, A., Stanley, E.G., Ward-van Oostwaard, D. and Mummery C., 2004. Regulation of human embryonic stem cell differentiation by BMP-2 and its antagonist noggin. *Journal of Cell Science*, 117(7), pp.1269-1280.

Perlman, R., 2016. Mouse Models of Human Disease: An Evolutionary Perspective. *Evolution, Medicine, and Public Health*, p.eow014.

Perry, A., Rimmer, K., Mertens, H., Waller, R., Mulhern, T., Lithgow, T. and Gooley, P., 2008. Structure, topology and function of the translocase of the outer membrane of mitochondria. *Plant Physiology and Biochemistry*, 46(3), pp.265-274.

Pias, E., Ekshyyan, O., Rhoads, C., Fuseler, J., Harrison, L. and Aw, T., 2003. Differential Effects of Superoxide Dismutase Isoform Expression on Hydroperoxide-induced Apoptosis in PC-12 Cells. *Journal of Biological Chemistry*, 278(15), pp.13294-13301.

Pietrocola, F., Lachkar, S., Enot, D., Niso-Santano, M., Bravo-San Pedro, J., Sica, V., Izzo, V., Maiuri, M., Madeo, F., Mariño, G. and Kroemer, G., 2014. Spermidine induces autophagy by inhibiting the acetyltransferase EP300. *Cell Death & Differentiation*, 22(3), pp.509-516.

Pua, H., Dzhagalov, I., Chuck, M., Mizushima, N. and He, Y., 2006. A critical role for the autophagy gene Atg5 in T cell survival and proliferation. *Journal of Experimental Medicine*, 204(1), pp.25-31.

Qi, Y., Zhang, X., Renier, N., Wu, Z., Atkin, T., Sun, Z., Ozair, M., Tchieu, J., Zimmer, B., Fattahi, F., Ganat, Y., Azevedo, R., Zeltner, N., Brivanlou, A., Karayiorgou, M., Gogos, J., Tomishima, M., Tessier-Lavigne, M., Shi, S. and Studer, L., 2017. Combined small-molecule inhibition accelerates the derivation of functional cortical neurons from human pluripotent stem cells. *Nature Biotechnology*, 35(2), pp.154-163.

Qu, X., Yu, J., Bhagat, G., Furuya, N., Hibshoosh, H., Troxel, A., Rosen, J., Eskelinen, E., Mizushima, N., Ohsumi, Y., Cattoretti, G. and Levine, B., 2003. Promotion of tumorigenesis by heterozygous disruption of the beclin 1 autophagy gene. *Journal of Clinical Investigation*, 112(12), pp.1809-1820.

Qu, X., Zou, Z., Sun, Q., Luby-Phelps, K., Cheng, P., Hogan, R., Gilpin, C. and Levine, B., 2007. Autophagy Gene-Dependent Clearance of Apoptotic Cells during Embryonic Development. *Cell*, 128(5), pp.931-946.

Rabinowitz, J. and White, E., 2010. Autophagy and Metabolism. *Science*, 330(6009), pp.1344-1348.

Rapaport, D., 2005. How does the TOM complex mediate insertion of precursor proteins into the mitochondrial outer membrane?. *Journal of Cell Biology*, 171(3), pp.419-423.

Ravikumar, B., Sarkar, S. and Rubinsztein, D., 2008. Clearance of Mutant Aggregate-Prone Proteins by Autophagy. *Autophagosome and Phagosome*, pp.195-211.

Ravikumar, B., Sarkar, S., Davies, J., Futter, M., Garcia-Arencibia, M., Green-Thompson, Z., Jimenez-Sanchez, M., Korolchuk, V., Lichtenberg, M., Luo, S., Massey, D., Menzies, F., Moreau, K., Narayanan, U., Renna, M., Siddiqi, F., Underwood, B., Winslow, A. and Rubinsztein, D., 2010. Regulation of Mammalian Autophagy in Physiology and Pathophysiology. *Physiological Reviews*, 90(4), pp.1383-1435.

Ravikumar, B., Vacher, C., Berger, Z., Davies, J., Luo, S., Oroz, L., Scaravilli, F., Easton, D., Duden, R., O'Kane, C. and Rubinsztein, D., 2004. Inhibition of mTOR

induces autophagy and reduces toxicity of polyglutamine expansions in fly and mouse models of Huntington disease. *Nature Genetics*, 36(6), pp.585-595.

Rodgers, J., Lerin, C., Haas, W., Gygi, S., Spiegelman, B. and Puigserver, P., 2005. Nutrient control of glucose homeostasis through a complex of PGC-1α and SIRT1. *Nature*, 434(7029), pp.113-118.

Roqué, P. and Costa, L., 2017. Co-Culture of Neurons and Microglia. *Current Protocols in Toxicology*, 74(1).

Rose, C., Menzies, F., Renna, M., Acevedo-Arozena, A., Corrochano, S., Sadiq, O., Brown, S. and Rubinsztein, D., 2010. Rilmenidine attenuates toxicity of polyglutamine expansions in a mouse model of Huntington's disease. *Human Molecular Genetics*, 19(11), pp.2144-2153.

Rosenstock, T., Carvalho, A., Jurkiewicz, A., Frussa-Filho, R. and Smaili, S., 2004. Mitochondrial calcium, oxidative stress and apoptosis in a neurodegenerative disease model induced by 3-nitropropionic acid. *Journal of Neurochemistry*, 88(5), pp.1220-1228.

Rubinsztein, D., 2006. The roles of intracellular protein-degradation pathways in neurodegeneration. *Nature*, 443(7113), pp.780-786.

Rubinsztein, D., Bento, C. and Deretic, V., 2015. Therapeutic targeting of autophagy in neurodegenerative and infectious diseases. *Journal of Experimental Medicine*, 212(7), pp.979-990.

Rubinsztein, D., Codogno, P. and Levine, B., 2012. Autophagy modulation as a potential therapeutic target for diverse diseases. *Nature Reviews Drug Discovery*, 11(9), pp.709-730.

Russell, R., Tian, Y., Yuan, H., Park, H., Chang, Y., Kim, J., Kim, H., Neufeld, T., Dillin, A. and Guan, K., 2013. ULK1 induces autophagy by phosphorylating Beclin-1 and activating VPS34 lipid kinase. *Nature Cell Biology*, 15(7), pp.741-750.

Sagot, Y., Dubois-Dauphin, M., Tan, S., de Bilbao, F., Aebischer, P., Martinou, J. and Kato, A., 1995. Bcl-2 overexpression prevents motoneuron cell body loss but not

axonal degeneration in a mouse model of a neurodegenerative disease. *The Journal of Neuroscience*, 15(11), pp.7727-7733.

Saha, K. and Jaenisch, R., 2009. Technical Challenges in Using Human Induced Pluripotent Stem Cells to Model Disease. *Cell Stem Cell*, 5(6), pp.584-595.

Saitoh, T., Fujita, N., Jang, M., Uematsu, S., Yang, B., Satoh, T., Omori, H., Noda, T., Yamamoto, N., Komatsu, M., Tanaka, K., Kawai, T., Tsujimura, T., Takeuchi, O., Yoshimori, T. and Akira, S., 2008. Loss of the autophagy protein Atg16L1 enhances endotoxin-induced IL-1β production. *Nature*, 456(7219), pp.264-268.

Sampath, P., Moideen, K., Ranganathan, U. and Bethunaickan, R., 2018. Monocyte Subsets: Phenotypes and Function in Tuberculosis Infection. *Frontiers in Immunology*, 9.

Sánchez, C., Diaz-Nido, J. and Avila, J., 2000. Phosphorylation of microtubule-associated protein 2 (MAP2) and its relevance for the regulation of the neuronal cytoskeleton function. *Progress in Neurobiology*, 61(2), pp.133-168.

Sandoval, H., Thiagarajan, P., Dasgupta, S., Schumacher, A., Prchal, J., Chen, M. and Wang, J., 2008. Essential role for Nix in autophagic maturation of erythroid cells. *Nature*, 454(7201), pp.232-235.

Sarkar, S., 2013. Regulation of autophagy by mTOR-dependent and mTOR-independent pathways: autophagy dysfunction in neurodegenerative diseases and therapeutic application of autophagy enhancers. *Biochemical Society Transactions*, 41(5), pp.1103-1130.

Sarkar, S., Carroll, B., Buganim, Y., Maetzel, D., Ng, A., Cassady, J., Cohen, M., Chakraborty, S., Wang, H., Spooner, E., Ploegh, H., Gsponer, J., Korolchuk, V. and Jaenisch, R., 2013. Impaired Autophagy in the Lipid-Storage Disorder Niemann-Pick Type C1 Disease. *Cell Reports*, 5(5), pp.1302-1315.

Sarkar, S., Davies, J., Huang, Z., Tunnacliffe, A. and Rubinsztein, D., 2006. Trehalose, a Novel mTOR-independent Autophagy Enhancer, Accelerates the Clearance of Mutant Huntingtin and α-Synuclein. *Journal of Biological Chemistry*, 282(8), pp.5641-5652.

Sarkar, S., Floto, R., Berger, Z., Imarisio, S., Cordenier, A., Pasco, M., Cook, L. and Rubinsztein, D., 2005. Lithium induces autophagy by inhibiting inositol monophosphatase. *Journal of Cell Biology*, 170(7), pp.1101-1111.

Sarkar, S., Korolchuk, V., Renna, M., Imarisio, S., Fleming, A., Williams, A., Garcia-Arencibia, M., Rose, C., Luo, S., Underwood, B., Kroemer, G., O'Kane, C. and Rubinsztein, D., 2011. Complex Inhibitory Effects of Nitric Oxide on Autophagy. *Molecular Cell*, 43(1), pp.19-32.

Sarkar, S., Korolchuk, V., Renna, M., Winslow, A. and Rubinsztein, D., 2009. Methodological considerations for assessing autophagy modulators: A study with calcium phosphate precipitates. *Autophagy*, 5(3), pp.307-313.

Sarkar, S., Krishna, G., Imarisio, S., Saiki, S., O'Kane, C. and Rubinsztein, D., 2007. A rational mechanism for combination treatment of Huntington's disease using lithium and rapamycin. *Human Molecular Genetics*, 17(2), pp.170-178.

Sarkar, S., Perlstein, E., Imarisio, S., Pineau, S., Cordenier, A., Maglathlin, R., Webster, J., Lewis, T., O'Kane, C., Schreiber, S. and Rubinsztein, D., 2007. Small molecules enhance autophagy and reduce toxicity in Huntington's disease models. *Nature Chemical Biology*, 3(6), pp.331-338.

Sarkar, S., Ravikumar, B. and Rubinsztein, D., 2009. Chapter 5 Autophagic Clearance of Aggregate-Prone Proteins Associated with Neurodegeneration. *Autophagy in Disease and Clinical Applications, Part C*, pp.83-110.

Sarkar, S., Ravikumar, B., Floto, R. and Rubinsztein, D., 2008. Rapamycin and mTOR-independent autophagy inducers ameliorate toxicity of polyglutamine-expanded huntingtin and related proteinopathies. *Cell Death & Differentiation*, 16(1), pp.46-56.

Saxton, R. and Sabatini, D., 2017. mTOR Signaling in Growth, Metabolism, and Disease. *Cell*, 169(2), pp.361-371.

Schiebler, M., Brown, K., Hegyi, K., Newton, S., Renna, M., Hepburn, L., Klapholz, C., Coulter, S., Obregón-Henao, A., Henao Tamayo, M., Basaraba, R., Kampmann, B., Henry, K., Burgon, J., Renshaw, S., Fleming, A., Kay, R., Anderson, K., Hawkins, P.,

Ordway, D., Rubinsztein, D. and Floto, R., 2014. Functional drug screening reveals anticonvulsants as enhancers of mTOR-independent autophagic killing of Mycobacterium tuberculosis through inositol depletion. *EMBO Molecular Medicine*, 7(2), pp.127-139.

Schöndorf, D., Ivanyuk, D., Baden, P., Sanchez-Martinez, A., De Cicco, S., Yu, C., Giunta, I., Schwarz, L., Di Napoli, G., Panagiotakopoulou, V., Nestel, S., Keatinge, M., Pruszak, J., Bandmann, O., Heimrich, B., Gasser, T., Whitworth, A. and Deleidi, M., 2018. The NAD+ Precursor Nicotinamide Riboside Rescues Mitochondrial Defects and Neuronal Loss in iPSC and Fly Models of Parkinson's Disease. *Cell Reports*, 23(10), pp.2976-2988.

Scott, I. and Youle, R., 2010. Mitochondrial fission and fusion. *Essays in Biochemistry*, 47, pp.85-98.

Sea, K., Sohn, S., Durazo, A., Sheng, Y., Shaw, B., Cao, X., Taylor, A., Whitson, L., Holloway, S., Hart, P., Cabelli, D., Gralla, E. and Valentine, J., 2014. Insights into the Role of the Unusual Disulfide Bond in Copper-Zinc Superoxide Dismutase. *Journal of Biological Chemistry*, 290(4), pp.2405-2418.

Sedlackova, L., Otten, E., Scialo, F., Shapira, D., Kataura, T., Carroll, B., Seranova, E., Rabanal-Ruiz, Y., Kelly, G., Stefanatos, R., Nelson, G., Urselli, F., Acharjee, A., Kenneth, N., Trushin, S., Zhang, T., Bascom, C., Tasseff, R., Isfort, R., Oblong, J., Trushina, E., Imoto, M., Saiki, S., Lazarou, M., Papamichos Chronakis, M., Maddoks, O., Sarkar, S., Sanz, A. and Korolchuk, V., 2020. Autophagy promotes cell and organismal survival by maintaining NAD(H) pools. *bioRxiv*, doi: https://doi.org/10.1101/2020.01.31.928424.

Senju, S., Haruta, M., Matsumura, K., Matsunaga, Y., Fukushima, S., Ikeda, T., Takamatsu, K., Irie, A. and Nishimura, Y., 2011. Generation of dendritic cells and macrophages from human induced pluripotent stem cells aiming at cell therapy. *Gene Therapy*, 18(9), pp.874-883.

Seranova, E., Connolly, K., Zatyka, M., Rosenstock, T., Barrett, T., Tuxworth, R. and Sarkar, S., 2017. Dysregulation of autophagy as a common mechanism in lysosomal storage diseases. *Essays in Biochemistry*, 61(6), pp.733-749.

Seranova, E., Palhegyi, A., Verma, S., Dimova, S., Lasry, R., Naama, M., Sun, C., Barrett, T., Rosenstock, T., Kumar, D., Cohen, M., Buganim, Y. and Sarkar, S., 2020. Human Induced Pluripotent Stem Cell Models of Neurodegenerative Disorders for Studying the Biomedical Implications of Autophagy. *Journal of Molecular Biology*, 432(8), pp.2754-2798.

Seranova, E., Ward, C., Chipara, M., Rosenstock, T. and Sarkar, S., 2019. In Vitro Screening Platforms for Identifying Autophagy Modulators in Mammalian Cells. *Methods in Molecular Biology*, pp.389-428.

Settembre, C., Di Malta, C., Polito, V., Arencibia, M., Vetrini, F., Erdin, S., Erdin, S., Huynh, T., Medina, D., Colella, P., Sardiello, M., Rubinsztein, D. and Ballabio, A., 2011. TFEB Links Autophagy to Lysosomal Biogenesis. *Science*, 332(6036), pp.1429-1433.

Settembre, C., Zoncu, R., Medina, D., Vetrini, F., Erdin, S., Erdin, S., Huynh, T., Ferron, M., Karsenty, G., Vellard, M., Facchinetti, V., Sabatini, D. and Ballabio, A., 2012. A lysosome-to-nucleus signalling mechanism senses and regulates the lysosome via mTOR and TFEB. *The EMBO Journal*, 31(5), pp.1095-1108.

Shacka, J., Klocke, B., Young, C., Shibata, M., Olney, J., Uchiyama, Y., Saftig, P. and Roth, K., 2007. Cathepsin D Deficiency Induces Persistent Neurodegeneration in the Absence of Bax-Dependent Apoptosis. *Journal of Neuroscience*, 27(8), pp.2081-2090.

Shaner, N., Steinbach, P. and Tsien, R., 2005. A guide to choosing fluorescent proteins. *Nature Methods*, 2(12), pp.905-909.

Sharma, V., Makhdoomi, M., Singh, L., Kumar, P., Khan, N., Singh, S., Verma, H., Luthra, K., Sarkar, S. and Kumar, D., 2020. Trehalose limits opportunistic mycobacterial survival during HIV co-infection by reversing HIV-mediated autophagy block. *Autophagy*, pp.1-20.

Sharma, V., Verma, S., Seranova, E., Sarkar, S. and Kumar, D., 2018. Selective Autophagy and Xenophagy in Infection and Disease. *Frontiers in Cell and Developmental Biology*, 6.

Shi, J., Xue, C., Liu, W. and Zhang, H., 2018. Differentiation of Human-Induced Pluripotent Stem Cells to Macrophages for Disease Modeling and Functional Genomics. *Current Protocols in Stem Cell Biology*, p.e74.

Shi, Y., Kirwan, P., Smith, J., Robinson, H. and Livesey, F., 2012. Human cerebral cortex development from pluripotent stem cells to functional excitatory synapses. *Nature Neuroscience*, 15(3), pp.477-486.

Shimada, K., Motoi, Y., Ishiguro, K., Kambe, T., Matsumoto, S., Itaya, M., Kunichika, M., Mori, H., Shinohara, A., Chiba, M., Mizuno, Y., Ueno, T. and Hattori, N., 2012. Long-term oral lithium treatment attenuates motor disturbance in tauopathy model mice: Implications of autophagy promotion. *Neurobiology of Disease*, 46(1), pp.101-108.

Shoji-Kawata, S., Sumpter, R., Leveno, M., Campbell, G., Zou, Z., Kinch, L., Wilkins, A., Sun, Q., Pallauf, K., MacDuff, D., Huerta, C., Virgin, H., Helms, J., Eerland, R., Tooze, S., Xavier, R., Lenschow, D., Yamamoto, A., King, D., Lichtarge, O., Grishin, N., Spector, S., Kaloyanova, D. and Levine, B., 2013. Identification of a candidate therapeutic autophagy-inducing peptide. *Nature*, 494(7436), pp.201-206.

Shtrichman, R. and Samuel, C., 2001. The role of gamma interferon in antimicrobial immunity. *Current Opinion in Microbiology*, 4(3), pp.251-259.

Siddiqi, F., Menzies, F., Lopez, A., Stamatakou, E., Karabiyik, C., Ureshino, R., Ricketts, T., Jimenez-Sanchez, M., Esteban, M., Lai, L., Tortorella, M., Luo, Z., Liu, H., Metzakopian, E., Fernandes, H., Bassett, A., Karran, E., Miller, B., Fleming, A. and Rubinsztein, D., 2019. Author Correction: Felodipine induces autophagy in mouse brains with pharmacokinetics amenable to repurposing. *Nature Communications*, 10(1).

Singh, R., Dwivedi, S., Gaharwar, U., Meena, R., Rajamani, P. and Prasad, T., 2019. Recent updates on drug resistance in Mycobacterium tuberculosis. *Journal of Applied Microbiology*, 128(6), pp.1547-1567.

Singh, S., Davis, A., Taylor, G. and Deretic, V., 2006. Human IRGM Induces Autophagy to Eliminate Intracellular Mycobacteria. *Science*, 313(5792), pp.1438-1441.

Slobodkin, M. and Elazar, Z., 2013. The Atg8 family: multifunctional ubiquitin-like key regulators of autophagy. *Essays in Biochemistry*, 55, pp.51-64.

Smith, T., Wolff, K. and Nguyen, L., 2012. Molecular Biology of Drug Resistance in Mycobacterium tuberculosis. *Current Topics in Microbiology and Immunology*, pp.53-80.

Soldner, F. and Jaenisch, R., 2018. Stem Cells, Genome Editing, and the Path to Translational Medicine. *Cell*, 175(3), pp.615-632.

Sou, Y., Waguri, S., Iwata, J., Ueno, T., Fujimura, T., Hara, T., Sawada, N., Yamada, A., Mizushima, N., Uchiyama, Y., Kominami, E., Tanaka, K. and Komatsu, M., 2008. The Atg8 Conjugation System Is Indispensable for Proper Development of Autophagic Isolation Membranes in Mice. *Molecular Biology of the Cell*, 19(11), pp.4762-4775.

Spence, J., Mayhew, C., Rankin, S., Kuhar, M., Vallance, J., Tolle, K., Hoskins, E., Kalinichenko, V., Wells, S., Zorn, A., Shroyer, N. and Wells, J., 2010. Directed differentiation of human pluripotent stem cells into intestinal tissue in vitro. *Nature*, 470(7332), pp.105-109.

Sperger, J., Chen, X., Draper, J., Antosiewicz, J., Chon, C., Jones, S., Brooks, J., Andrews, P., Brown, P. and Thomson, J., 2003. Gene expression patterns in human embryonic stem cells and human pluripotent germ cell tumors. *Proceedings of the National Academy of Sciences*, 100(23), pp.13350-13355.

Spilman, P., Podlutskaya, N., Hart, M., Debnath, J., Gorostiza, O., Bredesen, D., Richardson, A., Strong, R. and Galvan, V., 2010. Inhibition of mTOR by Rapamycin Abolishes Cognitive Deficits and Reduces Amyloid-β Levels in a Mouse Model of Alzheimer's Disease. *PLoS ONE*, 5(4), p.e9979.

Stafford, J., Neumann, N. and Belosevic, M., 2002. Macrophage-Mediated Innate Host Defense Against Protozoan Parasites. *Critical Reviews in Microbiology*, 28(3), pp.187-248.

Stavoe, A. and Holzbaur, E., 2019. Autophagy in Neurons. *Annual Review of Cell and Developmental Biology*, 35(1), pp.477-500.

Sterneckert, J., Reinhardt, P. and Schöler, H., 2014. Investigating human disease using stem cell models. *Nature Reviews Genetics*, 15(9), pp.625-639.

Stolz, A., Ernst, A. and Dikic, I., 2014. Cargo recognition and trafficking in selective autophagy. *Nature Cell Biology*, 16(6), pp.495-501.

Strohecker, A., Joshi, S., Possemato, R., Abraham, R., Sabatini, D. and White, E., 2015. Identification of 6-phosphofructo-2-kinase/fructose-2,6-bisphosphatase as a novel autophagy regulator by high content shRNA screening. *Oncogene*, 34(45), pp.5662-5676.

Sundaramurthy, V., Barsacchi, R., Samusik, N., Marsico, G., Gilleron, J., Kalaidzidis, I., Meyenhofer, F., Bickle, M., Kalaidzidis, Y. and Zerial, M., 2013. Integration of Chemical and RNAi Multiparametric Profiles Identifies Triggers of Intracellular Mycobacterial Killing. *Cell Host & Microbe*, 13(2), pp.129-142.

Svendsen, C., Skepper, J., Rosser, A., ter Borg, M., Tyres, P. and Ryken, T., 1997. Restricted growth potential of rat neural precursors as compared to mouse. *Developmental Brain Research*, 99(2), pp.253-258.

Takahashi, K. and Yamanaka, S., 2006. Induction of Pluripotent Stem Cells from Mouse Embryonic and Adult Fibroblast Cultures by Defined Factors. *Cell*, 126(4), pp.663-676.

Takahashi, K., Tanabe, K., Ohnuki, M., Narita, M., Ichisaka, T., Tomoda, K. and Yamanaka, S., 2007. Induction of Pluripotent Stem Cells from Adult Human Fibroblasts by Defined Factors. *Cell*, 131(5), pp.861-872.

Takahashi, Y., Coppola, D., Matsushita, N., Cualing, H., Sun, M., Sato, Y., Liang, C., Jung, J., Cheng, J., Mul, J., Pledger, W. and Wang, H., 2007. Bif-1 interacts with Beclin 1 through UVRAG and regulates autophagy and tumorigenesis. *Nature Cell Biology*, 9(10), pp.1142-1151.

Takasato, M., Er, P., Chiu, H., Maier, B., Baillie, G., Ferguson, C., Parton, R., Wolvetang, E., Roost, M., Chuva de Sousa Lopes, S. and Little, M., 2015. Kidney organoids from human iPS cells contain multiple lineages and model human nephrogenesis. *Nature*, 526(7574), pp.564-568.

Takata, K., Kozaki, T., Lee, C., Thion, M., Otsuka, M., Lim, S., Utami, K., Fidan, K., Park, D., Malleret, B., Chakarov, S., See, P., Low, D., Low, G., Garcia-Miralles, M., Zeng, R., Zhang, J., Goh, C., Gul, A., Hubert, S., Lee, B., Chen, J., Low, I., Shadan, N., Lum, J., Wei, T., Mok, E., Kawanishi, S., Kitamura, Y., Larbi, A., Poidinger, M., Renia, L., Ng, L., Wolf, Y., Jung, S., Önder, T., Newell, E., Huber, T., Ashihara, E., Garel, S., Pouladi, M. and Ginhoux, F., 2017. Induced-Pluripotent-Stem-Cell-Derived Primitive Macrophages Provide a Platform for Modeling Tissue-Resident Macrophage Differentiation and Function. *Immunity*, 47(1), pp.183-198.e6.

Takayama, K., Hagihara, Y., Toba, Y., Sekiguchi, K., Sakurai, F. and Mizuguchi, H., 2018. Enrichment of high-functioning human iPS cell-derived hepatocyte-like cells for pharmaceutical research. *Biomaterials*, 161, pp.24-32.

Tanaka, Y., Guhde, G., Suter, A., Eskelinen, E., Hartmann, D., Lüllmann-Rauch, R., Janssen, P., Blanz, J., von Figura, K. and Saftig, P., 2000. Accumulation of autophagic vacuoles and cardiomyopathy in LAMP-2-deficient mice. *Nature*, 406(6798), pp.902-906.

Teyssou, E., Takeda, T., Lebon, V., Boillée, S., Doukouré, B., Bataillon, G., Sazdovitch, V., Cazeneuve, C., Meininger, V., LeGuern, E., Salachas, F., Seilhean, D. and Millecamps, S., 2013. Mutations in SQSTM1 encoding p62 in amyotrophic lateral sclerosis: genetics and neuropathology. *Acta Neuropathologica*, 125(4), pp.511-522.

Thomson, J., 1998. Embryonic Stem Cell Lines Derived from Human Blastocysts. *Science*, 282(5391), pp.1145-1147.

Thomson, M., Liu, S., Zou, L., Smith, Z., Meissner, A. and Ramanathan, S., 2011. Pluripotency Factors in Embryonic Stem Cells Regulate Differentiation into Germ Layers. *Cell*, 145(6), pp.875-889.

Thoreen, C., Kang, S., Chang, J., Liu, Q., Zhang, J., Gao, Y., Reichling, L., Sim, T., Sabatini, D. and Gray, N., 2009. An ATP-competitive Mammalian Target of Rapamycin Inhibitor Reveals Rapamycin-resistant Functions of mTORC1. *Journal of Biological Chemistry*, 284(12), pp.8023-8032.

Thurston, T., Ryzhakov, G., Bloor, S., von Muhlinen, N. and Randow, F., 2009. The TBK1 adaptor and autophagy receptor NDP52 restricts the proliferation of ubiquitin-coated bacteria. *Nature Immunology*, 10(11), pp.1215-1221.

Tooze, S. and Yoshimori, T., 2010. The origin of the autophagosomal membrane. *Nature Cell Biology*, 12(9), pp.831-835.

Touboul, T., Hannan, N., Corbineau, S., Martinez, A., Martinet, C., Branchereau, S., Mainot, S., Strick-Marchand, H., Pedersen, R., Di Santo, J., Weber, A. and Vallier, L., 2009. Generation of functional hepatocytes from human embryonic stem cells under chemically defined conditions that recapitulate liver development. *Hepatology*, 51(5), pp.1754-1765.

Tsuchiya, S., Yamabe, M., Yamaguchi, Y., Kobayashi, Y., Konno, T. and Tada, K., 1980. Establishment and characterisation of a human acute monocytic leukemia cell line (THP-1). *International Journal of Cancer*, 26(2), pp.171-176.

Tsuganezawa, K., Shinohara, Y., Ogawa, N., Tsuboi, S., Okada, N., Mori, M., Yokoyama, S., Noda, N., Inagaki, F., Ohsumi, Y. and Tanaka, A., 2013. Two-Coloured Fluorescence Correlation Spectroscopy Screening for LC3-P62 Interaction Inhibitors. *Journal of Biomolecular Screening*, 18(9), pp.1103-1109.

Tumbarello, D., Manna, P., Allen, M., Bycroft, M., Arden, S., Kendrick-Jones, J. and Buss, F., 2015. The Autophagy Receptor TAX1BP1 and the Molecular Motor Myosin VI Are Required for Clearance of Salmonella Typhimurium by Autophagy. *PLOS Pathogens*, 11(10), p.e1005174.

Tumbarello, D., Waxse, B., Arden, S., Bright, N., Kendrick-Jones, J. and Buss, F., 2012. Autophagy receptors link myosin VI to autophagosomes to mediate Tom1-dependent autophagosome maturation and fusion with the lysosome. *Nature Cell Biology*, 14(10), pp.1024-1035.

Ueno, T. and Komatsu, M., 2017. Autophagy in the liver: functions in health and disease. *Nature Reviews Gastroenterology & Hepatology*, 14(3), pp.170-184.

Valente, A., Maddalena, L., Robb, E., Moradi, F. and Stuart, J., 2017. A simple ImageJ macro tool for analysing mitochondrial network morphology in mammalian cell culture. *Acta Histochemica*, 119(3), pp.315-326.

van der Zee, J., Van Langenhove, T., Kovacs, G., Dillen, L., Deschamps, W., Engelborghs, S., Matěj, R., Vandenbulcke, M., Sieben, A., Dermaut, B., Smets, K., Van Damme, P., Merlin, C., Laureys, A., Van Den Broeck, M., Mattheijssens, M., Peeters, K., Benussi, L., Binetti, G., Ghidoni, R., Borroni, B., Padovani, A., Archetti, S., Pastor, P., Razquin, C., Ortega-Cubero, S., Hernández, I., Boada, M., Ruiz, A., de Mendonça, A., Miltenberger-Miltényi, G., do Couto, F., Sorbi, S., Nacmias, B., Bagnoli, S., Graff, C., Chiang, H., Thonberg, H., Perneczky, R., Diehl-Schmid, J., Alexopoulos, P., Frisoni, G., Bonvicini, C., Synofzik, M., Maetzler, W., vom Hagen, J., Schöls, L., Haack, T., Strom, T., Prokisch, H., Dols-Icardo, O., Clarimón, J., Lleó, A., Santana, I., Almeida, M., Santiago, B., Heneka, M., Jessen, F., Ramirez, A., Sanchez-Valle, R., Llado, A., Gelpi, E., Sarafov, S., Tournev, I., Jordanova, A., Parobkova, E., Fabrizi, G., Testi, S., Salmon, E., Ströbel, T., Santens, P., Robberecht, W., De Jonghe, P., Martin, J., Cras, P., Vandenberghe, R., De Deyn, P., Cruts, M., Sleegers, K. and Van Broeckhoven, C., 2014. Rare mutations in SQSTM1 modify susceptibility to frontotemporal lobar degeneration. *Acta Neuropathologica*, 128(3), pp.397-410.

Vanhee, S., De Mulder, K., Van Caeneghem, Y., Verstichel, G., Van Roy, N., Menten, B., Velghe, I., Philippe, J., De Bleser, D., Lambrecht, B., Taghon, T., Leclercq, G., Kerre, T. and Vandekerckhove, B., 2014. In vitro human embryonic stem cell hematopoiesis mimics MYB-independent yolk sac hematopoiesis. *Haematologica*, 100(2), pp.157-166.

Vanier, M., 2010. Niemann-Pick disease type C. *Orphanet Journal of Rare Diseases*, 5(1).

Vanier, M., 2013. *Niemann-Pick Disease Type C*. 3rd ed. Handbook of Clinical Neurology, pp.1717-1721.

Vasileva, E., Shuvalov, O., Garabadgiu, A., Melino, G. and Barlev, N., 2015. Genome-editing tools for stem cell biology. *Cell Death & Disease*, 6(7), pp.e1831-e1831.

Vera, E., Bosco, N. and Studer, L., 2016. Generating Late-Onset Human iPSC-Based Disease Models by Inducing Neuronal Age-Related Phenotypes through Telomerase Manipulation. *Cell Reports*, 17(4), pp.1184-1192.

Verdin, E., 2015. NAD+ in aging, metabolism, and neurodegeneration. *Science*, 350(6265), pp.1208-1213.

Wang, C. and Youle, R., 2009. The Role of Mitochondria in Apoptosis. *Annual Review of Genetics*, 43(1), pp.95-118.

Wang, H., Sun, H., Zhu, X., Zhang, L., Albanesi, J., Levine, B. and Yin, H., 2015. GABARAPs regulate PI4P-dependent autophagosome:lysosome fusion. *Proceedings of the National Academy of Sciences*, 112(22), pp.7015-7020.

Wang, I., Guo, B., Liu, Y., Wu, C., Yang, C., Tsai, K. and Shen, C., 2012. Autophagy activators rescue and alleviate pathogenesis of a mouse model with proteinopathies of the TAR DNA-binding protein 43. *Proceedings of the National Academy of Sciences*, 109(37), pp.15024-15029.

Wang, J., Lian, H., Zhao, Y., Kauss, M. and Spindel, S., 2008. Vitamin D3 Induces Autophagy of Human Myeloid Leukemia Cells. *Journal of Biological Chemistry*, 283(37), pp.25596-25605.

Wang, Z., Miao, G., Xue, X., Guo, X., Yuan, C., Wang, Z., Zhang, G., Chen, Y., Feng, D., Hu, J. and Zhang, H., 2016. The Vici Syndrome Protein EPG5 Is a Rab7 Effector that Determines the Fusion Specificity of Autophagosomes with Late Endosomes/Lysosomes. *Molecular Cell*, 63(5), pp.781-795.

Warwick, C. and Usachev, Y., 2017. Culture, Transfection, and Immunocytochemical Analysis of Primary Macrophages. *Methods in Molecular Biology*, pp.161-173.

Watson, R., Bell, S., MacDuff, D., Kimmey, J., Diner, E., Olivas, J., Vance, R., Stallings, C., Virgin, H. and Cox, J., 2015. The Cytosolic Sensor cGAS Detects

Mycobacterium tuberculosis DNA to Induce Type I Interferons and Activate Autophagy. *Cell Host & Microbe*, 17(6), pp.811-819.

Weick, J., 2016. Functional Properties of Human Stem Cell-Derived Neurons in Health and Disease. *Stem Cells International*, 2016, pp.1-10.

Weiss, G. and Schaible, U., 2015. Macrophage defense mechanisms against intracellular bacteria. *Immunological Reviews*, 264(1), pp.182-203.

Westermann, B., 2010. Mitochondrial fusion and fission in cell life and death. *Nature Reviews Molecular Cell Biology*, 11(12), pp.872-884.

Wilgenburg, B., Browne, C., Vowles, J. and Cowley, S., 2013. Efficient, Long Term Production of Monocyte-Derived Macrophages from Human Pluripotent Stem Cells under Partly-Defined and Fully-Defined Conditions. *PLoS ONE*, 8(8), p.e71098.

Williams, A., Sarkar, S., Cuddon, P., Ttofi, E., Saiki, S., Siddiqi, F., Jahreiss, L., Fleming, A., Pask, D., Goldsmith, P., O'Kane, C., Floto, R. and Rubinsztein, D., 2008. Novel targets for Huntington's disease in an mTOR-independent autophagy pathway. *Nature Chemical Biology*, 4(5), pp.295-305.

Woo, M., Hakem, R., Soengas, M., Duncan, G., Shahinian, A., Kagi, D., Hakem, A., McCurrach, M., Khoo, W., Kaufman, S., Senaldi, G., Howard, T., Lowe, S. and Mak, T., 1998. Essential contribution of caspase 3/CPP32 to apoptosis and its associated nuclear changes. *Genes & Development*, 12(6), pp.806-819.

Wynn, T., Chawla, A. and Pollard, J., 2013. Macrophage biology in development, homeostasis and disease. *Nature*, 496(7446), pp.445-455.

Xia, Y., Nivet, E., Sancho-Martinez, I., Gallegos, T., Suzuki, K., Okamura, D., Wu, M., Dubova, I., Esteban, C., Montserrat, N., Campistol, J. and Belmonte, J., 2013. Directed differentiation of human pluripotent cells to ureteric bud kidney progenitor-like cells. *Nature Cell Biology*, 15(12), pp.1507-1515.

Xu, X., Lei, Y., Luo, J., Wang, J., Zhang, S., Yang, X., Sun, M., Nuwaysir, E., Fan, G., Zhao, J., Lei, L. and Zhong, Z., 2013. Prevention of β-amyloid induced toxicity in

human iPS cell-derived neurons by inhibition of Cyclin-dependent kinases and associated cell cycle events. *Stem Cell Research*, 10(2), pp.213-227.

Yamamoto, A., Tagawa, Y., Yoshimori, T., Moriyama, Y., Masaki, R. and Tashiro, Y., 1998. Bafilomycin A1 Prevents Maturation of Autophagic Vacuoles by Inhibiting Fusion between Autophagosomes and Lysosomes in Rat Hepatoma Cell Line, H-4-II-E Cells. *Cell Structure and Function*, 23(1), pp.33-42.

Yanez Arteta, M., Kjellman, T., Bartesaghi, S., Wallin, S., Wu, X., Kvist, A., Dabkowska, A., Székely, N., Radulescu, A., Bergenholtz, J. and Lindfors, L., 2018. Successful reprogramming of cellular protein production through mRNA delivered by functionalized lipid nanoparticles. *Proceedings of the National Academy of Sciences*, 115(15), pp.E3351-E3360.

Ye, L., Wang, J., Beyer, A., Teque, F., Cradick, T., Qi, Z., Chang, J., Bao, G., Muench, M., Yu, J., Levy, J. and Kan, Y., 2014. Seamless modification of wild-type induced pluripotent stem cells to the natural CCR5Δ32 mutation confers resistance to HIV infection. *Proceedings of the National Academy of Sciences*, 111(26), pp.9591-9596.

Ying, W., 2008. NAD+/NADH and NADP+/NADPH in Cellular Functions and Cell Death: Regulation and Biological Consequences. *Antioxidants & Redox Signaling*, 10(2), pp.179-206.

Yoshii, S. and Mizushima, N., 2017. Monitoring and Measuring Autophagy. *International Journal of Molecular Sciences*, 18(9), p.1865.

Yoshii, S., Kuma, A. and Mizushima, N., 2017. Transgenic rescue of Atg5-null mice from neonatal lethality with neuron-specific expression of ATG5: Systemic analysis of adult Atg5-deficient mice. *Autophagy*, 13(4), pp.763-764.

Yoshikawa, Y., Ogawa, M., Hain, T., Yoshida, M., Fukumatsu, M., Kim, M., Mimuro, H., Nakagawa, I., Yanagawa, T., Ishii, T., Kakizuka, A., Sztul, E., Chakraborty, T. and Sasakawa, C., 2009. Listeria monocytogenes ActA-mediated escape from autophagic recognition. *Nature Cell Biology*, 11(10), pp.1233-1240.

Youle, R. and Narendra, D., 2010. Mechanisms of mitophagy. *Nature Reviews Molecular Cell Biology*, 12(1), pp.9-14.

Yu, W., Gong, J., Ko, M., Garver, W., Yanagisawa, K. and Michikawa, M., 2005. Altered Cholesterol Metabolism in Niemann-Pick Type C1 Mouse Brains Affects Mitochondrial Function. *Journal of Biological Chemistry*, 280(12), pp.11731-11739.

Yuk, J., Shin, D., Lee, H., Yang, C., Jin, H., Kim, K., Lee, Z., Lee, S., Kim, J. and Jo, E., 2009. Vitamin D3 Induces Autophagy in Human Monocytes/Macrophages via Cathelicidin. *Cell Host & Microbe*, 6(3), pp.231-243.

Zachari, M. and Ganley, I., 2017. The mammalian ULK1 complex and autophagy initiation. *Essays in Biochemistry*, 61(6), pp.585-596.

Zhang, J., Zhou, Q., Chen, S. and Le, W., 2018. Repurposing carbamazepine for the treatment of amyotrophic lateral sclerosis in SOD1-G93A mouse model. *CNS Neuroscience & Therapeutics*, 24(12), pp.1163-1174.

Zhang, L., Zhang, S., Maezawa, I., Trushin, S., Minhas, P., Pinto, M., Jin, L., Prasain, K., Nguyen, T., Yamazaki, Y., Kanekiyo, T., Bu, G., Gateno, B., Chang, K., Nath, K., Nemutlu, E., Dzeja, P., Pang, Y., Hua, D. and Trushina, E., 2015. Modulation of Mitochondrial Complex I Activity Averts Cognitive Decline in Multiple Animal Models of Familial Alzheimer's Disease. *EBioMedicine*, 2(4), pp.294-305.

Zhang, S., Wernig, M., Duncan, I., Brüstle, O. and Thomson, J., 2001. In vitro differentiation of transplantable neural precursors from human embryonic stem cells. *Nature Biotechnology*, 19(12), pp.1129-1133.

Zhang, X., Heng, X., Li, T., Li, L., Yang, D., Zhang, X., Du, Y., Doody, R. and Le, W., 2011. Long-Term Treatment with Lithium Alleviates Memory Deficits and Reduces Amyloid-β Production in an Aged Alzheimer's Disease Transgenic Mouse Model. *Journal of Alzheimer's Disease*, 24(4), pp.739-749.

Zhao, Y. and Zhang, H., 2018. Autophagosome maturation: An epic journey from the ER to lysosomes. *Journal of Cell Biology*, 218(3), pp.757-770.

Zhou, C., Zhong, W., Zhou, J., Sheng, F., Fang, Z., Wei, Y., Chen, Y., Deng, X., Xia, B. and Lin, J., 2012. Monitoring autophagic flux by an improved tandem fluorescent-tagged LC3 (mTagRFP-mWasabi-LC3) reveals that high-dose rapamycin impairs autophagic flux in cancer cells. *Autophagy*, 8(8), pp.1215-1226.

Ziegler-Heitbrock, L., Ancuta, P., Crowe, S., Dalod, M., Grau, V., Hart, D., Leenen, P., Liu, Y., MacPherson, G., Randolph, G., Scherberich, J., Schmitz, J., Shortman, K., Sozzani, S., Strobl, H., Zembala, M., Austyn, J. and Lutz, M., 2010. Nomenclature of monocytes and dendritic cells in blood. *Blood*, 116(16), pp.e74-e80.

Zielonka, J., Zielonka, M. and Kalyanaraman, B., 2019. HPLC-Based Monitoring of Oxidation of Hydroethidine for the Detection of NADPH Oxidase-Derived Superoxide Radical Anion. *Methods in Molecular Biology*, pp.243-258.

Appendix

Appendix

Appendix 1: Publications of Elena Seranova

Only published articles are listed; papers submitted or in preparation are not listed.

Seranova, E., Connolly, K., Zatyka, M., Rosenstock, T., Barrett, T., Tuxworth, R. and Sarkar, S., 2017. Dysregulation of autophagy as a common mechanism in lysosomal storage diseases. *Essays in Biochemistry*, 61(6), pp.733-749.

Sharma, V., Verma, S., **Seranova, E.**, Sarkar, S. and Kumar, D., 2018. Selective autophagy and xenophagy in infection and disease. *Frontiers in Cell and Developmental Biology*, 6.

Seranova, E., Ward, C., Chipara, M., Rosenstock, T. and Sarkar, S., 2019. In vitro screening platforms for identifying autophagy modulators in mammalian cells. *Methods in Molecular Biology*, pp.389-428.

Panda, P., Fahrner, A., Vats, S., **Seranova, E.**, Sharma, V., Chipara, M., Desai, P., Torresi, J., Rosenstock, T., Kumar, D. and Sarkar, S., 2019. Chemical screening approaches enabling Drug discovery of autophagy modulators for biomedical applications in human diseases. *Frontiers in Cell and Developmental Biology*, 7.

Palhegyi, A., **Seranova, E.**, Dimova, S., Hoque, S. and Sarkar, S., 2019. Biomedical implications of autophagy in macromolecule storage disorders. *Frontiers in Cell and Developmental Biology*, 7.

Seranova, E., Palhegyi, A., Verma, S., Dimova, S., Lasry, R., Naama, M., Sun, C., Barrett, T., Rosenstock, T., Kumar, D., Cohen, M., Buganim, Y. and Sarkar, S., 2020. Human induced pluripotent stem cell models of neurodegenerative disorders for studying the biomedical implications of autophagy. *Journal of Molecular Biology*, 432(8), pp.2754-2798.

Klionsky, D.J. et al. including **Seranova, E.** and Sarkar, S. Guidelines for the use and interpretation of assays for monitoring autophagy (4th edition). *Autophagy* (In press).

Appendix 2: Cover of Journal of Molecular Biology (April 2020) featuring hESC-derived neurons generated by Elena Seranova in Sovan Sarkar lab

During this PhD work, an image of hESC-derived human neurons stained with TUJ1 (neuronal marker), DAPI (nuclear stain) and TUNEL (stain for apoptotic cells) was published in the cover of the April 2020 issue of Journal of Molecular Biology.

